# Application of cardiac imaging modalities in the assessment of coronary artery disease

Dr Jawad Mazhar

Thesis with published works

Submitted in fulfillment of the requirements for the degree of

Doctor of Philosophy


Sydney Medical School

Faculty of Medicine and Health

The University of Sydney

2024

## *Statement of originality*

This is to certify that to the best of my knowledge, the content of this thesis is my own work. This thesis has not been submitted for any degree or other purposes.

I certify that the intellectual content of this thesis is the product of my own work and that all the assistance received in preparing this thesis and sources have been acknowledged.

*Jawad Mazhar*

PhD Candidate

# TABLE OF CONTENTS

## Acknowledgements

I would like to thank and acknowledge all those that have made it possible for me undertake this PhD and complete this thesis.

Firstly, my supervisor, Professor Gemma Figtree. Thank you for your encouragement, patience and enthusiasm for this project and cardiovascular research more broadly. Your vision, leadership and advocacy are a source of inspiration for all those that have the privilege of working with you. Thank you for the encouragement to undertake this project and for the vast opportunities and collaborations you have facilitated.

I would also like to acknowledge and thank my co-supervisors, Dr Rebecca Kozor, Dr Ravinay Bhindi and Dr Stuart Grieve for their support and guidance. I could not have undertaken this without their support and encouragement.

I would also like to thank the staff and members of the team at Kolling Research Institute who helped me immensely while working on my research projects.

## Authorship Attribution Statement

This thesis is submitted to the University of Sydney in fulfilment of the requirement for the Degree of Doctor of Philosophy.

The work presented in this thesis is, to the best of my knowledge and belief, original except as acknowledged in the text. I hereby declare that I have not submitted this material, either in full or in part, for a degree at this or any other institution.

This thesis includes six original papers published in peer-reviewed journals. The core theme of this thesis is addressing the clinical challenges related to coronary artery disease using imaging modalities like coronary angiography, OCT, IVUS and cardiac MRI. The concepts, development and writing of all the papers included in this thesis were the principal responsibility of myself, the candidate, under the primary supervision of Professor Gemma Figtree, along with associate supervisor Dr Rebecca Kozor and Associate Professor Ravinay Bhindi.

The inclusion of co-authors in the papers reflects the fact that the work came from active collaboration between national and international researchers and acknowledges team-based research. I am first author on all papers included in this thesis.

| Thesis Chapter | Publication Title | Publication | Extent of Candidates Contribution |
|---|---|---|---|
| 3 | Automated quantification of myocardial salvage in a rat model of ischemia-reperfusion injury using 3D high-resolution magnetic resonance imaging (MRI). | J Am Heart Assoc. 2014 Jul 23;3(4):e000956. doi: 10.1161/JAHA.114.000956. PMID: 25146703 | 50%. I contributed to the design and analysis of the study. I performed the anaesthesia and surgery on animals. I injected the contrast agents and harvested the heart. I performed the TTC staining and methylene blue staining of the heart slices. I prepared the samples for MRI by storing them in agar gel. I perfomed the MRI acquisition of the heart samples. I performed the analysis of the MRI images. I drafted the publication. |
| 4 | Optical coherence tomography (OCT) as an adjunct to percutaneous coronary intervention; a single centre experience. | Int J Cardiol. 2013 Mar 10; 163(3):e49-e52. doi:10.1016/j.ijcard.2012.09.016. Epub 2012 Sep 30. PMID: 23031284. | 70%. I contributed to the design, collection of data and analysis of the study. I reviewed all the coronary angiograms and clinical information. I reviewed all the OCT images. I performed the literature search and drafted the publication. |
| 5 | Comparison of two dimensional quantitative coronary angiography (2D-QCA) with optical coherence tomography (OCT) in the | Int J Cardiol Heart Vasc. 2015 Jan 29;7:14-17. doi:10.1016/j.ijcha.2015.01.011. PMID: 28785639 | 70%. I contributed to the design, collection of data and analysis of the study. I reviewed all the coronary angiograms and clinical data. I performed 2D-QCA on all the images. I |

| | | | |
|---|---|---|---|
| | assessment of coronary artery lesion dimensions. | | analysed all the OCT images. I performed the literature search and drafted the publication. |
| 6 | Progression of coronary atherosclerosis in patients without standard modifiable risk factors. | Am J Prev Cardiol. 2020 Nov 24;4:100116. doi: 10.1016/j.ajpc.2020.100116. PMID: 34327476 | 70%. I contributed to the design and analysis of the study. I performed the literature search and drafted the publication. |
| 7 | Cardiovascular magnetic resonance characteristics and clinical outcomes of patients with ST-elevation myocardial infarction and no standard modifiable risk factors-A DANAMI-3 substudy. | Front Cardiovasc Med. 2022 Aug 3;9:945815. doi: 10.3389/fcvm.2022.945815. PMID: 35990971 | 50%. I contributed to the design and analysis of the study. I performed the literature search and drafted the publication. |

## Student's Statement

In addition to the statements above, in cases where I am not the corresponding author of a published item, permission to include the published material has been granted by the corresponding author.

*Jawad Mazhar*

18th January 2024

## Supervisor's Statement

As supervisor for the candidature upon which this thesis is based, I can confirm that the authorship attribution statements above are correct.

*Dr Rebecca Kozor*

18th January 2024

## Scientific Presentations:

I presented the results Chapter 3 as an abstract at the scientific sessions of American Heart Association conference in Chicago, USA in 2014.

## Additional publications during candidature

| Publication Title | Publication | Co-Authors |
|---|---|---|
| Cardiac magnetic resonance imaging of rapid VCAM-1 up-regulation in myocardial ischemia-reperfusion injury. | Eur Biophys J. 2013 Jan;42(1):61-70. doi: 10.1007/s00249-012-0857-x. Epub 2012 Sep 28. PMID: 23052973. | Grieve SM, Lønborg J, **Mazhar J**, Tan TC, Ho E, Liu CC, Lay W, Gill AJ, Kuchel P, Bhindi R, Figtree GA. |
| Predictors and outcome of no-reflow post primary percutaneous coronary intervention for ST elevation myocardial infarction. | Int J Cardiol Heart Vasc. 2015 Nov 6; 10:8-12. doi:10.1016/j.ijcha.2015.11.002. PMID: 28616509. | Jawad Mazhar, Mary Mashicharan, Ahmad Farshid |
| Clinical outcome of 2nd generation drug eluting stents versus bare-metal stents in percutaneous intervention on vein grafts. | Interv. Cardiol. (2015) 7(6), 511–517. | **Jawad Mazhar**, Ahmed Rehmani, Moyazur Rahman & Ahmad Farshid. |
| Clinical Outcomes in Patients With ST-Segment Elevation MI and No Standard Modifiable Cardiovascular Risk Factors. | JACC Cardiovasc Interv. 2022 Jun 13;15(11):1167-1175. doi: 10.1016/j.jcin.2022.03.036. PMID: 35680197. | Figtree GA, Redfors B, Kozor R, Vernon ST, Grieve SM, **Mazhar J**, Thiele H, Patel MR, Udelson JE, Selker HP, Ohman EM, Maehara A, Karmpaliotis D, Eitel I, Granger CB, Ben-Yehuda O, Stone GW, Kosmidou I. |

## Funding Statements:

**Chapter 3:** This work was supported by a grant from the North Shore Heart Research Foundation and by Project grant 632551 from the National Health & Medical Research Council (NHMRC), Australia. The animal magnetic resonance imaging facilities were funded by the Australian Research Council.

**Chapter 4:** No specific grant application but the PhD candidate was employed as an Imaging and Research fellow at Royal North Shore Hospital funded by the North Shore Heart Research Foundation.

**Chapter 5:** No specific grant application but the PhD candidate was employed as an Imaging and Research fellow at Royal North Shore Hospital funded by the North Shore Heart Research Foundation

**Chapter 6:** My supervisor Gemma Figtree receives funding from National Health and Medical Research Council (Australia) Practitioner Fellowship (GNT1135920) and Center for Research Excellence (GNT1196629), and New South Wales Office of Health and Medical Research (Senior Investigator grant).

**Chapter 7:** My supervisor Gemma Figtree receives funding from National Health and Medical Research Council (Australia) Practitioner Fellowship (GNT1135920) and Center for Research Excellence (GNT1196629), and New South Wales Office of

Health and Medical Research (Senior Investigator grant).and Medical Research (Senior Investigator grant)

## List of abbreviations:

| | |
|---|---|
| 2D-QCA | two-dimensional quantitative coronary angiography |
| 3D | Three dimensional |
| 3DGE | Three-dimensional gradient echo |
| AAR | Area at risk |
| ACE | Angiotensin converting enzyme |
| ACEi | Angiotensin converting enzyme inhibitor |
| ACS | Acute coronary syndrome |
| ARB | Angiotensin II receptor |
| AUC | Area under the curve |
| BMI | Body mass index |
| BNP | Brain natriuretic peptide |
| BP | Blood pressure |
| CABG | Coronary artery bypass graft surgery |
| CACS | Coronary artery calcium score |
| CAD | Coronary artery disease |
| CCS | Chronic Coronary Syndrome |
| CHD | Coronary heart disease |
| CHF | Chronic heart failure |

| | |
|---|---|
| CI | Confidence intervals |
| CMR | Cardiac magnetic resonance |
| CONCORDANCE | Cooperative National Registry of Acute Coronary Syndrome Care |
| CRP | C-reactive protein |
| CT | Computed tomography |
| CTCA | Computed tomography coronary angiography |
| CV | Cardiovascular |
| CVD | Cardiovascular disease |
| D1 | Diagonal branch 1 |
| D2 | Diagonal branch 2 |
| DANAMI-3 | Third DANish Study of Optimal Acute Treatment of Patients With ST-Segment Elevation Myocardial Infarction trial program |
| DCB | Drug Coated Balloon |
| DEFER | Deferred versus conventional stent implantation in patients with ST-segment elevation myocardial infarction; randomised controlled trial |
| DES-ISR | Drug Eluting Stent – Instent restenosis |
| DG-QFR | Diastolic Geometry Quantitative flow ratio |
| DMGV | dimethylguanidino valerate |
| DRD | Distal reference diameter |
| ECG | Electrocardiogram |
| EEL | External elastic lamina |
| EEM | External elastic membrane |

| | |
|---|---|
| FFR | Fractional flow reserve |
| FHS | Framingham Heart Study |
| FOV | Field of view |
| GGT | gamma-glutyl transferase |
| GRACE | Global Registry of Acute Coronary Events |
| GWAS | Genome wide association study |
| HbA1c | Glycated haemoglobin |
| HDL | High-density lipoprotein |
| HDL-C | High-density lipoprotein cholesterol |
| HF | Heart failure |
| HR | Hazard ratio |
| hs-CRP | High sensitive CRP |
| HU | Hounsfield unit |
| IHD | Ischaemic heart disease |
| IL | Interleukin |
| IMR | Index of Microvascular Resistance |
| IMRangio | Angiography-derived index of microcirculatory resistance |
| IPAQ | International Physical Activity Questionnaire |
| iPOST | Ischemic post conditioning |
| IQR | Interquartile range |
| IR | Ischemia reperfusion |
| ISR | In-stent restenosis |
| IVUS | Intravascular ultrasound |

| | |
|---|---|
| LAD | Left anterior descending artery |
| LCx | Left circumflex artery |
| LDL | Low-density lipoprotein |
| LDL-C | Low-density lipoprotein cholesterol |
| LGE | Late gadolinium enhancement |
| LMCA | Left main coronary artery |
| Lp(a) | Lipoprotein(a) |
| LV | Left ventricle |
| LVEF | Left ventricular ejection fraction |
| LVEDV | Left ventricle end diastolic volume |
| LVESV | left ventricle end systolic volume |
| MACE | Major adverse cardiovascular events |
| MEMRI | Manganese Enhanced Magnetic Resonance Imaging |
| MHz | Megahertz |
| MI | Myocardial infarction |
| MLA | Minimum luminal area |
| MLD | Minimum luminal diameter |
| MPIO | Microparticles of iron oxide |
| MRI | Magnetic resonance imaging |
| MSA | Minimum stent area |
| MSI | Myocardial salvage index |
| MVD | Multivessel disease |
| MVO | Microvascular obstruction |

| | |
|---|---|
| NA | Number of averages |
| NHMRC | National Health and Medical Research Council |
| NIH | National Institute of Health |
| NSTEMI | Non-ST elevation myocardial infarction |
| NT-proBNP | N-terminal-pro B-type natriuretic peptide |
| OCT | Optical coherence tomography |
| OM1 | Obtuse marginal branch 1 |
| OM2 | Obtuse marginal branch 2 |
| OR | Odds ratio |
| OSA | Obstructive Sleep Apnoea |
| PAI-1 | Plasminogen Activator Inhibitor-1 |
| PAV | Percent atheroma volume |
| PCI | Percutaneous coronary intervention |
| PDA | Posterior descending artery |
| PhD | Doctor of philosophy |
| PLB | Posterolateral branch |
| PM | Particulate Matter |
| PRD | Proximal reference diameter |
| PRIMULTI | Complete revascularisation versus treatment of the culprit lesion only in patients with ST-segment elevation myocardial infarction and multivessel disease (DANAMI-3—PRIMULTI): an open-label, randomised controlled trial |
| PVC | Polyvinyl Chloride |

| | |
|---|---|
| QCA | Quantitative coronary angiography |
| QFR | Quantitative flow ratio |
| RANZCR | Royal Australian and New Zealand College of Radiologists |
| RCA | Right coronary artery |
| RF | Risk factor |
| SBP | Systolic blood pressure |
| SA | Short axis |
| SD | Standard deviation |
| SEM | Standard Error of Mean |
| SG-QFR | Systolic Geometry Quantitative flow ratio |
| SMuRF-less | No standard modifiable cardiovascular risk factors |
| SMuRFs | Standard modifiable cardiovascular risk factors |
| SSFP | steady-state free precession |
| STEMI | ST elevation myocardial infarction |
| STIR | short tau inversion-recovery sequence |
| SWEDEHEART | Swedish Web-system for Enhancement and Development of Evidence-based care in Heart disease Evaluated According to Recommended Therapies |
| T2DM | Type 2 diabetes mellitus |
| TAV | Total atheroma volume |
| TA-QFR | Time Averaged Quantitative flow ratio |
| TCFA | Thin cap fibroatheroma |
| TE | Echo time |

| | |
|---|---|
| TI | Inversion time |
| TIA | Transient ischaemic accident |
| TFC | TIMI frame count |
| TIMI | Thrombolysis in myocardial infarction |
| TMAO | trimethylamine N-oxide |
| TR | Repetition time |
| TTC | Triphenyl Tetrazolium Chloride |
| UA | Uric Acid |
| vFFR | Vessel Fractional Flow Reserve |

# **Chapter 1.** Introduction

## *The global burden of coronary artery disease*

Coronary artery disease remains the leading cause of death in adults worldwide[1]. Based on the most recent estimates from global burden of disease dataset, coronary artery disease affects around 126 million individuals (1,655 per 100,000) worldwide[1]. It estimates that the current prevalence rate of 1,655 per 100,000 population is expected to exceed 1,845 by the year 2030[1]. In 2017, around 9 million deaths were due to coronary artery disease making it the leading cause of death worldwide[1]. Coronary artery disease is also the leading cause of death in Australia and was responsible for 17,500 deaths in 2018[2]. This represents 11% of all deaths annually and 42% of these deaths were due to myocardial infarction[2]. The prevalence of coronary artery disease increases with age for both men and women.

## *Pathophysiology of Coronary artery disease*

Coronary artery disease is caused by a pathologic process called atherosclerosis that leads to build up of atherosclerotic plaque within the wall of the coronary artery. Chronic exposure to certain risk factors like hypertension, hyperlipidemia, hyperglycemia and smoking etc. causes chronic injury to endothelial cells which leads to endothelial dysfunction with increased permeability and increased expression of surface adhesion molecules[3]. The first step in atherogenesis is trapping and accumulation of lipoproteins within the arterial wall[3]. The circulating monocytes bind to endothelial cells that express adhesion molecules and migrate into the wall of the coronary artery[4]. Once inside the arterial wall, monocytes become macrophages[4]. Oxidation of lipoproteins releases chemoattractants that activate endothelial cells, T cells and macrophages[3]. Macrophages take up the oxidized lipoproteins and become

foam cells[3]. Certain chemokines cause smooth muscle cells from the media to migrate towards the luminal side of the vessel and synthesize extracellular matrix which forms the fibrous cap of the plaque[3]. The fibrous cap is composed of collagen-rich fibre tissues, smooth muscle cells, macrophages and T lymphocytes[3]. All of them form the mature atherosclerosis plaque and bulge into the vessel lumen and compromise the blood flow[3]. The histologic stages of atherosclerotic plaque are as follows.

*Fatty streaks and intimal thickening*

Atherosclerosis begins with fatty streaks and thickening of the intima[3]. Fatty streaks are focal accumulations of lipid laden macrophages within the wall of the coronary artery while intimal thickening mainly consists of layers of smooth muscle cells mixed in proteoglycan matrix near the lumen[3].

*Pathologic Intimal thickening*

This is the second stage in the progression of atherosclerosis. It is characterized by extracellular lipid pools without necrosis[4]. The lipid pools are rich in hyaluronan and proteoglycans with no smooth muscle cells or inflammatory cells[4].

*Fibroatheroma*

Fibroatheroma is the next stage in the evolution of atherosclerotic plaque. It consists of an acellular necrotic core that is covered by a thick fibrous cap[4]. The necrotic core is caused by the death of foam cells. Foam cells contain cholesterol esters and free cholesterol. As plaques progress, the free cholesterol content of the plaque lesion

increases. A high ratio of free cholesterol to phospholipid in cellular membrane has been shown to be toxic to cells and may contribute to foam cell necrosis.

*Thin-cap Fibroatheroma or Vulnerable plaque*

Thin-cap fibroatheroma have a necrotic core and a thin fibrous cap measuring <65µm[4]. Also known as vulnerable plaque as they are prone to rupture and causing luminal thrombosis. The fibrous cap is heavily infiltrated by macrophages and to a lesser extent T-lymphocytes. The fibrous cap lacks smooth muscle cells.

## *Clinical manifestations of coronary artery disease*

Coronary artery disease is a chronic disease due to accumulation of atherosclerotic plaque that can have a wide range of symptoms and clinical outcomes. Patients may present with stable angina that occurs as there is myocardial ischemia due to supply and demand mismatch due to a fixed obstructive coronary artery lesion. Coronary artery lesions that cause angina are usually considered stable lesions with small lipid core, more fibrosis and calcification and thick fibrous caps[5]. The risk of major adverse events is low in this group of patients and are usually treated with risk factor modification with medications and lifestyle changes[6]. These patients can have long stable periods but can become unstable at any point due to plaque rupture or plaque erosion[7].

Unstable coronary artery lesions may cause an acute coronary syndrome which can have further clinical consequences that can range from myocardial infarction, cardiac arrhythmias, cardiogenic shock, and heart failure. Myocardial infarction occurs due to disruption of the fibrous cap overlying the atherosclerotic plaque and exposing the inner

core of the plaque to blood leading to activation of platelets, formation of thrombus and sudden occlusion of vessel[5]. The disruption of fibrous cap can occur due to plaque rupture or plaque erosion[4]. Plaques that are prone to rupture usually have a large necrotic core, high lipid content and a thin (<65μm) inflamed fibrous cap[4].

## *SMuRFless Patients*

Major advances have been made in the identification and treatment of standard modifiable risk factors for coronary artery disease - particularly hypercholesterolemia, hypertension, diabetes mellitus and smoking[8]. However, it is not uncommon for a patient to present with extensive atherosclerosis and life-threatening heart attack that is not clearly explained by Standard Modifiable Risk Factors (SMuRFs). In a large Canadian acute coronary syndrome registry study (n = 13 686), 14.5% of participants were identified as SMuRF-less[9]. A large myocardial infarction registry of 542 008 patients in the United States identified 14.4% of patients presenting with an initial myocardial infarction (STEMI and NSTEMI) had no SMuRFs[10]. This is also highlighted by our recently published data where around 27% of patients presenting to our Institution with identified plaque rupture and life-threatening ST elevation myocardial infarction had none of the SMuRFs[11]. This proportion has risen from 13% over 10 years, at a steady rate at our institution[11].

Surprisingly, a number of large observational studies have shown that SMuRFless patients have a higher in-hospital and 30-day mortality compared to patients with SMuRFs[10,12-14]. The mechanism of this paradox is not well understood. The underlying

pathology and clinical progression of coronary atherosclerosis in patients whose disease cannot be attributed to the presence of traditional risk factors has not been well studied. Specifically, the SMuRFless patients have not been well studied in large IVUS trials. We sought to compare the coronary plaque characteristics of SMuRFless patients and patients with >1 standard modifiable risk factor (SMuRF) to see if there is a difference in coronary plaque characteristics that may explain this. In this thesis (Chapter 6) I utilised serial IVUS data from a pooled cohort of 5823 patients enrolled in ten clinical trials to examine rates of plaque progression in patients who had no standard modifiable risk factors versus individuals with risk factors who were matched on age, sex and use of statins.

## *Imaging modalities to assess coronary artery disease*

Cardiac imaging modalities are commonly used in clinical cardiology to assess coronary artery disease (e.g., characterisation of atherosclerosis, plaque burden) and to assess the consequences (e.g., myocardial infarction, heart failure, cardiac structural and functional changes). There are multiple different imaging modalities/techniques available in clinical practice and for research, both non-invasive techniques (echocardiography, nuclear medicine, magnetic resonance imaging, CT coronary angiography) and invasive techniques (coronary angiography, intravascular ultrasound, optical coherence tomography). Cardiac imaging is arguably the centre of cardiology as it provides great insights into cardiac diseases and has expanding applications in both the clinical and research domains. Relevant to clinicians is translating cardiac imaging discoveries to clinical practice and making a positive impact on patient care and outcomes. It is the application of different cardiac imaging techniques that is the focus

of this thesis. In my clinical practice as an interventional cardiologist in Australia, the bulk of my work relates to coronary artery disease, infarction and ischemia. Therefore, I chose to focus my research on this area because of its clinical relevance.

**General hypothesis:** The overarching hypotheses is that cardiac imaging is able to improve the detection and characterisation of coronary artery disease, facilitate diagnosis, risk stratification, and contribute to knowledge in this field. In this thesis I have used cardiac magnetic resonance imaging and intravascular imaging to address some of the challenges in the assessment of myocardial infarction and coronary artery disease. The first study involves the development and validation of a novel method of quantifying myocardial infarction and area at risk in a rodent model using high resolution magnetic resonance imaging while the subsequent four studies use intravascular imaging and cardiac magnetic resonance imaging in human clinical trials. These studies have been published in peer reviewed journals and are listed here:

1. Automated Quantification of Myocardial Salvage in a Rat Model of Ischemia–Reperfusion Injury using 3D High-Resolution Magnetic Resonance Imaging (MRI)
2. Optical coherence tomography (OCT) as an adjunct to percutaneous coronary intervention; a single centre experience
3. Comparison of two-dimensional quantitative coronary angiography (2D-QCA) with optical coherence tomography (OCT) in the assessment of coronary artery lesion dimensions

4. Progression of coronary atherosclerosis in patients without standard modifiable risk factors
5. Cardiovascular magnetic resonance characteristics and clinical outcomes of patients with ST-elevation myocardial infarction and no Standard Modifiable Risk Factors - A DANAMI-3 substudy.

An introduction and rationale behind each individual study is as follows.

## *Automated Quantification of Myocardial Salvage in a Rat Model of Ischemia–Reperfusion Injury using 3D High-Resolution Magnetic Resonance Imaging (MRI)*

Ischemic heart disease remains the leading cause of death worldwide[1]. Improvements in the techniques and speed with which patients receive reperfusion therapy have significantly decreased mortality and morbidity of patients suffering myocardial infarction (MI)[1]. However, restoration of flow at the time of reperfusion also leads to a specific myocardial injury in addition to the injury caused by ischemia that is known as myocardial ischemia–reperfusion (IR) injury[15]. This myocardial IR injury manifests itself clinically in the form of arrhythmias, reversible contractile dysfunction (myocardial stunning), endothelial dysfunction, and cell death[16,17]. Contributing factors include postischemic low ATP and high phosphate levels, intracellular and mitochondrial calcium overload, oxidative stress and rapid increases in pH, endothelial dysfunction, and apoptosis[16,18]. The inflammatory response is also thought to play an important role, and several experimental studies have demonstrated a reduction in MI size with anti-inflammatory treatment[19-23].

Rodent models of cardiovascular disease provide a valuable means to understand the molecular and physiological mechanisms that influence outcome. The ability to measure infarct size accurately is important in rodent models as it allows the assessment of response to novel therapies. The current "gold standard" method uses a combination of selective perfusion of the heart with Evan's Blue and staining of the post-mortem sectioned heart with triphenyl tetrazolium chloride (TTC) to quantitate the area at risk (AAR) and degree of completed infarct[24,25]. Importantly, this approach accounts for variability in coronary artery anatomical supply, and can allow investigators to quantify the amount of salvaged myocardium. This method, although widely used and considered the "gold standard," also has documented problems relating to the accurate and reproducible delineation of the border of the infarct and AAR zones[26]. The accuracy of the delineation of the border zone between infarct and area at risk by this method has been questioned[26,27]. The requirement of manual slicing of tissue is labor intensive, and slices are relatively thick. This requires assumptions to be made about the surface borders reflecting the whole thickness of the slice. Questions have also been raised regarding the sensitivity of TTC staining in the setting of a gradient of viability, as would be common in the setting of IR injury[27].

Magnetic resonance imaging (MRI) is well recognized for its high spatial resolution (25 to 100 μm at fields higher than 3 T) and excellent soft-tissue discrimination. Cardiac MRI (CMR) has been developed to provide accurate functional data, although this requires an expert team to optimize cardiac and respiratory gating at high fields when applied to rodents[28], which may be a rate-limiting step in the majority of laboratories. Central to the clinical use of MRI to assess the ischemic heart is the use of delayed

gadolinium-enhanced images to define infarcted tissue[29]. The enhancement seen in the setting of an acute infarct using this method is based on the increased permeability of the cell membrane associated with necrosis, and has been shown to correlate extremely well with histology[30].

Delineation of AAR is considered a holy grail for cardiac MRI researchers. T2 sequences have been used to delineate areas of higher water content/edema. Although some studies have provided evidence for this approach[31,32] there is considerable controversy regarding this with concerns over reliability and robustness of the measure across different laboratories[33,34]. Microparticles of iron oxide (MPIO) provide excellent negative contrast even at low concentrations, are inert, and remain intravascular[35]. In this study, I compared the standard Evan's Blue/TTC method of AAR/infarct delineation against a novel method that uses a combination of T2* contrast from MPIO to define the borders of the perfused/unperfused myocardium, together with gadolinium-based T1- weighted enhancement to define the established infarct zone. I propose that this method has potential to provide rapid and accurate quantitation of these parameters in animal models of IR injury.

A method using cardiac MRI of whole heart could provide three-dimensional imaging of whole heart and reduce the assumptions made with the current method. In chapter 3 of this thesis, I describe a novel high resolution magnetic resonance imaging method of measuring area at risk and infarct size in a rodent model using two contrast agents, iron microparticles and gadolinium.

## *Optical coherence tomography (OCT) as an adjunct to percutaneous coronary intervention; a single centre experience*

Optical coherence tomography (OCT) is an intravascular imaging catheter that uses light to create a cross-sectional image of the coronary vessel[36]. It creates an image by measuring the echo time delay and the intensity of light that is reflected back from the coronary vessel[36]. It has a resolution of 10–20 μm which is 10 times higher than intravascular ultrasound [37]. However, its depth of tissue penetration is lower, around 1-2mm, while IVUS is higher around 4-8mm[37].

Due to its high-resolution images, OCT is able to differentiate the three layers of the arterial wall, intima, media and external elastic membrane which is not possible with IVUS[36]. The media appears as a dark band in between the intima and external elastic lamina[36]. OCT provides better visualisation of the lumen and arterial wall interface when compared with IVUS, this allows measurement of lumen areas and volumes[36]. OCT measurements of luminal area are highly reproducible with a high degree of correlation when two serial pullbacks are performed[36].

OCT can identify different components of atherosclerotic plaque. This includes fibrous plaque, lipid rich plaque, calcification and thrombus. Fibrous plaques have high reflectivity and low attenuation[36]. Calcifications within a plaque are usually well delineated with low reflectivity and low attenuation[36]. Lipid rich plaques are less well delineated with high reflectivity and high attenuation[36]. Thrombi are seen as masses protruding into the lumen with high reflectivity and signal-free shadowing[36]. OCT can

also identify dissection within plaque which is seen as rim of tissue extending into the lumen[36].

Although OCT can identify plaque characteristics and has been used predominantly in research settings, the indications for its use in clinical settings are not known. Most of the clinical trials have used IVUS rather than OCT during PCI. A metanalysis of 8 randomized clinical trials comparing IVUS with coronary angiography showed reduced angiographic restenosis, repeat revascularisation and MACE but no effect on MI or death[38]. OCT is more accurate than angiography or IVUS in detecting subtle morphological details like malapposition of stent struts, residual thrombus, plaque prolapse, and residual dissections, however the significance of these findings is uncertain[38]. OCT has some limitations; it requires complete clearance of blood from within the lumen of the vessel by injecting additional volume of contrast. Also, OCT has lower penetration compared to IVUS and is not able to measure the complete plaque burden. In Chapter 4 we sought to clarify the role OCT may have in the clinical setting of percutaneous coronary intervention in a single major tertiary centre.

### *Comparison of two-dimensional quantitative coronary angiography (2D-QCA) with optical coherence tomography (OCT) in the assessment of coronary artery lesion dimensions*

Suboptimal stent deployment has been shown to be associated with increased incidence of target vessel revascularization[39-41]. Reasons for target vessel revascularisation can be in-stent restenosis or stent thrombosis. Under sizing of the coronary artery stent is one of the predictors of stent thrombosis and in-stent restenosis[42,43]. Hence, an accurate

assessment of intracoronary lumen dimensions is essential in the diagnosis and treatment of coronary artery disease.

Coronary angiography involves selective engagement of a coronary artery with a catheter and injecting contrast media which in combination with x-rays allows visualisation of the lumen of the coronary vessels. Coronary lumen dimensions can be assessed by a visual estimate but this is dependent on the experience of the operator. Coronary lumen dimensions can also be assessed by quantitative coronary angiography (QCA) or by more invasive techniques like intravascular ultrasound or optical coherence tomography (OCT).

Intracoronary lumen dimensions assessed by OCT correlate well with IVUS, however OCT measurements are usually smaller than IVUS [44,45]. Although intravascular catheters like IVUS and OCT can provide an accurate assessment of the coronary artery lumen dimensions, they are invasive, expensive, time consuming and may require use of additional contrast. QCA uses an automated edge detection software to detect the contrast filled lumen of the coronary artery. QCA is mainly limited by foreshortening of vessel, overlapped vessels and inadequate filling of vessel with contrast. Previous studies comparing OCT and 2D/3D-QCA show a satisfactory to good correlation; however, QCA measurements are usually smaller than OCT[45-48]. Although these studies describe a correlation between QCA and OCT but do not describe how well they agree with each other.

Our aim was to assess the correlation between 2D-QCA and OCT for coronary lumen dimensions prior to stent implantation and to quantify the agreement between the two modalities by Bland–Altman analysis. We hypothesized that if the QCA measurements are within 0.5 mm of the OCT measurement, then it would be considered as an acceptable agreement between the two modalities. In Chapter 5 we have compared luminal measurements of coronary vessels performed by OCT with two-dimensional quantitative coronary angiography (2D-QCA) as 2D-QCA has the advantage of being non-invasive, inexpensive, less time consuming and does not require additional contrast.

## *Progression of coronary atherosclerosis in patients without standard modifiable risk factors*

Intravascular ultrasound is an intravascular imaging catheter with a miniature ultrasound probe at the tip of the catheter[49]. It emits ultrasound waves that can be either transmitted through the tissue or reflected depending on the mechanical impedance of the tissue[49]. For example, a calcified plaque is associated with acoustic shadowing i.e., a complete reflection of the ultrasound waves[49]. Non-calcified plaques allow partial transmission of ultrasound waves and a small percentage of the ultrasound waves are reflected[49]. The reflected signal is converted into an electrical signal and post processed into an image[49]. It typically has an axial resolution around 80–100 μm and lateral resolution around 200–250 μm, whereas tissue penetration is ~6–12 mm[50]. It allows assessment of plaque burden and plaque morphology i.e., lipid rich, fibrous or calcified plaque. IVUS imaging has been performed serially to evaluate the impact of medical therapies on progression of plaque in a number of clinical trials[51-60]. There is a wealth

of comprehensive IVUS imaging data collected in these clinical trials that can be interrogated to examine plaque burden and progression.

SMuRFless patients represent a significant proportion of patients who present with a myocardial infarction and range from 10.5% to 30% in large observational studies[10-13]. In a large study of 542,008 patients presenting with first myocardial infarction, in-hospital mortality was inversely related to the number of risk factors and patients with no risk factors had the highest in-hospital mortality compared to patients with >1 traditional risk factor, even after adjusting for different confounders including age and gender[10]. Also, patients with fewer risk factors are more likely to present with ST elevation myocardial infarction and cardiac arrest[9]. The mechanism of this paradox is not well understood. We sought to compare these two groups, i.e., patients with and without standard modifiable risk factors, to see if there is a difference in coronary plaque characteristics that may explain this. In Chapter 6, I utilised serial IVUS data from a pooled cohort of 5823 patients enrolled in ten clinical trials to examine rates of plaque progression in patients who had no standard modifiable risk factors versus individuals with risk factors who were matched on age, sex and use of statins.

### *Cardiovascular magnetic resonance characteristics and clinical outcomes of patients with ST-elevation myocardial infarction and no Standard Modifiable Risk Factors - A DANAMI-3 substudy.*

Cardiac MRI is considered the gold standard for quantifying ventricle volumes, mass, ejection fraction, infarct size and microvascular obstruction given its high reproducibility[61]. Cardiac MRI uses the late gadolinium enhancement technique to

assess infarct size[61-63]. Gadolinium is an extracellular contrast agent that accumulates in areas of extracellular expansion such as in myocardial infarction, and appears bright on T1 weighted imaging due to its T1 shortening property[62]. It is a robust technique that has been well validated and is highly reproducible with low interobserver variability[61-63]. After an intravenous injection of gadolinium, it perfuses locally through myocardial capillaries and diffuses within the interstitial compartment but does not enter myocytes as it is an extracellular agent. In acute myocardial infarction, the rupture of cardiac cells increases the interstitial volume, which reduces the washout rate, and results in an increase in the concentration of gadolinium in the infarcted area. The gadolinium persists within the infarct zone for a longer time than in healthy tissue leading to a regional hyperintense (bright) area on T1 weighted imaging

Myocardial salvage is defined as the difference between the area at risk and the final infarct size, where area at risk is the myocardium distal to the coronary stenosis that is at risk of ischemia. Ischemia in the area at risk leads to accumulation of fluid and edema which can be detected using a T2 weighted MRI sequence. T2 weighted short tau inversion recovery (T2-STIR) turbo spin echo sequence allows visualisation of edema and is comparable to SPECT and histopathology[64]. In order to compare the effect of therapy on infarcts of different sizes, the myocardial salvage index can be calculated as the proportion of non-necrotic myocardium inside the area at risk[65]. An area of myocardium can remain hypo-perfused even after restoration of flow by primary percutaneous coronary intervention in an occluded coronary artery in the setting of ST elevation myocardial infarction[66]. This occurs due to distal embolization of plaque or thrombus and leading to microvascular obstruction[66].

Microvascular obstruction appears as a hypo-intense area within an area of infarction seen with late gadolinium enhancement[66]. The extent of infarct size after a myocardial infarction is associated with mortality and hospitalization for heart failure[67]. Myocardial salvage index (MSI) and microvascular obstruction are both strong predictors of major adverse cardiac events[65,66].

Cardiac MRI can also assess ventricular size and function. Four patterns of left ventricle remodelling have been defined after an ST elevation myocardial infarction[61].

1. Reverse remodelling is defined as ≥12% decrease in left ventricle end systolic volume (LVESV).
2. No LV remodelling is defined as <12% change in left ventricle end diastolic volume (LVEDV) and LVESV.
3. Adverse LV remodelling with compensation is defined as >12% increase in LVEDV only.
4. Adverse left ventricle remodelling is defined as ≥ 12% increase in both LV end diastolic volume (LVEDV) and LV end systolic volume (LVESV).

Adverse left ventricle remodelling at 6 months is associated with worse clinical outcomes at 5 years in terms of all-cause mortality and hospitalization for heart failure in comparison to other 3 patterns[61]. Hence, cardiac MRI allows the measurement of infarct size, myocardial salvage index, microvascular obstruction and adverse LV remodelling. In Chapter 7 of this thesis, we evaluate the clinical outcomes and cardiac

MRI imaging characteristics in patients with and without SMuRFs who presented with first-presentation ST elevation myocardial infarction (STEMI).

## *Summary*

This thesis concentrates on exploring the application of cardiac imaging modalities in coronary artery disease, the most common clinical cardiology condition. The aim is to show that the techniques used in this thesis offer potential in terms of disease characterisation and diagnosis in addition to providing further insights into the knowledge of heart disease.

## *References:*


1. Khan MA, Hashim MJ, Mustafa H, Baniyas MY, Al Suwaidi S, AlKatheeri R, Alblooshi FMK, Almatrooshi M, Alzaabi MEH, Al Darmaki RS, et al. Global Epidemiology of Ischemic Heart Disease: Results from the Global Burden of Disease Study. *Cureus*. 2020;12:e9349. doi: 10.7759/cureus.9349

2. Health AIo, Welfare. Coronary heart disease. In: Canberra: AIHW; 2020.

3. Rafieian-Kopaei M, Setorki M, Doudi M, Baradaran A, Nasri H. Atherosclerosis: process, indicators, risk factors and new hopes. *Int J Prev Med*. 2014;5:927-946.

4. Bergheanu SC, Bodde MC, Jukema JW. Pathophysiology and treatment of atherosclerosis : Current view and future perspective on lipoprotein modification treatment. *Neth Heart J*. 2017;25:231-242. doi: 10.1007/s12471-017-0959-2

5. Libby P, Theroux P. Pathophysiology of coronary artery disease. *Circulation*. 2005;111:3481-3488. doi: 10.1161/circulationaha.105.537878

6. Ferraro R, Latina JM, Alfaddagh A, Michos ED, Blaha MJ, Jones SR, Sharma G, Trost JC, Boden WE, Weintraub WS, et al. Evaluation and Management of Patients With Stable Angina: Beyond the Ischemia Paradigm: JACC State-of-the-Art Review. *J Am Coll Cardiol*. 2020;76:2252-2266. doi: 10.1016/j.jacc.2020.08.078

7. Knuuti J, Wijns W, Saraste A, Capodanno D, Barbato E, Funck-Brentano C, Prescott E, Storey RF, Deaton C, Cuisset T, et al. 2019 ESC Guidelines for the diagnosis and management of chronic coronary syndromes. *Eur Heart J*. 2020;41:407-477. doi: 10.1093/eurheartj/ehz425

8. Jellinger PS, Handelsman Y, Rosenblit PD, Bloomgarden ZT, Fonseca VA, Garber AJ, Grunberger G, Guerin CK, Bell DSH, Mechanick JI, et al. AMERICAN ASSOCIATION

OF CLINICAL ENDOCRINOLOGISTS AND AMERICAN COLLEGE OF ENDOCRINOLOGY GUIDELINES FOR MANAGEMENT OF DYSLIPIDEMIA AND PREVENTION OF CARDIOVASCULAR DISEASE. *Endocr Pract*. 2017;23:1-87. doi: 10.4158/EP171764.APPGL

9. Wang JY, Goodman SG, Saltzman I, Wong GC, Huynh T, Dery JP, Leiter LA, Bhatt DL, Welsh RC, Spencer FA, et al. Cardiovascular Risk Factors and In-hospital Mortality in Acute Coronary Syndromes: Insights From the Canadian Global Registry of Acute Coronary Events. *Can J Cardiol*. 2015;31:1455-1461. doi: 10.1016/j.cjca.2015.04.007

10. Canto JG, Kiefe CI, Rogers WJ, Peterson ED, Frederick PD, French WJ, Gibson CM, Pollack CV, Jr., Ornato JP, Zalenski RJ, et al. Number of coronary heart disease risk factors and mortality in patients with first myocardial infarction. *Jama*. 2011;306:2120-2127. doi: 10.1001/jama.2011.1654

11. Vernon ST, Coffey S, Bhindi R, Soo Hoo SY, Nelson GI, Ward MR, Hansen PS, Asrress KN, Chow CK, Celermajer DS, et al. Increasing proportion of ST elevation myocardial infarction patients with coronary atherosclerosis poorly explained by standard modifiable risk factors. *Eur J Prev Cardiol*. 2017;24:1824-1830. doi: 10.1177/2047487317720287

12. Vernon ST, Coffey S, D'Souza M, Chow CK, Kilian J, Hyun K, Shaw JA, Adams M, Roberts-Thomson P, Brieger D, et al. ST-Segment-Elevation Myocardial Infarction (STEMI) Patients Without Standard Modifiable Cardiovascular Risk Factors-How Common Are They, and What Are Their Outcomes? *J Am Heart Assoc*. 2019;8:e013296. doi: 10.1161/jaha.119.013296

13. Roe MT, Halabi AR, Mehta RH, Chen AY, Newby LK, Harrington RA, Smith SC, Jr., Ohman EM, Gibler WB, Peterson ED. Documented traditional cardiovascular risk factors

and mortality in non-ST-segment elevation myocardial infarction. *Am Heart J*. 2007;153:507-514. doi: 10.1016/j.ahj.2006.12.018

14. Nauta ST, Deckers JW, van der Boon RM, Akkerhuis KM, van Domburg RT. Risk factors for coronary heart disease and survival after myocardial infarction. *European journal of preventive cardiology*. 2014;21:576-583. doi: 10.1177/2047487312460514

15. Keeley EC, Boura JA, Grines CL. Primary angioplasty versus intravenous thrombolytic therapy for acute myocardial infarction: a quantitative review of 23 randomised trials. *Lancet (London, England)*. 2003;361:13-20. doi: 10.1016/S0140-6736(03)12113-7

16. Wang QD, Pernow J, Sjöquist PO, Rydén L. Pharmacological possibilities for protection against myocardial reperfusion injury. *Cardiovasc Res*. 2002;55:25-37. doi: 10.1016/s0008-6363(02)00261-4

17. Kloner RA, Rezkalla SH. Cardiac protection during acute myocardial infarction: where do we stand in 2004? *J Am Coll Cardiol*. 2004;44:276-286. doi: 10.1016/j.jacc.2004.03.068

18. Ambrosio G, Tritto I. Reperfusion injury: experimental evidence and clinical implications. *Am Heart J*. 1999;138:S69-75. doi: 10.1016/s0002-8703(99)70323-6

19. Litt MR, Jeremy RW, Weisman HF, Winkelstein JA, Becker LC. Neutrophil depletion limited to reperfusion reduces myocardial infarct size after 90 minutes of ischemia. Evidence for neutrophil-mediated reperfusion injury. *Circulation*. 1989;80:1816-1827. doi: 10.1161/01.cir.80.6.1816

20. Hayward R, Campbell B, Shin YK, Scalia R, Lefer AM. Recombinant soluble P-selectin glycoprotein ligand-1 protects against myocardial ischemic reperfusion injury in cats. *Cardiovasc Res*. 1999;41:65-76. doi: 10.1016/s0008-6363(98)00266-1

21. Zhao ZQ, Lefer DJ, Sato H, Hart KK, Jefforda PR, Vinten-Johansen J. Monoclonal antibody to ICAM-1 preserves postischemic blood flow and reduces infarct size after ischemia-reperfusion in rabbit. *J Leukoc Biol*. 1997;62:292-300. doi: 10.1002/jlb.62.3.292

22. Entman ML, Smith CW. Postreperfusion inflammation: a model for reaction to injury in cardiovascular disease. *Cardiovasc Res*. 1994;28:1301-1311. doi: 10.1093/cvr/28.9.1301

23. Jolly SR, Kane WJ, Hook BG, Abrams GD, Kunkel SL, Lucchesi BR. Reduction of myocardial infarct size by neutrophil depletion: effect of duration of occlusion. *Am Heart J*. 1986;112:682-690. doi: 10.1016/0002-8703(86)90461-8

24. Gao E, Lei YH, Shang X, Huang ZM, Zuo L, Boucher M, Fan Q, Chuprun JK, Ma XL, Koch WJ. A novel and efficient model of coronary artery ligation and myocardial infarction in the mouse. *Circ Res*. 2010;107:1445-1453. doi: 10.1161/CIRCRESAHA.110.223925

25. Virag JA, Lust RM. Coronary artery ligation and intramyocardial injection in a murine model of infarction. *J Vis Exp*. 2011. doi: 10.3791/2581

26. Holmbom B, Näslund U, Eriksson A, Virtanen I, Thornell LE. Comparison of triphenyltetrazolium chloride (TTC) staining versus detection of fibronectin in experimental myocardial infarction. *Histochemistry*. 1993;99:265-275. doi: 10.1007/bf00269099

27. Freeman I, Grunwald AM, Robin B, Rao PS, Bodenheimer MM. Effect of early reperfusion on use of triphenyltetrazolium chloride to differentiate viable from non-viable myocardium in area of risk. *Cardiovasc Res*. 1990;24:109-114. doi: 10.1093/cvr/24.2.109

28. Schneider JE, Cassidy PJ, Lygate C, Tyler DJ, Wiesmann F, Grieve SM, Hulbert K, Clarke K, Neubauer S. Fast, high-resolution in vivo cine magnetic resonance imaging in normal and failing mouse hearts on a vertical 11.7 T system. *J Magn Reson Imaging*. 2003;18:691-701. doi: 10.1002/jmri.10411

29. Kim RJ, Fieno DS, Parrish TB, Harris K, Chen EL, Simonetti O, Bundy J, Finn JP, Klocke FJ, Judd RM. Relationship of MRI delayed contrast enhancement to irreversible injury, infarct age, and contractile function. *Circulation*. 1999;100:1992-2002. doi: 10.1161/01.cir.100.19.1992

30. Arheden H, Saeed M, Higgins CB, Gao DW, Bremerich J, Wyttenbach R, Dae MW, Wendland MF. Measurement of the distribution volume of gadopentetate dimeglumine at echo-planar MR imaging to quantify myocardial infarction: comparison with 99mTc-DTPA autoradiography in rats. *Radiology*. 1999;211:698-708. doi: 10.1148/radiology.211.3.r99jn41698

31. Aletras AH, Tilak GS, Natanzon A, Hsu LY, Gonzalez FM, Hoyt RF, Arai AE. Retrospective determination of the area at risk for reperfused acute myocardial infarction with T2-weighted cardiac magnetic resonance imaging: histopathological and displacement encoding with stimulated echoes (DENSE) functional validations. *Circulation*. 2006;113:1865-1870. doi: 10.1161/CIRCULATIONAHA.105.576025

32. Friedrich MG, Abdel-Aty H, Taylor A, Schulz-Menger J, Messroghli D, Dietz R. The salvaged area at risk in reperfused acute myocardial infarction as visualized by cardiovascular magnetic resonance. *J Am Coll Cardiol*. 2008;51:1581-1587. doi: 10.1016/j.jacc.2008.01.019

33. Mewton N, Rapacchi S, Augeul L, Ferrera R, Loufouat J, Boussel L, Micolich A, Rioufol G, Revel D, Ovize M, et al. Determination of the myocardial area at risk with pre- versus post-reperfusion imaging techniques in the pig model. *Basic Res Cardiol*. 2011;106:1247-1257. doi: 10.1007/s00395-011-0214-8

34. Eitel I, Friedrich MG. T2-weighted cardiovascular magnetic resonance in acute cardiac disease. *Journal of cardiovascular magnetic resonance : official journal of the Society for Cardiovascular Magnetic Resonance*. 2011;13:13. doi: 10.1186/1532-429X-13-13

35. McAteer MA, Sibson NR, von Zur Muhlen C, Schneider JE, Lowe AS, Warrick N, Channon KM, Anthony DC, Choudhury RP. In vivo magnetic resonance imaging of acute brain inflammation using microparticles of iron oxide. *Nat Med*. 2007;13:1253-1258. doi: 10.1038/nm1631

36. Prati F, Regar E, Mintz GS, Arbustini E, Di Mario C, Jang IK, Akasaka T, Costa M, Guagliumi G, Grube E, et al. Expert review document on methodology, terminology, and clinical applications of optical coherence tomography: physical principles, methodology of image acquisition, and clinical application for assessment of coronary arteries and atherosclerosis. *Eur Heart J*. 2010;31:401-415. doi: 10.1093/eurheartj/ehp433

37. Terashima M, Kaneda H, Suzuki T. The role of optical coherence tomography in coronary intervention. *Korean J Intern Med*. 2012;27:1-12. doi: 10.3904/kjim.2012.27.1.1

38. Neumann FJ, Sousa-Uva M, Ahlsson A, Alfonso F, Banning AP, Benedetto U, Byrne RA, Collet JP, Falk V, Head SJ, et al. 2018 ESC/EACTS Guidelines on myocardial revascularization. *Eur Heart J*. 2019;40:87-165. doi: 10.1093/eurheartj/ehy394

39. Costa MA, Angiolillo DJ, Tannenbaum M, Driesman M, Chu A, Patterson J, Kuehl W, Battaglia J, Dabbons S, Shamoon F, et al. Impact of stent deployment procedural factors on long-term effectiveness and safety of sirolimus-eluting stents (final results of the multicenter prospective STLLR trial). *Am J Cardiol*. 2008;101:1704-1711. doi: 10.1016/j.amjcard.2008.02.053

40. Lemos PA, Saia F, Ligthart JM, Arampatzis CA, Sianos G, Tanabe K, Hoye A, Degertekin M, Daemen J, McFadden E, et al. Coronary restenosis after sirolimus-eluting stent implantation: morphological description and mechanistic analysis from a consecutive series of cases. *Circulation*. 2003;108:257-260. doi: 10.1161/01.CIR.0000083366.33686.11

41. Aminian A, Kabir T, Eeckhout E. Treatment of drug-eluting stent restenosis: an emerging challenge. *Catheter Cardiovasc Interv*. 2009;74:108-116. doi: 10.1002/ccd.21938

42. van Werkum JW, Heestermans AA, Zomer AC, Kelder JC, Suttorp MJ, Rensing BJ, Koolen JJ, Brueren BR, Dambrink JH, Hautvast RW, et al. Predictors of coronary stent thrombosis: the Dutch Stent Thrombosis Registry. *J Am Coll Cardiol*. 2009;53:1399-1409. doi: 10.1016/j.jacc.2008.12.055

43. Condello F, Spaccarotella C, Sorrentino S, Indolfi C, Stefanini GG, Polimeni A. Stent Thrombosis and Restenosis with Contemporary Drug-Eluting Stents: Predictors and Current Evidence. *J Clin Med*. 2023;12. doi: 10.3390/jcm12031238

44. Gonzalo N, Serruys PW, García-García HM, van Soest G, Okamura T, Ligthart J, Knaapen M, Verheye S, Bruining N, Regar E. Quantitative ex vivo and in vivo comparison of lumen dimensions measured by optical coherence tomography and intravascular ultrasound in human coronary arteries. *Rev Esp Cardiol*. 2009;62:615-624. doi: 10.1016/s1885-5857(09)72225-x

45. Okamura T, Onuma Y, Garcia-Garcia HM, van Geuns RJ, Wykrzykowska JJ, Schultz C, van der Giessen WJ, Ligthart J, Regar E, Serruys PW. First-in-man evaluation of intravascular optical frequency domain imaging (OFDI) of Terumo: a comparison with intravascular ultrasound and quantitative coronary angiography. *EuroIntervention*. 2011;6:1037-1045. doi: 10.4244/eijv6i9a182

46. Puri R, Nelson AJ, Liew GY, Nicholls SJ, Carbone A, Wong DT, Harvey JE, Uno K, Copus B, Leong DP, et al. Variations in coronary lumen dimensions measured in vivo. *JACC Cardiovasc Imaging*. 2012;5:123-124. doi: 10.1016/j.jcmg.2011.07.012

47. Tu S, Xu L, Ligthart J, Xu B, Witberg K, Sun Z, Koning G, Reiber JH, Regar E. In vivo comparison of arterial lumen dimensions assessed by co-registered three-dimensional (3D) quantitative coronary angiography, intravascular ultrasound and optical coherence tomography. *Int J Cardiovasc Imaging*. 2012;28:1315-1327. doi: 10.1007/s10554-012-0016-6

48. Gutierrez-Chico JL, Serruys PW, Girasis C, Garg S, Onuma Y, Brugaletta S, Garcia-Garcia H, van Es GA, Regar E. Quantitative multi-modality imaging analysis of a fully bioresorbable stent: a head-to-head comparison between QCA, IVUS and OCT. *The international journal of cardiovascular imaging*. 2012;28:467-478. doi: http://dx.doi.org/10.1007/s10554-011-9829-y

49. Mintz GS, Nissen SE, Anderson WD, Bailey SR, Erbel R, Fitzgerald PJ, Pinto FJ, Rosenfield K, Siegel RJ, Tuzcu EM, et al. American College of Cardiology clinical expert consensus document on standards for acquisition, measurement and reporting of intravascular ultrasound studies (ivus)31When citing this document, the American College of Cardiology would appreciate the following citation format: Mintz GS, Nissen SE, Anderson WD, Bailey SR, Erbel R, Fitzgerald PJ, Pinto FJ, Rosenfield K, Siegel RJ, Tuzcu EM, Yock PG. ACC Clinical Expert Consensus Document on Standards for the acquisition, measurement and reporting of intravascular ultrasound studies: a report of the American College of Cardiology Task Force on Clinical Expert Consensus Documents (Committee to Develop a Clinical Expert Consensus Document on Standards for Acquisition, Measurement and Reporting of Intravascular Ultrasound Studies [IVUS]). J Am Coll Cardiol2001;37:1478–92.33Address for reprints: This document is available on the ACC Website at www.acc.org. Reprints of this document are available for $5.00 each by calling 800-253-4636 (U.S. only) or writing to the Resource Center, American College of Cardiology, Educational Services, 9111 Old Georgetown Road, Bethesda, MD 20814-1699. *Journal of the American College of Cardiology*. 2001;37:1478-1492. doi: 10.1016/s0735-1097(01)01175-5

50. Xu J, Lo S. Fundamentals and role of intravascular ultrasound in percutaneous coronary intervention. *Cardiovasc Diagn Ther*. 2020;10:1358-1370. doi: 10.21037/cdt.2020.01.15

51. Nissen SE, Tuzcu EM, Brewer HB, Sipahi I, Nicholls SJ, Ganz P, Schoenhagen P, Waters DD, Pepine CJ, Crowe TD, et al. Effect of ACAT inhibition on the progression of coronary atherosclerosis. *The New England journal of medicine*. 2006;354:1253-1263. doi: 10.1056/NEJMoa054699

52. Nissen SE, Nicholls SJ, Sipahi I, Libby P, Raichlen JS, Ballantyne CM, Davignon J, Erbel R, Fruchart JC, Tardif JC, et al. Effect of very high-intensity statin therapy on regression of coronary atherosclerosis: the ASTEROID trial. *Jama*. 2006;295:1556-1565. doi: 10.1001/jama.295.13.jpc60002

53. Nissen SE, Tardif JC, Nicholls SJ, Revkin JH, Shear CL, Duggan WT, Ruzyllo W, Bachinsky WB, Lasala GP, Tuzcu EM. Effect of torcetrapib on the progression of coronary atherosclerosis. *The New England journal of medicine*. 2007;356:1304-1316. doi: 10.1056/NEJMoa070635

54. Nissen SE, Nicholls SJ, Wolski K, Nesto R, Kupfer S, Perez A, Jure H, De Larochellière R, Staniloae CS, Mavromatis K, et al. Comparison of pioglitazone vs glimepiride on progression of coronary atherosclerosis in patients with type 2 diabetes: the PERISCOPE randomized controlled trial. *Jama*. 2008;299:1561-1573. doi: 10.1001/jama.299.13.1561

55. Nissen SE, Nicholls SJ, Wolski K, Rodés-Cabau J, Cannon CP, Deanfield JE, Després JP, Kastelein JJ, Steinhubl SR, Kapadia S, et al. Effect of rimonabant on progression of atherosclerosis in patients with abdominal obesity and coronary artery disease: the STRADIVARIUS randomized controlled trial. *Jama*. 2008;299:1547-1560. doi: 10.1001/jama.299.13.1547

56. Nicholls SJ, Ballantyne CM, Barter PJ, Chapman MJ, Erbel RM, Libby P, Raichlen JS, Uno K, Borgman M, Wolski K, et al. Effect of two intensive statin regimens on

progression of coronary disease. *The New England journal of medicine*. 2011;365:2078-2087. doi: 10.1056/NEJMoa1110874

57. Nicholls SJ, Puri R, Anderson T, Ballantyne CM, Cho L, Kastelein JJ, Koenig W, Somaratne R, Kassahun H, Yang J, et al. Effect of Evolocumab on Progression of Coronary Disease in Statin-Treated Patients: The GLAGOV Randomized Clinical Trial. *JAMA*. 2016;316:2373-2384. doi: 10.1001/jama.2016.16951

58. Nicholls SJ, Bakris GL, Kastelein JJ, Menon V, Williams B, Armbrecht J, Brunel P, Nicolaides M, Hsu A, Hu B, et al. Effect of aliskiren on progression of coronary disease in patients with prehypertension: the AQUARIUS randomized clinical trial. *JAMA*. 2013;310:1135-1144. doi: 10.1001/jama.2013.277169

59. Nissen SE, Tuzcu EM, Schoenhagen P, Brown BG, Ganz P, Vogel RA, Crowe T, Howard G, Cooper CJ, Brodie B, et al. Effect of intensive compared with moderate lipid-lowering therapy on progression of coronary atherosclerosis: a randomized controlled trial. *Jama*. 2004;291:1071-1080. doi: 10.1001/jama.291.9.1071

60. Brener SJ, Ivanc TB, Poliszczuk R, Chen M, Tuzcu EM, Hu T, Frid DJ, Nissen SE. Antihypertensive therapy and regression of coronary artery disease: insights from the Comparison of Amlodipine versus Enalapril to Limit Occurrences of Thrombosis (CAMELOT) and Norvasc for Regression of Manifest Atherosclerotic Lesions by Intravascular Sonographic Evaluation (NORMALISE) trials. *Am Heart J*. 2006;152:1059-1063. doi: 10.1016/j.ahj.2006.07.022

61. Bulluck H, Carberry J, Carrick D, McEntegart M, Petrie MC, Eteiba H, Hood S, Watkins S, Lindsay M, Mahrous A, et al. Redefining Adverse and Reverse Left Ventricular Remodeling by Cardiovascular Magnetic Resonance Following ST-Segment-Elevation Myocardial Infarction and Their Implications on Long-Term Prognosis. *Circulation Cardiovascular imaging*. 2020;13:e009937. doi: 10.1161/circimaging.119.009937

62. Ibanez B, Aletras AH, Arai AE, Arheden H, Bax J, Berry C, Bucciarelli-Ducci C, Croisille P, Dall'Armellina E, Dharmakumar R, et al. Cardiac MRI Endpoints in Myocardial Infarction Experimental and Clinical Trials: JACC Scientific Expert Panel. *J Am Coll Cardiol*. 2019;74:238-256. doi: 10.1016/j.jacc.2019.05.024

63. Thiele H, Kappl MJ, Conradi S, Niebauer J, Hambrecht R, Schuler G. Reproducibility of chronic and acute infarct size measurement by delayed enhancement-magnetic resonance imaging. *J Am Coll Cardiol*. 2006;47:1641-1645. doi: 10.1016/j.jacc.2005.11.065

64. Lønborg J, Vejlstrup N, Mathiasen AB, Thomsen C, Jensen JS, Engstrøm T. Myocardial area at risk and salvage measured by T2-weighted cardiovascular magnetic resonance: reproducibility and comparison of two T2-weighted protocols. *Journal of cardiovascular magnetic resonance : official journal of the Society for Cardiovascular Magnetic Resonance*. 2011;13:50. doi: 10.1186/1532-429x-13-50

65. Kendziora B, Dewey M. Prognostic value of the myocardial salvage index measured by T2-weighted and T1-weighted late gadolinium enhancement magnetic resonance imaging after ST-segment elevation myocardial infarction: A systematic review and meta-regression analysis. *PloS one*. 2020;15:e0228736. doi: 10.1371/journal.pone.0228736

66. de Waha S, Patel MR, Granger CB, Ohman EM, Maehara A, Eitel I, Ben-Yehuda O, Jenkins P, Thiele H, Stone GW. Relationship between microvascular obstruction and adverse events following primary percutaneous coronary intervention for ST-segment elevation myocardial infarction: an individual patient data pooled analysis from seven randomized trials. *Eur Heart J*. 2017;38:3502-3510. doi: 10.1093/eurheartj/ehx414

67. Stone GW, Selker HP, Thiele H, Patel MR, Udelson JE, Ohman EM, Maehara A, Eitel I, Granger CB, Jenkins PL, et al. Relationship Between Infarct Size and Outcomes Following Primary PCI: Patient-Level Analysis From 10 Randomized Trials. *J Am Coll Cardiol*. 2016;67:1674-1683. doi: 10.1016/j.jacc.2016.01.069

# **Chapter 2.** Methods

Each of the original results chapters of this thesis are published manuscripts. A description of the methods of imaging performed in these chapters and the strategies behind these are as follows.

## *Automated Quantification of Myocardial Salvage in a Rat Model of Ischemia–Reperfusion Injury using 3D High-Resolution Magnetic Resonance Imaging (MRI)*

The pathophysiology of coronary no-reflow post primary PCI is multifactorial and includes myocardial reperfusion injury that may occur after restoration of blood flow with accumulation of neutrophils and platelets that release inflammatory mediators and vasoconstrictors. Small animal models of myocardial ischemia reperfusion closely mimic the clinical scenario of ischemic perfusion injury after restoration of flow in patients with STEMI. Novel therapies targeting ischemia reperfusion injury are usually tested in these small animal models. An accurate assessment of myocardial "area at risk" (AAR) and myocardial infarction (MI) zone is critical when testing these therapies. The current "gold-standard" method involves perfusing the animal heart with Evan's Blue and staining with triphenyl tetrazolium chloride (TTC) and requires manual slicing and analysis.

We aimed to develop and validate a high-resolution 3-dimensional (3D) magnetic resonance imaging (MRI) method for quantifying MI and AAR. In chapter 3, Sprague–Dawley rats (weight 250 to 300 g) were acclimatized for a period of 1 week before surgery. The animals were kept in the animal house at the Kolling Institute, Royal North Shore Hospital, for 1 week to allow them to get use to their new environment. Procedures were conducted with the approval of the Royal North Shore Hospital Animal Care and Ethics Committee. After 1 week of acclimatization, myocardial ischemia reperfusion (IR) was induced as previously described using an open-chest approach[1,2]. Anaesthesia was induced by placing the animal in an induction chamber, with vaporised isoflurane 2%, and was performed by myself. Once anaesthetized, the animal was then positioned supine (on its back) on an operating table on top of a heating pad. The trachea was intubated with an 18-gauge intravenous cannula tubing and connected to the ventilator. The rats were ventilated and kept anaesthetized using 2% isoflurane. The hair on the

front of chest were removed with a hair clipper. After confirmation of deep anaesthesia, under aseptic measures, a lateral incision on the left side of chest was made in between the fourth and fifth rib. A retractor was used to keep the ribs apart. The pericardium was opened by pulling it up with a small forceps and cutting with a small scissor. Ischemia was induced for 30 minutes by transient suture ligation of the left anterior coronary artery 2 to 3 mm distal to the junction of pulmonary artery and left atrial appendage. The ligature was then released and the chest was closed with 4.0 silk suture. The rats were allowed to recover for 48 hours.

Under repeat anaesthesia, gadopentetate dimeglumine 0.15 mmol/kg was infused via the tail vein. After 10 minutes, the left anterior coronary artery was re-occluded and a solution containing microparticles of iron oxide (MPIO) at dose of 4.5 mg/kg body weight (as determined in pilot studies) mixed with 3% Evan's Blue, in a total volume of 5 mL, was injected via the tail vein. After a 2-minute interval, the heart was then excised, sectioned into 2-mm short-axis slices, and placed in TTC 1% in phosphate-buffered saline for 20 minutes at 37°C[3]. Slices were photographed and then fixed in 10% normal buffered formalin. To reduce sample movement during MRI imaging, whole hearts and sections were set in agar gel. They were then stored at 4°C and imaged within 1 week of each experiment.

**Iron-Oxide Microparticles**

MyOneTosyl-activated iron microparticles (MPIO: diameter 1.08 µm, iron content 26%) were purchased from Life Technologies. The MPIO particles were diluted in phosphate buffered saline prior to use.

**Magnetic Resonance Imaging: Protocol and Analysis**

MRI data were acquired on a vertical 9.4-T magnet (Biospec, Bruker, Ettlingen, Germany). Three-dimensional gradient echo, inversion recovery (2-dimensional multislice spin-echo), and T2 sequences were acquired with parameters optimized in order to achieve anatomical detail as well as T1 and T2/T2* contrast. Details of imaging parameters are below in Table 1. Resolution was 81 μm3 for 3-dimensional (3D) gradient echo, 163x325x400 μm for inversion recovery, and 120 μm3 for T2 sequences. T1 maps of sectioned MRI images were created from the inversion-recovery images (TI range 100 ms—1500 ms), respectively, and along with T2* images were registered to a common coordinate system for region-of-interest analysis.

Table 1. Technical Details of the Parameters Used for Acquiring MRI Data

| Sequence | Parameters |
|---|---|
| 3DGE | NA=4. TE=4 ms, TR=40 ms, flip angle=30°, FOV=20.8x20.8x5.1mm, matrix=256x256x64, resolution=81x81x 81μm (zero-filled to 40 μm3 isotropic) imaging time = 44 min. |
| Inversion recovery sequence (2D multislice spin-echo) | NA=1, TE=12.5 ms, TR=4000 ms, FOV=20.8x20.8, matrix=128x 64, 8 contiguous slices of 400 μm, in-plane resolution=163x325 μm (zero-filled to 81x81 μm), TI=100–1500 ms (6 steps: 300, 400, 600, 800, 1000, 1500 ms), Imaging time=34 min (per TI value). |
| Spin-echo images | TE=42 ms, TR=400, NE=3, resolution=120x120x120 μm (zero-filled to 60x60 μm), imaging time=27 min |

3DGE indicates 3-dimensional gradient echo; NA, Number of averages; TE, echo time; TR, repetition time; FOV, field of view; MRI, magnetic resonance imaging; TI, inversion time.

The 3 image stacks (T1 map, T2*, and T2) were used for each heart section. For comparison with Evan's Blue/TTC stained slices, analysis of the MRI data was restricted to 8 evenly spaced slices. The MRI images were pre-processed to define left and right ventricular epicardium and

left ventricular endocardium by 1 observer (the PhD candidate). Regions of interest for the AAR and MI were then manually contoured by 4 blinded observers, and by 1 observer twice with 1 week between analyses. AAR was identified by an absence of signal voids from MPIO in the T2* image stack, and MI was identified by high intensity on an inverted T1 map (i.e., longitudinal relativity, R1). In the case of any discrepancy, any region that was defined as MI was included as AAR. Regions of confluent signal within the MI, most likely representing microhemorrhage[4], were included as infarct zone. The T2 image was used to assist with anatomical definition of the AAR and MI zones.

The same analysis technique was used for the MR whole heart images following reformatting of the data to present the data in left ventricle short-axis (SA) orientation. For the whole-heart MRI analysis technique, 20 SA slices (650-lm slice spacing) were generated covering the whole heart. In addition, an automatic segmentation of the AAR and MI regions in the whole-heart MRI volumes was carried out. A 3D minimum filter was applied to accentuate the signal voids due to MPIO, followed by a 2D 9x9 pixel standard deviation filter, which resulted in low signal in the region of AAR, and high signal outside of the AAR where signal voids were present. Within the region detected as AAR, thresholding of the T1 map images was used to define MI regions. The T1 threshold was chosen based on a single manual segmentation. As the T1 value is an intrinsic material property of the heart tissue depending on its pathological state that has been extracted by the MRI technique and cleaned of noise by the image processing technique described, a single manual investigation was necessary to define the T1 value that gave a clear threshold between AAR tissue and MI tissue. The photographed heart sections were also pre-processed to define left and right epicardium and left endocardium borders before being analysed by the same observers, identifying AAR and MI on the apical side of each heart

section following standard protocols[3]. Custom code written in Matlab (The MathWorks Co, Natick, MA) was used for all analysis.

***Statistical Analysis***

Statistical analysis was performed within Matlab and SPSS v20 (IBM, NY). The Bland Altman statistical test was used to assess intra- and interobserver variability, with the results presented graphically including mean differences and 95% limits of agreement. Summary results are presented as mean ± Standard error of the mean (SEM).

**Candidate's contribution:** I performed the anaesthesia and the surgery on the animals. I injected the contrast agents i.e., gadolinium and iron microparticles via the tail vein. I harvested the heart at the end of the procedure. I sliced the hearts and stained with TTC. I prepared the heart slices for MRI by storing them in small tubes of agar gel. I was present at the time of acquisition of MRI with my supervisor. I performed the analysis of the MRI images.

## *Optical coherence tomography (OCT) as an adjunct to percutaneous coronary intervention; a single centre experience*

Optical coherence tomography (OCT) is a relatively new intravascular imaging catheter in comparison to intravascular ultrasound[5]. The clinical indications for use of OCT were not well defined in 2013 when this study was performed. In chapter 4, we sought to clarify the potentially under-appreciated clinical role that OCT may play in PCI. We reported a single centre experience where OCT was used to help guide management in routine clinical practice. Between November 2010 and February 2012 all cases where OCT was performed for clinical indications during PCI at Royal North Shore Hospital, Sydney, Australia were retrospectively analysed. The OCT acquisition was performed by local cardiologists using the C7 Dragonfly™ intracoronary imaging catheter and the ILUMIEN™ PCI Optimization System (St. Jude

Medical, Inc. USA). All images were acquired using a non-occlusive technique with injection of isosmolar iodixanol (Visipaque™by GE healthcare) contrast to clear the coronary artery lumen of blood[6]. The steps of the procedure were as follows:

1. OCT catheter was prepared by connecting the side port of the catheter with a 3ml syringe filled with 100% contrast.
2. The OCT catheter was then purged by flushing it with contrast until 3-5 drops of contrast were seen exiting the tip of the catheter.
3. The drive motor and optical controller (DOC) was draped in a plastic sleeve to maintain a sterile environment.
4. The back end of OCT catheter was connected to the DOC by aligning it with the notches on the DOC and turning clockwise until it locks.
5. The LED lights flash as the catheter is connected with DOC and the system performs an automatic calibration.
6. The OCT software confirms the connection.
7. The OCT catheter was loaded on the coronary wire and advanced to the target area under fluoroscopic guidance.
8. The catheter was than auto calibrated by clicking “Auto Calibrate” on the screen or the “Enable button” on the DOC. The image is correctly calibrated when the outermost “ring” of the catheters is centred between the 4 calibration marks
9. The catheter was purged by injecting ~0.1 mL contrast using the 3 mL syringe to ensure no blood has diffused into the catheter lumen
10. A small puff of contrast was injected through the guide catheter to determine adequate blood clearance of the distal vessel. This helped determine guide catheter alignment and position prior to image acquisition.

11. Once ready to acquire the image, the operator clicked “Enable Pullback” followed by stepping on the cine pedal to begin the flush protocol.
12. The operator would step off the cine pedal after the OCT pullback
13. The flush protocol was performed by a pressure injector connected to the manifold.

**Candidate's contribution:** I reviewed all the coronary angiograms and OCT images to confirm the findings observed at the time of the procedure. I collected all the demographic details of the patients, OCT vessel information and OCT indications to understand the impact of the OCT images on clinical decision making. I discussed the cases with the interventional cardiologist performing the procedure to understand how it changed management for the case.

### *Comparison of two-dimensional quantitative coronary angiography (2D-QCA) with optical coherence tomography (OCT) in the assessment of coronary artery lesion dimensions*

An accurate assessment of intracoronary lumen dimensions is essential in the diagnosis and treatment of coronary artery disease. Although intravascular catheters like IVUS and OCT can provide an accurate assessment of the coronary artery lumen dimensions, they are invasive, expensive, time consuming and may require use of extra contrast. Also, these intravascular catheters may not be available in some cardiac catheterisation laboratories. 2D-QCA is available in most cardiac catheterisation laboratories as a software. It uses automated edge detection software to detect the contrast filled lumen of the coronary artery[7]. Our aim was to assess the correlation between 2D-QCA and OCT for coronary lumen dimensions prior to stent implantation and also to quantify the agreement between the two modalities by Bland–Altman analysis. Therefore, in chapter 5, patients undergoing OCT for various clinical indications at Royal North Shore Hospital, Sydney, Australia were reviewed. The OCT acquisition was performed using the C7 Dragonfly™ intracoronary imaging catheter and the ILUMIEN™ PCI

Optimization System (St. Jude Medical). All images were acquired using a non-occlusive technique with injection of isosmolar iodixanol (Visipaque™ by GE healthcare) contrast using automatic injection to clear the vessel of blood[6]. The lesion was crossed using a routine angioplasty wire. The imaging catheter was then advanced over the wire. Once the catheter was positioned distal to the lesion it was pull backed using an automated motor at a speed of 15 mm/s. Two-dimensional quantitative coronary angiography (2D-QCA) was performed offline using automated software. Measurements were performed on image sequences adequately filled with contrast and when the vessel was not foreshortened. Calibration was performed on the contrast filled segment of the guiding catheter. Measurements were performed on the lesion of interest using the automated software. Proximal and distal reference diameters were performed manually to measure the diameter of the normal segment of the vessel.

Minimum luminal diameter (MLD), proximal reference diameter (PRD) and distal reference diameter (DRD) were measured for each lesion. PRD was defined as the diameter of the normal vessel proximally but within 10 mm of the lesion and DRD as the diameter of the normal vessel distally but within 10 mm of the lesion.

Lesions that were not suitable for analysis were excluded e.g., OCT images with poor clearance of blood or inadequate short runs were excluded. Lesions that were dilated prior to performing OCT were excluded. Lesions with poor angiographic images not suitable for quantitative coronary angiography (QCA) were also excluded, e.g., foreshortened images or images with overlapping vessels. All 2D-QCA and OCT images were reviewed and analysed by the PhD candidate.

***Statistical analysis***

Statistical analysis was performed using GraphPad Prism 6 for windows. Continuous variables are expressed as means. Means were compared using Student's t test. A p value of b0.05 was considered to be significant. The association between the measurements by QCA and OCT was tested by plotting a scatter plot and measuring the correlation coefficient 'r' by Pearson's method. Bland–Altman plots were constructed to test the agreement between the two methods by plotting the average of the QCA and OCT measurements on x axis and the difference between the QCA and OCT measurements on y axis.

**Candidate's contributions:** I contributed to the design, collection of data and analysis of the study. I reviewed all the coronary angiograms and collected the demographic data. I performed 2D-QCA analysis on all the coronary angiogram images and measured the luminal dimensions. I analysed all of the OCT images for luminal dimensions. I performed all of the statistical analysis on GraphPad Prism 6. I performed the literature search and drafted the publication.

## *Progression of coronary atherosclerosis in patients without standard modifiable risk factors*

It is not uncommon for a patient to present with extensive atherosclerosis and acute coronary syndrome in the absence of traditional risk factors for coronary artery disease. These patients have not been well studied in randomized clinical trials. Observational studies show that these patients have higher in-hospital and 30-day mortality rates after myocardial infarction compared to patients with at least one of the major 4 modifiable risk factors[8-11]. Intravascular ultrasound [5] permits quantification of coronary plaque burden and has been employed to evaluate the impact of medical therapies on disease progression in randomized clinical trials[12-19]. We aimed to utilise IVUS data from clinical trials to assess plaque burden, plaque characteristics and plaque progression in patients with no standard modifiable risk factors.

Therefore, in chapter 6, we investigated a pooled cohort of 5823 patients with angiographic CAD who underwent serial IVUS imaging in ten clinical trials evaluating the impact of medical therapies on plaque progression[13-22]. Of the 5823 patients, we identified 214 to have no standard modifiable risk factors (3.7%), including smoking, hypertension, diabetes and hypercholesterolemia, recorded on the basis of self-reporting. On review of the baseline systolic blood pressure and lipids of the patients in the no risk factor group, it was noted that these were elevated in some patients. Out of the 214 patients, 49 were noted to have either systolic blood pressure of >140 mmHg or total cholesterol >213 mg/dl or LDL >135 mg/dl at baseline. These patients were excluded. For the purpose of this analysis, patients with no standard modifiable risk factors (n = 165) were compared with patients with at least one such risk factor after matching (3:1) on age, sex and use of statins during the trials (n = 492).

***Acquisition of IVUS images***

The IVUS images had already been acquired at the time of the randomised controlled trials. The data was collected from these trials for analysis. The method of acquisition of the IVUS images in these trials was performed as follows. Patients were imaged with either a 40 MHz Atlantis SR Pro (Boston Scientific Scimed, Inc., Maple Grove, MN, USA) or a 45 MHz Revolution (Volcano Corporation, San Diego, CA, USA) catheter. The target vessel for imaging was required to have at least 20% but not more than 50% stenosis on the coronary angiogram, at least 30 mm in length, with no prior revascularization and not planned for revascularization. After appropriate anticoagulation and intra-coronary nitrate, the IVUS imaging catheter was advanced beyond the lesion into the distal segment of the coronary artery. A pullback was performed at a constant speed of 0.5mm/s and a continuous image of the coronary artery was acquired at 30 frames per second. IVUS images were matched with the coronary angiogram by identifying the proximal and distal side branches. Follow up IVUS

imaging, after 18–24 months, was performed in the same coronary segment by using these side branches as landmarks. Images were stored and sent to a core lab for analysis.

For each pull back, cross sectional images spaced 1 mm apart were selected for measurement. For each selected cross-sectional image, the leading edge of the lumen and the external elastic membrane (EEM) were manually traced to measure the lumen area and EEM area. IVUS images were analysed in a core laboratory by personnel blinded to all patient characteristics and treatment status. A number of plaque measures were derived from this analysis. Percent atheroma volume [23] was determined as the proportion of the whole vessel wall occupied by plaque throughout the entire length of artery studied[14].

$$PAV = \frac{\sum(EEM\ area - lumen\ area)}{\sum(EEM\ area)}\ x\ 100$$

Total atheroma volume (TAV) was determined by summation of atheroma area in all evaluable cross-sectional images [11].

$$TAV = \sum(EEM\ area - lumen\ area)$$

To account for potential differences in segment length between patients, TAV was subsequently normalized, by multiplying the average plaque area in a segment by the median number of evaluable images for all patients in the study.

$$Normalised\ TAV = \frac{\sum(EEM\ area - lumen\ area)}{n}\ x\ Median\ number\ of\ images\ in\ cochort$$

The quantitation of plaque calcium has been described previously[24]. The presence of calcium in each measured image was assigned a grade from 0 to 2. Grade 0 representing no calcium, grade 1 representing calcium with acoustic shadowing <90°, grade 2 representing calcium with shadowing >90°. In images that contained multiple calcium deposits, the grade represented the summation of all angles of acoustic shadows present. The degree of calcification is expressed as the percentage of images containing ≥1 grade of calcium. From serial imaging, changes in PAV and TAV were calculated as the difference from baseline to follow up and the percentage of images containing ≥1 grade of calcium at each time point were directly compared. The percentage of patients demonstrating any degree of progression or regression of either PAV or TAV were also determined.

***Statistical analysis***

Patients were identified with no standard modifiable risk factors (n = 165) and then those with at least one such risk factor were matched in a 3:1 fashion based on age, sex and use of statins during the trials (n = 492). These two groups were then compared on baseline clinical characteristics, use of secondary prevention medications, blood pressure, serum lipids, CRP, IVUS measurements, proportion of patients with >1 grade of calcium, and proportion of patients showing progression or regression. Continuous variables were compared between groups using Student's t-test or Wilcoxon rank-sum test, depending on if normally or non-normally distributed, respectively. Mean ± standard deviation or median (interquartile range) are reported. Changes from baseline were assessed to see if significantly different than zero using the paired t-test or Wilcoxon signed-rank test, as appropriate. Categorical variables were compared between the two risk factor groups using Pearson's chi squared or Fisher's exact test. Percentages are reported. Annualized changes in IVUS measurements were compared between

the two groups using mixed models adjusting for baseline counterparts and with trial set as a random factor to control for heterogeneity across the ten studies. Least-squares means ± standard error is reported. Given that each trial's duration varied from 18 to 24 months, annualized change in PAV is the interpolated value of change in PAV at 1 year. All tests were two tailed with a significance level of 0.05. Analyses were performed using SAS software, version 9.4 (SAS Institute, Cary, NC, USA).

**Candidate's contributions:** I contributed to the design of the study. I collaborated with the lead investigator in these clinical trials. I collected the IVUS imaging data from the ten randomised clinical trials. I interpreted the data and performed the statistical analysis. I performed the literature search and drafted the publication.

## *Cardiovascular magnetic resonance characteristics and clinical outcomes of patients with ST-elevation myocardial infarction and no Standard Modifiable Risk Factors - A DANAMI-3 substudy.*

The reasons for the higher mortality rates in patients without standard modifiable cardiovascular risk factors (SMuRFs) following myocardial infarction are not well described. The higher mortality in this group of patients may be due to differences in myocardial infarct size, microvascular obstruction and adverse left ventricle remodelling as these characteristics are known to be associated with poor outcomes[25-28]. Cardiac magnetic resonance imaging allows assessment of these characteristics and has been employed in clinical trials to assess outcomes[29-32]. Therefore, in chapter 7, we aimed to explore cardiovascular magnetic resonance (CMR) imaging and clinical outcomes in patients with and without standard modifiable cardiovascular risk factors (SMuRFs) who presented with STEMI. The Third DANish Study of Optimal Acute Treatment of Patients With ST-Segment Elevation Myocardial Infarction (DANAMI-3) trial program (NCT 01960933, NCT01435408) consisted of three randomized

controlled STEMI trials performed at four large primary percutaneous coronary intervention [33] centres in Denmark between March 2011 and February 2014[34-37]. The studies examined the effect of ischemic postconditioning (iPOST), deferred stenting (DEFER) and fractional flow reserve (FFR)-guided complete revascularization (PRIMULTI) in patients following STEMI. Patients were primarily randomized to either iPOST or DEFER. A secondary randomization was subsequently performed, randomizing patients with multivessel disease (MVD) in the PRIMULTI trial. For the current study, patients from all the DANAMI-3 trials with first-presentation STEMI were classified into patients with no SMuRFs versus those with at least one SMuRF, to assess for any significant differences in clinical outcomes. SMuRFless patients were defined as patients with no standard modifiable cardiovascular risk factors- diabetes mellitus, hypertension, hyperlipidemia and current smoker. A patient was classified as having diabetes, hypertension or hyperlipidemia if the patient reported a history of such, was on treatment of these conditions at time of presentation or LDL at the time of admission was ≥3.5 mmol/L. A patient was defined as a current smoker if they reported to be smoking regularly prior to admission. The clinical outcomes of the two groups were compared as per the primary and secondary end points defined in the DANAMI-3 trial[34-37]. Baseline clinical characteristics, procedural data, medications at discharge as well as clinical outcomes were obtained.

A subgroup of DANAMI-3 patients recruited at one centre (Righospitalet, Copenhagen University Hospital) had CMR performed according to a standard protocol to evaluate the effects of randomizations on a surrogate marker. This CMR-subgroup provided an optimal opportunity to examine for any potential differences in CMR variables such as AAR, infarct size, MVO and LV remodelling between individuals with no SMuRFs versus those with at least one SMuRF. Patients were included in the sub study if they had baseline and/or follow-up CMR performed (Figure 1).

***Acquisition and analysis of CMR Images***

CMR imaging was performed during index admission at the clinical trial sites following primary PCI using a 1.5 Tesla scanner (Avanto; Siemens, Erlangen, Germany). CMR was also repeated three months after the index admission. Images were analysed by an independent observer, blinded to all clinical data, using dedicated software (CVI42, Circle Cardiovascular Imaging Inc, Calgary, Alberta, Canada), and validated by a second experienced independent observer. These observers were study investigators of the original clinical trials. Left ventricular function and mass were calculated on short-axis steady-state free precession (SSFP) cine images on index and follow-up CMRs. Infarct size was assessed on late gadolinium enhancement (LGE) images, which was obtained 10 minutes after intravenous injection of 0.1 mmol/kg body weight of gadolinium-based contrast (Gadovist; Bayer Schering, Berlin, Germany) on 8mm sliced short-axis images with full-LV coverage and no gap[30]. Myocardial infarction was defined as hyper-enhanced myocardium with a signal intensity of >5 standard deviations of the mean intensity of normal reference myocardium[38]. Infarct size was calculated as a percentage of left ventricular mass and reported on both index and follow-up CMRs. AAR was identified as edema on the index scan using a T2-weighted short tau inversion-recovery sequence (STIR)[29,31]. Edema was defined as an area with signal intensity of >2 standard deviations above the signal intensity in remote normal myocardium[38]. Microvascular obstruction (MVO) was assessed on the LGE images in the index scans as hypointense areas within the acute infarct region. Myocardial salvage index (MSI) was calculated as the difference between area at risk and infarct size, divided by area at risk[39].

***Statistical analysis***

The DANAMI-3 patients with first-presentation STEMI were identified and classified into patients with no SMuRF (SMuRFless) and those with at least one SMuRF. Continuous variables were compared using Student's t-test (if normal distribution) or Mann–Whitney U test (if not normal distribution). Mean ± SD or median (interquartile range, IQR) or percentages are reported. Changes in baseline to follow-up CMR measures were assessed using the paired t-test. Categorical variables were compared using Pearson's chi-squared or Fisher's exact test as appropriate. Multivariable linear regression analyses were performed using SMuRFless patients as a predictor for final infarct size or final MSI adjusting for pre-specified clinically relevant variables: male sex, age, ECG–to-wire time, former smoking, thrombolysis in myocardial infarction (TIMI) flow 0–1 pre-PCI and culprit left anterior descending artery (LAD). A Cox proportional hazards regression model was used to assess the individual risk of a clinical outcome in SMuRFless patients. Finally, an additional logistic regression model was performed to determine the independent predictors of TIMI 0-1 flow, adjusting for pre-specified clinically relevant variables, namely, male sex, age, symptom to wire time, multivessel disease, culprit LAD, heart rate, systolic blood pressure and SMuRFless status. A result was considered significant when it was below a two-sided p-value of 0.05. The statistical analyses were performed with SPSS version 25.

**Candidate's contribution:** I contributed to the design of the study. I collaborated with the lead investigators in these clinical trials. I collected the cardiac MRI imaging data from the three randomised clinical trials. I interpreted the data and performed the statistical analysis. I performed the literature search and drafted the publication.

## *References:*


1. Bhindi R, Khachigian LM, Lowe HC. DNAzymes targeting the transcription factor Egr-1 reduce myocardial infarct size following ischemia-reperfusion in rats. *J Thromb Haemost*. 2006;4:1479-1483. doi: 10.1111/j.1538-7836.2006.02022.x
2. Samsamshariat SA, Samsamshariat ZA, Movahed MR. A novel method for safe and accurate left anterior descending coronary artery ligation for research in rats. *Cardiovasc Revasc Med*. 2005;6:121-123. doi: 10.1016/j.carrev.2005.07.001
3. Bhindi R, Witting PK, McMahon AC, Khachigian LM, Lowe HC. Rat models of myocardial infarction. Pathogenetic insights and clinical relevance. *Thromb Haemost*. 2006;96:602-610.
4. Grieve SM, Lønborg J, Mazhar J, Tan TC, Ho E, Liu CC, Lay W, Gill AJ, Kuchel P, Bhindi R, et al. Cardiac magnetic resonance imaging of rapid VCAM-1 up-regulation in myocardial ischemia-reperfusion injury. *Eur Biophys J*. 2013;42:61-70. doi: 10.1007/s00249-012-0857-x
5. Hong SJ, Mintz GS, Ahn CM, Kim JS, Kim BK, Ko YG, Kang TS, Kang WC, Kim YH, Hur SH, et al. Effect of Intravascular Ultrasound-Guided Drug-Eluting Stent Implantation: 5-Year Follow-Up of the IVUS-XPL Randomized Trial. *JACC Cardiovasc Interv*. 2020;13:62-71. doi: 10.1016/j.jcin.2019.09.033
6. Prati F, Cera M, Ramazzotti V, Imola F, Giudice R, Albertucci M. Safety and feasibility of a new non-occlusive technique for facilitated intracoronary optical coherence tomography (OCT) acquisition in various clinical and anatomical scenarios. *EuroIntervention : journal of EuroPCR in collaboration with the Working Group on Interventional Cardiology of the European Society of Cardiology*. 2007;3:365-370.

7. Garrone P, Biondi-Zoccai G, Salvetti I, Sina N, Sheiban I, Stella PR, Agostoni P. Quantitative coronary angiography in the current era: principles and applications. *Journal of interventional cardiology*. 2009;22:527-536. doi: http://dx.doi.org/10.1111/j.1540-8183.2009.00491.x

8. Vernon ST, Coffey S, D'Souza M, Chow CK, Kilian J, Hyun K, Shaw JA, Adams M, Roberts-Thomson P, Brieger D, et al. ST-Segment-Elevation Myocardial Infarction (STEMI) Patients Without Standard Modifiable Cardiovascular Risk Factors-How Common Are They, and What Are Their Outcomes? *Journal of the American Heart Association*. 2019;8:e013296. doi: 10.1161/jaha.119.013296

9. Roe MT, Halabi AR, Mehta RH, Chen AY, Newby LK, Harrington RA, Smith SC, Jr., Ohman EM, Gibler WB, Peterson ED. Documented traditional cardiovascular risk factors and mortality in non-ST-segment elevation myocardial infarction. *Am Heart J*. 2007;153:507-514. doi: 10.1016/j.ahj.2006.12.018

10. Canto JG, Kiefe CI, Rogers WJ, Peterson ED, Frederick PD, French WJ, Gibson CM, Pollack CV, Jr., Ornato JP, Zalenski RJ, et al. Number of coronary heart disease risk factors and mortality in patients with first myocardial infarction. *Jama*. 2011;306:2120-2127. doi: 10.1001/jama.2011.1654

11. Nauta ST, Deckers JW, van der Boon RM, Akkerhuis KM, van Domburg RT. Risk factors for coronary heart disease and survival after myocardial infarction. *European journal of preventive cardiology*. 2014;21:576-583. doi: 10.1177/2047487312460514

12. Andrews J, Puri R, Kataoka Y, Nicholls SJ, Psaltis PJ. Therapeutic modulation of the natural history of coronary atherosclerosis: lessons learned from serial imaging studies. *Cardiovascular diagnosis and therapy*. 2016;6:282-303. doi: 10.21037/cdt.2015.10.02

13. Nissen SE, Tuzcu EM, Brewer HB, Sipahi I, Nicholls SJ, Ganz P, Schoenhagen P, Waters DD, Pepine CJ, Crowe TD, et al. Effect of ACAT inhibition on the progression of coronary atherosclerosis. *The New England journal of medicine*. 2006;354:1253-1263. doi: 10.1056/NEJMoa054699

14. Nissen SE, Nicholls SJ, Sipahi I, Libby P, Raichlen JS, Ballantyne CM, Davignon J, Erbel R, Fruchart JC, Tardif JC, et al. Effect of very high-intensity statin therapy on regression of coronary atherosclerosis: the ASTEROID trial. *Jama*. 2006;295:1556-1565. doi: 10.1001/jama.295.13.jpc60002

15. Nissen SE, Tardif JC, Nicholls SJ, Revkin JH, Shear CL, Duggan WT, Ruzyllo W, Bachinsky WB, Lasala GP, Tuzcu EM. Effect of torcetrapib on the progression of coronary atherosclerosis. *The New England journal of medicine*. 2007;356:1304-1316. doi: 10.1056/NEJMoa070635

16. Nissen SE, Nicholls SJ, Wolski K, Nesto R, Kupfer S, Perez A, Jure H, De Larochellière R, Staniloae CS, Mavromatis K, et al. Comparison of pioglitazone vs glimepiride on progression of coronary atherosclerosis in patients with type 2 diabetes: the PERISCOPE randomized controlled trial. *Jama*. 2008;299:1561-1573. doi: 10.1001/jama.299.13.1561

17. Nissen SE, Nicholls SJ, Wolski K, Rodés-Cabau J, Cannon CP, Deanfield JE, Després JP, Kastelein JJ, Steinhubl SR, Kapadia S, et al. Effect of rimonabant on progression of atherosclerosis in patients with abdominal obesity and coronary artery disease: the STRADIVARIUS randomized controlled trial. *Jama*. 2008;299:1547-1560. doi: 10.1001/jama.299.13.1547

18. Nicholls SJ, Ballantyne CM, Barter PJ, Chapman MJ, Erbel RM, Libby P, Raichlen JS, Uno K, Borgman M, Wolski K, et al. Effect of two intensive statin regimens on

progression of coronary disease. *The New England journal of medicine*. 2011;365:2078-2087. doi: 10.1056/NEJMoa1110874

19. Nicholls SJ, Puri R, Anderson T, Ballantyne CM, Cho L, Kastelein JJ, Koenig W, Somaratne R, Kassahun H, Yang J, et al. Effect of Evolocumab on Progression of Coronary Disease in Statin-Treated Patients: The GLAGOV Randomized Clinical Trial. *JAMA*. 2016;316:2373-2384. doi: 10.1001/jama.2016.16951
20. Nicholls SJ, Bakris GL, Kastelein JJ, Menon V, Williams B, Armbrecht J, Brunel P, Nicolaides M, Hsu A, Hu B, et al. Effect of aliskiren on progression of coronary disease in patients with prehypertension: the AQUARIUS randomized clinical trial. *JAMA*. 2013;310:1135-1144. doi: 10.1001/jama.2013.277169
21. Nissen SE, Tuzcu EM, Schoenhagen P, Brown BG, Ganz P, Vogel RA, Crowe T, Howard G, Cooper CJ, Brodie B, et al. Effect of intensive compared with moderate lipid-lowering therapy on progression of coronary atherosclerosis: a randomized controlled trial. *JAMA*. 2004;291:1071-1080. doi: 10.1001/jama.291.9.1071
22. Brener SJ, Ivanc TB, Poliszczuk R, Chen M, Tuzcu EM, Hu T, Frid DJ, Nissen SE. Antihypertensive therapy and regression of coronary artery disease: insights from the Comparison of Amlodipine versus Enalapril to Limit Occurrences of Thrombosis (CAMELOT) and Norvasc for Regression of Manifest Atherosclerotic Lesions by Intravascular Sonographic Evaluation (NORMALISE) trials. *Am Heart J*. 2006;152:1059-1063. doi: 10.1016/j.ahj.2006.07.022
23. Katritsis DG, Pantos I, Korovesis S, Hadjipavlou M, Tzanalaridou E, Lockie T, Redwood S, Voridis E, Efstathopoulos EP. Three-dimensional analysis of vulnerable segments in the left anterior descending artery. *Coron Artery Dis*. 2009;20:199-206. doi: 10.1097/MCA.0b013e32832397fe

24. Nicholls SJ, Tuzcu EM, Wolski K, Sipahi I, Schoenhagen P, Crowe T, Kapadia SR, Hazen SL, Nissen SE. Coronary artery calcification and changes in atheroma burden in response to established medical therapies. *J Am Coll Cardiol*. 2007;49:263-270. doi: 10.1016/j.jacc.2006.10.038

25. Stone GW, Selker HP, Thiele H, Patel MR, Udelson JE, Ohman EM, Maehara A, Eitel I, Granger CB, Jenkins PL, et al. Relationship Between Infarct Size and Outcomes Following Primary PCI: Patient-Level Analysis From 10 Randomized Trials. *J Am Coll Cardiol*. 2016;67:1674-1683. doi: 10.1016/j.jacc.2016.01.069

26. Durante A, Laricchia A, Benedetti G, Esposito A, Margonato A, Rimoldi O, De Cobelli F, Colombo A, Camici PG. Identification of High-Risk Patients After ST-Segment-Elevation Myocardial Infarction: Comparison Between Angiographic and Magnetic Resonance Parameters. *Circulation Cardiovascular imaging*. 2017;10:e005841. doi: 10.1161/circimaging.116.005841

27. de Waha S, Patel MR, Granger CB, Ohman EM, Maehara A, Eitel I, Ben-Yehuda O, Jenkins P, Thiele H, Stone GW. Relationship between microvascular obstruction and adverse events following primary percutaneous coronary intervention for ST-segment elevation myocardial infarction: an individual patient data pooled analysis from seven randomized trials. *Eur Heart J*. 2017;38:3502-3510. doi: 10.1093/eurheartj/ehx414

28. Bulluck H, Carberry J, Carrick D, McEntegart M, Petrie MC, Eteiba H, Hood S, Watkins S, Lindsay M, Mahrous A, et al. Redefining Adverse and Reverse Left Ventricular Remodeling by Cardiovascular Magnetic Resonance Following ST-Segment-Elevation Myocardial Infarction and Their Implications on Long-Term Prognosis. *Circulation Cardiovascular imaging*. 2020;13:e009937. doi: 10.1161/circimaging.119.009937

29. Lønborg J, Vejlstrup N, Mathiasen AB, Thomsen C, Jensen JS, Engstrøm T. Myocardial area at risk and salvage measured by T2-weighted cardiovascular magnetic resonance: reproducibility and comparison of two T2-weighted protocols. *Journal of cardiovascular magnetic resonance : official journal of the Society for Cardiovascular Magnetic Resonance*. 2011;13:50. doi: 10.1186/1532-429x-13-50

30. Kim RJ, Fieno DS, Parrish TB, Harris K, Chen EL, Simonetti O, Bundy J, Finn JP, Klocke FJ, Judd RM. Relationship of MRI delayed contrast enhancement to irreversible injury, infarct age, and contractile function. *Circulation*. 1999;100:1992-2002. doi: 10.1161/01.cir.100.19.1992

31. Abdel-Aty H, Zagrosek A, Schulz-Menger J, Taylor AJ, Messroghli D, Kumar A, Gross M, Dietz R, Friedrich MG. Delayed enhancement and T2-weighted cardiovascular magnetic resonance imaging differentiate acute from chronic myocardial infarction. *Circulation*. 2004;109:2411-2416. doi: 10.1161/01.cir.0000127428.10985.c6

32. Touboul C, Angoulvant D, Mewton N, Ivanes F, Muntean D, Prunier F, Ovize M, Bejan-Angoulvant T. Ischaemic postconditioning reduces infarct size: systematic review and meta-analysis of randomized controlled trials. *Archives of cardiovascular diseases*. 2015;108:39-49. doi: 10.1016/j.acvd.2014.08.004

33. Ali ZA, Maehara A, Généreux P, Shlofmitz RA, Fabbiocchi F, Nazif TM, Guagliumi G, Meraj PM, Alfonso F, Samady H, et al. Optical coherence tomography compared with intravascular ultrasound and with angiography to guide coronary stent implantation (ILUMIEN III: OPTIMIZE PCI): a randomised controlled trial. *Lancet (London, England)*. 2016;388:2618-2628. doi: 10.1016/S0140-6736(16)31922-5

34. Høfsten DE, Kelbæk H, Helqvist S, Kløvgaard L, Holmvang L, Clemmensen P, Torp-Pedersen C, Tilsted HH, Bøtker HE, Jensen LO, et al. The Third DANish Study of

Optimal Acute Treatment of Patients with ST-segment Elevation Myocardial Infarction: Ischemic postconditioning or deferred stent implantation versus conventional primary angioplasty and complete revascularization versus treatment of culprit lesion only: Rationale and design of the DANAMI 3 trial program. *Am Heart J*. 2015;169:613-621. doi: 10.1016/j.ahj.2015.02.004

35. Engstrøm T, Kelbæk H, Helqvist S, Høfsten DE, Kløvgaard L, Holmvang L, Jørgensen E, Pedersen F, Saunamäki K, Clemmensen P, et al. Complete revascularisation versus treatment of the culprit lesion only in patients with ST-segment elevation myocardial infarction and multivessel disease (DANAMI-3—PRIMULTI): an open-label, randomised controlled trial. *Lancet (London, England)*. 2015;386:665-671. doi: 10.1016/s0140-6736(15)60648-1

36. Kelbæk H, Høfsten DE, Køber L, Helqvist S, Kløvgaard L, Holmvang L, Jørgensen E, Pedersen F, Saunamäki K, De Backer O, et al. Deferred versus conventional stent implantation in patients with ST-segment elevation myocardial infarction (DANAMI 3-DEFER): an open-label, randomised controlled trial. *Lancet (London, England)*. 2016;387:2199-2206. doi: 10.1016/s0140-6736(16)30072-1

37. Engstrøm T, Kelbæk H, Helqvist S, Høfsten DE, Kløvgaard L, Clemmensen P, Holmvang L, Jørgensen E, Pedersen F, Saunamaki K, et al. Effect of Ischemic Postconditioning During Primary Percutaneous Coronary Intervention for Patients With ST-Segment Elevation Myocardial Infarction: A Randomized Clinical Trial. *JAMA Cardiology*. 2017;2:490-497. doi: 10.1001/jamacardio.2017.0022

38. Nepper-Christensen L, Lønborg J, Ahtarovski KA, Høfsten DE, Kyhl K, Ghotbi AA, Schoos MM, Göransson C, Bertelsen L, Køber L, et al. Left Ventricular Hypertrophy Is Associated With Increased Infarct Size and Decreased Myocardial Salvage in Patients With ST-Segment Elevation Myocardial Infarction Undergoing Primary

Percutaneous Coronary Intervention. *Journal of the American Heart Association*. 2017;6. doi: 10.1161/jaha.116.004823

39. Friedrich MG, Abdel-Aty H, Taylor A, Schulz-Menger J, Messroghli D, Dietz R. The salvaged area at risk in reperfused acute myocardial infarction as visualized by cardiovascular magnetic resonance. *Journal of the American College of Cardiology*. 2008;51:1581-1587. doi: 10.1016/j.jacc.2008.01.019

# **Chapter 3.** Automated Quantification of Myocardial Salvage in a Rat Model of Ischemia–Reperfusion Injury using 3D High-Resolution Magnetic Resonance Imaging (MRI)


## Summary:

The pathophysiology of coronary no-reflow post primary PCI is multifactorial and includes myocardial reperfusion injury that may occur after restoration of blood flow with accumulation of neutrophils and platelets that release inflammatory mediators and vasoconstrictors. In chapter 6 we explored the clinical predictors of coronary no-reflow. A larger infarct size is a clinical consequence of no-reflow which can be measured by cardiac MRI as demonstrated in chapter 7. Novel therapies targeting ischemia reperfusion injury are usually tested in small animal models. An accurate assessment of infarct size and area at risk (AAR) is critical when assessing new therapies for myocardial ischemia reperfusion (IR) injury. In chapter 8, we aimed to develop and validate a high-resolution 3-dimensional (3D) magnetic resonance imaging (MRI) method for quantifying infarct size and AAR in a rodent model. Current "gold-standard" methods perfuse the heart with Evan's Blue and stain with triphenyl tetrazolium chloride (TTC), requiring manual slicing and analysis. The manual slicing is labor intensive and the slices are thick. The analysis requires assumptions to be made about the surface borders reflecting that of the mid slice tissue. In this chapter, we describe a novel MRI technique that allows precise assessment of infarct and AAR zones. It removes the need for tissue slicing and provides opportunity for 3D digital analysis at high anatomical resolution.

American Heart Association | American Stroke Association

## Automated Quantification of Myocardial Salvage in a Rat Model

# of Ischemia–Reperfusion Injury Using 3D High-Resolution Magnetic Resonance Imaging (MRI)

Stuart M. Grieve, MBBS, DPhil;* Jawad Mazhar, MBBS;* Fraser Callaghan, PhD; Cindy Y. Kok, PhD; Sarah Tandy, PhD; Ravinay Bhindi, MBBS, PhD; Gemma A. Figtree, MBBS, DPhil, FRACP, FAHA

*Background*—Quantification of myocardial "area at risk" (AAR) and myocardial infarction (MI) zone is critical for assessing novel therapies targeting myocardial ischemia–reperfusion (IR) injury. Current "gold-standard" methods perfuse the heart with Evan's Blue and stain with triphenyl tetrazolium chloride (TTC), requiring manual slicing and analysis. We aimed to develop and validate a high-resolution 3-dimensional (3D) magnetic resonance imaging (MRI) method for quantifying MI and AAR.

*Methods and Results*—Forty-eight hours after IR was induced, rats were anesthetized and gadopentetate dimeglumine was administered intravenously. After 10 minutes, the coronary artery was re-ligated and a solution containing iron oxide microparticles and Evan's Blue was infused (for comparison). Hearts were harvested and transversally sectioned for TTC staining. Ex vivo MR images of slices were acquired on a 9.4-T magnet. T2* data allowed visualization of AAR, with microparticle-associated signal loss in perfused regions. T1 data demonstrated gadolinium retention in infarcted zones. Close correlation ($r$=0.92 to 0.94; $P$<0.05) of MRI and Evan's Blue/TTC measures for both AAR and MI was observed when the combined techniques were applied to the same heart slice. However, 3D MRI acquisition and analysis of whole heart reduced intra-observer variability compared to assessment of isolated slices, and allowed automated segmentation and analysis, thus reducing interobserver variation.

Anatomical resolution of 81 $1m^3$ was achieved (versus ⧠2 mm with manual slicing).

*Conclusions*—This novel, yet simple, MRI technique allows precise assessment of infarct and AAR zones. It removes the need for tissue slicing and provides opportunity for 3D digital analysis at high anatomical resolution in a streamlined manner accessible for all laboratories already performing IR experiments. (*J Am Heart Assoc*. 2014;3:e000956 doi: 10.1161/JAHA.114.000956)

Key Words: magnetic resonance imaging • molecular imaging • myocardial ischemia–reperfusion • ventricular remodeling

Ischemic heart disease remains the number 1 cause of death in Western society. Improvements in the techniques and speed with which patients receive reperfusion therapy have significantly decreased mortality and morbidity of patients suffering myocardial infarction (MI).[1] However, regeneration of flow at the time of reperfusion also leads to a specific myocardial injury in addition to the injury caused by ischemia that is known as myocardial ischemia–reperfusion (IR) injury.[2] This myocardial IR injury manifests itself clinically in the form of arrhythmias, reversible contractile dysfunction (myocardial stunning), endothelial dysfunction, and cell death.[3,4] Contributing factors include postischemic low ATP and high phosphate levels, intracellular and mitochondrial calcium overload, oxidative stress and rapid increases in pH, endothelial dysfunction, and apoptosis.[3,5] The inflammatory response is also thought to play an important role, and several experimental studies have demonstrated a reduction in MI size with anti-inflammatory treatment.[6–10]

Rodent models of cardiovascular disease provide a valuable means to understand the molecular and physiological mechanisms that influence outcome. The ability to accurately quantitate outcome measures such as the extent

*From the North Shore Heart Research Group Kolling Institute (S.M.G., J.M., C.Y.K., R.B., G.A.F., S.T. ) and Sydney Translational Imaging Laboratory, Sydney Medical School (S.M.G.), University of Sydney Australia; Department of Radiology Royal Prince Alfred Hospital Sydney Australia (S.M.G., F.C.); Department of Cardiology, Royal North Shore Hospital, Sydney, Australia (J.M., R.B., G.A.F.).*

*Grieve and Mazhar are equal first authors.

An accompanying Movies S1 and S2 are available at http://jaha.ahajournals.org/content/3/4/e000956/suppl/DC1

Correspondence to: Gemma A. Figtree, MBBS, DPhil, FRACP, FAHA, North Shore Heart Research Group, Kolling Institute (University of Sydney), Royal North Shore Hospital, St Leonards, New South Wales 2065, Australia. E-mail: gemma.figtree@sydney.edu.au

Received March 18, 2014; accepted June 5, 2014.

of infarction permits assessment of response to novel therapeutic strategies. In this article, we address the problem of measuring the volume of infarction in animal models of IR injury. Current "gold standard" methods use a combination of selective perfusion of the heart with Evan's Blue and staining of the postmortem sectioned heart with triphenyl tetrazolium chloride (TTC) to quantitate the area at risk (AAR) and degree of completed infarct.[11,12] Importantly, this approach accounts for variability in coronary artery anatomical supply, and can allow investigators to quantify the amount of salvaged myocardium. This method, although widely used and considered the "gold standard," also has documented problems relating to the accurate and reproducible delineation of the border of the infarct and AAR zones.[13] The requirement of manual slicing of tissue is labor intensive, and slices are relatively thick. This requires assumptions to be made about the surface borders reflecting that of the midslice tissue. Questions have also been raised regarding the sensitivity of TTC staining in the setting of a gradient of viability, as would be common in the setting of IR injury.[14]

Magnetic resonance imaging (MRI) is well recognized for its high spatial resolution (25 to 100 µm at fields higher than 3 T) and excellent soft-tissue discrimination. Cardiac MRI (CMR) has been developed to provide accurate functional data, although this requires an expert team to optimize cardiac and respiratory gating at high fields when applied to rodents,[15] which may be a rate-limiting step in the majority of laboratories. Central to the clinical use of MRI to assess the ischemic heart is the use of delayed gadolinium-enhanced images to define infarcted tissue.[16] The enhancement seen in the setting of an acute infarct using this method is based on the increased permeability of the cell membrane associated with necrosis, and has been shown to correlate extremely well with histology.[17]

Delineation of AAR is considered a holy grail for cardiac MRI researchers. T2 sequences have been used to delineate areas of higher water content/edema. Although some studies have provided evidence for this approach,[18,19] there is considerable controversy regarding this with concerns over reliability and robustness of the measure across different laboratories.[20,21] Microparticles of iron oxide (MPIO) provide excellent negative contrast even at low concentrations, are inert, and remain intravascular.[22] In this study, we compare the standard Evan's Blue/TTC method of AAR/infarct delineation against a novel method that uses a combination of T2* contrast from MPIO to define the borders of the perfused/unperfused myocardium, together with gadolinium-based T1- weighted enhancement to define the established infarct zone. We propose that this method has potential to provide rapid and accurate quantitation of these parameters in animal models of IR injury.

# Methods

## Animals and Experimental Model of Myocardial IR Injury

Sprague–Dawley rats (weight 250 to 300 g) were acclimatized for a period of 1 week before surgery. Procedures were conducted with the approval of the Royal North Shore Hospital Animal Care and Ethics Committee. Myocardial IR was induced as previously described using an open-chest approach.[23]

Ischemia was induced for 30 minutes by transient suture ligation of the left anterior coronary artery 2 to 3 mm distal to the junction of pulmonary artery and left atrial appendage.

The ligature was then released and the rats recovered for 48 hours. Under repeat anesthesia, gadopentetate dimeglumine 0.15 mmol/kg was infused via the tail vein. After 10 minutes, the left anterior coronary artery was re-occluded and a solution containing MPIO (4.5 mg/kg body weight, as determined in pilot studies) mixed with 3% Evan's Blue, in a total volume of 5 mL, was infused. After a 2-minute interval, the heart was then excised, sectioned into 2-mm short-axis slices, and placed in TTC 1% in phosphate-buffered saline for 20 minutes at 37°C.[24] Slices were photographed and then fixed in 10% normal buffered formalin. To reduce sample movement during MRI imaging, whole hearts and sections were set in agar gel. They were then stored at 4°C and imaged within 1 week of each experiment. A schematic illustration of both techniques is shown in Figure 1.

## Iron-Oxide Microparticles

MyOneTosyl-activated iron microparticles (MPIO: diameter 1.08 1m, iron content 26%) were purchased from Life Technologies. The MPIO particles were diluted in phosphate- buffered saline prior to use.

## Magnetic Resonance Imaging: Protocol and Analysis

MRI data were acquired on a vertical 9.4-T magnet (Biospec, Bruker, Ettlingen, Germany). Three-dimensional gradient echo, inversion recovery (2-dimensional multislice spin-echo), and T2 sequences were acquired with parameters optimized in order to achieve anatomical detail as well as T1 and T2/T2* contrast. Details of imaging parameters are found in Table 1, and illustration of our process of sequence optimization is shown in Figure 2). Resolution was 81 $1m^3$ for 3-dimensional (3D) gradient echo, 163x325x400 µm for inversion recovery, and 120 $µm^3$ for T2 sequences. T1 maps of sectioned MRI images were created from the inversion-recovery images (TI range 100 ms—1500 ms), respectively, and along with T2* images were registered to a common coordinate system for region-of-interest analysis.

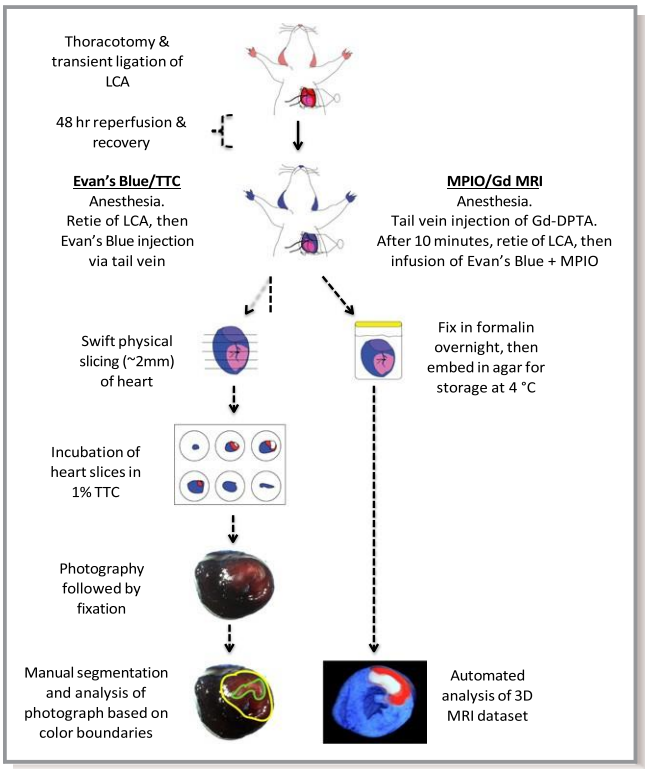


Figure 1. Schematic illustration comparing the steps involved in the traditional Evan's Blue/TTC technique, versus the auto- mated MPIO/Gd 3D MRI technique. Gd-DPTA indicates gadopentetate dimeglumine; LCA, left anterior coronary artery; MPIO/ Gd, microparticles of iron oxide/gadolinium; MRI, magnetic resonance imaging; TTC, triphenyl tetrazolium chloride.

The 3 image stacks (T1 map, T2*, and T2) were used for each heart section. For comparison with Evan's Blue/TTC stained slices, analysis of the MRI data was restricted to 8 evenly spaced slices. Figure 2D and 2F shows representative segmentation on a 3D gradient echo (T2) image and T1- weighted image. The MRI images were preprocessed to define left and right ventricular epicardium and left ventricular endocardium by 1 observer. Regions of interest for the AAR and MI were then manually contoured by 4 blinded observers, and by 1 observer twice, with 1 week between analyses. AAR was identified by an absence of signal voids from MPIO in the T2* image stack, and MI was identified by high intensity on an inverted T1 map (ie, longitudinal relativity, R1). In the case of any discrepancy, any region that was defined as MI was included as AAR. Regions of confluent signal within the MI, most likely representing microhemorrhage,[25] were included as infarct zone. The T2 image was used to assist with anatomical definition of the AAR and MI zones.

The same analysis technique was used for the MR whole heart images following reformatting of the data to present the data in left ventricle short-axis (SA) orientation. For the whole-heart MRI analysis technique, 20 SA slices (650-1m slice spacing) were generated covering the whole heart. In addition, an automatic segmentation of the AAR and MI regions in the whole-heart MRI volumes was carried out. A 3D minimum filter was applied to accentuate the signal voids due to MPIO, followed by a 2D 9x9 pixel standard deviation filter, which resulted in low signal in the region of AAR, and high signal outside of the AAR where signal voids were present. Within the region detected as AAR, thresholding of the T1 map images was used to define MI regions. The T1 threshold was chosen based on a single manual segmentation.

The photographed heart sections were also preprocessed to define left and right epicardium and left endocardium borders before being analyzed by the same observers, identifying AAR and MI on the apical side of each heart section following standard protocols.[24] Custom code written in Matlab (The MathWorks Co, Natick, MA) was used for all analysis.

## Statistical Analysis

Statistical analysis was performed within Matlab and SPSS v20 (IBM, NY). The Bland Altman statistical test was used to assess intra- and interobserver variability, with the results presented graphically including mean differences and 95% limits of agreement. Summary results are presented as mean

± SEM.

Table 1. Technical Details of the Parameters Used for Acquiring MRI Data

| Sequence | Parameters |
|---|---|
| 3DGE | NA=4. TE=4 ms, TR=40 ms, flip angle=30°, FOV=20.89 20.895.1 mm, matrix=2569256964, resolution=81x81x81 µm (zero-filled to 40 1m$^3$ isotropic) imaging time=44 min. |
| Inversion recovery sequence (2D multislice spin-echo) | NA=1, TE=12.5 ms, TR=4000 ms, FOV=20.8x20.8, matrix=128x 64, 8 contiguous slices of 400 µm, in-plane resolution=163x325 µm (zero-filled to 81x81 µm), TI=100–1500 ms (6 steps: 300, 400, 600, 800, 1000, 1500 ms), imaging time=34 min (per TI value). |
| Spin-echo images | TE=42 ms, TR=400, NE=3, resolution=120x120x120 µm (zero-filled to 60x60 µm), imaging time=27 min |

3DGE indicates 3-dimensional gradient echo; NA, Number of averages; TE, echo time; TR, repetition time; FOV, field of view; MRI, magnetic resonance imaging; TI, inversion time.

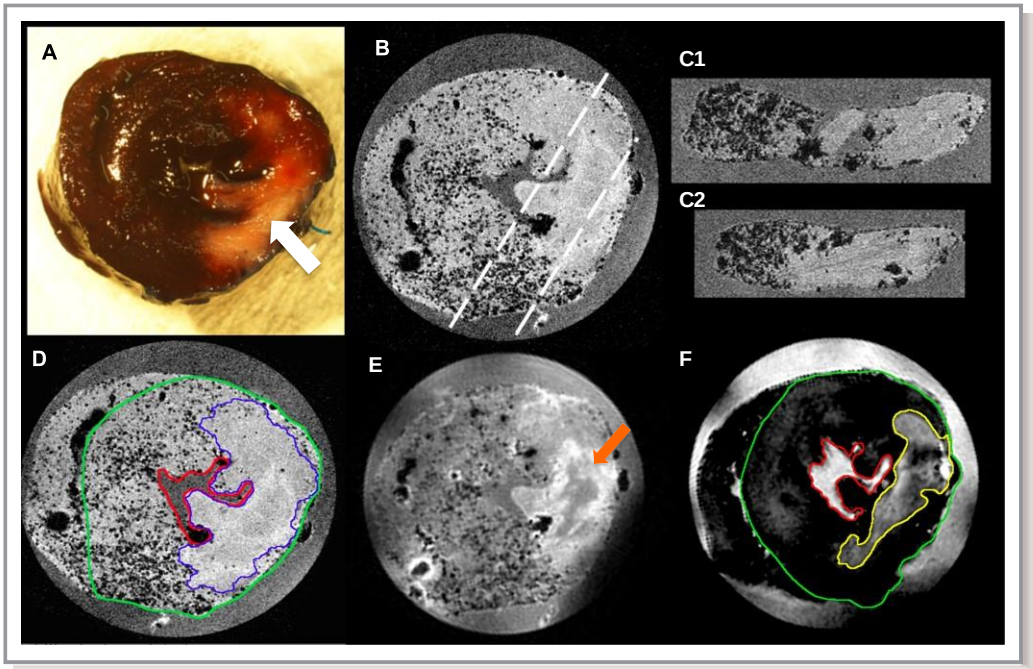


Figure 2. Visual comparison of traditional Evan's Blue/TTC and novel high-field MRI technique for defining myocardial salvage zone. A, Photograph of sliced rat heart prepared using standard Evan's Blue TTC technique. The AAR is determined as the region of the heart that is not stained blue by Evan's Blue dye. Within the AAR the MI zone is seen as the central white zone (white arrow). The pink/red zone within the AAR defines the viable myocardium stained by TTC. Slice thickness is ~2 mm. B, 3DGE (TE 4 ms) image of the same representative slice shown in A, illustrating the perfused myocardium appearance containing numerous signal voids (black dots), and clear delineation of perfused and nonperfused myocardium. Resolution: 81 $1m^3$. The dashed white lines indicate the reformatted slices C1 and C2. D, 3DGE image of same slice with TE=8 ms showing increased T2* contrast within the perfused territory from the MPIOs (border zone of AAR delineated by blue line). Resolution: 81 $\mu m^3$. E, Spin echo MRI image (TE=42 ms, TR=600 ms) of same slice highlighting T2 contrast within the MI zone, while also showing signal voids from MPIO. Some low-intensity signal (orange arrow) can be seen centrally within the MI zone likely secondary to microvascular obstruction. Resolution: 120 $\mu m^3$. F, Inversion recovery image of the same slice shown in E, highlighting the T1 contrast caused by gadolinium within the MI zone (yellow line). Resolution: 163x325x400 µm. The LV epicardial contour is shown in D and F by a green line and the endocardial surface by a red line. AAR indicates area at risk; DGE, delayed gadolinium enhanced; LV, left ventricular; MI, myocardial infarction; MPIO, microparticles of iron oxide; MRI, magnetic resonance imaging; TE, echo time; TTC, triphenyl tetrazolium chloride.

# Results

## MPIO to Delineate AAR

Initial visual inspection of the MRI data, focusing on the T2 and T2* data, found evenly spread foci of signal loss (observed as "black dots") in regions that remained perfused outside the territory of the ligated coronary artery, and no "dots" in the area perfused by the coronary artery (AAR) (Figure 2). The presence of small microbubbles did not compromise visualization of AAR borders, and was minimized through careful sample prepara- tion. The small number of bubbles present could easily be differentiated from microparticles due to size and position (bubbles are larger and more peripheral).

Consistent with our previous observations,[25] regions in the MI region of some hearts demonstrated signal loss in a midwall distribution with a more confluent pattern than that of the discrete signal loss attributed to MPIO (Figure 2). We have previously demonstrated by histological techniques that this corresponds to microhemorrhage at the core of the MI.[25] Similar MRI signal loss has been reported in human CMR images, and has been associated with MI size and prognosis.[26] We examined the correlation of AAR using the traditional Evan's Blue technique, and that determined by MPIO/MRI technique, using the calculated AAR as a percentage of myocardial mass (Figure 3). This direct comparison required MRI and analysis to be performed on sliced myocardium, taking away a major advantage of MRI related to examining an intact 3D dataset, and being able to easily examine adjacent regions "above" or "below." Figure 3A provides a scatterplot comparing the AAR calculated using the 2 methods. While the size of the AAR varied between animals, the correlation between the

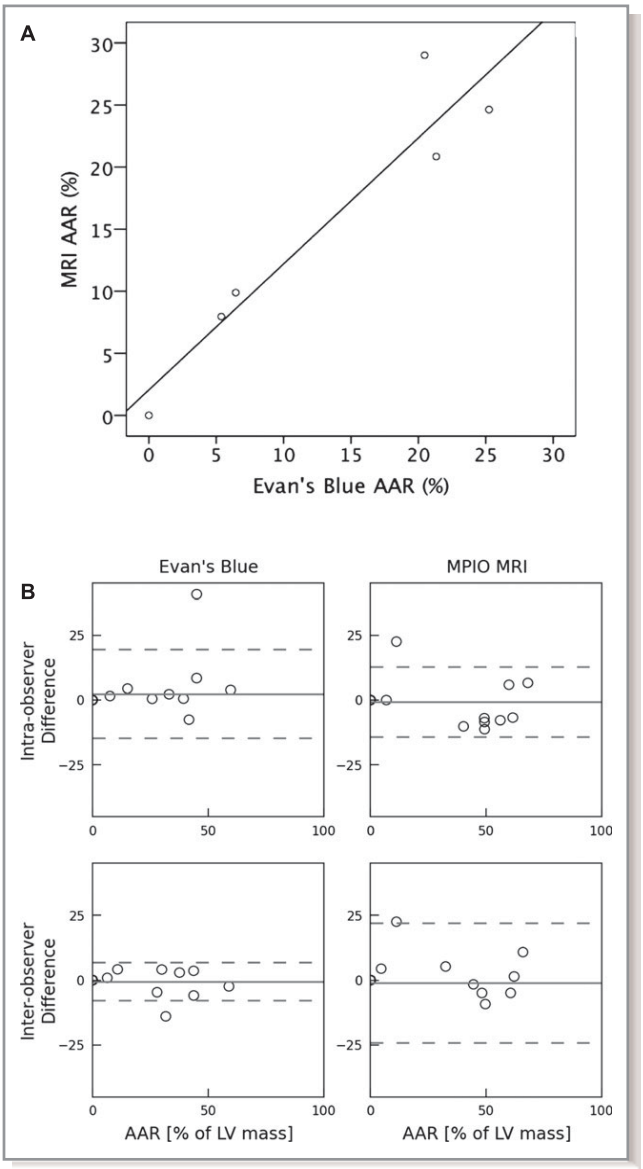


Figure 3. Comparison between AAR measurements obtained using MPIO MRI vs traditional Evan's Blue methods. A, Scatterplot of the calculated AAR (expressed as % of LV mass) for MPIO MRI method vs Evan's Blue method performed on same isolated tissue slices ($r$=0.94; $P$=0.004). B, Bland-Altman plot examining the intra- observer (top 2 panels) and interobserver (bottom 2 panels) variability for the 2 methods when both were applied to the same tissue slices. The dashed lines represent the 95% level of agreement. AAR indicates area at risk; MPIO, microparticles of iron oxide; MRI, magnetic resonance imaging; LV, left ventricular.

measurements was high ($r$=0.95, $P$=0.004). The intra- and interobserver variability was assessed using a Bland-Altman plot for both techniques (Figure 3B). The particulate nature of the MPIO avoids the diffusional blurring seen using Evan's Blue. This superior edge definition that results from using the MPIO/Gd (microparticles of iron oxide/gadolinium) MRI technique is demonstrated in Figure 4.

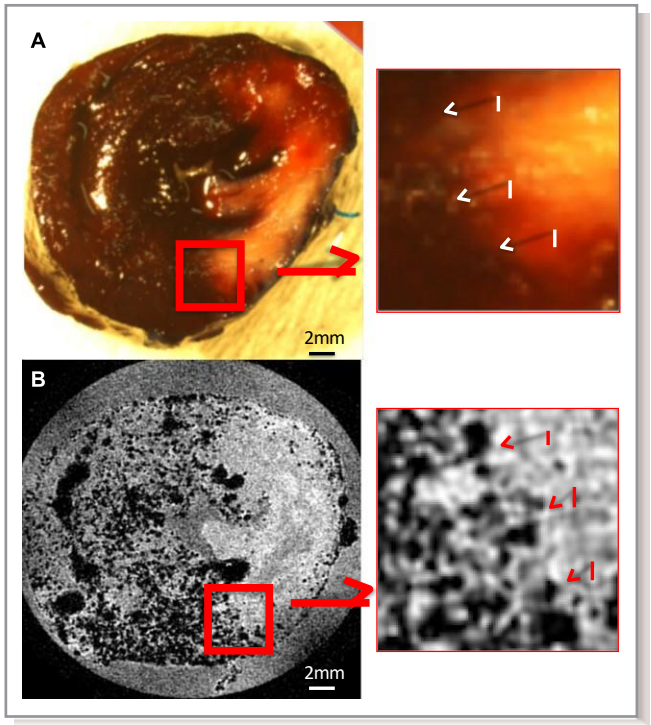


Figure 4. Comparison between the borderzone definition of the AAR using Evan's Blue (A) and MPIO (B). The edge definition (white arrows, A; red arrows, B) using Evan's Blue appears indistinct due to diffusion of the stain and the reduced contrast between Evan's Blue–positive area and the TTC-positive staining. In contrast, the particulate nature of the MPIO, and the T-weighted image acquisition, create a sharp definition of the border between the AAR and the perfused territory. Insets show magnified image. Two millimeter magnified views are provided to the right of A and B. AAR indicates area at risk; MPIO, microparticles of iron oxide; TTC, triphenyl tetrazolium chloride.

## Gadolinium Enhancement to Delineate MI

Initial visual inspection of the MRI images showed that using longitudinal relaxivity (R1) data (ie, an inverted T1 map), in which the MI zone appears as high intensity, was preferable to using either the raw T1-weighted inversion recovery data or an orthodox presentation of the T1 maps (in which the MI zone appears as a region of low intensity). The regions of T1 shortening correlated closely with the distribution of infarction defined by TTC on corresponding images (e.g, Figure 2). Figure 5A shows a comparison between the MI mass measured using the Evan's Blue/TTC method versus using the MPIO/Gd MRI method in the same slices. There was a good correlation between 2 methods for the measurement of MI ($r$=0.93, $P$=0.020). A Bland-Altman plot of the 2 methods is presented in Figure 5B, demonstrating adequate inter- and intra-observer variability when applying the MPIO/Gd MRI method to sliced heart slabs where the majority of points fall between the 95% limits of agreement. For the TTC data, there is a nonsignificant trend toward positive differences at low

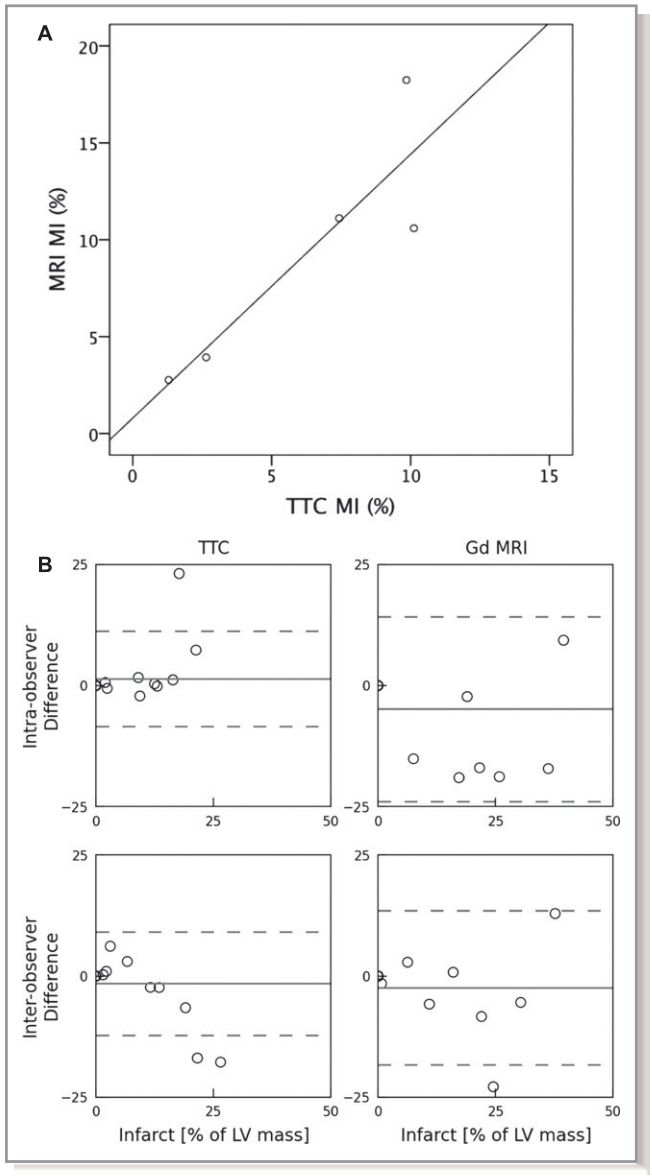


Figure 5. Comparison between MI quantification obtained using Gd MRI vs traditional TTC method. A, Scatterplot of calculated MI volume (expressed as % of LV) for the Gd MRI vs traditional TTC method performed on same isolated tissue slices ($r$=0.93; $P$=0.04). B, Bland-Altman plot examining the intraobserver (top 2 panels) and interobserver (bottom 2 panels) variability for the 2 methods when both were applied to the same tissue slices. The dashed lines represent the 95% level of agreement. LV indicates left ventricular; MI, myocardial infarction; MRI, magnetic resonance imaging; TTC, triphenyl tetrazolium chloride; Gd, gadolinium.

percent infarct and negative differences at high percent infarct.

## Analysis of AAR and MI in Whole Hearts

In order to comprehensively assess the potential benefits of the MPIO/Gd MRI technique, an additional 4 hearts were assessed, but were imaged as intact hearts, thereby preserving the 3D information inherently provided by this technique. Figure 6 demonstrates the continuity of both the AAR and MI zones in both short-axis (SA, top 2 rows), and long-axis views (4 chamber—left, and LVLA—right). At the 4 SA levels chosen as representative slices, the definition and extent of the AAR and MI zones are clearly demarcated. The ability to scroll between slices acts to further clarify any unclear regions, meaning that little ambiguity is present when assigning regions manually. The anatomical relationships of the segmented territories are also clearly identified, making it easier for the investigator to exclude artifactual changes in signal.

Figure 7A shows a plot of the AAR and MI masses for each of the whole heart samples. Figure 7B shows a Bland-Altman plot of the intra-observer and interobserver variation for manual quantitation of both AAR and MI mass. Compared with the conventional AAR/MI measures (Evan's Blue/TTC staining of the sliced hearts assessed in Figures 3B and 5B), MRI- derived AAR and MI from whole hearts show tighter intra- observer limits of agreement for both measures, and similar interobserver agreement.

We next explored automated methods for segmenting and quantitating the AAR and MI zones, since the high-contrast and digital 3D nature of the MRI data is inherently suited to an algorithmic, automated approach. Figure 8 shows a 3D representation of the segmented heart, with the MI color- coded in white, the AAR as red, and the unaffected myocardium coded as blue. The left anterior oblique (LAO) projection shows how the zonal nature of the AAR and MI regions are precisely captured by our automated approach, and the SA and 4-chamber views demonstrate the clear delineation of the borders of each zone. The ability of the investigator to scroll through the digital dataset, in order to appreciate anatomic relationships, is highlighted by Movie S1 and S2.

Figure 9 shows Bland-Altman plots comparing the inter-observer variability between the manual and automatic segmentation of the whole heart for and MI zones. These show good agreement between the segmentation strategies.

## Discussion

In this study, we have applied high-field cardiac MRI to precisely assess MI size and AAR in a rat model of myocardial IR. This removes the need for physical slicing of the fresh, postmortem heart, offering the possibility for reducing the error of measurements and providing the opportunity for high- resolution, automated 3D digital analysis.

Given the clinical importance of MI and its complications, investigators have been looking to animal models to assist them in understanding the pathogenesis, and to assess efficacy of novel therapies. Due to cost and ease of

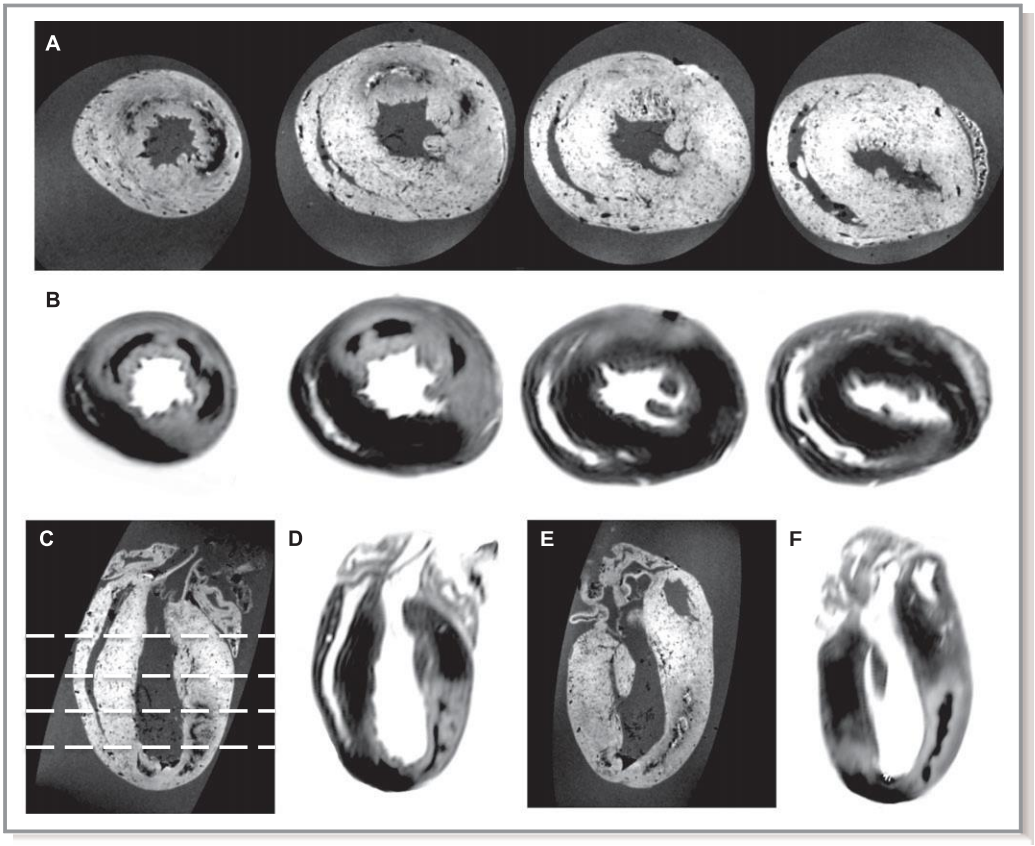


Figure 6. Selected images from 3D MRI volumetric images of a whole rat heart following IR and preparation using the MPIO/Gd method. A, Short-axis GE slices from the apex to base demonstrating clear definition of the AAR. The border of the MPIO signal voids delineates the AAR from the myocardium not perfused by the occluded vessel. The position of the slices is shown in C. B, Co-registered slices from a 3D R1 map (ie, inverted T1), clearly demonstrating the MI zone as high-signal against a low-signal background of normal myocardium. Note the low signal contained within the MI zone due to microhemorrhage. C, D, 4 chamber and (E, F) LVLA reformats of both GE and R1 map data showing the transmural nature of the MI and the full extent of the endocardial extension reformats of GE and R1 map data. AAR indicates area at risk; GE, gradient echo; MI, myocardial infarction; MPIO/Gd, microparticles of iron oxide/gadolinium; MRI, magnetic resonance imaging; IR, ischemia–reperfusion; LVLA, left ventricle long axis.

management, the use of mouse and rats has predominated. Providing genetic modification is not required, the rat has advantages of not only being convenient to house, and relatively inexpensive, but also, compared to the mouse, being technically easier on which to perform the required cardiac surgery. In regions of complete MI, achieved with a complete ligation model, histopathology in the rat has been found to be similar to that in humans, although with an accelerated time- course, and less polymorph infiltration.[27] In the case of temporary ligation, and myocardial IR injury, the histopatho-logic changes are more patchy than in humans.[24] The surgical transient ligation model, as we have performed in this study, is the most commonly used technique to achieve myocardial IR injury.[24] The occlusion time of 30 minutes is usually chosen, with longer periods resulting in larger areas of infarction and associated higher mortality.[28,29] Although investigators may ligate the left coronary artery at what appears to be the "same place" for every animal, the variation in coronary anatomy and the territory of myocardium supplied by the vessel means that there is considerable variation in the area of threatened myocardium or AAR. If only MI size was measured, without this denominator of AAR, the noise of experimental data would be greatly increased. In contrast, precise assessment of AAR allows for the MI size to be expressed in relation to this, and the effect of therapy on salvaged myocardium to be fully appreciated. For this purpose, Evan's Blue injection, with the vessel re-ligated, has become indispensable to researchers for decades, and is widely accepted as the "gold standard" technique. However, even experienced researchers will acknowledge difficulties with the technique.

We have developed a user-friendly technique, in which AAR is defined by perfusion border zones of MPIO instead of Evan's Blue, and the MI region is highlighted by gadolinium

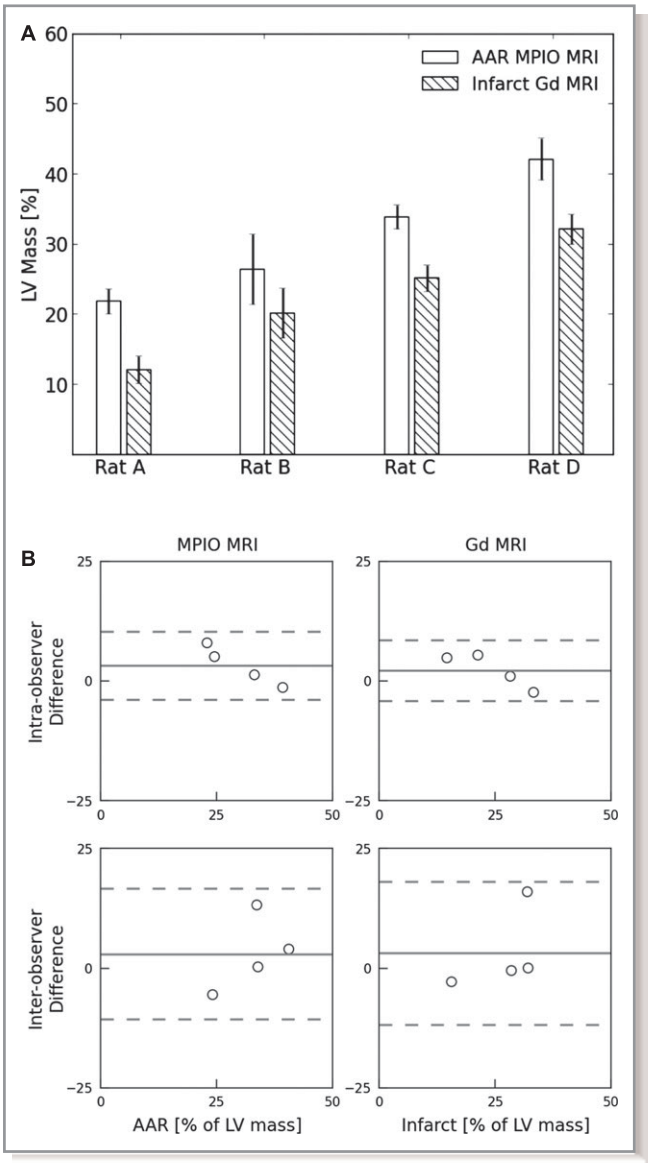


Figure 7. Summary of AAR and MI measurements in whole rat hearts (n=4 readers) following IR using the MPIO/Gd MRI method. A, AAR and infarct zones (expressed as a percentage of LV myocardial mass ±SEM). B, Bland-Altman plots examining the intra-observer (top 2 panels) and interobserver (bottom 2 panels) variability for determination of AAR (left) and MI zones (right). The dashed lines represent the 95% level of agreement. AAR indicates area at risk; LV, left ventricular; MI, myocardial infarction; MPIO/ Gd, microparticles of iron oxide/gadolinium; MRI, magnetic resonance imaging; IR, ischemia–reperfusion.

uptake. MRI then provides a high-resolution digital dataset, and removes the requirement for manual slicing of fresh postmortem heart. Given that the physical principles delineating perfused and nonperfused myocardial segments are similar in the 2 techniques, and that late gadolinium enhancement (LGE) and TTC techniques have previously been highly correlated,[16] it is not unexpected that the 2 approaches provided very similar MI/AAR measurements for corresponding slices. However, the major benefits of the MRI technique are realized through whole-heart analysis. The 3D digital dataset allows the operator to scroll through adjacent slices (Figure 8 and Movie S1 and S2), and for automated segmentation and quantification to be performed. Improved ability to examine anatomic relationships of the segments also helps ensure that artifacts are excluded.

Access of investigators to an entire high-resolution 3D dataset (effective isotropic resolution 40 to 80 1m, depending on acquisition time available), rather than just the surface of five ~2-mm slices, ensures that any regional effects of intramyocardially applied therapies such as stem cell injections will not be overlooked. These methodological improvements not only improve the ease of the measurements, but also will likely result in less intra-observer variability (Fig- ure 7B), and if automated strategies are used, removal of the nonsystematic components of interobserver variability.

Although the ex-vivo nature of our 3D MRI technique has limitations in regard to serial studies, and assessing functional correlations, it does open up the possibility of an easily accessible technique for laboratories that may not have direct access to high-field MRI facilities and staff expert in high-field, cardiac-gated MRI. It is emminently feasible, using this technique, for research teams to prepare the hearts, and have them imaged at high resolution by a core facility, with the prepared hearts being suitable for postal delivery. In the case of this study, hearts were imaged within 1 week. Although previous studies have identified issues with relatively rapid dispersion of gadolinium (within hours),[30] this did not cause significant problems in our hands using heart tissue that was rapidly fixed postmortem. Furthermore, we observed stability of the AAR border zones with the MPIO compared with our experience using Evan's Blue, where we often found postmortem diffusion of the blue agent making the borders blurry. The ex-vivo nature or novel approach also overcomes issues related to cardiac movement, and engineering challenges of imaging the high heart rate of the smaller animal. This allows high-resolution imaging to be acquired. The 3D nature of the data obtained using this technique also allows for digital analysis and automated segmentation. The technique is applicable to both smaller (e.g, mouse) and larger animals. A comparison of the advantages and disadvantages of the traditional Evan's Blue/TTC technique and the 3D MPIO/Gd MRI technique is provided in Table 2.

Hopes have been pinned on CMR by investigators studying myocardial salvage in the setting of IR and infarction in vivo. The most successful technique of imaging the AAR to date, based on higher T2 signal intensity in the edematous myocardium postischemia, requires highly expert teams to interpret and acquire the data and is poorly reproducible across laboratories.[20] Recent advances in T2-weighted CMR, including with free-breathing, motion-correction,[31,32] and T2

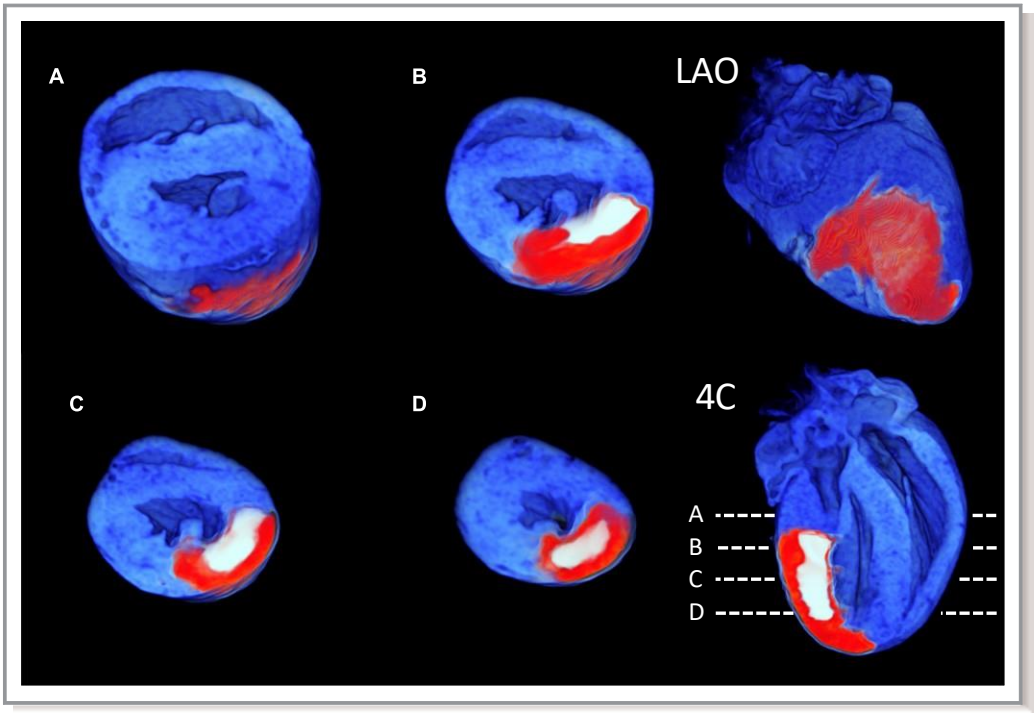


Figure 8. A 3D reformat of a whole rat heart following automated segmentation of the AAR and MI zones. The AAR is coded as red, the MI as white, and the myocardium beyond the AAR as blue. Short-axis views from the base to apex demonstrating the clear delineation of the MI. A through D, The level of the slices is shown in the 4-chamber (4C) view. An LAO projection shows the surface distribution of the occluded AAR territory following an expected distribution over the anterior and lateral walls of the LV. AAR indicates area at risk; MI, myocardial infarction; LAO, left anterior oblique; LV, left ventricle.

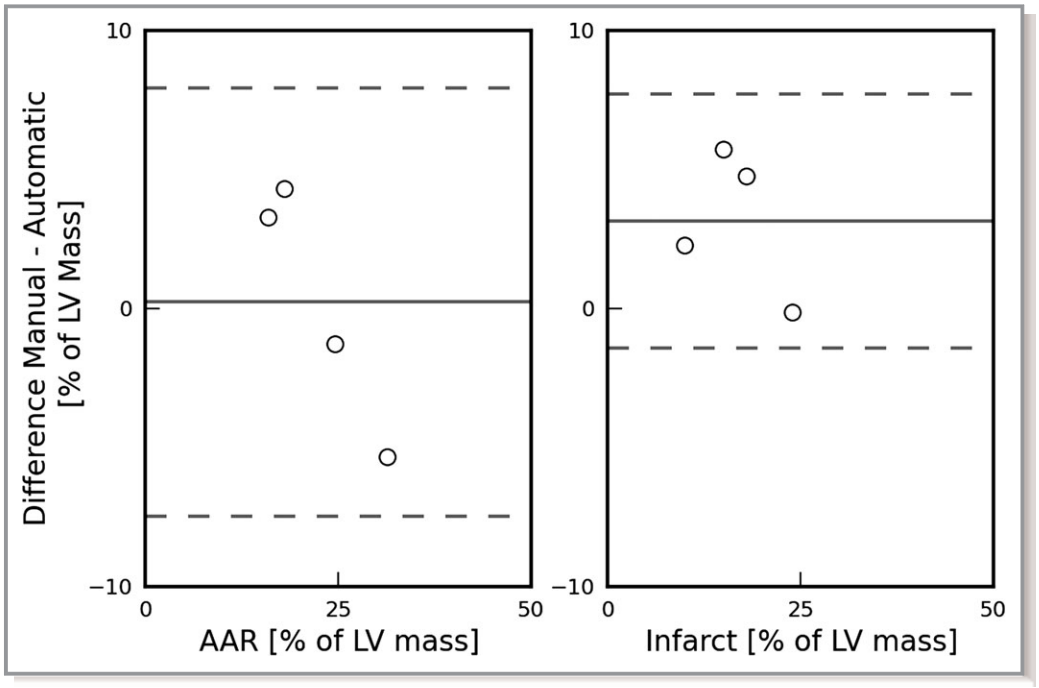


Figure 9. Bland-Altman plots comparing manual and automatic detection of the AAR (left) and MI (right) zones in intact (nonsliced) rat heart (n=4) using the MPIO/Gd technique. The dashed lines represent the 95% level of agreement. AAR indicates area at risk; MI, myocardial infarction; MPIO/Gd, microparticles of iron oxide/gadolinium.

Table 2. Advantages and Disadvantages of the Traditional Evan's Blue/TTC Technique, Vs the 3D MPIO/Gd MRI Approach

| Evan's Blue/TTC | 3D MPIO/Gd MRI |
|---|---|
| Requires IV tail injections | Requires IV tail injections |
| Requires re-ligation of culprit vessel | Requires re-ligation of culprit vessel |
| Assessment is postmortem, excluding possibility of serial study | Assessment is postmortem, excluding possibility of serial study |
| Relies on physical cutting of 2-mm slices of fresh postmortem heart, on average resulting in 5 slices for 1 rat heart | High resolution, with slice thickness not limited at a practical level (eg, we acquired 48 "slices" for 1 heart) |
| Assumptions made that AAR/MI same across the volume of the 2-mm slice | No requirement for assumptions due to high number of slices and high resolution |
| Evan's Blue can diffuse across the border zones, making rapid assessment essential, and reducing the clarity of measurement | MPIO appears to be more restricted in its diffusion, and the border zones are seen clearly even 1 week postfixation |
| Requires manual tracing of borders, and calculation of volumes for MI and AAR | Extremely suited to 3D digital analysis and automated segmentation |
| Difficult to easily assess corresponding myocardium between slices | Extremely easy for operator to scroll through slices, and examine anatomic relationships to reduce error |

AAR indicates area at risk; 3D, 3-dimensional; MI, myocardial infarction; MPIO/Gd, microparticles of iron oxide/gadolinium; MRI, magnetic resonance imaging; TTC, triphenyl tetrazolium chloride.

mapping, have partially alleviated problems related to inher- ently low signal-to-noise ratio, and inconsistent image qual- ity.[21] Furthermore, precontrast T1 mapping has shown potential to provide more robust definition of the AAR.[33] Despite these major breakthroughs, recent clinical studies highlight remaining practical difficulties in applying edema- imaging techniques to larger clinical studies, with the need to exclude a significant portion of patients from myocardial salvage assessment by CMR due to insufficient image quality.[34] The technical difficulty of cardiac gating with rapid heart rates of mice and rats in a small-bore, high-field magnet exacerbates these issues. The application to preclinical research is hampered further by the fact that therapies, including ischemic preconditioning, can influence water content and T2 signal intensity, independently of the true AAR.[35] Combined, these factors make current in vivo assessment of myocardial IR injury and myocardial salvage by CMR not only technically challenging, but also far less reliable than the high-resolution, postmortem histological approach, and, as such, in vivo MRI approaches to this methodological challenge in rodents is not comparable to our current study findings.

## Conclusions

IR injury is considered a major contributor to the residual morbidity and mortality resulting from MI. Improved robust- ness and precision in quantifying salvaged myocardium is key to the success of research programs aimed at minimizing myocardial IR injury. We have developed a novel, automatable 3D MRI technique that improves the robustness of measure- ment of the salvaged myocardium, and is accessible to any laboratory capable of performing standard Evan's Blue/TTC assessment.

## Acknowledgments

The authors are grateful for the technical assistance of Dr Bob Chapman, who assisted in the acquisition of CMR data.

## Sources of Funding

This work was supported by a grant from the North Shore Heart Research Foundation and by Project grant 632551 from the National Health & Medical Research Council (NHMRC), Australia. Grieve and Figtree acknowledge the support of the Sydney University Medical Foundation. Figtree was supported by NHMRC/Heart Foundation cofunded Career Development Fellowship. Animal NMR imaging facilities were funded by the Australian Research Council.

## Disclosures

None.

## References

1. Goldberg RJ, Currie K, White K, Brieger D, Steg PG, Goodman SG, Dabbous O, Fox KA, Gore JM. Six-month outcomes in a multinational registry of patients hospitalized with an acute coronary syndrome (the Global Registry of Acute Coronary Events [GRACE]). *Am J Cardiol*. 2004;93:288–293.
2. Keeley EC, Boura JA, Grines CL. Primary angioplasty versus intravenous thrombolytic therapy for acute myocardial infarction: a quantitative review of 23 randomised trials. *Lancet*. 2003;361:13–20.
3. Wang QD, Pernow J, Sjoquist PO, Ryden L. Pharmacological possibilities for protection against myocardial reperfusion injury. *Cardiovasc Res*. 2002;55:25– 37.
4. Kloner RA, Rezkalla SH. Cardiac protection during acute myocardial infarction: where do we stand in 2004? *J Am Coll Cardiol*. 2004;44:276–286.

5. Ambrosio G, Tritto I. Reperfusion injury: experimental evidence and clinical implications. *Am Heart J*. 1999;138:S69–S75.
6. Litt MR, Jeremy RW, Weisman HF, Winkelstein JA, Becker LC. Neutrophil depletion limited to reperfusion reduces myocardial infarct size after 90 minutes of ischemia: evidence for neutrophil-mediated reperfusion injury. *Circulation*. 1989;80:1816–1827.
7. Hayward R, Campbell B, Shin YK, Scalia R, Lefer AM. Recombinant soluble P-selectin glycoprotein ligand-1 protects against myocardial ischemic reper- fusion injury in cats. *Cardiovasc Res*. 1999;41:65–76.
8. Zhao ZQ, Lefer DJ, Sato H, Hart KK, Jefforda PR, Vinten-Johansen J. Monoclonal antibody to ICAM-1 preserves post-ischemic blood flow and reduces infarct size after ischemia-reperfusion in rabbit. *J Leukoc Biol*. 1997;62:292–300.
9. Entman ML, Smith CW. Postreperfusion inflammation: a model for reaction to injury in cardiovascular disease. *Cardiovasc Res*. 1994;28:1301–1311.
10. Jolly SR, Kane WJ, Hook BG, Abrams GD, Kunkel SL, Lucchesi BR. Reduction of myocardial infarct size by neutrophil depletion: effect of duration of occlusion. *Am Heart J*. 1986;112:682–690.
11. Gao E, Lei YH, Shang X, Huang ZM, Zuo L, Boucher M, Fan Q, Chuprun JK, Ma XL, Koch WJ. A novel and efficient model of coronary artery ligation and myocardial infarction in the mouse. *Circ Res*. 2010;107:1445–1453.
12. Virag JA, Lust RM. Coronary artery ligation and intramyocardial injection in a murine model of infarction. *J Vis Exp*. 2011;52:2581.
13. Holmbom B, Naslund U, Eriksson A, Virtanen I, Thornell LE. Comparison of triphenyltetrazolium chloride (TTC) staining versus detection of fibronectin in experimental myocardial infarction. *Histochemistry*. 1993;99:265–275.
14. Freeman I, Grunwald AM, Robin B, Rao PS, Bodenheimer MM. Effect of early reperfusion on use of triphenyltetrazolium chloride to differentiate viable from non-viable myocardium in area of risk. *Cardiovasc Res*. 1990;24:109–114.
15. Schneider JE, Cassidy PJ, Lygate C, Tyler DJ, Wiesmann F, Grieve SM, Hulbert K, Clarke K, Neubauer S. Fast, high-resolution in vivo cine magnetic resonance imaging in normal and failing mouse hearts on a vertical 11.7 T system. *J Magn Reson Imaging*. 2003;18:691–701.
16. Kim RJ, Fieno DS, Parrish TB, Harris K, Chen EL, Simonetti O, Bundy J, Finn JP, Klocke FJ, Judd RM. Relationship of MRI delayed contrast enhancement to irreversible injury, infarct age, and contractile function. *Circulation*. 1999;100:1992–2002.
17. Arheden H, Saeed M, Higgins CB, Gao DW, Bremerich J, Wyttenbach R, Dae MW, Wendland MF. Measurement of the distribution volume of gadopentetate dimeglumine at echo-planar MR imaging to quantify myocardial infarction: comparison with 99mTc-DTPA autoradiography in rats. *Radiology*. 1999;211:698–708.
18. Aletras AH, Tilak GS, Natanzon A, Hsu L-Y, Gonzalez FM, Hoyt RF, Arai AE. Retrospective determination of the area at risk for reperfused acute myocardial infarction with T2-weighted cardiac magnetic resonance imaging: histopathological and displacement encoding with stimulated echoes (DENSE) functional validations. *Circulation*. 2006;113:1865–1870.
19. Friedrich MG, Abdel-Aty H, Taylor A, Schulz-Menger J, Messroghli D, Dietz R. The salvaged area at risk in reperfused acute myocardial infarction as visualized by cardiovascular magnetic resonance. *J Am Coll Cardiol*. 2008;51:1581–1587.
20. Mewton N, Rapacchi S, Augeul L, Ferrera R, Loufouat J, Boussel L, Micolich A, Rioufol G, Revel D, Ovize M, Croisille P. Determination of the myocardial area at risk with pre- versus post-reperfusion imaging techniques in the pig model. *Basic Res Cardiol*. 2011;106:1247–1257.
21. Eitel I, Friedrich MG. T2-weighted cardiovascular magnetic resonance in acute cardiac disease. *J Cardiovasc Magn Reson*. 2011;13:13.
22. McAteer MA, Sibson NR, von ZurMuhlen C, Schneider JE, Lowe AS, Warrick N, Channon KM, Anthony DC, Choudhury RP. In vivo magnetic resonance imaging of acute brain inflammation using microparticles of iron oxide. *Nat Med* 2007;13:1253–1258.
23. Bhindi R, Khachigian LM, Lowe HC. DNAzymes targeting the transcription factor Egr-1 reduce myocardial infarct size following ischemia-reperfusion in rats. *J Thromb Haemost*. 2006;4:1479–1483.
24. Bhindi R, Witting PK, McMahon AC, Khachigian LM, Lowe HC. Rat models of myocardial infarction—pathogenetic insights and clinical relevance. *Thromb Haemost*. 2006;96:602–610.
25. Grieve SM, Lonborg J, Mazhar J, Tan TC, Ho E, Liu CC, Lay W, Gill AJ, Kuchel P, Bhindi R, Figtree GA. Cardiac magnetic resonance imaging of rapid VCAM-1 up-regulation in myocardial ischemia-reperfusion injury. *Eur Biophys J*. 2013;42:61–70.
26. Wu KC, Zerhouni EA, Judd RM, Lugo-Olivieri CH, Barouch LA, Schulman SP, Blumenthal RS, Lima JAC. Prognostic significance of microvascular obstruction by magnetic resonance imaging in patients with acute myocardial infarction. *Circulation*. 1998;97:765–772.
27. Fishbein MC, Maclean D, Maroko PR. Experimental myocardial infarction in the rat: qualitative and quantitative changes during pathologic evolution. *Am J Pathol*. 1978;90:57–70.
28. Wayman NS, McDonald MC, Chatterjee PK, Thiemermann C. Models of coronary artery occlusion and reperfusion for the discovery of novel antiischemic and antiinflammatory drugs for the heart. *Methods Mol Biol*. 2003;225:199–208.
29. Chimenti S, Carlo E, Masson S, Bai A, Latini R. Myocardial infarction: animal models. *Methods Mol Med*. 2004;98:217–226.
30. Schelbert EB, Hsu L, Anderson SA, Mohanty BD, Karim SM, Kellman P, Aletras AH, Arai AE. Late gadolinium enhancement cardiac magnetic resonance identifies post infarction myocardial fibrosis and the border zone at the near cellular level in ex vivo rat hearts. *Circ Cardiovasc Imaging*. 2010;3:743–752.
31. Kellman P, Aletras AH, Mancini C, McVeigh ER, Arai AE. T2-prepared SSFP improves diagnostic confidence in edema imaging in acute myocardial infarction compared to turbo spin echo. *Magn Reson Med*. 2007;57:891–897.
32. Aletras AH, Kellman P, Derbyshire JA, Arai AE. Acute TSE-SSFP: A hybrid method for T2-weighted imaging of edema in the heart. *Magn Reson Med*. 2008;59:229–235.
33. Ugander M, Bagi PS, Oki AJ, Chen B, Hsu L-Y, Aletras AH, Shah S, Greiser A, Kellman P, Arai AE. Myocardial edema as detected by pre-contrast T1 and T2 CMR delineates area at risk associated with acute myocardial infarction. *JACC Cardiovasc Imaging*. 2012;5:596–603.
34. Masci PG, Andreini D, Francone M, Bertella E, De Luca L, Coceani M, Mushtaq S, Mariani M, Carbone I, Pontone G, Agati L, Bogaert J, Lombardi M. Prodromal angina is associated with myocardial salvage in acute ST- segment elevation myocardial infarction. *Eur Heart J Cardiovasc Imaging*. 2013;14:1041–1048.
35. Thuny F, Lairez O, Roubille F, Mewton N, Rioufol G, Sportouch C, Sanchez I, Bergerot C, Thibault H, Cung TT, Finet G, Argaud L, Revel D, Derumeaux G, Bonnefoy-Cudraz E, Elbaz M, Piot C, Ovize M, Croisille P. Post-conditioning reduces infarct size and edema in patients with ST-segment elevation myocardial infarction. *J Am Coll Cardiol*. 2012;59:2175–2181.

Journal of the American Heart Association
OPEN ACCESS

# Automated Quantification of Myocardial Salvage in a Rat Model of Ischemia–Reperfusion Injury Using 3D High-Resolution Magnetic Resonance Imaging (MRI)

Stuart M. Grieve, Jawad Mazhar, Fraser Callaghan, Cindy Y. Kok, Sarah Tandy, Ravinay Bhindi and Gemma A. Figtree

*J Am Heart Assoc.* 2014;3:e000956; originally published July 23, 2014; doi: 10.1161/JAHA.114.000956
The *Journal of the American Heart Association* is published by the American Heart Association, 7272 Greenville Avenue, Dallas, TX 75231
Online ISSN: 2047-9980

# **Chapter 4.** Optical coherence tomography (OCT) as an adjunct to percutaneous coronary intervention; a single centre experience


## Summary:

Although chapter 3 demonstrates that 2D-QCA may be a reasonable alternative to OCT in assessment of proximal and distal reference diameter of a lesion, optical coherence tomography (OCT) provides additional information regarding lesion morphology that is not possible with 2D-QCA. Unlike IVUS (Intravascular ultrasound) which uses ultrasound waves, OCT creates an image by directing an optical beam of infrared light onto the tissue and measuring the reflected intensity of light. OCT is a relatively new intravascular imaging catheter in comparison to IVUS and indications for its use are not well defined. In this chapter we report a single centre experience where OCT was used to help guide management in routine clinical practice. It may help physicians identify the clinical indications for using OCT in percutaneous coronary intervention.

International Journal of Cardiology 163 (2013) e49–e52

Contents lists available at SciVerse ScienceDirect

International Journal of Cardiology

journal homepage: www.elsevier.com/locate/ijcard

Letter to the Editor

# Optical coherence tomography (OCT) as an adjunct to percutaneous coronary intervention; a single centre experience

J. Mazhar *, J.C. Murphy, G. Figtree, P. Hansen, G.I. Nelson, R. Bhindi

*Royal North Shore Hospital, Sydney, Australia*

article info

*Article history:*
Received 11 July 2012
Accepted 4 September 2012
Available online 30 September 2012

*Keywords:*
Optical coherence tomography (OCT)
Intracoronary imaging

Intravascular imaging of coronary arteries has become increasingly common. Optical coherence tomography (OCT) and intravascular ultra- sound (IVUS) are the two most recognized modalities utilized. Unlike IVUS which uses ultrasound waves, OCT creates an image by directing an optical beam of infrared light onto the tissue and measuring the reflected intensity of light [1]. Until recently OCT has predominantly been used in the research setting, though it has been shown to be safe and feasible to use in the clinical setting [2,3].

IVUS guided percutaneous coronary intervention has been shown to reduce target lesion revascularisation in certain patient cohorts [4,5] and although no similar outcome studies currently exist with OCT, it is arguable that the indications for its use would be similar to those established for IVUS. We sought to clarify the potentially under-appreciated clinical role that OCT may play in PCI. We report a single centre experience where OCT was used to help guide management in routine clinical practice.

Between November 2010 and February 2012 all cases where OCT performed for clinical indications during PCI in our centre were retrospectively analysed. The OCT acquisition was performed using the C7 Dragonfly™ intracoronary imaging catheter and the ILUMIEN™ PCI Optimization System (St. Jude Medical). All images were acquired using a non-occlusive technique with injection of isosmolar iodixonoal (Visipaque™ by GE healthcare) contrast to clear the vessel of blood [3].

Demographic details of the patients, OCT vessel, OCT indications and impact of OCT on decision making was collated. The authors certify compliance with the principles of ethical publishing in the International Journal of Cardiology.

The main indications for use of OCT were categorised into 4 main sub-groups (see Table 1):

1–To assess cause of stent thrombosis (n=6);

2–to assess in-stent restenosis (n=11);
3–to assess hazy or ambiguous lesions (n=23); and
4–to optimise stent selection/size (n=7).

Forty seven patients had OCT performed for clinical indications during the study period. The mean age was 68±12 years and 40 (86%) were male. The clinical presentations were ST elevation myocardial infarction [STEMI] (10), non ST elevation myocardial infarction [NSTEMI] (16), unstable angina (7) and stable angina (14). A femoral approach was used in 15 cases and radial approach in 32 (68%) cases. The vessels assessed were left anterior descending artery (16), saphenous vein graft (11), right coronary artery (8), diagonal artery (4), left main stem (3), circumflex (3), obtuse marginal (1) and ramus (1). OCT identified intracoronary pathologies like plaque rupture (6), intra-coronary dissection (4), cause of stent thrombosis (6) and intracoronary thrombus (3), see Fig. 1. It added to angiographic interpretation in 33 (70%) cases and changed management in 23 (49%) cases (see Table 2). There were no complications related to the OCT procedures. The details for each indication are as follows:

Out of the 6 cases of stent thrombosis, OCT added to angiographic interpretation in 5 (83%) cases. It showed malapposed stent (1), well apposed stents (2), exposed (not endothelialized) stent struts (1), and suboptimally dilated stents (2). This led to a change in management in 3 (50%) cases. The reasons for change in management were: only balloon dilatation done in two cases as stents were well apposed and it helped in selecting an appropriate size stent in the third case.

Out of the 11 cases of in-stent restenosis (ISR), OCT added to angiographic interpretation in 7 (63%) cases. It added to angio- graphic interpretation by showing radial stent collapse (1), plaque rupture (1), showed ISR rather than stent thrombosis (2), no significant ISR in a case suspicious of severe ISR on angiogram (1), undersized stent (1) and a well apposed stent suggesting intima formation as cause of ISR (1). This led to a change in management in 3 (27%) cases: It showed plaque rupture rather than ISR in a

* Corresponding author. Tel.: +61 422040611.
*E-mail address:* jawadmc2@gmail.com (J. Mazhar).

0167-5273/$ - see front matter  http://dx.doi.org/10.1016/j.ijcard.2012.09.016

Table 1
Clinical details of the forty seven patients in whom OCT was performed. To assess stent thrombosis

| No. | Presentation | Vessel | OCT indication | OCT findings. | Did OCT add to angiographic interpretation | Did it change management? | Outcome or How did it change management? |
|---|---|---|---|---|---|---|---|
| 1 | Anterior STEMI | LAD | Very late ST | Confirmed ST and showed malapposed stent struts. | Yes | No | PCI performed. |
| 2 | STEMI | Ramus | ? ST ?ISR had stent 2 weeks earlier, ? cause of ST | Confirmed ST No stent malapposition. | Yes | Yes | PTCA performed as stent well apposed. |
| 3 | Inferior STEMI | RCA | Reinfarction 2/7 following PCI after starting plasmaphoresis for GB syndrome. | Stent well apposed, ST due to washout of antiplatelet drugs due to plasmaphoresis | Yes | Yes | Confirmed that ST due to plasmaphoresis rather than stent malapposition. |
| 4 | Inferior STEMI | RCA | Late ST | Exposed stent struts | Yes | No | PCI performed |
| 5 | NSTEMI | Diagonal | Sub-acute ST | Suboptimally dilated mid segment of stent (also noted on angiogram) | No | No | PTCA performed. |
| 6 | STEMI | RCA | Sub-acute ST (previous PCI to RCA 3 days ago) | Suboptimally deployed stent, although could be seen angiographically as well. | Yes (confirms underdeployed stent) | Yes (Helped in sizing the stent). | PCI performed. |
| *To assess in-stent restenosis* | | | | | | | |
| 1 | Unstable angina | RCA | ISR/ST | Confirmed aggressive ISR and probable radial stent collapse. | Yes | No | PCI performed |
| 2 | Unstable angina | Cx/OM2 | ISR | Confirmed ISR | No | No | PCI performed |
| 3 | Unstable angina | LAD | ? ISR | Plaque rupture prior to stent. No ISR | Yes | Yes (as it showed plaque rupture although FFR normal) | PCI performed |
| 4 | Stable angina | LAD | ?ISR?ST | Confirmed ISR | No | No | PCI performed |
| 5 | NSTEMI | RCA | ISR | Confirmed ISR | No | No | PCI performed |
| 6 | NSTEMI | RCA | ?ISR?ST | Showed ISR rather than ST. | Yes | No | PCI performed |
| 7 | NSTEMI | Cx | ISR | Confirmed severe ISR | No | No | PCI performed |
| 8 | Stable angina | LAD | Severity of ISR | No significant ISR on OCT, MLA 5.2 $mm^2$ | Yes | Yes | Medical treatment |
| 9 | Stable angina | RCA | ISR | Yes (stent well apposed and ISR due to intima formation) | Yes | No | PCI performed. |
| 10 | Unstable angina | D1 | ?ST?ISR | ISR. | Yes | Yes | PTCA done as stent well apposed. |
| 11 | Stable angina | LAD | ISR | Undersized stent (gives mechanistic reason of ISR) | Yes | No | PCI performed. |
| *To assess angiographically ambiguous lesions* | | | | | | | |
| 1 | Anterior STEMI | LAD | ?ostial LAD dissection | No dissection (IVUS 3 months later also showed it to be a non-significant lesion) | Yes | Yes (LAD lesion not treated) | PCI performed to culprit lesin in circumflex. |
| 2 | Stable angina | LM/CX | ? guide dissection | No dissection but severe LM-Cx lesion. | Yes | Yes | PCI performed |
| 3 | Anterior STEMI | LAD | ?plaque rupture ? Dissection | Plaque rupture with thrombus. | Yes | Yes | PCI performed |
| 4 | NSTEMI | CX | Filling defect | In-stent dissection | Yes | Yes | Medical treatment. |
| 5 | Anterior STEMI | LAD | ? proximal edge dissection | Edge dissection LM not involved | Yes | Yes | Medical treatment |
| 6 | NSTEMI | LM | LM abnormality noted after PCI to Cx. ?Significant LM disease or guide dissection | Severe LM disease | Yes | Yes | Helped in sizing of LM stent |
| 7 | Stable angina | SVG | Filling defect at ostium | Dissection | Yes | Yes | PCI performed |
| 8 | Anterior STEMI | LAD | Hazy at proximal and distal edge with good TIMI flow. | Stent malapposition with plaque rupture and thrombus. | Yes | Yes | PTCA. Stent not implanted as patient has myeloproliferative disorder and aspirin allergy. |
| 9 | Stable angina | RCA | ? calcified lesion | Soft plaque in the lesion. Diffuse calcification otherwise | No (can be appreciated on angiogram) | No | PCI performed |
| 10 | Stable angina | | | | SVG | Unable to pass filter wire retrieval device past proximal edge of deployed stent. | |

| | | | | | | | | |
|---|---|---|---|---|---|---|---|---|
| Disrupted (inwardly deformed) proximal edge of stent | | Yes proximal edge | No | PCI to cover | | | | |
| 11 | NSTEMI | LAD | Hazy proximal LAD. | Atheroma with plaque rupture. | Yes | | No | PCI done |
| 12 | NSTEMI | SVG | Occluded vein graft, thrombus aspirated, and two sequential lesions visualized. ? Atypical distal lesion or residual thrombus. | Tight lesion confirmed. | | Yes | Yes | No further aspiration and proceeded to PCI. |

Table 1 (*continued*)

| No. | Presentation | Vessel | OCT indication | OCT findings. | Did OCT add to angiographic interpretation | Did it change management? | Outcome or How did it change management? |
|---|---|---|---|---|---|---|---|
| To assess stent thrombosis | | | | | | | |
| 13 | NSTEMI | LAD | Hazy proximal LAD, ? Spontaneous coronary artery dissection | Atheroma with plaque rupture | Yes | No | PCI performed |
| 14 | Stable angina | LAD | Hazy lesion ostial LAD | Severe lesion with thrombus | Yes | Yes | CABG performed. |
| 15 | STEMI | Cx | Hazy lesion mid circumflex | Thrombus | No | No | PCI performed. |
| 16 | NSTEMI | SVG | Severe lesion on angiogram | Severe lesion. | No | No | PCI performed |
| 17 | NSTEMI | LAD | Hazy mid LAD lesion (appeared signifi cant on angio) | Mild disease on OCT (FFR nor- mal). Probably a kink in the vessel made it appear as significant lesion. | Yes | Yes | Medical treatment. |
| 18 | NSTEMI | LAD | Severe lesion on angiogram | Severe lesion. | No | No | PCI performed. |
| 19 | STEMI | LAD | Hazy prox LAD lesion (poor images due to obesity) | Severe lesion | Yes | Yes | PCI performed. |
| 20 | Unstable angina | Diagonal | Severe lesion in diagonal artery. | Severe lesion | No | No | PCI performed |
| 21 | NSTEMI | Diagonal | To see if thrombus in diagonal artery is embolic. | plaque rupture and dissection plane, although could be due to balloon predilation. | Yes | Yes (if embolic, PCI would not have been done) | PCI performed. |
| 22 | Stable angina | SVG | Intermediate lesion on angiogram | Severe lesion on OCT (MLA of lesion 6 $mm^2$ and MLA of nor- mal part 14 $mm^2$) | Yes | Yes | PCI performed. |
| 23 | NSTEMI | LAD | Filling defect within stent, ? ISR ? ST. | Severe ISR | Yes | No | PCI performed |
| *To assess vessel size prior to stent deployment* | | | | | | | |
| 1 | Stable angina | SVG | To measure size and length of lesion | True diameter of vessel determined. True diameter of vessel | No | No | |
| 2 | Unstable angina | SVG | To measure size and length of lesion | determined. | No | No | |
| 3 | Unstable angina | SVG | To measure size and length of lesion | True diameter of vessel determined. | No | No | |
| 4 | Stable angina | SVG | SVG to PDA occluded. To measure size and length of lesion | True diameter of vessel determined. | No | No | |
| 5 | NSTEMI | SVG | Occluded stent in ostium of SVG to Cx. | True diameter of vessel determined. | Yes | Yes | Led to choosing a larger stent. |
| 6 | Stable angina | SVG | ISR | Confirmed severe ostial ISR | Yes | Yes | Helped in sizing the stent |
| 7 | Unstable angina | LM | 80% lesion in distal LM. | True diameter of vessel determined. | Yes | Yes | Led to choosing a larger stent. |

Legend: Cx = circumflex artery, D1 = diagonal, GB = Guillian Barre, ISR = in-stent restenosis, LAD = left anterior descending, LM = left main, MLA = minimum luminal area. NSTEMI = non ST elevation myocardial infarction, OM = obtuse marginal, OCT = optical coherence tomography, PTCA = percutaneous coronary angioplasty, PCI = percutaneous coronary intervention, RCA = right coronary artery, STEMI = ST elevation myocardial infarction, ST = stent thrombosis, SVG = saphenous vein graft, PDA = posterior descending artery.

case of unstable angina which led to percutaneous coronary intervention (PCI). It showed no significant ISR with minimum luminal area 5.2 $mm^2$ in a case where there was suspicion of significant ISR on angiogram. It showed well apposed stent in a case of ISR, so only balloon dilatation done.

Out of the 23 cases of angiographically ambiguous lesions, OCT added to angiographic interpretation in 18 (78%) cases. Lesions were considered ambiguous if they appeared hazy or as filing defects on coronary angiogram. In these lesions, OCT added to angiographic interpretation by excluding dissection (2), showing atheroma with plaque rupture (2), plaque rupture with thrombus (1), plaque rupture and dissection plane (1), intracoronary dissection (3), stent malapposition with thrombus (1), disrupted (inwardly deformed) proximal edge of stent (1), severe lesions (6) and mild disease in LAD which appeared significant on angiogram (1). This led to change in management in 14 (60%) cases.

In 7 cases, OCT was done to assess vessel size prior to stent deployment. OCT added to angiographic interpretation in 3 (43%) cases by measuring the accurate intraluminal diameter. This led to choosing a larger stent size in 3 cases (43%).

OCT provides cross sectional images of the coronary artery with a resolution up to 10 μm [6] which is approximately ten times higher than that of IVUS [6,7]. This allows OCT to demonstrate vessel morphology and stent deployment in greater detail then other currently clinically available technologies [8]. OCT demonstrates more clearly differentiation of lumen to arterial wall interface or the lumen border, when compared with IVUS [2]. This makes it superior to IVUS in identifying plaque rupture [9] coronary artery dissection and intracoronary thrombus [8,9]. In our case series it identified intraluminal pathologies like atheromatous plaque, coronary artery dissection, intracoronary thrombosis, plaque rupture and stent malapposition. Although OCT has limited depth penetration (b 2 mm) [2], it adequately visualized 11 cases of saphenous vein graft in this cohort.

Our single centre study confirms that OCT is a safe procedure and can be used clinically to add to information obtained angiographically and importantly to change management for the patient. Whilst long term prospective studies are necessary to define a role for OCT guided angiography and PCI, the present study supports its use for selected clinical indications.

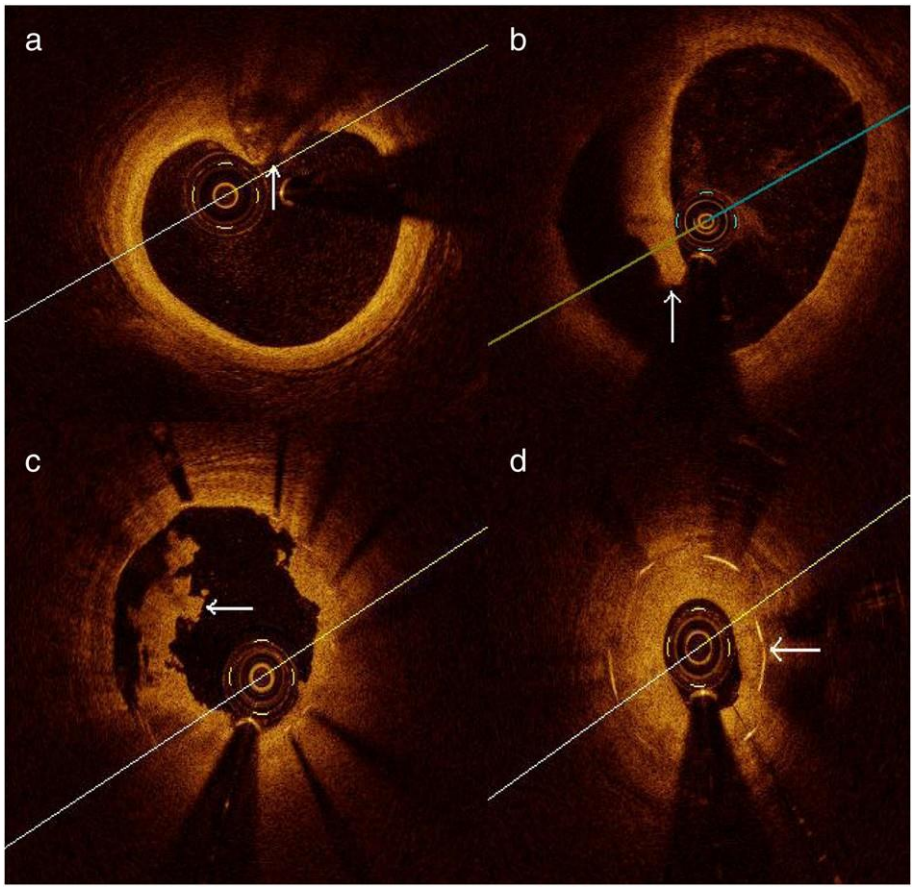


Fig. 1. Intraluminal pathologies seen on OCT. Figure 1a: Atheroma with plaque rupture (arrow). Figure 1b: Intracoronary dissection flap (arrow) in a saphenous vein graft. Figure 1c: Stent thrombosis (arrow). Figure 1d: In-stent restenosis, arrow points to stent struts.

Table 2
Change in management in each group.

| Indication for OCT | Total no. of patients in each group. | No. of patients in which it added to angiographic interpretation (%) | No. of patients in which it changed management (%) |
|---|---|---|---|
| Stent thrombosis | 6 | 5 (83%) | 3 (50%) |
| In-stent restenosis | 11 | 7 (63%) | 3 (27%) |
| Ambiguous lesion | 23 | 18 (78%) | 14 (60%) |
| Vessel size | 7 | 3 (43%) | 3 (43%) |

## References


[1] Lowe HC, Narula J, Fujimoto JG, Jang IK. Intracoronary optical diagnostics, current status, limitations and potential. J Am Coll Cardiol: Cardiovasc Interv 2011 Dec;4(12):1257-70, doi:10.1016/j.jcin.2011.08.015 [Review].

[2] Yamaguvhi T, Terashima M, Akasaka T, Hayashi T, Mizuno K, Muramatsu T, et al. Safety and feasibility of an intravascular optical coherence tomography image wire system in the clinical setting. Am J Cardiol 2008;101:562-7.

[3] Prati Francesco, Cera Maria, Ramazzotti Vito, Imola Fabrizio, Giudice Rocco, Albertucci Mario. Safety and feasibility of a new non-occlusive technique for facil- itated intracoronary optical coherence tomography (OCT) acquisition in various clinical and anatomical scenarios. EuroInterv 2007;3:365-70.

[4] AURusso RJ, Silva PD, Teirstein PS, et al. A randomized controlled trial of angiogra- phy versus intravascular ultrasound-directed bare-metal coronary stent placement (The AVID Trial). Circ Cardiovasc Interv 2009;2:113.

[5] Oemrawsingh PV, Mintz GS, Schalij MJ, Zwinderman AH, Jukema JW, van der Wall EE. Intravascular ultrasound guidance improves angiographic and clinical outcome of stent implantation for long coronary artery stenoses: final results of a randomized comparison with angiographic guidance (TULIP Study). TULIP Study. Throm- bocyte activity evaluation and effects of Ultrasound guidance in Long Intracoronary stent Placement. Circulation 2003;107(1):62.

[6] Tearney GJ, Brezinski ME, Bouma BE, Boppart SA, Pitris C, Southern JF, et al. In vivo endoscopic optical biopsy with optical coherence tomography. Science 1997 Jun 27;276(5321):2037-9.

[7] Jang IK, Bouma BE, Kang DH, et al. Visualization of coronary atherosclerotic plaques in patients using optical coherence tomography: comparison with intravascular ul- trasound. J Am Coll Cardiol 2002;39:604-9.

[8] Bouma BE, Tearney GJ, Yabushita H, et al. Evaluation of intracoronary stenting by intravascular optical coherence tomography. Heart 2003;89:317-21.

[9] Kubo T, Imanishi T, Takarada S, Kuroi A, Ueno S, Yamano T, et al. Assessment of culprit lesion morphology in acute myocardial infarction: ability of optical coherence tomography compared with intravascular ultrasound and coronary angioscopy. J Am Coll Cardiol 2007;50:933-9.

# Chapter 5. Comparison of two-dimensional quantitative coronary angiography (2D-QCA) with optical coherence tomography (OCT) in the assessment of coronary artery lesion dimensions


## Summary:

An accurate assessment of intracoronary lumen dimensions is essential in the diagnosis and treatment of coronary artery disease. Although intravascular catheters like IVUS and OCT can provide an accurate assessment of the coronary artery lumen dimensions, they are invasive, expensive, time consuming and may require use of additional contrast. There is limited data on how well 2D-QCA and OCT agree with each other for measurement of coronary artery lumen dimensions. In this chapter we aimed to assess the agreement between the two modalities and found that there is a good correlation and agreement between 2D-QCA and OCT for measurement of proximal and distal reference diameters of a coronary vessel. However, the minimum luminal diameter (MLD) was underestimated by 2D-QCA.

IJC Heart & Vasculature 7 (2015) 14-17

Contents lists available at ScienceDirect

IJC Heart & Vasculature

journal homepage: http://www.journals.elsevier.com/ijc-heart-and-vasculature

# Comparison of two dimensional quantitative coronary angiography (2D-QCA) with optical coherence tomography (OCT) in the assessment of coronary artery lesion dimensions☆

J. Mazhar [a,c,*], E. Shaw [b], U.K. Allahwala [b], G.A. Figtree [b,c], R. Bhindi [b,c]

[a] The Canberra Hospital, Canberra, Australia
[b] Royal North Shore Hospital, Sydney, Australia
[c] North Shore Heart Research Group, Kolling Institute, University of Sydney, Sydney, Australia

## article info

*Article history:*
Received 2 July 2014
Received in revised form 9 January 2015
Accepted 20 January 2015
Available online 29 January 2015

*Keywords:*
Quantitative coronary angiography Optical coherence tomography Coronary artery lesion

## abstract

*Objectives:* There is limited data on how well 2D-QCA and OCT agree with each other for measurement of coronary artery lumen dimensions. We aimed to assess the agreement between the two modalities.

*Methods:* Patients undergoing OCT for assessment of coronary artery lesions were reviewed. Minimum luminal diameter (MLD), proximal reference diameter and distal reference diameter were measured for each lesion prior to stenting.

*Results:* OCT was performed in 64 patients and 40 lesions were suitable for analysis. There was a good correlation for proximal and distal reference diameters ($r = 0.86$, $p < 0.0001$ and $r = 0.92$, $p < 0.0001$ respectively). There was good agreement on Bland–Altman analysis; the proximal and distal reference diameters measured by QCA were on average 0.09 mm (95% CI, −0.52 to 0.53 mm) and 0.1 mm (95% CI, −0.59 to 0.6 mm) smaller than OCT respectively. There was a satisfactory correlation ($r = 0.63$, $p < 0.0001$) between QCA and OCT for MLD. However, the MLD by QCA was 0.49 mm (95% CI, −1.57 to 0.59 mm) smaller than OCT, suggesting a poor agreement for MLD.

*Conclusions:* There is a good correlation and agreement between QCA and OCT for measurement of proximal and distal reference diameters. However, the MLD was underestimated by QCA.



## 1. Introduction

Suboptimal stent deployment has been shown to be associated with increased incidence of target vessel revascularization [1-3]. An accurate assessment of intracoronary lumen dimensions is essential in the diagnosis and treatment of coronary artery disease. Coronary lumen dimensions can be assessed by a visual estimate by an experienced op- erator, by quantitative coronary angiography (QCA) or by more invasive techniques like intravascular ultrasound (IVUS) or optical coherence tomography (OCT).

Intracoronary lumen dimensions assessed by OCT correlate well with IVUS, however OCT measurements are usually smaller than IVUS [4-6]. Previous studies comparing OCT and 2D/3D-QCA show a satisfactory to good correlation; however QCA measurements are usually smaller than OCT [5-8]. Our aim was to assess the correlation between 2D-QCA and OCT for coronary lumen dimensions prior to stent implantation and to quantify the agreement between the two modalities by Bland–Altman analysis. We hypothesized that if the QCA measurements are within 0.5 mm of the OCT measurement, then it would be considered as an acceptable agreement between the two modalities.

## 2. Methods

### 2.1. OCT acquisition

Patients undergoing OCT for various clinical indications at our institution were reviewed. The OCT acquisition was performed using the C7 Dragonfly™ intracoronary imaging catheter and the ILUMIEN™ PCI Optimization System (St. Jude Medical). All images were acquired using a non-occlusive technique with injection of isosmolar iodixonoal (Visipaque™ by GE healthcare) contrast using automatic injection to clear the vessel of blood [9]. The lesion was crossed using a routine angioplasty wire. The imaging catheter was then advanced over the wire. Once the catheter was positioned distal to the lesion it was pull backed using an automated motor at a speed of 15 mm/s.

☆ This work was performed at Royal North Shore Hospital, Sydney, Australia.

* Corresponding author at: The Canberra Hospital, Yamba Drive, Canberra, ACT, Australia. Tel.: +61 422040611.
*E-mail address:* Jawadmc2@gmail.com (J. Mazhar).

http://dx.doi.org/10.1016/j.ijcha.2015.01.011

### 2.2. 2D-QCA

2D-QCA was performed offline using automated software. Measurements were performed on image sequences adequately filled with contrast and when the vessel was not foreshortened. Calibration was performed on the contrast filled segment of the guiding catheter. Measurements were performed on the lesion of interest using the auto- mated software. Proximal and distal reference diameters were performed manually to measure the diameter of the normal segment of the vessel.

### 2.3. Measurements

Minimum luminal diameter (MLD), proximal reference diameter (PRD) and distal reference diameter (DRD) were measured for each lesion. PRD was defined as the diameter of the normal vessel proximally but within 10 mm of the lesion and DRD as the diameter of the normal vessel distally but within 10 mm of the lesion.

### 2.4. Lesions excluded

Lesions that were not suitable for analysis were excluded. OCT images with poor clearance of blood or inadequate short runs were excluded. Lesions that were dilated prior to performing OCT were excluded. Lesions with poor angiographic images not suitable for QCA were also excluded, e.g. foreshortened images or images with overlapping vessels.

### 2.5. Statistical analysis

Statistical analysis was performed using GraphPad Prism 6 for windows. Continuous variables are expressed as means. Means were compared using Student's $t$ test. A p value of b 0.05 was considered to be significant. The association between the measurements by QCA and OCT was tested by plotting a scatter plot and measuring the correlation coefficient 'r' by Pearson's method. Bland–Altman plots were construct- ed to test the agreement between the two methods by plotting the average of the QCA and OCT measurements on x axis and the difference between the QCA and OCT measurements on y axis.

## 3. Results

64 patients underwent OCT between November 2010 and August 2012. 40 lesions in 38 patients were suitable for analysis by QCA and OCT. Mean age was 68 years with 28 males and 10 females. Majority of the cases were done by radial approach (87%). Clinical presentations were stable angina (10), unstable angina (6), non-ST elevation myocardial infarction (14) and ST elevation myocardial infarction (8). Vessels assessed were left anterior descending artery (17), right coronary artery (8), circumflex artery (5), obtuse marginal (1) and saphenous vein graft (7).

### 3.1. Proximal reference diameter

30 lesions were suitable for measurement of PRD by QCA and OCT. There was no significant difference between the mean PRD measured by QCA and OCT (3.15 vs. 3.24 mm, p = 0.56), see Fig. 1a. There was a good correlation (r = 0.86, 95% confidence interval 0.72 to 0.93, p = b 0.0001) between QCA and OCT (Fig. 1b). Bland–Altman plot showed a bias of −0.09 mm with 95% confidence interval from −0.52 to 0.53 mm, suggesting that on average the PRD by QCA was 0.09 mm smaller than that by OCT (Fig. 1c).

### 3.2. Distal reference diameter

28 lesions were suitable for measurement of DRD by QCA and OCT. There was no significant difference between the mean DRD measured by QCA and OCT (3.25 vs. 3.35 mm, p = 0.66), see Fig. 2a. There was a good correlation (r = 0.92, 95% confidence interval 0.84 to 0.96, p = b 0.0001) between QCA and OCT (Fig. 2b). Bland–Altman plot showed a bias of −0.1 mm with 95% confidence interval from −0.59 to 0.6 mm, suggesting that on average the DRD by QCA was 0.1 mm smaller than that by OCT (Fig. 2c).

### 3.3. Minimum luminal diameter

37 lesions were suitable for measurement of MLD by QCA and OCT. There was a satisfactory correlation (r = 0.63, 95% confidence interval 0.38 to 0.79, p = b 0.0001) between QCA and OCT, however the mean MLD measured by QCA was significantly lower compared to OCT (1.40 vs. 1.90 mm, p = 0.001), see Fig. 3a and b. Bland–Altman plot showed a bias of −0.49 mm with 95% confidence interval from −1.57 to 0.59 mm, suggesting that on average the MLD by QCA was 0.49 mm smaller than that by OCT (Fig. 3c). Hence there was a poor agreement for estimation of MLD.

## 4. Discussion

Visual estimation is commonly used to quantify the severity of a coronary artery lesion in the catheterization laboratory but is limited by significant inter-observer variability [10]. QCA is more precise than visual estimation and has less inter-observer variability [11,12]. It has been in use as a clinical and research tool since the 1980s [12]. It uses automated edge detection software to detect the contrast filled lumen of the coronary artery [12].

OCT and IVUS are the two main intra-coronary imaging modalities in clinical use. Unlike IVUS which uses ultrasound waves, OCT creates an image by directing an optical beam of infrared light onto the tissue and measuring the reflected intensity of light [13]. It has a resolution of 10–20 μm which is 10 times higher than IVUS [13]. In an ex-vivo study assessing coronary lumen dimensions, IVUS and OCT

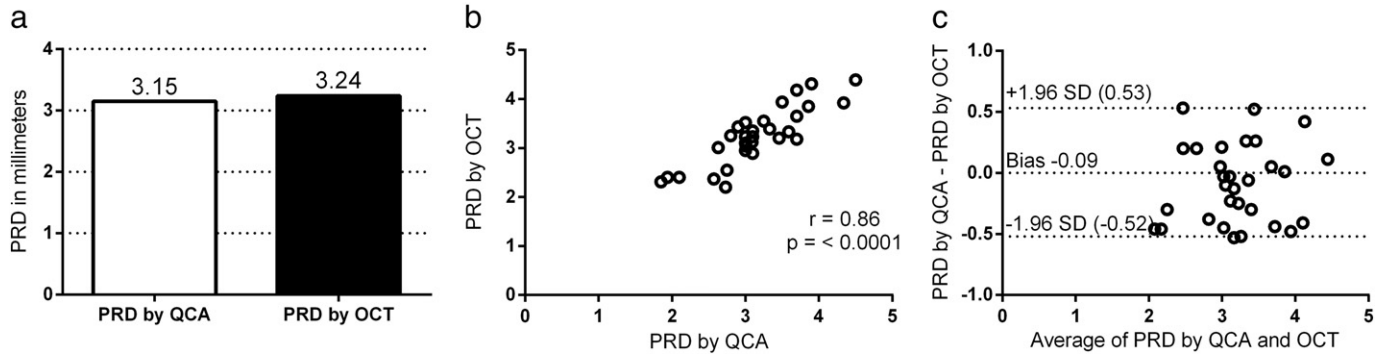


Fig. 1. Fig. 1a shows the mean PRD by QCA and OCT, p = 0.65. Fig. 1b shows a scatter plot of the correlation between QCA and OCT for PRD. Fig. 1c shows the Bland–Altman plot for PRD. PRD = proximal reference diameter, QCA = quantitative coronary angiography, OCT = optical coherence tomography.

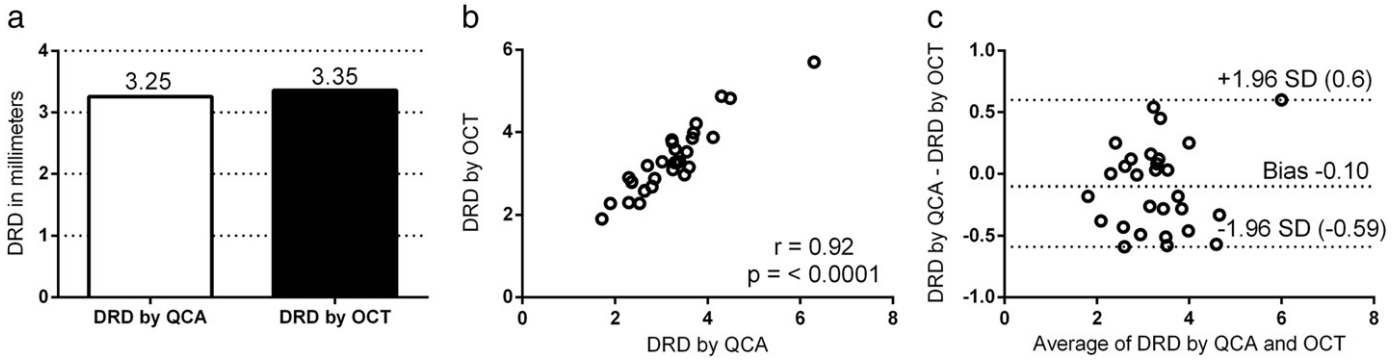


Fig. 2. Fig. 2a shows the mean DRD by QCA and OCT, p = 0.66. Fig. 2b shows a scatter plot of the correlation between QCA and OCT for PRD. Fig. 2c shows the Bland–Altman plot for PRD. DRD = distal reference diameter, QCA = quantitative coronary angiography, OCT = optical coherence tomography.

measurements were larger than histologic specimens, but this may have been due to tissue shrinkage when preparing specimens for histology [4]. In clinical studies, OCT measurements are usually smaller than IVUS and QCA measurements even smaller than OCT [4-6]. In a study using a phantom model of known dimension, OCT measured the lumen area accurately while IVUS overestimated the lumen area [14]. This may be due to poor border detection by IVUS, whereas, OCT has the advantage of higher resolution with a clear lumen to vessel interface [15] (15). Hence, OCT is emerging as the new gold standard for measuring coronary lumen dimensions. It also has less inter-observer variability than IVUS in measuring lumen dimensions [14,16].

Proximal and distal reference diameters are crucial dimensions needed for selecting the appropriate stent size during coronary angioplasty. This is even more important when selecting bioresorbable vascular scaffolds (BVS), due to their limited distensibility [17]. Previous studies comparing OCT and 2D-QCA show a good correlation, but how well the two agree with each other has not been well studied [5,8]. This study shows a good correlation and agreement between 2D-QCA and OCT for estimating PRD and DRD. There was no significant difference in the mean PRD and DRD in both groups. On average, the PRD by 2D-QCA was 0.09 mm smaller and the DRD by 2D-QCA was 0.1 mm smaller than the OCT measurements. Importantly, most of the reference diameter measurements by 2D-QCA were within 0.5 mm of the OCT measurements. Although OCT is the gold standard in measuring coronary lumen dimensions, this study shows that in the absence or non-availability of OCT, 2D-QCA can be used to estimate reference vessel diameters for sizing of stent prior to angioplasty. This is also supported by the ABSORB EXTEND study in which mandatory use of QCA prior to implantation of BVS showed a reduction in the undersizing of BVS [17].

QCA has the advantage of being non-invasive, inexpensive and less time consuming. The main technical challenge with QCA is selection of an appropriate image sequence. The accuracy of QCA is improved by selecting an image with minimal foreshortening and minimal overlap with other vessels or other radio-opaque structures [12].

The MLD measured by QCA was significantly smaller compared to OCT. On average the MLD by QCA was 0.49 mm smaller than the OCT measurements. The possible reasons for this difference may be poor border detection by QCA or foreshortening of the image or incomplete filling of the vessel with contrast.

### 4.1. Limitations

Although the reference diameters on the two modalities were matched as closely as possible, the measurements were not done at exactly the same point in the vessel, as it was not possible to make an exact match. However, the measurements were done as it would be in routine clinical practice to measure the reference diameters for a lesion. Lesion lengths were not measured as it was difficult to correlate exactly the start and end of a lesion on the two modalities. However, fusion technology is now available that can match QCA with IVUS or OCT and allows exact correlation of plaque seen on angiography with IVUS or OCT [18,19].

## 5. Conclusion

There is a good correlation and agreement between QCA and OCT for measurement of proximal and distal reference diameters of a lesion. There was no significant difference in the mean proximal and distal reference diameters in both groups. The MLD was underestimated by QCA.

## Conflict of interest

None.

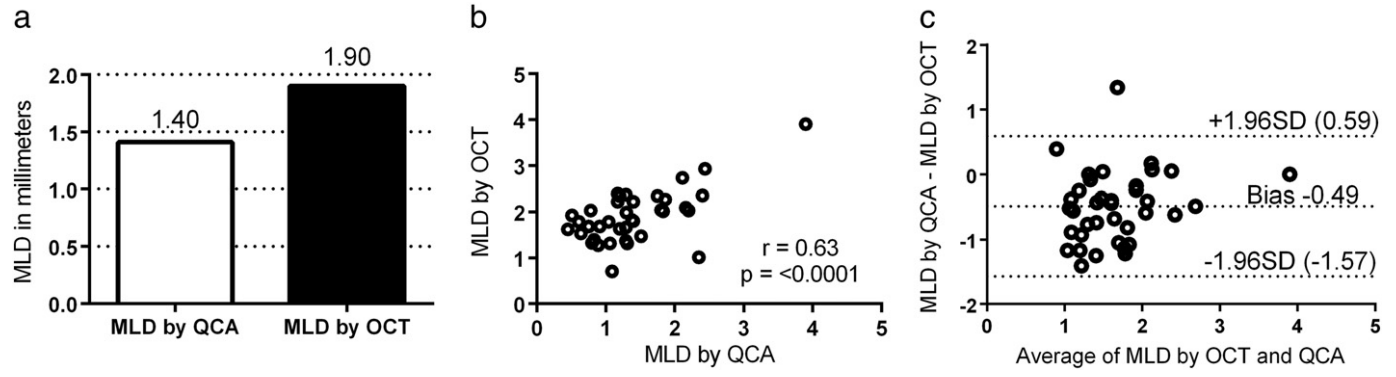


Fig. 3. Fig. 3a shows the mean MLD by QCA and OCT, p = 0.001. Fig. 3b shows a scatter plot of the correlation between QCA and OCT for MLD. Fig. 3c shows the Bland–Altman plot for MLD. MLD = minimum luminal diameter, QCA = quantitative coronary angiography, OCT = optical coherence tomography.

## Acknowledgement

We would like to acknowledge the radiographers at our department, especially chief radiographer Nadeem Mughal for maintaining the imaging database.

## References

[1] Costa MA, Angiolillo DJ, Tannenbaum M, Driesman M, Chu A, Patterson J, et al. Impact of stent deployment procedural factors on long-term effectiveness and safety of sirolimus-eluting stents (final results of the multicenter prospective STLLR trial). Am J Cardiol Jun 15 2008;101(12):1704-11 [PubMed PMID: 18549844. Epub 2008/06/14. eng].

[2] Lemos PA, Saia F, Ligthart JM, Arampatzis CA, Sianos G, Tanabe K, et al. Coronary restenosis after sirolimus-eluting stent implantation: morphological description and mechanistic analysis from a consecutive series of cases. Circulation Jul 22 2003;108(3):257-60 [PubMed PMID: 12860901. Epub 2003/07/16. eng].

[3] Aminian A, Kabir T, Eeckhout E. Treatment of drug-eluting stent restenosis: an emerging challenge. Catheter Cardiovasc Interv Jul 1 2009;74(1):108-16 [PubMed PMID: 19199365. Epub 2009/02/10. eng].

[4] Gonzalo N, Serruys PW, Garcia-Garcia HM, van Soest G, Okamura T, Ligthart J, et al. Quantitative ex vivo and in vivo comparison of lumen dimensions measured by optical coherence tomography and intravascular ultrasound in human coronary arteries. Rev Esp Cardiol Jun 2009;62(6):615-24 [PubMed PMID: 19480757. Epub 2009/06/02. Eng spa].

[5] Okamura T, Onuma Y, Garcia-Garcia HM, van Geuns RJ, Wykrzykowska JJ, Schultz C, et al. First-in-man evaluation of intravascular optical frequency domain imaging (OFDI) of Terumo: a comparison with intravascular ultrasound and quantitative coronary angiography. EuroIntervention Apr 2011;6(9):1037-45 [PubMed PMID: 21518674. Epub 2011/04/27. eng].

[6] Puri R, Nelson AJ, Liew GY, Nicholls SJ, Carbone A, Wong DT, et al. Variations in coronary lumen dimensions measured in vivo. JACC Cardiovasc Imaging Jan 2012;5(1): 123–4 [PubMed PMID: 22239902. Epub 2012/01/14. eng].

[7] Tu S, Xu L, Ligthart J, Xu B, Witberg K, Sun Z, et al. In vivo comparison of arterial lumen dimensions assessed by co-registered three-dimensional (3D) quantitative coronary angiography, intravascular ultrasound and optical coherence tomography. Int J Cardiovasc Imaging Aug 2012;28(6):1315-27 [PubMed PMID: 22261998. Pubmed Central PMCID: PMC3463784. English].

[8] Gutierrez-Chico JL, Serruys PW, Girasis C, Garg S, Onuma Y, Brugaletta S, et al. Quantitative multi-modality imaging analysis of a fully bioresorbable stent: a head-to-head comparison between QCA, IVUS and OCT. Int J Cardiovasc Imaging Mar 2012;28(3):467-78 [PubMed PMID: 21359517. Pubmed Central PMCID: PMC3326362. English].

[9] Prati F, Cera M, Ramazzotti V, Imola F, Giudice R, Albertucci M. Safety and feasibility of a new non-occlusive technique for facilitated intracoronary optical coherence tomography (OCT) acquisition in various clinical and anatomical scenarios. EuroIntervention Nov 2007;3(3):365-70 [PubMed PMID: 19737719. Epub 2007/11/01. eng].

[10] Shub C, Vlietstra RE, Smith HC, Fulton RE, Elveback LR. The unpredictable progression of symptomatic coronary artery disease: a serial clinical–angiographic analysis. Mayo Clin Proc Mar 1981;56(3):155-60 [PubMed PMID: 7206792. Epub 1981/03/01. eng].

[11] Goldberg RK, Kleiman NS, Minor ST, Abukhalil J, Raizner AE. Comparison of quantitative coronary angiography to visual estimates of lesion severity pre and post PTCA. Am Heart J Jan 1990;119(1):178-84 [PubMed PMID: 2404387. Epub 1990/01/01. eng].

[12] Garrone P, Biondi-Zoccai G, Salvetti I, Sina N, Sheiban I, Stella PR, et al. Quantitative coronary angiography in the current era: principles and applications. J Interv Cardiol Dec 2009;22(6):527-36 [PubMed PMID: 19627430. English].

[13] Lowe HC, Narula J, Fujimoto JG, Jang IK. Intracoronary optical diagnostics current status, limitations, and potential. JACC Cardiovasc Interv Dec 2011;4(12):1257-70 [PubMed PMID: 22192367. Epub 2011/12/24. eng].

[14] Kubo T, Akasaka T, Shite J, Suzuki T, Uemura S, Yu B, et al. OCT compared with IVUS in a coronary lesion assessment: the OPUS-CLASS study. JACC Cardiovasc Imaging Oct 2013;6(10):1095-104 [PubMed PMID: 24011777. Epub 2013/09/10. eng].

[15] Guagliumi G, Virmani R. The race to achieve the gold standard in coronary imaging. Rev Esp Cardiol Jun 2009;62(6):599-602 [PubMed PMID: 19480754. Epub 2009/06/02. Eng spa].

[16] Abnousi F, Waseda K, Kume T, Otake H, Kawarada O, Yong CM, et al. Variability in quantitative and qualitative analysis of intravascular ultrasound and frequency domain optical coherence tomography. Catheter Cardiovasc Interv Sep 1 2013; 82(3):E192–9 [PubMed PMID: 23412754. Epub 2013/02/16. eng].

[17] Farooq V, Gomez-Lara J, Brugaletta S, Gogas BD, Garcia-Garcia HM, Onuma Y, et al. Proximal and distal maximal luminal diameters as a guide to appropriate deployment of the ABSORB everolimus-eluting bioresorbable vascular scaffold: a sub-study of the ABSORB Cohort B and the on-going ABSORB EXTEND Single Arm Study. Catheter Cardiovasc Interv May 1 2012;79(6):880-8 [PubMed PMID: 22514149. Epub 2012/04/20. eng].

[18] Schuurbiers JC, Lopez NG, Ligthart J, Gijsen FJ, Dijkstra J, Serruys PW, et al. In vivo validation of CAAS QCA-3D coronary reconstruction using fusion of angiography and intravascular ultrasound (ANGUS). Catheter Cardiovasc Interv Apr 1 2009; 73(5):620-6 [PubMed PMID: 19309696. Epub 2009/03/25. eng].

[19] Tu S, Holm NR, Koning G, Huang Z, Reiber JH. Fusion of 3D QCA and IVUS/OCT. Int J Cardiovasc Imaging Feb 2011;27(2):197-207 [PubMed PMID: 21264684. Pubmed Central PMCID: PMC3078305. English].

# **Chapter 6.** Progression of coronary atherosclerosis in patients without standard modifiable risk factors


## Summary:

There has been an increase in the prevalence of myocardial infarction in patient who have no standard modifiable cardiovascular risk factors i.e., diabetes, hypertension, hyperlipidemia, and current smoker. Large observational studies have shown that these patients have higher in-hospital and 30-day mortality rates after myocardial infarction compared to patients with at least one of the major 4 modifiable risk factors. Intravascular ultrasound (IVUS) permits quantification of coronary atheroma burden. Patients without standard modifiable risk factors have not been well studied in randomized clinical trials. In this chapter I analysed serial IVUS data from a pooled cohort of 5823 patients enrolled in ten randomized clinical trials to examine rates of plaque progression in patients who had no standard modifiable risk factors versus individuals with risk factors who were matched on age, sex and use of statins. Patients without traditional risk factors demonstrated a 2.3% lower degree of plaque burden. Degree of calcification was 4.3% less than those with at least one SMuRF. The rate of plaque progression was similar to patients with risk factors. Despite having lower plaque burden, these patients still had clinical events which requires further studies to identify unknown risk factors that increase susceptibility to atherosclerosis.

American Journal of Preventive Cardiology 4 (2020) 100116

Contents lists available at ScienceDirect

American Journal of Preventive Cardiology

journal homepage: www.journals.elsevier.com/the-american-journal-of-preventive-cardiology

Original Research

# Progression of coronary atherosclerosis in patients without standard modifiable risk factors

Jawad Mazhar [a], Gemma Figtree [a], Stephen T. Vernon [a], Keyvan Karimi Galougahi [b], Julie Carlo [c], Steven E. Nissen [c], Stephen J. Nicholls [d,*]

[a] Kolling Research Institute, University of Sydney, Sydney, Australia
[b] Royal Prince Alfred Hospital, Camperdown, Australia
[c] CSResearch, Department of Cardiovascular Medicine, Heart, Vascular, and Thoracic Institute, Cleveland Clinic, Australia
[d] Monash Cardiovascular Research Centre, Victorian Heart Institute, Monash University, Australia

ARTICLE INFO

*Keywords:*
Atherosclerosis
Coronary artery disease
Intravascular ultrasound (IVUS)
Standard modifiable risk factors

ABSTRACT

*Background and aims:* The outcome of patients with clinical coronary artery disease despite traditional risk factors is poorly understood.

*Methods:* Clinical characteristics and plaque burden on serial intravascular ultrasonography were compared in patients without (n = 165) and with (n = 492) standard modifiable risk factors after matching on age, sex and use of statins from a database of 5823 patients participating in clinical trials of anti-atherosclerotic therapies.

*Results:* Patients without standard modifiable risk factors had lower baseline systolic blood pressure (118 ± 12 vs. 129 ± 17 mmHg, $p < 0.001$), low-density lipoprotein cholesterol (87 ± 21 vs. 104 ± 34 mg/dl, $p < 0.001$), triglycerides [106 vs. 136 mg/dl, $p < 0.001$)] and *C*-reactive protein [1.5 vs. 2.1 mg/l, $p = 0.001$]. At baseline, patients without modifiable risk factors had a lower percent atheroma volume (35.7 ± 8.6 vs. 38 ± 8.8%, $p = 0.004$) and total atheroma volume (174.7 ± 80 vs. 190.9 ± 84 $mm^3$, $p = 0.03$) and less images with calcification (22.2 vs. 26.5%, $p = 0.025$). The use of aspirin and statin prior to and during the trials was similar. The use of ACE inhibitors and beta blockers was lower in the no risk factor group prior to and during the trials. The change in percent atheroma volume (−0.2 ± 2.8 vs. −0.1 ± 3.6%, $p = 0.71$), total atheroma volume (−5.5 ± 23.4 vs. −3.8 ± 22.7 $mm^3$, $p = 0.42$), and the percentage of patients demonstrating any degree of progression (50.9% vs 45.1%, $p = 0.20$) were similar in those without and with standard modifiable risk factors, respectively.

*Conclusion:* Patients who develop clinical coronary atherosclerosis without standard modifiable risk factors have similar rates of plaque progression to those with traditional risk factors.

## 1. Introduction

Despite the common perception that coronary artery disease (CAD) is well understood and managed, it remains the leading cause of mortality in adults worldwide [1]. Major advances have been made in the identification and treatment of standard modifiable risk factors for CAD - particularly hypercholesterolemia, hypertension, diabetes mellitus and smoking [2,3]. However, at an individual level, it is not uncommon for a patient to present with extensive atherosclerosis and acute coronary syndrome that is not clearly explained by such risk factors. We have previously reported an increase in prevalence of myocardial infarction patients presenting with no standard modifiable cardiovascular risk factors from 13% to 27% over a 10 year period [4], confirmed by findings of a large, nation-wide cohort [5].

Despite the perceived low risk of CAD in patients with no standard modifiable risk factors, large observational studies have shown that these patients have higher in-hospital and 30 day mortality rates after myocardial infarction compared to patients with at least one of the major 4 modifiable risk factors [5–8]. Data from the National Registry of Myocardial infarction demonstrated this relationship, even after adjusting for age and other clinical factors, and identified an inverse association between the number of standard modifiable risk factors and the risk for in-hospital mortality [7]. The reasons for these apparently paradoxical differences in the mortality rates following myocardial infarction are not well understood.

Intravascular ultrasound (IVUS) permits quantitation of coronary

* Corresponding author. Monash Cardiovascular Research Centre, 246 Clayton Road, Clayton, VIC, 3168, Australia.
*E-mail address:* stephen.nicholls@monash.edu (S.J. Nicholls).

https://doi.org/10.1016/j.ajpc.2020.100116
Received 16 September 2020; Received in revised form 11 October 2020; Accepted 18 October 2020

atheroma burden and on serial imaging has been employed to evaluate the impact of medical therapies on disease progression [9–16]. We utilised serial IVUS data from a pooled cohort of 5823 patients enrolled in ten clinical trials [10–19] to examine rates of plaque progression in patients who had no standard modifiable risk factors versus individuals with risk factors who were matched on age, sex and use of statins.

## 2. Materials & methods

The current analysis investigated a pooled cohort of 5823 patients with angiographic CAD who underwent serial IVUS imaging in ten clinical trials evaluating the impact of medical therapies on plaque progression, the details of which have been discussed previously [10–16]. Of the 5823 patients, we identified 214 to have no standard modifiable risk factors (3.7%), including smoking, hypertension, diabetes and hypercholesterolemia, recorded on the basis of self-reporting. On review of the baseline systolic blood pressure and lipids of the patients in the no risk factor group, it was noted that these were elevated in some patients. Out of the 214 patients, 49 were noted to have either systolic blood pressure of >140 mmHg or total cholesterol >213 mg/dl or LDL >135 mg/dl at baseline. These patients were excluded. For the purpose of this analysis, patients with no standard modifiable risk factors (n = 165) were compared with patients with at least one such risk factor after matching (3:1) on age, sex and use of statins during the trials (n = 492).

## 3. Acquisition of IVUS images

Patients were imaged with either a 40 MHz Atlantis SR Pro (Boston Scientific Scimed, Inc., Maple Grove, MN, USA) or a 45 MHz Revolution (Volcano Corporation, San Diego, CA, USA) catheter. The target vessel for imaging was required to have at least 20% but not more than 50% stenosis on the coronary angiogram, at least 30 mm in length, with no prior revascularization and not planned for revascularization. After appropriate anticoagulation and intra-coronary nitrate, the IVUS imaging catheter was advanced beyond the lesion into the distal segment of the coronary artery. A pullback was performed at a constant speed of 0.5 mm/s and a continuous image of the coronary artery was acquired at 30 frames per second. IVUS images were matched with the coronary angiogram by identifying the proximal and distal side branches. Follow up IVUS imaging, after 18–24 months, was performed in the same coronary segment by using these side branches as landmarks. Images were stored and sent to a core lab for analysis.

## 4. Analysis of IVUS images

For each pull back, cross sectional images spaced 1 mm apart were selected for measurement. For each selected cross-sectional image, the leading edge of the lumen and the external elastic membrane (EEM) were manually traced to measure the lumen area and EEM area. IVUS images were analysed in a core laboratory by personnel blinded to all patient characteristics and treatment status. A number of plaque measures were derived from this analysis.

Percent atheroma volume (PAV) was determined as the proportion of the whole vessel wall occupied by plaque throughout the entire length of artery studied [11].

$$PAV = \frac{\sum(EEM\ area - lumen\ area)}{\sum(EEM\ area)} \times 100$$

Total atheroma volume (TAV) was determined by summation of atheroma area in all evaluable cross-sectional images [11].

$$TAV = \sum(EEM\ area - lumen\ area)$$

To account for potential differences in segment length between patients, TAV was subsequently normalized, by multiplying the average plaque area in a segment by the median number of evaluable images for all patients in the study.

$$Normalised\ TAV = \frac{\sum(EEM\ area - lumen\ area)}{n} \times Median\ number\ of\ images\ in\ cochort$$

The quantitation of plaque calcium has been described previously [20]. The presence of calcium in each measured image was assigned a grade from 0 to 2. Grade 0 representing no calcium, grade 1 representing calcium with acoustic shadowing <90°, grade 2 representing calcium with shadowing >90°. In images that contained multiple calcium deposits, the grade represented the summation of all angles of acoustic shadows present. The degree of calcification is expressed as the percentage of images containing ≥1 grade of calcium. From serial imaging, changes in PAV and TAV were calculated as the difference from baseline to follow up and the percentage of images containing ≥1 grade of calcium at each time point were directly compared. The percentage of patients demonstrating any degree of progression or regression of either PAV or TAV were also determined.

## 5. Statistical analysis

Patients were identified with no standard modifiable risk factors (n = 165) and then those with at least one such risk factor were matched in a 3:1 fashion based on age, sex and use of statins during the trials (n = 492). These two groups were then compared on baseline clinical characteristics, use of secondary prevention medications, blood pressure, serum lipids, CRP, IVUS measurements, proportion of patients with >1 grade of calcium, and proportion of patients showing progression or regression. Continuous variables were compared between groups using Student's t-test or Wilcoxon rank-sum test, depending on if normally or non-normally distributed, respectively. Mean ± standard deviation or median (interquartile range) are reported. Changes from baseline were assessed to see if significantly different than zero using the paired *t*-test or Wilcoxon signed-rank test, as appropriate. Categorical variables were compared between the two risk factor groups using Pearson's chi-squared or Fisher's exact test. Percentages are reported. Annualized changes in IVUS measurements were compared between the two groups using mixed models adjusting for baseline counterparts and with trial set as a random factor to control for heterogeneity across the ten studies. Least-squares means ± standard error are reported. Given that each trial's duration varied from 18 to 24 months, annualized change in PAV is the interpolated value of change in PAV at 1 year. All tests were two-tailed with a significance level of 0.05. Analyses were performed using SAS software, version 9.4 (SAS Institute, Cary, NC, USA).

## 6. Results

### 6.1. Clinical characteristics

Baseline demographics and medications are shown in Table 1 for patients with no risk factors matched on age (mean 55.7 ± 9.4 years), sex (17% females) and use of statins during the trials (93.9 vs. 94.1%, $p$ = 0.78). Patients with at least one standard modifiable risk factor were more likely to have a history of congestive heart failure (3.9 vs. 0.6%, $p$ = 0.035) or to have undergone prior percutaneous coronary intervention (36 vs 22%, $p = 0.001$) compared to those with no identifiable risk factors. Baseline use of aspirin (94.5 vs 91.7%, $p = 0.23$) and statins (74.5 vs. 77.4%, $p = 0.45$) was similar between the two groups but use of baseline beta blockers (61.8 vs. 74.6%, $p = 0.002$) and ACE inhibitors (29.7% vs. 51.8%, $p < 0.001$) was lower in patients without standard modifiable risk factors. The use of aspirin (96.4 vs. 92.1%, $p = 0.06$) and statins (93.9 vs. 94.5%, $p = 0.78$) during the trials was similar in both groups. The use of beta blockers (57.6 vs. 76.6%, $p < 0.001$) and ACE inhibitors (34.5 vs. 55.7%, $p < 0.001$) was lower in patients without standard modifiable risk factors during the trials.

**Table 1**
Demographics and medications at baseline. Results expressed as mean ± SD or percentage.

| Parameter | No Risk Factors n = 165 | Risk Factors n = 492 | *p*-value |
|---|---|---|---|
| Age, years | 55.7 ± 9.4 | 55.7 ± 9.4 | 0.99 |
| Female, % | 17.0 | 16.5 | 0.88 |
| Caucasian, % | 96.4 | 93.3 | 0.15 |
| Current Smoker | 0 | 31.0 | <0.001 |
| BMI, kg/m$^2$ | 28.6 ± 4.7 | 30.6 ± 5.7 | <0.001 |
| Hypertension, % | 0 | 81.7 | <0.001 |
| Diabetes, % | 0 | 28.5 | <0.001 |
| Hyperlipidemia, % | 0 | 77.8 | <0.001 |
| Angina, % | 31.5 | 45.7 | 0.002 |
| History of CHF, % | 0.6 | 3.9 | 0.035 |
| History of MI, % | 34.5 | 30.9 | 0.38 |
| History of stroke, % | 0 | 2.2 | 0.07 |
| History of PCI, % | 21.8 | 36.4 | 0.001 |
| History of CABG, % | 1.8 | 1.9 | 1.0 |
| Medication use prior to study entry | | | |
| Aspirin, % | 94.5 | 91.7 | 0.23 |
| Statins, % | 74.5 | 77.4 | 0.45 |
| Beta Blockers, % | 61.8 | 74.6 | 0.002 |
| ACE Inhibitors, % | 29.7 | 51.8 | <0.001 |
| Medication use during studies | | | |
| Aspirin, % | 96.4 | 92.1 | 0.06 |
| Statins, % | 93.9 | 94.5 | 0.78 |
| Beta Blockers, % | 57.6 | 76.6 | <0.001 |
| ACE Inhibitors, % | 34.5 | 55.7 | <0.001 |

ACE inhibitors = Angiotensin converting enzyme inhibitors, CHF = Congestive heart failure, CABG = Coronary artery bypass graft, MI = Myocardial infarction, PCI = percutaneous coronary intervention, SD = standard deviation.

### 6.2. Metabolic and BP parameters

Risk factor control is summarized in Table 2. Patients without standard modifiable risk factors had lower baseline levels of LDL cholesterol (87.4 ± 20.5 vs. 103.6 ± 34.3 mg/dl, $p < 0.001$), triglycerides [106.2 (75.6, 150.5) vs. 136 (101, 197) mg/dl, ($p < 0.001$)], systolic (118 ± 12 vs. 129 ± 17 mmHg, $p < 0.001$) and diastolic (73.7 ± 8.2 vs. 77.3 ± 9.8 mmHg, $p < 0.001$) blood pressure, and a higher HDL cholesterol (44.9 ± 11.9 vs. 42.8 ± 11.6 mg/dl, $p = 0.05$). During the course of the studies, patients without risk factors had a greater increase in systolic blood pressure (2.9 ± 12 vs. 0.3 ± 15, $p = 0.04$) and HDL cholesterol (9.5 ± 13.7 vs. 4.4 ± 9.8 mg/dl, $p < 0.001$) and a lesser reduction in LDL cholesterol (−11.0 ± 26.8 vs. −23.9 ± 38.3 mg/dl, $p < 0.001$) compared to patients with risk factors. Patients with standard modifiable risk factors had higher hsCRP levels at baseline [2.1 (1.0, 4.8) vs. 1.5 (0.8, 3.2) mg/l, $p = 0.001$] however the change in hsCRP was similar in both groups during the studies [-0.2 (−1.4, 0.5) vs. −0.1 (−0.9, 0.4) mg/l, $p = 0.38$].

### 6.3. Plaque burden and progression

Measures of plaque burden and calcification at baseline and serial changes are summarized in Table 3. At baseline, patients without standard modifiable risk factors demonstrated a lower PAV (35.7 ± 8.6 vs. 38.0 ± 8.8%, $p = 0.004$) and TAV (174.7 ± 80.2 vs. 190.9 ± 84.2 mm$^3$, $p = 0.03$) compared with those with at least one risk factor. Similar reductions in PAV (−0.2 ± 2.8 vs. −0.1 ± 3.6%, $p = 0.71$) and TAV (−5.5 ± 23.4 vs. −3.8 ± 22.7 mm$^3$, $p = 0.42$), as well as the percentage of patients demonstrating any degree of regression of plaque (49.1 vs. 54.9%, $p = 0.20$) with study treatment were observed in patients without and with modifiable risk factors. Patients without standard modifiable risk factors had less plaque calcification [22.2 (5.1, 38.5) vs. 26.5 (10.9, 45.8) %, $p = 0.025$], however a similar change in plaque calcification [(1.4 (0.0, 6.9) vs. 2.5 (0, 8.1)%, $p = 0.51$] was observed compared to patients with risk factors, respectively. Results were similarly non-significant in comparing the adjusted annualized changes between groups.

**Table 2**
Blood pressure, Lipids and CRP at baseline and follow up. Results expressed as mean ± SD or median (interquartile range).

| Parameter | No Risk Factors n = 165 | Risk Factors n = 492 | *p*-value |
|---|---|---|---|
| Systolic blood pressure (mmHg) | | | |
| Baseline | 118 ± 12 | 129 ± 17 | <0.001 |
| Follow-up | 121 ± 11 | 129 ± 13 | <0.001 |
| Absolute change | 2.9 ± 12 | 0.3 ± 15 | 0.04 |
| *P* value for change within group | 0.003 | 0.69 | |
| Diastolic blood pressure (mmHg) | | | |
| Baseline | 73.7 ± 8.2 | 77.3 ± 9.8 | <0.001 |
| Follow-up | 74.8 ± 7.4 | 77.3 ± 7.8 | <0.001 |
| Absolute change | 1.2 ± 8.1 | 0 ± 9.4 | 0.15 |
| *P* value for change within group | 0.065 | 0.99 | |
| LDL cholesterol (mg/dL) | | | |
| Baseline | 87.4 ± 20.5 | 103.6 ± 34.3 | <0.001 |
| Follow-up | 76.4 ± 22.2 | 79.9 ± 29.7 | 0.17 |
| Absolute change | −11.0 ± 26.8 | −23.9 ± 38.3 | <0.001 |
| *P* value for change within group | <0.001 | <0.001 | |
| HDL cholesterol (mg/dL) | | | |
| Baseline | 44.9 ± 11.9 | 42.8 ± 11.6 | 0.052 |
| Follow-up | 54.3 ± 19.0 | 47.3 ± 14.3 | <0.001 |
| Absolute change | 9.5 ± 13.7 | 4.4 ± 9.8 | <0.001 |
| *P* value for change within group | <0.001 | <0.001 | |
| Triglycerides (mg/dL) | | | |
| Baseline | 106.2 (75.6, 150.5) | 136 (101, 197) | <0.001 |
| Follow-up | 99.9 (73.7, 135.8) | 131 (95.6, 175.7) | <0.001 |
| Absolute change | −2.5 (−27.6, 13.0) | −6 (−37.2, 22.0) | 0.42 |
| *P* value for change within group | 0.14 | <0.001 | |
| CRP (mg/L) | | | |
| Baseline | 1.5 (0.8, 3.2) | 2.1 (1.0, 4.8) | 0.001 |
| Follow-up | 1.2 (0.6, 2.9) | 1.7 (0.9, 3.7) | 0.005 |
| Absolute change | −0.1 (−0.9, 0.4) | −0.2 (−1.4, 0.5) | 0.38 |
| *P* value for change within group | 0.10 | <0.001 | |

BP = blood pressure, CRP = C-reactive protein, HDL = high density lipoprotein, LDL = low density Lipoprotein, TG = Triglycerides.

## 7. Discussion

The underlying pathology and clinical progression of coronary atherosclerosis in patients whose disease cannot be attributed to the presence of traditional risk factors has not been well studied. This study compared coronary plaque burden and longitudinal changes, as assessed by serial IVUS, in patients presenting with angiographic coronary disease in the presence and absence of established risk factors. We observed that while patients without traditional risk factors demonstrated a lower degree of both plaque burden and calcification, they demonstrated a similar response to patients with such risk factors, in terms of plaque progression with medical therapy. This suggests the absence of traditional risk factors does not impact the potential modifiability of atherosclerotic plaque in these patients.

Patients without traditional risk factors have been reported to account for 10–30% of patients in large observational studies of acute coronary syndromes [4–8]. A study of 542,008 patients presenting with their first myocardial infarction reported that in-hospital mortality inversely associated with the number of risk factors, a finding which persisted after adjusting for clinical variables, including age and sex [7]. The presence of traditional risk factors may also potentially influence the clinical presentation of acute coronary syndromes, with reports that patients with fewer risk factors are more likely to present with STEMI and cardiac arrest [21]. While the mechanisms underlying these worse outcomes in the acute setting remain to be understood, the current analysis permitted examination of plaque progression.

The ability to image atherosclerotic plaque in a serial fashion has permitted the opportunity to study the potential impact of both risk

**Table 3**
IVUS parameters: plaque burden, vessel wall dimension, calcification and progression. Results expressed as mean ± SD or median (interquartile range).

| Parameter | No Risk Factors n = 165 | Risk Factors n = 492 | p-value |
|---|---|---|---|
| Percent atheroma volume (%) | | | |
| Baseline | 35.7 ± 8.6 | 38.0 ± 8.8 | 0.004 |
| Follow up | 35.5 ± 8.8 | 37.9 ± 9.0 | 0.003 |
| Absolute change | −0.2 ± 2.8 | −0.1 ± 3.6 | 0.71 |
| P value for change within groups | 0.43 | 0.73 | |
| Adjusted annualized change[a] | −0.08 ± 0.17 | −0.02 ± 0.13 | 0.64 |
| Total atheroma volume ($mm^3$) | | | |
| Baseline | 174.7 ± 80.2 | 190.9 ± 84.2 | 0.03 |
| Follow up | 169.2 ± 82.5 | 187.1 ± 84.0 | 0.02 |
| Absolute change | −5.5 ± 23.4 | −3.8 ± 22.7 | 0.42 |
| P value for change within groups | 0.003 | <0.001 | |
| Adjusted annualized change[a] | −2.1 ± 1.1 | −2.0 ± 0.8 | 0.90 |
| EEM volume ($mm^3$) | | | |
| Baseline | 483.2 ± 169.6 | 500.1 ± 181.7 | 0.30 |
| Follow up | 470.4 ± 174.2 | 490.5 ± 178.9 | 0.21 |
| Absolute change | −12.8 ± 49.9 | −9.6 ± 39.7 | 0.41 |
| P value for change within groups | 0.001 | <0.001 | |
| Adjusted annualized change[a] | −3.9 ± 2.2 | −5.0 ± 1.5 | 0.63 |
| Lumen volume ($mm^3$) | | | |
| Baseline | 308.5 ± 109.1 | 309.2 ± 118.2 | 0.95 |
| Follow up | 301.2 ± 111.1 | 303.4 ± 116.5 | 0.83 |
| Absolute change | −7.3 ± 36.3 | −5.8 ± 33.2 | 0.63 |
| P value for change within groups | 0.01 | <0.001 | |
| Adjusted annualized change[a] | −2.1 ± 1.8 | −3.4 ± 1.2 | 0.40 |
| Percent of images with calcium ≥1 | | | |
| Baseline | 22.2 (5.1, 38.5) | 26.5 (10.9, 45.8) | 0.025 |
| Follow up | 26.4 (4.5, 44.4) | 31.3 (13.4, 50.5) | 0.03 |
| Absolute change | 1.4 (0.0, 6.9) | 2.5 (0, 8.1) | 0.51 |
| P value for change within groups | <0.001 | <0.001 | |
| PAV | | | |
| Progressors (%) | 50.9 | 45.1 | 0.20 |
| Regressors (%) | 49.1 | 54.9 | |

EEM = external elastic membrane, PAV = percent atheroma volume.
[a] Adjusting for trial and respective baseline measures. Least-squares means ± standard error reported.

factors and medical therapies on disease progression [9]. These studies have largely confirmed the importance of traditional risk factors associating with both disease burden and progression over time. For example, multiple studies have demonstrated the beneficial effects of lowering LDL cholesterol, while trials have reported variable effects of infusing HDL and that modest increases in HDL cholesterol levels associate with the beneficial effects of statins [9]. Increasing levels of blood pressure, including those within the prehypertensive range, associate with greater disease progression [22]. Diabetes is associated with more diffuse and extensive atherosclerotic plaque, with evidence of less regression in response to use of lipid lowering therapy [23]. Atherogenic dyslipidemia, as evidenced by the triglyceride/HDL cholesterol ratio, closely associates with disease progression in patients with diabetes [24]. The contribution of multiple metabolic risk factors to cardiovascular risk in diabetes is further supported by evidence that more intensive targeting of these parameters results in an incremental benefit on coronary atherosclerosis [9,25]. These studies reinforce the importance of traditional risk factors underlying atherosclerotic disease in many patients.

However, the absence of these risk factors in some patients presenting with myocardial infarction has stimulated the search to identify additional factors that may potentially influence the underlying disease within the artery wall. While increasing attention has highlighted the importance of inflammation in atherosclerosis, even in the absence of traditional risk factors [26], this was not an explanation for disease in those without risk factors, with lower levels of hsCRP in this group compared to patients with risk factors. Given that all patients in these studies had presented for a clinically indicated coronary angiogram, both the absence of traditional risk factors or the presence of less atherosclerotic plaque in this group did not prevent their clinical presentation. Further work will be required to determine what other factors may have driven the heightened susceptibility to atherosclerosis and clinical presentation in these individuals. For example, repetitive long term exposure to air pollution promotes atherosclerosis and increases the risk of myocardial infarction [27]. Genome wide association studies have identified more than 50 loci associated with risk of coronary artery disease and genetic risk score based on these alleles can identify individuals at high risk of coronary artery disease [28]. Interestingly, in subjects with high genetic risk, a favorable lifestyle can reduce the relative risk of coronary artery disease by 50% when compared with unfavorable lifestyle [28].

A number of caveats should be noted with regard to this analysis. Patients were selected from trials using different pharmacologic interventions which may have influenced the results, however, patients were taken from all 10 trials and this prevented any one therapy from predominating in the whole cohort. As the role of statins in lowering plaque progression is well established, therefore, both groups were matched for use of statins. Any further selection based on therapies was not possible as this would have significantly reduced the number of patients with no risk factors. All patients had undergone coronary angiography on the basis of a symptomatic presentation. It is uncertain whether the findings translate to the asymptomatic population. The studies employed IVUS imaging with measurements of plaque burden, the implications for measures of plaque composition are unknown. While several reports have demonstrated the association between disease burden and progression with cardiovascular events [29], the current analysis lacked power to directly compare clinical outcomes in the two groups. Differences in medication use were observed between the groups, which may reflect a potential clinical bias to undertreat patients without risk factors, despite the presence of clinically manifest coronary atherosclerosis. Importantly, these findings do suggest a similar degree of modifiability of disease when intensive risk factor targeted therapies are used. The distinction between patients with and without risk factors may not be binary but rather a graded continuous relationship. Sipahi et al. have demonstrated progression of coronary artery disease over a wide blood pressure range from 100 mmHg into the hypertensive range [22]. There may also be a variation in the degree of control of risk factors. Atheroma progression has been observed in patients with early diabetes even after achieving optimal glycemic control due to residual risk factors which emphasizes the need to control all risk factors [30]. Furthermore, studies with more intensive treatment of risk factors have demonstrated less progression of plaque and even regression [15,22].

In summary, the absence of traditional risk factors associates with less extensive atherosclerotic plaque in a cohort recruited with known clinically significant coronary disease. Whilst these patients were less likely to receive evidence-based therapies, the progression of their disease in serial IVUS evaluation appeared similar to the patients with risk factors. Increased use of evidence-based agents in these "low risk" patients may produce greater benefit, although this requires further investigation. This study highlights an ongoing need to better understand the factors that do influence the pathophysiology in these patients, in order to develop new strategies for cardiovascular disease prevention and treatments relevant to this group of patients and beyond.

## Author contributions

JM, GF, KK, SV and SJN contributed to the conception of the work. JM and JC contributed to data analysis. JM, GF and SJN drafted the manuscript. SEN critically revised the manuscript. All gave final approval and

agree to be accountable for all aspects of work ensuring integrity and accuracy.

## Declaration of interests

GF is supported by a National Health and Medical Research Council of Australia Practitioner Fellowship, as well as New South Wales Office of Health and Medical Research and Heart Research Australia. SV receives support from Heart Research Australia. SJN receives support as a Senior Principal Research Fellow from the National Health and Medical Research Council of Australia, is a recipient of a Principal Research Fellowship from the National Health and Medical Research Council of Australia and reports having received research support from AstraZeneca, Amgen Inc., Anthera, Eli Lilly, Novartis, Cerenis, The Medicines Company, Resverlogix, InfraReDx, Roche,Sanofi-Regeneron, and LipoScience; Consulting fees and honoraria from AstraZeneca, Eli Lilly, Anthera, Omthera, Merck, Takeda, Resverlogix, Sanofi-Regeneron, CSL Behring, Esperion, and Boehringer Ingelheim.

## References

[1] Piepoli MF, Hoes AW, Agewall S, Albus C, Brotons C, et al. 2016 European guidelines on cardiovascular disease prevention in clinical practice: the sixth joint task force of the European society of cardiology and other societies on cardiovascular disease prevention in clinical practice (constituted by representatives of 10 societies and by invited experts)Developed with the special contribution of the European association for cardiovascular prevention & rehabilitation (EACPR). Eur Heart J 2016;37(29):2315–81.

[2] Jellinger PS, Handelsman Y, Rosenblit PD, Bloomgarden ZT, Fonseca VA, et al. AMERICAN association OF clinical endocrinologists and AMERICAN college OF endocrinology guidelines for management OF dyslipidemia and prevention OF cardiovascular disease. Endocr Pract : official journal of the American College of Endocrinology and the American Association of Clinical Endocrinologists. 2017; 23(Suppl 2):1–87.

[3] Mahmood SS, Levy D, Vasan RS, Wang TJ. The Framingham Heart Study and the epidemiology of cardiovascular disease: a historical perspective. Lancet 2014; 383(9921):999–1008.

[4] Vernon ST, Coffey S, Bhindi R, Soo Hoo SY, Nelson GI, et al. Increasing proportion of ST elevation myocardial infarction patients with coronary atherosclerosis poorly explained by standard modifiable risk factors. European journal of preventive cardiology 2017;24(17):1824–30.

[5] Vernon ST, Coffey S, D'Souza M, Chow CK, Kilian J, et al. ST-Segment-Elevation myocardial infarction (STEMI) patients without standard modifiable cardiovascular risk factors-how common are they, and what are their outcomes? Journal of the American Heart Association 2019;8(21):e013296.

[6] Roe MT, Halabi AR, Mehta RH, Chen AY, Newby LK, et al. Documented traditional cardiovascular risk factors and mortality in non-ST-segment elevation myocardial infarction. Am Heart J 2007;153(4):507–14.

[7] Canto JG, Kiefe CI, Rogers WJ, Peterson ED, Frederick PD, et al. Number of coronary heart disease risk factors and mortality in patients with first myocardial infarction. Jama 2011;306(19):2120–7.

[8] Nauta ST, Deckers JW, van der Boon RM, Akkerhuis KM, van Domburg RT. Risk factors for coronary heart disease and survival after myocardial infarction. European journal of preventive cardiology 2014;21(5):576–83.

[9] Andrews J, Puri R, Kataoka Y, Nicholls SJ, Psaltis PJ. Therapeutic modulation of the natural history of coronary atherosclerosis: lessons learned from serial imaging studies. Cardiovasc Diagn Ther 2016;6(4):282–303.

[10] Nissen SE, Tuzcu EM, Brewer HB, Sipahi I, Nicholls SJ, et al. Effect of ACAT inhibition on the progression of coronary atherosclerosis. N Engl J Med 2006; 354(12):1253–63.

[11] Nissen SE, Nicholls SJ, Sipahi I, Libby P, Raichlen JS, et al. Effect of very high-intensity statin therapy on regression of coronary atherosclerosis: the ASTEROID trial. Jama 2006;295(13):1556–65.

[12] Nissen SE, Tardif JC, Nicholls SJ, Revkin JH, Shear CL, et al. Effect of torcetrapib on the progression of coronary atherosclerosis. N Engl J Med 2007;356(13):1304–16.

[13] Nissen SE, Nicholls SJ, Wolski K, Nesto R, Kupfer S, et al. Comparison of pioglitazone vs glimepiride on progression of coronary atherosclerosis in patients with type 2 diabetes: the PERISCOPE randomized controlled trial. Jama 2008; 299(13):1561–73.

[14] Nissen SE, Nicholls SJ, Wolski K, Rodes-Cabau J, Cannon CP, et al. Effect of rimonabant on progression of atherosclerosis in patients with abdominal obesity and coronary artery disease: the STRADIVARIUS randomized controlled trial. Jama 2008;299(13):1547–60.

[15] Nicholls SJ, Ballantyne CM, Barter PJ, Chapman MJ, Erbel RM, et al. Effect of two intensive statin regimens on progression of coronary disease. N Engl J Med 2011; 365(22):2078–87.

[16] Nicholls SJ, Puri R, Anderson T, Ballantyne CM, Cho L, et al. Effect of evolocumab on progression of coronary disease in statin-treated patients: the GLAGOV randomized clinical trial. Jama 2016;316(22):2373–84.

[17] Nicholls SJ, Bakris GL, Kastelein JJ, Menon V, Williams B, et al. Effect of aliskiren on progression of coronary disease in patients with prehypertension: the AQUARIUS randomized clinical trial. Jama 2013;310(11):1135–44.

[18] Nissen SE, Tuzcu EM, Schoenhagen P, Brown BG, Ganz P, et al. Effect of intensive compared with moderate lipid-lowering therapy on progression of coronary atherosclerosis: a randomized controlled trial. Jama 2004;291(9):1071–80.

[19] Brener SJ, Ivanc TB, Poliszczuk R, Chen M, Tuzcu EM, et al. Antihypertensive therapy and regression of coronary artery disease: insights from the comparison of amlodipine versus enalapril to limit occurrences of thrombosis (CAMELOT) and norvasc for regression of manifest atherosclerotic lesions by intravascular sonographic evaluation (NORMALISE) trials. Am Heart J 2006;152(6):1059–63.

[20] Nicholls SJ, Tuzcu EM, Wolski K, Sipahi I, Schoenhagen P, et al. Coronary artery calcification and changes in atheroma burden in response to established medical therapies. J Am Coll Cardiol 2007;49(2):263–70.

[21] Wang JY, Goodman SG, Saltzman I, Wong GC, Huynh T, et al. Cardiovascular risk factors and in-hospital mortality in acute coronary syndromes: insights from the Canadian global Registry of acute coronary events. Can J Cardiol 2015;31(12): 1455–61.

[22] Sipahi I, Tuzcu EM, Schoenhagen P, Wolski KE, Nicholls SJ, et al. Effects of normal, pre-hypertensive, and hypertensive blood pressure levels on progression of coronary atherosclerosis. J Am Coll Cardiol 2006;48(4):833–8.

[23] Nicholls SJ, Tuzcu EM, Kalidindi S, Wolski K, Moon KW, et al. Effect of diabetes on progression of coronary atherosclerosis and arterial remodeling: a pooled analysis of 5 intravascular ultrasound trials. J Am Coll Cardiol 2008;52(4):255–62.

[24] Musunuru K. Atherogenic dyslipidemia: cardiovascular risk and dietary intervention. Lipids 2010;45(10):907–14.

[25] Nicholls SJ, Tuzcu EM, Wolski K, Bayturan O, Lavoie A, et al. Lowering the triglyceride/high-density lipoprotein cholesterol ratio is associated with the beneficial impact of pioglitazone on progression of coronary atherosclerosis in diabetic patients: insights from the PERISCOPE (Pioglitazone Effect on Regression of Intravascular Sonographic Coronary Obstruction Prospective Evaluation) study. J Am Coll Cardiol 2011;57(2):153–9.

[26] Ridker PM, Cook N. Clinical usefulness of very high and very low levels of C-reactive protein across the full range of Framingham Risk Scores. Circulation 2004; 109(16):1955–9.

[27] Rajagopalan S, Al-Kindi SG, Brook RD. Air pollution and cardiovascular disease: JACC state-of-the-art review. J Am Coll Cardiol 2018;72(17):2054–70.

[28] Khera AV, Emdin CA, Drake I, Natarajan P, Bick AG, et al. Genetic risk, adherence to a healthy lifestyle, and coronary disease. N Engl J Med 2016;375(24):2349–58.

[29] Forbes C, Quek RG, Deshpande S, Worthy G, Ross J, et al. Relationship between changes in coronary atherosclerotic plaque burden measured by intravascular ultrasound and cardiovascular disease outcomes: a systematic literature review. Curr Med Res Opin 2016;32(6):1143–50.

[30] Kataoka Y, Yasuda S, Miyamoto Y, Sase K, Kosuge M, et al. Clinical predictors of atheroma progression despite optimal glycemic control in early-stage diabetic patients with coronary artery disease: insight from the DIANA study. J Atherosclerosis Thromb 2014;21(5):509–18.

# **Chapter 7.** Cardiovascular magnetic resonance characteristics and clinical outcomes of patients with ST-elevation myocardial infarction and no Standard Modifiable Risk Factors - A DANAMI-3 substudy.


## Summary:

In chapter 6, we examined the plaque burden and rates of plaque progression in patients with no standard modifiable risk factors. In order to understand the potential mechanism of higher mortality in these patients in observational studies, this chapter evaluates the clinical outcomes and CMR imaging characteristics of patients with and without SMuRFs who presented with first-presentation STEMI. We collaborated with physicians from major tertiary centres in Denmark. The Third DANish Study of Optimal Acute Treatment of Patients with ST-Segment Elevation Myocardial Infarction (DANAMI-3) trial programme consists of three randomized controlled STEMI trials performed at four large centres in Denmark. Patients from DANAMI-3 were classified into those with no SMuRFs vs. those with at least one SMuRF. There was no difference in 30-day mortality however SMuRFless patients had a larger infarct size and a smaller myocardial salvage index. This association was mediated by a larger proportion of left anterior descending artery (LAD) culprits and poor TIMI flow pre-PCI. Interestingly, the proportion of patients with culprit LAD and TIMI 0-1 flow pre-PCI was significantly higher in SMuRFless patients. Whether SMuRFless patients truly have a higher predisposition for the involvement of LAD and if there are any biological mechanisms predisposing them to a higher incidence of poor flow (TIMI 0-1) pre-PCI requires further investigation.

frontiers | Frontiers in Cardiovascular Medicine

TYPE Original Research
PUBLISHED 03 August 2022
DOI 10.3389/fcvm.2022.945815



OPEN ACCESS

EDITED BY
Alessia Gimelli,
Gabriele Monasterio Tuscany Foundation (CNR), Italy

REVIEWED BY
Federico Fortuni,
Leiden University Medical Center, Netherlands
Giuseppe Muscogiuri,
Italian Auxological Institute (IRCCS), Italy

*CORRESPONDENCE
Gemma A. Figtree
gemma.figtree@sydney.edu.au

SPECIALTY SECTION
This article was submitted to Cardiovascular Imaging, a section of the journal Frontiers in Cardiovascular Medicine

RECEIVED 17 May 2022
ACCEPTED 30 June 2022
PUBLISHED 03 August 2022

CITATION
Mazhar J, Ekström K, Kozor R, Grieve SM, Nepper-Christensen L, Ahtarovski KA, Kelbæk H, Høfsten DE, Køber L, Vejlstrup N, Vernon ST, Engstrøm T, Lønborg J and Figtree GA (2022) Cardiovascular magnetic resonance characteristics and clinical outcomes of patients with ST-elevation myocardial infarction and no standard modifiable risk factors–A DANAMI-3 substudy. *Front. Cardiovasc. Med.* 9:945815. doi: 10.3389/fcvm.2022.945815



# Cardiovascular magnetic resonance characteristics and clinical outcomes of patients with ST-elevation myocardial infarction and no standard modifiable risk factors–A DANAMI-3 substudy

Jawad Mazhar[1], Kathrine Ekström[2], Rebecca Kozor[1], Stuart M. Grieve[3,4], Lars Nepper-Christensen[2], Kiril A. Ahtarovski[2], Henning Kelbæk[5], Dan E. Høfsten[2], Lars Køber[2], Niels Vejlstrup[2], Stephen T. Vernon[1], Thomas Engstrøm[2,6], Jacob Lønborg[2] and Gemma A. Figtree[1]*

[1]Kolling Research Institute, University of Sydney, Sydney, NSW, Australia, [2]Department of Cardiology, The Heart Centre, Rigshospitalet, Copenhagen University Hospital, Copenhagen, Denmark, [3]Imaging and Phenotyping Laboratory, Faculty of Medicine and Health, Charles Perkins Centre, University of Sydney, Sydney, NSW, Australia, [4]Department of Radiology, Royal Prince Alfred Hospital, Camperdown, NSW, Australia, [5]Department of Cardiology, Zealand University Hospital, Roskilde, Denmark, [6]Department of Cardiology, Lund University Hospital, Lund, Sweden

Introduction: A higher 30-day mortality has been observed in patients with first-presentation ST elevation myocardial infarction (STEMI) who have no standard modifiable cardiovascular risk factors (SMuRFs), i. e., diabetes, hypertension, hyperlipidemia, and current smoker. In this study, we evaluate the clinical outcomes and CMR imaging characteristics of patients with and without SMuRFs who presented with first-presentation STEMI.

Methods: Patients from the Third DANish Study of Acute Treatment of Patients With ST-Segment Elevation Myocardial Infarction (DANAMI-3) with first-presentation STEMI were classified into those with no SMuRFs vs. those with at least one SMuRF.

Results: We identified 2,046 patients; 283 (14%) SMuRFless and 1,763 (86%) had >0 SMuRF. SMuRFless patients were older (66 vs. 61 years, $p < 0.001$) with more males (84 vs. 74%, $p < 0.001$), more likely to have left anterior descending artery (LAD) as the culprit artery (50 vs. 42%, $p = 0.009$), and poor pre- PCI (percutaneous coronary intervention) TIMI (thrombolysis in myocardial infarction) flow ≤1 (78 vs. 64%; $p < 0.001$). There was no difference in all- cause mortality, non-fatal reinfarction, or hospitalization for heart failure at 30 days or at long-term follow-up. CMR imaging was performed on 726 patients. SMuRFless patients had larger acute infarct size (17 vs. 13%, $p = 0.04$) and a smaller myocardial salvage index (42 vs. 50%, $p = 0.02$). These differences were

attenuated when the higher LAD predominance and/or TIMI 0-1 flow were included in the model.

Conclusion: Despite no difference in 30-day mortality, SMuRFless patients had a larger infarct size and a smaller myocardial salvage index following first- presentation STEMI. This association was mediated by a larger proportion of LAD culprits and poor TIMI flow pre-PCI.

Clinical trial registration: clinicaltrials.gov, unique identifier: NCT01435408 (DANAMI 3-iPOST and DANAMI 3-DEFER) and NCT01960933 (DANAMI 3- PRIMULTI).

KEYWORDS

coronary artery disease, ST elevation myocardial infarction, cardiovascular risk factors, atherosclerosis, cardiovascular magnetic resonance

# Introduction

Despite the common perception that coronary artery disease (CAD) is well understood and managed, it remains the leading cause of mortality in adults worldwide (1). Major advances have been made in the identification and treatment of standard modifiable risk factors (SMuRFs) for CAD—particularly hypercholesterolemia, hypertension, diabetes mellitus, and smoking (2, 3). However, at an individual level, it is not uncommon for a patient to present with extensive atherosclerosis and acute coronary syndrome that is not clearly explained by such risk factors. We have previously reported an increase in the prevalence of myocardial infarction patients presenting with no standard modifiable cardiovascular risk factors in Australia from 11 to 27% over a 10-year period (4), confirmed in a large, nation-wide cohort (5).

A number of large observational studies have shown, somewhat unexpectedly, that SMuRFless STEMI patients have higher in-hospital and 30-day mortality rates after myocardial infarction compared to patients with at least one of the major risk factors (4–9). A recent analysis of 62,048 patients with first presentation ST-segment elevation myocardial infarction (STEMI) in the SWEDEHEART (Swedish Healthcare Registry on Heart Disease) registry showed that SMuRFless patients had a ∼1.5 times higher 30-day mortality rate compared to patients with >0 SMuRFs (9). SMuRFless women had the highest 30- day mortality (18%), with the heightened susceptibility factors presumably driving atherosclerosis compounding their already recognized poor outcomes post-STEMI compared with men (9). The reasons for these higher mortality rates in SMuRFless patients following myocardial infarction are not well described, but current data suggests they may be driven by arrhythmia rather than reinfarction or heart failure (9). Differences in myocardial infarct size and microvascular obstruction (MVO) may also contribute to the higher 30-day mortality rates, but this remains to be investigated.

Cardiac magnetic resonance (CMR) imaging allows direct quantitation of the area at risk (AAR), myocardial infarct size, and MVO. Both myocardial infarct size and MVO are associated with poor outcome (10–12). CMR has also been employed to evaluate the impact of medical therapies on left ventricular remodeling post-myocardial infarction (13–16). In this study, we evaluate the clinical outcome and CMR measures of infarct characteristics and LV remodeling in patients with and without SMuRFs who presented with first-presentation STEMI.

# Methods

## Study population

The Third DANish Study of Optimal Acute Treatment of Patients With ST-Segment Elevation Myocardial Infarction (DANAMI-3) trial programme (NCT 01960933, NCT01435408)
consisted of three randomized controlled STEMI trials performed at four large primary percutaneous coronary intervention (PCI) centers in Denmark between March 2011 and February 2014 (17–20). The studies examined the effect of ischemic postconditioning (iPOST), deferred stenting (DEFER), and fractional flow reserve (FFR)-guided complete revascularization (PRIMULTI) in patients following STEMI. Patients were primarily randomized to either iPOST or DEFER. A secondary randomization was subsequently performed, randomizing patients with multivessel disease (MVD) in the PRIMULTI trial. For the current study, patients from all the DANAMI-3 trials with first-presentation STEMI were classified into patients with no SMuRFs vs. those with at least one SMuRF, to assess for any significant differences in clinical outcomes. SMuRFless patients were defined as patients with no standard modifiable cardiovascular risk factors—diabetes mellitus, hypertension, hyperlipidaemia, and current smoker. A patient was classified as having diabetes, hypertension, or

hyperlipidaemia if the patient reported a history of such, was on the treatment of these conditions at the time of presentation, or LDL at the time of admission was ≥3.5 mmol/L. A patient was defined as a current smoker if they reported being smoking regularly prior to admission. The clinical outcomes of the two groups were compared as per the primary and secondary endpoints defined in the DANAMI-3 trial (17–20). Baseline clinical characteristics, procedural data, medications at discharge as well as clinical outcomes were obtained.

## The CMR sub-study

A subgroup of DANAMI-3 patients recruited at one center (Righospitalet, Copenhagen University Hospital) had CMR performed according to a standard protocol to evaluate the effects of randomizations on a surrogate marker. This CMR-subgroup provided an optimal opportunity to examine any potential differences in CMR variables such as AAR, infarct size, MVO, and LV remodeling between individuals with no SMuRFs vs. those with at least one SMuRF. Patients were included in the sub-study if they had baseline and/or follow-up CMR performed (Figure 1).

## Acquisition and analysis of CMR images

The CMR protocol has been described in detail previously (21). Briefly, CMR was performed during index admission following primary PCI using a 1.5 Tesla scanner (Avanto; Siemens, Erlangen, Germany). CMR was also repeated 3 months after the index admission. Images were analyzed by an independent observer, blinded to all clinical data, using dedicated software (CVI42, Circle Cardiovascular Imaging Inc, Calgary, Alberta, Canda), and validated by a second experienced independent observer. Left ventricular function and mass were calculated on short-axis steady-state free precession (SSFP) cine images on index and follow-up CMRs. Infarct size was assessed on late gadolinium enhancement images, which were obtained 10 min after intravenous injection of 0.1 mmol/kg body weight of gadolinium-based contrast (Gadovist; Bayer Schering, Berlin, Germany) on 8 mm sliced short-axis images with full- LV coverage and no gap (14). Myocardial infarction was defined as hyperenhanced myocardium with a signal intensity of >5 SDs of the mean intensity of normal reference myocardium. Infarct size was calculated as a percentage of left ventricular mass and reported on both index and follow-up CMRs. AAR was identified as oedema on the index scan using a T2-weighted short tau inversion-recovery sequence (STIR) (13, 15). Oedema was defined as an area with a signal intensity of >2 SDs above the signal intensity in remote normal myocardium. Microvascular obstruction (MVO) was assessed on the LGE images in the index scans as hypointense areas within the acute infarct region.

Myocardial salvage index (MSI) was calculated as the difference between area at risk and infarct size, divided by area at risk (22).

## Statistical analysis

The DANAMI-3 patients with first-presentation STEMI were identified and classified into patients with no SMuRF (SMuRFless) and those with at least one SMuRF. Continuous variables were compared using Student's *t*-test (if normal distribution) or Mann–Whitney *U* test (if not normal distribution). Mean ± SD or median (interquartile range, IQR) or percentages are reported. Changes in baseline to follow-up CMR measures were assessed using the paired *t*-test. Categorical variables were compared using Pearson's chi-squared or Fisher's exact test as appropriate. Multivariable linear regression analyses were performed using SMuRFless patients as a predictor for final infarct size or final MSI adjusting for pre-specified clinically relevant variables: male sex, age, ECG–to-wire time, former smoking, thrombolysis in myocardial infarction (TIMI) flow 0–1 pre-PCI and culprit left anterior descending artery (LAD). A Cox proportional hazards regression model was used to assess the individual risk of a clinical outcome in SMuRFless patients. Finally, an additional logistic regression model was performed to determine the independent predictors of TIMI 0-1 flow, adjusting for pre-specified clinically relevant variables, namely, male sex, age, symptom to wire time, multivessel disease, culprit LAD, heart rate, systolic blood pressure, (23) and SMuRFless status. A result was considered significant when it was below a two-sided *p*-value of 0.05. The statistical analyses were performed with SPSS version 25.

# Results

## Study population

A total of 2,217 patients were included in the DANAMI-3 trial program. After excluding 160 patients with previous acute myocardial infarction, PCI, and coronary artery bypass grafting (CABG), and 11 patients with missing SMuRF data, the total study population was comprised of 2,046 patients. Of these, 283 (14%) were SMuRFless and 1,763 (86%) had >0 SMuRFs. A total of 726 (13%) patients underwent baseline and/or follow-up CMR imaging: 688 (95%) had CMR at baseline and 639 (88%) had CMR at follow up. A total of 87 patients had only baseline CMR and 38 had only follow-up CMR performed. Of the 726 patients in the CMR sub-group, 61 (8%) were SMuRFless, and 665 (92%) had >0 SMuRFs (Figure 1).

In the CMR subgroup, the proportion of SMuRF-less and SMuRF patients in the three randomized trials was similar (Appendix Table A1). In the total DANAMI-3 population, the proportion of SMuRFless and SMuRF patients was

10.3389/fcvm.2022.945815

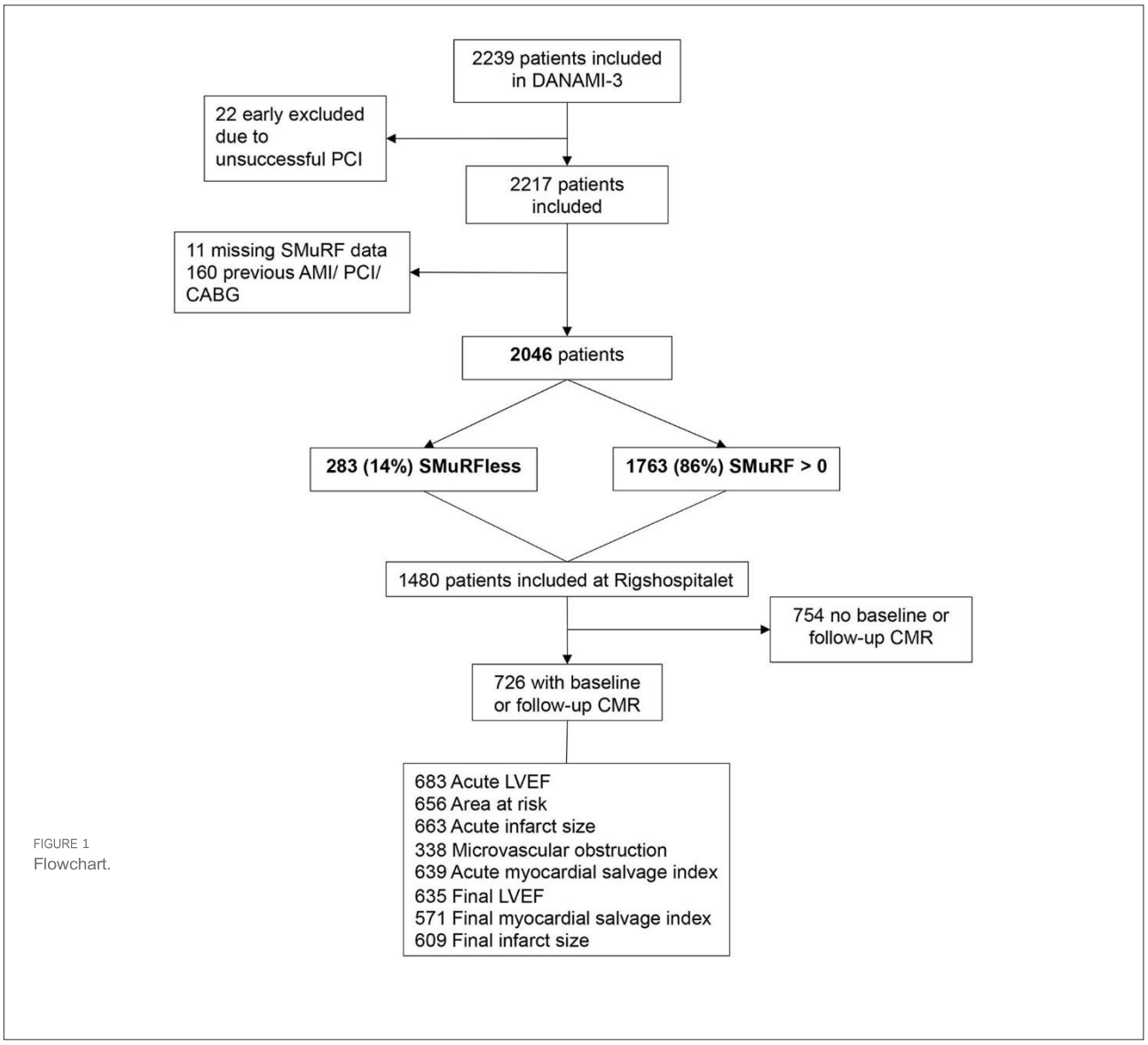


FIGURE 1
Flowchart.

similar in PRIMULTI and iPOST but not similar in DEFER (Appendix Table A1). Additional analyses were performed to ensure, that there was no effect of randomizations on the results. There was no interaction between SMuRFs and either of the treatment arms in DANAMI-3 with regards to acute infarct size (DEFER $p = 0.45$, iPOST $p = 0.70$, and PRIMULTI $p = 0.89$).

## Baseline clinical characteristics

The baseline clinical characteristics for the total population and the CMR subgroup are presented in Table 1. In the total study population, SMuRFless patients were older with more males, a larger proportion were former smokers, but fewer had a family history of ischemic heart disease. In the CMR sub-group, the SMuRFless patients were older, but the proportion of males was similar and likewise, a larger proportion were former smokers.

## Procedural characteristics

Procedural characteristics for both populations are presented in Table 2. In the total study population and the CMR sub-group, the SMuRFless and SMuRF patients were similar in terms of the number of arteries treated, number of implanted stents, stent diameter, total stent length, and the use of periprocedural medications such as heparin, glycoprotein IIb/IIIa, and bivalirudin. In the total study population, the number of patients with multivessel disease (MVD) was less

TABLE 1 Baseline characteristics between SMuRFless and patients with more than one SMuRF, total DANAMI-3 and CMR sub-population.

| Parameter | *Total population* | | | *CMR sub-population* | | |
|---|---|---|---|---|---|---|
| | **SMuRFless** $n = 283$ (14%) | **SMuRF > 0** $n = 1{,}763$ (86%) | ***p*-value** | **SmuRFless** $n = 61$ (8%) | **SMuRF > 0** $n = 665$ (92%) | ***p*-value** |
| Age, years | 66 ± 12 | 61 ± 12 | <0.001 | 63 ± 11 | 58 ± 11 | 0.003 |
| Male, % | 238 (84) | 1,322 (75) | <0.001 | 51 (84) | 523 (79) | 0.42 |
| SMuRFs | | | | | | |
| Hypertension, % | 0 (0) | 758 (43) | | 0 (0) | 245 (37) | |
| Diabetes, % | 0 (0) | 172 (10) | | 0 (0) | 59 (9) | |
| Hyperlipidemia, % | 0 (0) | 1,019 (73) | | 0 (0) | 487 (74) | |
| Current smoker | 0 (0) | 1,043 (59) | | 0 (0) | 395 (59) | |
| Former smoker | 148 (52) | 420 (24) | <0.001 | 34 (56) | 115 (23) | <0.001 |
| Pre-existing chronic heart failure, % | 69 (24) | 312 (18) | 0.007 | 15 (25) | 105 (16) | 0.08 |
| Pre-existing chronic kidney disease, % | 1 (1) | 25 (2) | 0.33 | 0 (0) | 4 (1) | 0.52 |
| Pre-existing stroke, % | 3 (2) | 59 (4) | 0.24 | 2 (3) | 21 (3) | 0.96 |
| BMI, kg/m$^2$ | 27 ± 4 | 27 ± 4 | 0.95 | 28 ± 4 | 27 ± 4 | 0.11 |
| Family history of IHD, % | 93 (35) | 785 (46) | 0.001 | 26 (43) | 328 (50) | 0.35 |
| Time from first ecg to wire, minutes | 87 (73–118) | 87 (71–114) | 0.64 | 91 (76–115) | 85 (69–114) | 0.31 |
| Admission eGFR < 60 mL/min/ 1,73 m$^2$, % | 16 (12) | 140 (11) | 0.75 | 1 (2) | 29 (5) | 0.30 |
| Admission Hgb < 6.0 mmol/L, % | 4 (1) | 11 (1) | 0.15 | 1 (2) | 2 (0.3) | 0.12 |

in the SMuRFless group, however, in the CMR sub-group the number of patients with MVD was similar. The proportion of patients with TIMI flow 0–1 before PCI was higher in the SMuRFless group in both the total study population (78 vs. 64%, $p = 0.001$) and the CMR subgroup (75 vs. 61%, $p = 0.02$). In the total study population, the left anterior descending artery (LAD) was the culprit artery in a higher proportion of SMuRFless patients (50 vs. 42%, $p = 0.009$). In the CMR sub-group, the proportion was not significantly different (44 vs. 41%, $p = 0.60$).

## Discharge medications

Appendix Table A2 summarizes discharge medications for both groups. In the total population, a significantly higher proportion of SMuRFless patients were discharged with clopidogrel or ticagrelor treatment vs. a higher proportion of patients with SMuRFs treated with prasugrel. No substantial group-level differences in the CMR subgroup were demonstrated.

## CMR endpoints

Of the 726 patients in the CMR sub-group, 688 (95%) patients had a baseline CMR performed at a median of 0 days [IQR: 0–1] after primary PCI, and 639 (88%) patients had a follow-up CMR performed after a median of 90 days [IQR: 88–96]).

## Infarct size, microvascular obstruction, and myocardial salvage index

CMR results are presented in Table 3. At baseline, SMuRFless patients had significantly larger acute and final infarct sizes with a similar-sized AAR compared to their counterparts. After adjusting for the AAR, there remained an association between larger acute infarct size and SMuRFless status (B 2.3% LV mass, 95% CI (0.1–4.4%), $p = 0.04$) compared to patients with >0 SMuRFs. The increased infarct size to AAR is presented in Figure 2. This is reflected in the lower acute MSI in SMuRFless patients. MVO was similar to those with or without SMuRFs.

In a multivariable regression model, the association of SMuRFless status with larger acute infarct size remained significant independent of age, sex, former smoking, and ECG- to-wire time. However, this association was no longer observed if culprit LAD and/or TIMI 0-1 flow pre-PCI were included in the model (Table 4). As TIMI 0-1 flow pre-PCI was a strong predictor of infarct size, a logistic regression analysis was performed to determine the predictors of TIMI 0-1 flow pre- PCI (Table 5). This model included clinically relevant variables, namely, male sex, age, symptom-to-wire time, multivessel disease, culprit LAD, heart rate, systolic blood pressure, and being SMuRFless. The predictors of TIMI 0-1 flow pre-PCI in

TABLE 2 Procedural data and medication given at discharge, total DANAMI-3 and CMR sub-population.

| | *Total population* | | | *CMR sub-population* | | |
|---|---|---|---|---|---|---|
| | **SMuRFless** $n = 283$ **(14%)** | **SMuRF** $> 0$ $n = 1{,}763$ **(86%)** | ***p*-value** | **SmuRFless** $n = 61$ **(8%)** | **SMuRF** $> 0$ $n = 665$ **(92%)** | ***p*-value** |
| No. of main arteries treated per patient, mean[a] | 1 (1–1) | 1 (1–1) | 0.89 | 1 (1–1) | 1 (1–1) | 0.85 |
| No. of implanted stents, *n* (IQR) | 1 (1–2) | 1 (1–2) | 0.80 | 1 (1–2) | 1 (1–2) | 0.81 |
| Stent diameter, mean, mm | 3.4 ± 0.5 | 3.5 ± 0.5 | 0.52 | 3.4 ± 0.7 | 3.5 ± 0.6 | 0.21 |
| Total stent length, mm (IQR) | 18 (15–33) | 23 (15–33) | 0.80 | 21 (18–36) | 23 (18–33) | 0.87 |
| Stent type | | | 0.16 | | | 0.70 |
| None | 1 (0) | 21 (1) | | 0 (0) | 8 (1) | |
| POBA | 16 (6) | 79 (5) | | 4 (7) | 50 (5) | |
| Bare-metal | 6 (2) | 37 (2) | | 1 (2) | 12 (2) | |
| Drug-eluting | 258 (92) | 1,607 (92) | | 55 (92) | 607 (92) | |
| Pretreatment with heparin | 268 (96) | 1,645 (96) | 0.94 | 58 (97) | 606 (95) | 0.56 |
| Use of glycoprotein IIb/IIIa inhibitor | 49 (18) | 318 (19) | 0.68 | 15 (25) | 139 (22) | 0.57 |
| Use of bivalirudin | 220 (79) | 1,308 (76) | 0.38 | 43 (72) | 463 (73) | 0.88 |
| Thrombus aspiration | 158 (56) | 1,016 (58) | 0.57 | 39 (64) | 392 (59) | 0.45 |
| Killip class III-IV heart failure at any time | 6 (2) | 25 (1) | 0.37 | 0 (0) | 3 (1) | 0.60 |
| Multivessel disease | 90 (32) | 709 (40) | 0.006 | 21 (34) | 280 (42) | 0.23 |
| Location of culprit lesion | | | | | | |
| LM | 0 (0) | 3 (0) | 0.49 | 0 (0) | 1 (0) | 0.76 |
| LAD | 142 (50) | 736 (42) | 0.009 | 27 (44) | 271 (41) | 0.60 |
| RCA | 104 (37) | 759 (43) | 0.04 | 22 (36) | 293 (44) | 0.22 |
| LCx | 37 (13) | 261 (15) | 0.44 | 12 (20) | 99 (15) | 0.32 |
| TIMI flow grade 0/1 before PCI[b] | 222 (78) | 1,130 (64) | <0.001 | 46 (75) | 402 (61) | 0.02 |
| TIMI flow grade 2/3 after PCI[b] | 282 (99) | 1,752 (99) | 0.58 | 61 (100) | 661 (99) | 0.54 |
| Radial access | 8 (3) | 113 (7) | 0.02 | 3 (5) | 44 (7) | 0.58 |

Results expressed as mean±SD, interquartile range (IQR), or percentage. LCx, left circumflex artery; LAD, left anterior descending artery; LM, left main artery; POBA, plain old balloon angioplasty; RCA, right coronary artery; TIMI, thrombolysis in myocardial infarction.
[a]Includes diagonal, obtuse marginal, posterolateral coronary artery, and posterior descending coronary artery.
[b]Grades range from 0 to 3, with 3 indicating higher flow.

this model were SMuRFless status (OR 1.6, CI (1.03–2.4), $p = 0.03$), male sex (OR 1.4, CI (1.1–1.9), $p = 0.006$), culprit LAD (OR 0.7, CI (0.6–0.9), $p = 0.005$), and symptom-to-wire time (OR 1.0, CI 1.0–1.0, $p = 0.001$).

## Left ventricle function and remodeling

At baseline CMR, there was no difference in indexed left ventricle end diastolic volume (LVEDV), indexed left ventricular end systolic volume (LVESV), or left ventricular ejection fraction (LVEF), which were relatively preserved in both groups (Table 3).

We next examined CMR measurements of ventricular remodeling between baseline and follow-up scans within each individual participant (Table 3). There was an increase in LVEDV, decrease in LVESV, increase in LVEF, and a reduction in infarct size in both SMuRFless and SMuRF groups ($p < 0.001$ for all). The increase in LVEDV tended to be greater in SMuRF- less participants ($p = 0.06$). However, this was not significant when indexed for body surface area. The proportion of patients reaching ≥12% increase in LVEDV was equivalent in both groups. All other CMR ventricular remodeling measurements were similar between patients with or without SMuRFs (Table 3).

## Clinical outcomes

The clinical outcomes at 30 days are presented in Table 6. Kaplan–Meier survival curves illustrating the 30-day risk and long-term risk of all-cause mortality and hospitalization for heart failure in patients with SMuRF vs. SMuRFless is shown in Figure 3. All the rates of all-cause mortality (3 vs. 2%), non-fatal reinfarction (0 vs. 1%), hospital admission for heart failure (1 vs. 1%), and the combined all-cause mortality/hospital admission

TABLE 3 CMR variables at baseline and follow-up.

| Parameter | SmuRFless $n = 61$ (8%) | SMuRF $> 0$ $n = 665$ (92%) | *p*-value |
|---|---|---|---|
| **Baseline** | | | |
| LV EDV (ml) | 172 ± 39 | 165 ± 38 | 0.20 |
| LV EDV index (ml/m$^2$) | 86 ± 18 | 83 ± 16 | 0.13 |
| LV ESV (ml) | 88 ± 34 | 83 ± 29 | 0.23 |
| LV ESV index (ml/m$^2$) | 44 ± 17 | 41 ± 14 | 0.22 |
| LVEF (%) | 50 ± 11 | 51 ± 10 | 0.74 |
| Acute infarct size (% LV)* | 17 ± 2 | 13 ± 2 | 0.04 |
| AAR (% LV) | 35 ± 10 | 33 ± 11 | 0.24 |
| MVO (% LV)* | 3 ± 3 | 3 ± 2 | 0.78 |
| Acute MSI (%) | 42 ± 22 | 50 ± 25 | 0.02 |
| **Follow-up** | | | |
| LV EDV (ml) | 186 ± 44 | 170 ± 40 | 0.006 |
| LV EDV index (ml/m$^2$) | 93 ± 19 | 86 ± 18 | 0.006 |
| LV ESV (ml) | 83 ± 34 | 74 ± 30 | 0.03 |
| LV ESV index (ml/m$^2$) | 41 ± 16 | 37 ± 15 | 0.06 |
| LVEF (%) | 57 ± 10 | 58 ± 9 | 0.42 |
| Final infarct size (% LV)* | 12 ± 2 | 8 ± 3 | 0.03 |
| Final MSI (%) | 60 ± 22 | 64 ± 24 | 0.23 |
| A **Baseline to follow-up** | | | |
| LV EDV (ml) | 13 ± 26 ** | 5 ± 27 ** | 0.06 |
| LV EDV index (ml/m$^2$) | 6 ± 13 ** | 3 ± 13 ** | 0.10 |
| LV ESV (ml) | −7 ± 21 ** | −9 ± 22 ** | 0.58 |
| LV ESV index (ml/m$^2$) | −4 ± 11 ** | −4 ± 11 ** | 0.69 |
| LVEF (%) | 7 ± 10** | 7 ± 8 ** | 0.50 |
| Infarct size (% LV) | −1.6 ± 1.7 ** | −1.5 ± 1.8 ** | 0.30 |
| LV EDV % change from baseline – follow-up CMR | 8 ± 17 | 4 ± 17 | 0.14 |
| LV ESV % change from baseline – follow-up CMR | −5 ± 25 | −8 ± 25 | 0.31 |
| Patients with ≥ 12% increase in LV EDV and LV ESV from baseline to follow-up, *n* (%) | 6 (11) | 72 (13) | 0.68 |

Data are expressed as mean±SD.
* Logarithm transferred.
** p-Value within groups $< 0.001$, paired t-test.
AAR, area at risk; EDV, end-diastolic volume; ESV, end-systolic volume; LV, left ventricular; LVEF, left ventricular ejection fraction; MVO, microvascular obstruction.

for heart failure rate (3 vs. 3%) were low and similar between the two groups (SMuRFless vs. SMuRFs). Patients had a long-term clinical follow-up of a median of 3.1 years (IQR: 2.4–3.8) and no patients were lost to follow-up. Event rates continued to be low and there were no differences in any of the clinical outcomes at long-term follow up, when comparing SMuRFless patients to patients with >0 SMuRFs (Table 6).

## Discussion

In recent studies, we have reported excess early mortality in STEMI patients who have developed CAD in the absence of modifiable risk factors. Contrary to previous publications, we did not find any difference in 30-day clinical endpoints. However, the CMR imaging of the DANAMI-3 trials allowed us to examine potential differences in acute infarct size and myocardial remodeling after the first presentation of STEMI in patients with no SMuRFs vs. those with at least one SMuRF. Whilst we did not find any difference in 30-day clinical endpoints, myocardial remodeling, or MVO in the DANAMI- 3 study cohort, we did observe an increased acute and final infarct size in SMuRFless patients. This appeared to be at least partially mediated by a higher proportion of culprit locations in the LAD-territory and pre-PCI TIMI 0-1 flow among SMURFLESS patients.

SMuRFless patients are often an invisible subgroup in randomized clinical trials and subsequently, evidence-based guidelines for STEMI patients. Indeed, of the 256 controlled trials referenced in the ESC (European Society of Cardiology)

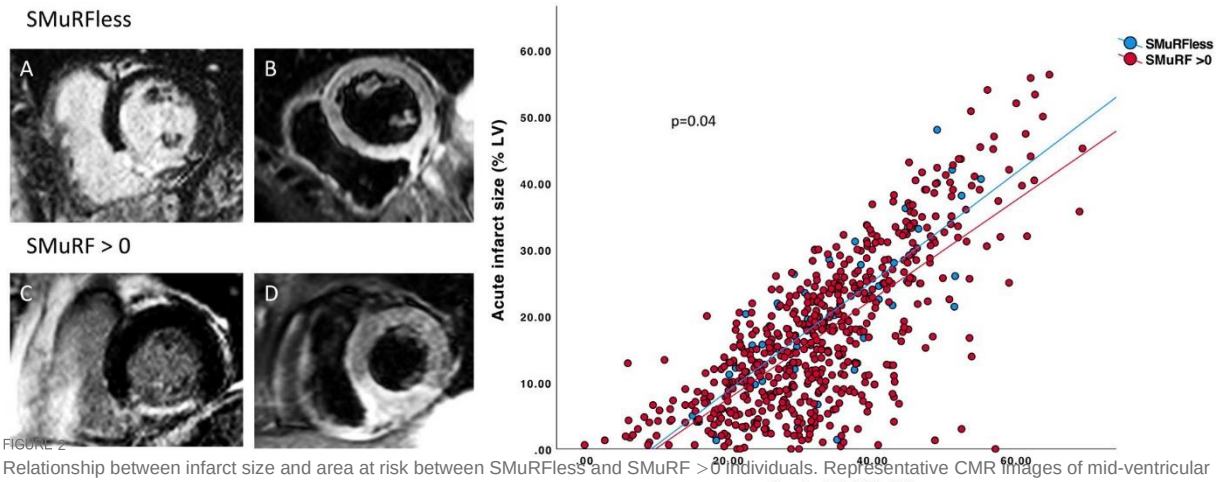


FIGURE 2
Relationship between infarct size and area at risk between SMuRFless and SMuRF >0 individuals. Representative CMR images of mid-ventricular LGE and T2-weighed STIR slices at baseline. SMuRFless patient: (A) LGE contrast enhanced slice showing area with hyperintense signal in the inferior-septal region indicating infarction. (B) T2-weighed STIR slice showing hyperintense signal in the same region indicating the AAR (oedema) and thus acute infarction. Same images are shown for a patient with SMuRF >0: (C) LGE image of the infarction with corresponding (D) T2-weighed STIR image of the AAR. Scatterplot (right panel) of the acute infarct size and AAR in SMuRFless vs. SMuRF patients showing a larger infarct size in SMuRFless patients after adjustment for AAR.

and AHA (American Heart Association) STEMI guidelines, the proportion of patients with diabetes mellitus, hypertension, hypercholesterolemia, and smoking is a common feature of the baseline characteristics in Table 1, but not a single study reported the proportion of patients without SMuRFs (24–26). It is important to note that this proportion cannot be derived from the number of patients with one or more of the four SMuRFs reported. In the current study of 1st presentation STEMI patients in the combined DANAMI 3 studies, we confirm that a substantial proportion (14%) were unknown SMuRFless according to our definition. However, the proportion was smaller than initially reported (27%) (4, 5). In regard to their non-modifiable risk factors that may have contributed to their event, SMuRFless patients were older, were more likely to be male, and had a higher rate of prior smoking, but were less likely to have a family history of ischemic heart disease than their STEMI counterparts with at least one SMuRF. It is, however, important to bear in mind that the definitions of SMuRFs were based on electronic medical records and patients were categorized as having hypertension, hypercholesterolemia, or diabetes if the diagnosis was present at the time of enrolment or if LDL ≥3.5 mmol/L upon admission. Serum glucose was not incorporated in the diagnosis of diabetes due to the influence of AMI on glucose levels. Importantly, there may be a risk of patients neglecting to report their actual smoking habits leading to a falsely high number of patients reporting being prior smokers as well as unknown hypertension. We have accounted for this in the multivariable analyses.

In the recent study of the SWEDEHEART Registry, 30- day mortality rates were ∼50% higher in SMuRFless STEMI patients (11.3%) vs. those with at least one modifiable risk factor (7.9%; $p < 0.0001$) (9). In comparison, the mortality rate was much lower overall in the DANAMI series (2%), and not significantly different between the groups. This lower mortality rate may reflect a degree of selection bias, with severely unwell patients being unsuitable for randomization to clinical trials, as well as potential higher rates of secondary prevention medications that are recognized to occur in the setting of a rigorous clinical trial vs. a "real-world" registry. It may also relate to the lower than expected proportion of women in the DANAMI study population, given women have an excess early mortality post STEMI (9, 27). On the other hand, register-based data are more prone to bias as regards the existence of comorbidities and risk factors, which may be even more pronounced among the most critically ill who also carry the highest mortality rate. The presence of multi- vessel disease in the overall population was higher in the SMuRF group (41 vs. 34%, $p = 0.02$), however, despite this the incidence of clinical outcomes like all-cause mortality, non- fatal reinfarction, or hospitalization for heart failure at 30 days or long-term follow up was not higher in the SMuRF group. Hence, the presence of higher multivessel disease in the SMuRF group probably did not have an effect on outcomes. The main emphasis of our study was the CMR subgroup to assess CMR imaging features in the two groups. In the CMR subgroup, there was no difference in the presence of multi-vessel

TABLE 4 Multivariable linear regression analysis for predictors of acute infarct size and MSI.

| | *Acute infarct size* | | | | *Myocardial salvage index* | | | |
|---|---|---|---|---|---|---|---|---|
| | **Univariable** | | **Multivariable** | | **Univariable** | | **Multivariable** | |
| | **B** | ***P*-value** | **B** | ***P*-value** | **B** | ***P*-value** | **B** | ***P*-value** |
| **Model 1** | | | | | | | | |
| Male sex | 3.2 | 0.004 | 3.9 | <0.001 | −4.4 | 0.07 | −5.3 | 0.04 |
| Age, years | 0.1 | 0.01 | 0.1 | 0.007 | −0.2 | 0.05 | −0.1 | 0.12 |
| Former smoker | −0.1 | 0.92 | −1.5 | 0.18 | −0.4 | 0.87 | 1.7 | 0.48 |
| ECG-to-wire-time, min | 0.02 | 0.08 | 0.02 | 0.08 | −0.06 | 0.01 | −0.06 | 0.006 |
| SMuRFless | 3.5 | 0.03 | 3.3 | 0.04 | −7.8 | 0.02 | −7.7 | 0.03 |
| **Model 2–TIMI flow** | | | | | | | | |
| Male sex | | | 3.7 | <0.001 | | | −4.8 | 0.04 |
| Age, years | | | 0.1 | 0.06 | | | −0.1 | 0.16 |
| Former smoker | | | −1.5 | 0.14 | | | 1.9 | 0.38 |
| ECG-to-wire-time, min | | | 0.02 | 0.02 | | | −0.06 | 0.002 |
| SMuRFless | | | 2.2 | 0.15 | | | −5.4 | 0.10 |
| TIMI 0-1 pre-PCI | 9.1 | <0.001 | 8.8 | <0.001 | −20.7 | <0.001 | 20.6 | <0.001 |
| **Model 3–culprit LAD** | | | | | | | | |
| Male sex | | | 3.7 | 0.001 | | | −5.2 | 0.04 |
| Age, years | | | 0.1 | 0.03 | | | −0.1 | 0.43 |
| Former smoker | | | −1.0 | 0.35 | | | 1.5 | 0.52 |
| ECG-to-wire-time, min | | | 0.01 | 0.20 | | | −0.05 | 0.02 |
| SMuRFless | | | 3.1 | 0.05 | | | −7.6 | 0.03 |
| Culprit LAD | 5.1 | <0.001 | 5.2 | <0.001 | −2.2 | 0.26 | −2.0 | 0.32 |
| **Model 4–full model** | | | | | | | | |
| Male sex | | | 3.5 | <0.001 | | | −4.7 | 0.04 |
| Age, years | | | 0.1 | 0.04 | | | −0.1 | 0.22 |
| Former smoker | | | −1.0 | 0.32 | | | 1.6 | 0.46 |
| ECG-to-wire-time, min | | | 0.02 | 0.08 | | | −0.06 | 0.003 |
| SMuRFless | | | 1.8 | 0.21 | | | 5.1 | 0.12 |
| TIMI 0-1 pre-PCI | | | 9.5 | <0.001 | | | 21.1 | <0.001 |
| culprit LAD | | | 6.2 | <0.001 | | | −4.5 | 0.02 |

TABLE 5 Uni and multivariable logistic regression analysis for predictors of TIMI 0-1 flow pre-PCI.

| | **Univariable** | | **Multivariable** | |
|---|---|---|---|---|
| | **Odds Ratio (95% CI)** | ***P*-value** | **Odds Ratio (95% CI)** | ***P*-value** |
| Male sex | 1.3 (1.1–1.7) | 0.005 | 1.4 (1.1–1.9) | 0.006 |
| Age, years | 1.0 (0.99–1.01) | 0.86 | 0.99 (0.99–1.00) | 0.81 |
| Symptom-wire time, min | 1.001 (1.001–1.002) | 0.003 | 1.0 (1.0–1.0) | 0.001 |
| Multivessel disease | 1.0 (0.8–1.3) | 0.7 | 0.9 (0.7–1.2) | 0.60 |
| Culprit LAD | 0.8 (0.7–0.95) | 0.01 | 0.7 (0.6–0.9) | 0.005 |
| Heart rate, bpm | 0.99 (0.98–0.99) | 0.008 | 0.99 (0.98–1.0) | 0.08 |
| Systolic blood pressure | 1.0 (1.0–1.001) | 0.83 | 1.0 (1.0–1.0) | 0.46 |
| SMuRFless | 2.0 (1.5–2.8) | <0.001 | 1.6 (1.03–2.4) | 0.03 |

10.3389/fcvm.2022.945815

TABLE 6 Clinical outcomes, total DANAMI-3 population.

| | SMuRFless $n = 283$ (14%) | SMuRF $> 0$ $n = 1,763$ (86%) | Hazard ratio (95% CI) | *p*-value |
|---|---|---|---|---|
| 30-days follow-up | | | | |
| All-cause mortality, *n* (%) | 8 (3) | 31 (2) | 1.7 (0.8–3.6) | 0.20 |
| Non-fatal reinfarction | 0 (0) | 26 (1) | 0.04 (0.0–1.6) | 0.30 |
| Hospital admission for heart failure | 2 (1) | 20 (1) | 1.1 (0.2–4.5) | 0.94 |
| All-cause mortality or hospital admission for heart failure, *n* (%) | 9 (3) | 47 (3) | 1.4 (0.7–2.9) | 0.31 |
| Long-term follow-up | | | | |
| All-cause mortality, *n* (%) | 22 (8) | 122 (7) | 1.2 (0.7–1.8) | 0.54 |
| Non-fatal reinfarction | 9 (3) | 104 (6) | 0.5 (0.3–1.1) | 0.08 |
| Hospital admission for heart failure | 7 (5) | 72 (4) | 0.6 (0.3–1.3) | 0.23 |
| All-cause mortality or hospital admission for heart failure, *n* (%) | 26 (9) | 173 (10) | 0.96 (0.6–1.4) | 0.84 |

Data are number of events (%).

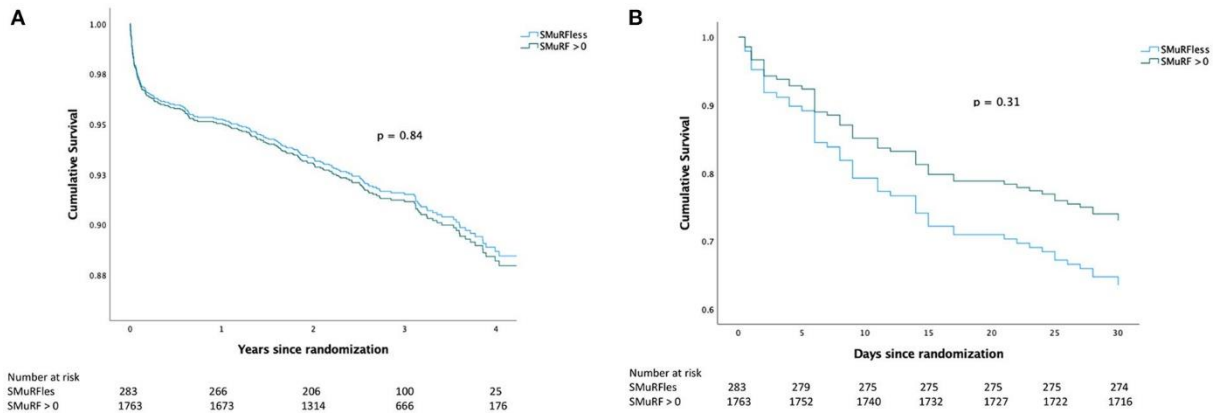


FIGURE 3
Kaplan-Meier curves. (A) Shows the Kaplan–Meier curve for the long-term composite endpoint of all-cause mortality and hospitalization for heart failure. (B) Shows the Kaplan–Meier curve for the composite endpoint of all-cause mortality and hospitalization for heart failure at 30 days.

disease between SMuRFs and SMuRFless patients (39 vs. 42%, $p = 0.56$).

The detailed CMR imaging data available enabled us to explore any potential differences in myocardial infarction and remodeling characteristics as a potential explanation of the early mortality. It could be hypothesized that factors involved in heightened susceptibility to coronary artery disease against a background of minimal risk factors may be a reflection of increased inflammatory and pathophysiological signaling downstream of the risk factors. Such signaling may also impact the myocardial response to a myocardial infarction and ischemia-reperfusion injury. However, this hypothesis cannot be confirmed in the present study as SMuRF was not an independent predictor of infarct size and myocardial salvage after adjusting for LAD territory and TIMI 0-1 flow.

The most significant predictors of infarct size were a culprit LAD lesion and TIMI 0–1 flow pre-PCI. This is consistent with the established literature, with extensive data demonstrating that STEMI due to LAD as the culprit vessel is associated with larger infarct size, worse left ventricle function, and higher mortality when compared with STEMI due to non-LAD arteries (28, 29). Interestingly, the proportion of patients with culprit LAD and TIMI 0-1 flow pre-PCI was also significantly higher in SMuRFless patients similar to what we had observed in the SWEDEHEART Registry (9), and CONCORDANCE (5) (Cooperative National Registry of Acute Coronary Syndrome Care) registry in Australia. The observed higher proportion of LAD culprit lesions in SMuRFless STEMI patients vs. those with at least one risk factor in SWEDEHEART (9) (42 vs. 37%) and CONCORDANCE (5) (46 vs. 37%) was initially considered

to be due to chance. However, whilst chance may still be an explanation for the observation due to the many statistical comparisons, the consistent signal in the DANAMI series of LAD territory culprits in the SMuRFless group (50 vs. 42%) raises the possibility of an underlying biological mechanism that warrants further investigation (30, 31).

Poor pre-procedural TIMI flow in STEMI patients is associated with larger infarct size, higher fatal arrhythmia events, higher in-hospital, and one-year mortality (23, 32, 33). Some of the known predictors of pre-procedural TIMI 3 flow are high systolic blood pressure and fast heart rate on admission, diabetes, longer delay to PCI, smoking, and extensive coronary disease (23). Other studies have demonstrated prothrombotic and inflammatory markers like neutrophil to lymphocyte ratio, platelet count and reactivity, mean platelet volume, and uric acid levels to be associated with patency of infarct-related arteries before PCI (23). Plaque composition may also contribute to poor pre-procedural flow in STEMI patients. An intravascular imaging study of 111 STEMI patients demonstrated that patients with pre-procedural TIMI 0-1 flow had greater lipid burden, larger vessel size, and larger plaque areas (34). Interestingly, in our multivariate analysis of predictors of TIMI 0-1 flow pre-PCI, SMuRFless status was one of the independent predictors. Whether SMuRFless patients truly have a higher predisposition for the involvement of LAD and if there are any biological mechanisms predisposing them to a higher incidence of poor flow (TIMI 0-1) pre-PCI is unknown. Other important differences between the groups may also contribute to these observations e.g., age, gender, former smokers, and baseline cardiovascular medications (aspirin, statins, ACE -inhibitors, beta-blockers, etc.) with cardioprotective abilities prescribed due to the risk factors. It is possible that being on these medications pre-STEMI may provide a cardioprotective effect in patients with standard modifiable risk factors. Unfortunately, information on pre- STEMI prescribed medications is not available.

CMR is the gold standard for measuring left ventricle volumes and ejection fraction due to its high reproducibility (35). The DANAMI series inclusion of serial CMR allowed us to examine potential associations with adverse remodeling post-STEMI. The average increase in LVEDV tended to be larger in the SMuRFless STEMI patients than in those with at least one risk factor. No differences were seen in the change of ESV or LVEF over the 3 months between the groups. A previous study showed that adverse left ventricle remodeling after STEMI with ≥12% increase in both LVEDV and LVESV at 6 months was associated with worse clinical outcomes at 5 years in terms of all-cause mortality and hospitalization for heart failure in comparison to their counterparts (35). The proportion of patients reaching this cut off was equivalent in both our groups (11% of SmuRFless vs. 13% of patients with at least one SMuRF) (Table 3). There was no difference in MVO between the two groups. At baseline, the infarct size was larger in SMuRFless patients even after adjusting for the area at risk. Infarct size, as a percent of LV mass, decreased equally over the 3 months in both groups by 1.5%.

Although three different treatment strategies were used in the three randomized controlled STEMI trials of the DANAMI- 3 trial program, there was no difference in clinical outcomes in these trials due to the interventions. Therefore, including patients from three different STEMI trials should not have influenced the clinical outcomes in our study. Furthermore, there was no interaction between the infarct size and either of the treatment arms. The limitations of the study include the low mortality rate and the potential for selection bias of a clinical trial, which contributing to this vs. real-world registries. This must be weighed against the benefits of prospectively collected data in randomized trials, which are less susceptible to missing data than registries. Many comparisons were made leading to the risk of type 1 error. Finally, many patients were lost to CMR, and it is well known that patients suitable for CMR are at lower risk compared to the CMR drop-outs.

## Conclusion

SMuRFless patients had a larger infarct size and smaller MSI following first-presentation STEMI, but this association was mediated by a higher proportion of LAD- territory events and pre-PCI TIMI 0-1 flow. Despite of this observation, mortality was not significantly different. Whether the finding of LAD territory and flow reduction preponderance in SMuRFless STEMI patients is a chance finding or related to unknown differences in biology remains to be examined.

## Data availability statement

The original contributions presented in the study are included in the article/supplementary material, further inquiries can be directed to the corresponding author.

## Ethics statement

The studies involving human participants were reviewed and approved by the Third DANish Study of Optimal Acute Treatment of Patients with ST- Segment Elevation Myocardial Infarction (DANAMI-3) trial program (NCT 01960933, NCT01435408; ethics approved by the Ethical Committee of the capital region of Denmark: H-4-2010-076. The patients/participants provided their written informed consent to participate in this study.

## Author contributions

GF, JM, SG, RK, and SV conceived the study. JL and KE conceived and designed the analysis approach. GF, JM, JL, and KE led the interpretation of the data for the work and drafted the work. RK, SG, LN-C, KA, HK, DH, LK, NV, and TE revised the manuscript critically and contributed important intellectual content. GF and JL approved the final version of the manuscript for publication and agree to be accountable for all aspects of the work. All authors contributed to the article and approved the submitted version.

## Funding

GF receives funding from National Health and Medical Research Council (Australia) Practitioner Fellowship (GNT1135920) and Center for Research Excellence (GNT1196629), and New South Wales Office of Health and Medical Research (Senior Investigator grant).

## Acknowledgments

Dedicated project nurses and staff at the Department of Cardiology, Rigshospitalet, Copenhagen University Hospital are thanked for their participation in the DANAMI-3 trial.

## Conflict of interest

Author LK reports Speakers honorarium from Novo, Novartis, AstraZeneca and Bohringer, unrelated to this manuscript. TE reports personal fees from Abbott, Bayer, and AstraZeneca outside the submitted work. GF reports personal consulting fees from CSL and grants from Abbott Diagnostic outside the submitted work.

The remaining authors declare that the research was conducted in the absence of any commercial or financial relationships that could be construed as a potential conflict of interest.

## Publisher's note



## References

1. Piepoli MF, Hoes AW, Agewall S, Albus C, Brotons C, Catapano AL, et al. Binno S and Group ESCSD. 2016 European Guidelines on cardiovascular disease prevention in clinical practice: The Sixth Joint Task Force of the European Society of Cardiology and Other Societies on Cardiovascular Disease Prevention in Clinical Practice (constituted by representatives of 10 societies and by invited experts)Developed with the special contribution of the European Association for Cardiovascular Prevention & Rehabilitation (EACPR). *Eur Heart J.* (2016) 37:2315–81. doi: 10.1093/eurheartj/ehw106

2. Jellinger PS, Handelsman Y, Rosenblit PD, Bloomgarden ZT, Fonseca VA, Garber AJ, et al. American association of clinical endocrinologists and american college of endocrinology guidelines for management of dyslipidemia and prevention of cardiovascular disease. *Endocr Pract.* (2017) 23:1–87. doi: 10.4158/EP171764.APPGL

3. Mahmood SS, Levy D, Vasan RS, Wang TJ. The Framingham Heart Study and the epidemiology of cardiovascular disease: a historical perspective. *Lancet.* (2014) 383:999–1008. doi: 10.1016/S0140-6736(13)61752-3

4. Vernon ST, Coffey S, Bhindi R, Soo Hoo SY, Nelson GI, Ward MR, et al. Increasing proportion of ST elevation myocardial infarction patients with coronary atherosclerosis poorly explained by standard modifiable risk factors. *Eur J Prev Cardiol.* (2017) 24:1824–30. doi: 10.1177/2047487317720287

5. Vernon ST, Coffey S, D'Souza M, Chow CK, Kilian J, Hyun K, et al. ST-Segment-Elevation Myocardial Infarction (STEMI) Patients Without Standard Modifiable Cardiovascular Risk Factors-How Common Are They, and What Are Their Outcomes? *J Am Heart Assoc.* (2019) 8:e013296. doi: 10.1161/JAHA.119.013296

6. Roe MT, Halabi AR, Mehta RH, Chen AY, Newby LK, Harrington RA, et al. Documented traditional cardiovascular risk factors and mortality in non-ST-segment elevation myocardial infarction. *Am Heart J.* (2007) 153:507–14. doi: 10.1016/j.ahj.2006.12.018

7. Canto JG, Kiefe CI, Rogers WJ, Peterson ED, Frederick PD, French WJ, et al. Number of coronary heart disease risk factors and mortality in patients with first myocardial infarction. *JAMA.* (2011) 306:2120–7. doi: 10.1001/jama.2011.1654

8. Nauta ST, Deckers JW, van der Boon RM, Akkerhuis KM, van Domburg RT. Risk factors for coronary heart disease and survival after myocardial infarction. *Eur J Prev Cardiol.* (2014) 21:576–83. doi: 10.1177/2047487312460514

9. Figtree GA, Vernon ST, Hadziosmanovic N, Sundström J, Alfredsson J, Arnott C, et al. Mortality in STEMI patients without standard modifiable risk factors: a sex-disaggregated analysis of SWEDEHEART registry data. *Lancet.* (2021) 397:1085–94. doi: 10.1016/S0140-6736(21)00272-5

10. Stone GW, Selker HP, Thiele H, Patel MR, Udelson JE, Ohman EM, et al. Relationship between infarct size and outcomes following primary PCI: patient-level analysis from 10 randomized trials. *J Am Coll Cardiol.* (2016) 67:1674–83. doi: 10.1016/j.jacc.2016.01.069

11. Durante A, Laricchia A, Benedetti G, Esposito A, Margonato A, Rimoldi O, et al. Identification of high-risk patients after ST-segment-elevation myocardial infarction: comparison between angiographic and magnetic resonance parameters. *Circ Cardiovasc Imaging.* (2017) 10:e005841. doi: 10.1161/CIRCIMAGING.116.005841

12. de Waha S, Patel MR, Granger CB, Ohman EM, Maehara A, Eitel I, et al. Relationship between microvascular obstruction and adverse events following primary percutaneous coronary intervention for ST-segment elevation myocardial infarction: an individual patient data pooled analysis from seven randomized trials. *Eur Heart J.* (2017) 38:3502–10. doi: 10.1093/eurheartj/ehx414

13. Lønborg J, Vejlstrup N, Mathiasen AB, Thomsen C, Jensen JS, Engstrøm T. Myocardial area at risk and salvage measured by T2-weighted cardiovascular magnetic resonance: reproducibility and comparison of two T2-weighted protocols. *J Cardiovasc Magn Reson.* (2011) 13:50. doi: 10.1186/1532-429X-13-50

14. Kim RJ, Fieno DS, Parrish TB, Harris K, Chen EL, Simonetti O, et al. Relationship of MRI delayed contrast enhancement to irreversible injury, infarct age, and contractile function. *Circulation.* (1999) 100:1992–2002. doi: 10.1161/01.CIR.100.19.1992

15. Abdel-Aty H, Zagrosek A, Schulz-Menger J, Taylor AJ, Messroghli D, Kumar A, et al. Delayed enhancement and T2-weighted cardiovascular magnetic resonance imaging differentiate acute from chronic myocardial infarction. *Circulation.* (2004) 109:2411–6. doi: 10.1161/01.CIR.0000127428.10985.C6

16. Touboul C, Angoulvant D, Mewton N, Ivanes F, Muntean D, Prunier F, et al. Ischaemic postconditioning reduces infarct size: systematic review and meta-analysis of randomized controlled trials. *Arch Cardiovasc Dis.* (2015) 108:39–49. doi: 10.1016/j.acvd.2014.08.004

17. Høfsten DE, Kelbæk H, Helqvist S, Kløvgaard L, Holmvang L, Clemmensen P, et al. The Third DANish Study of Optimal Acute Treatment of Patients with ST-segment Elevation Myocardial Infarction: Ischemic postconditioning or deferred stent implantation versus conventional primary angioplasty and complete revascularization versus treatment of culprit lesion only: Rationale and design of the DANAMI 3 trial program. *Am Heart J.* (2015) 169:613–21. doi: 10.1016/j.ahj.2015.02.004

18. Engstrøm T, Kelbæk H, Helqvist S, Høfsten DE, Kløvgaard L, Holmvang L, et al. Complete revascularisation versus treatment of the culprit lesion only in patients with ST-segment elevation myocardial infarction and multivessel disease (DANAMI-3—PRIMULTI): an open-label, randomised controlled trial. *Lancet.* (2015) 386:665–71. doi: 10.1016/S0140-6736(15)60648-1

19. Kelbæk H, Høfsten DE, Køber L, Helqvist S, Kløvgaard L, Holmvang L, et al. Deferred versus conventional stent implantation in patients with ST-segment elevation myocardial infarction (DANAMI 3-DEFER): an open-label, randomised controlled trial. *Lancet.* (2016) 387:2199–206. doi: 10.1016/S0140-6736(16)30072-1

20. Engstrøm T, Kelbæk H, Helqvist S, Høfsten DE, Kløvgaard L, Clemmensen P, et al. Investigators ftTDSoOAToPWSEMIIP. Effect of ischemic postconditioning during primary percutaneous coronary intervention for patients with ST-segment elevation myocardial infarction: a randomized clinical trial. *JAMA Cardiol.* (2017) 2:490–7. doi: 10.1001/jamacardio.2017.0022

21. Nepper-Christensen L, Lønborg J, Ahtarovski KA, Høfsten DE, Kyhl K, Ghotbi AA, et al. Left ventricular hypertrophy is associated with increased infarct size and decreased myocardial salvage in patients with ST-segment elevation myocardial infarction undergoing primary percutaneous coronary intervention. *J Am Heart Assoc*. (2017) 6:e004823. doi: 10.1161/JAHA.116.004823

22. Friedrich MG, Abdel-Aty H, Taylor A, Schulz-Menger J, Messroghli D, Dietz R. The salvaged area at risk in reperfused acute myocardial infarction as visualized by cardiovascular magnetic resonance. *J Am Coll Cardiol.* (2008) 51:1581–7. doi: 10.1016/j.jacc.2008.01.019

23. Hashimoto T, Ako J, Nakao K, Ozaki Y, Kimura K, Noguchi T, et al. Pre-procedural thrombolysis in myocardial infarction flow in patients with ST-segment elevation myocardial infarction. *Int Heart J.* (2018) 59:920–5. doi: 10.1536/ihj.17-518

24. O'Gara PT, Kushner FG, Ascheim DD, Casey DE Jr, Chung MK, de Lemos JA, et al. 2013 ACCF/AHA guideline for the management of ST-elevation myocardial infarction: a report of the American College of Cardiology Foundation/American Heart Association Task Force on Practice Guidelines. *Circulation.* (2013) 127:e362–425. doi: 10.1161/CIR.0b013e3182742cf6

25. Ibanez B, James S, Agewall S, Antunes MJ, Bucciarelli-Ducci C, Bueno H, et al. 2017 ESC Guidelines for the management of acute myocardial infarction in patients presenting with ST-segment elevation: the task force for the management of acute myocardial infarction in patients presenting with ST-segment elevation of the European Society of Cardiology (ESC). *Eur Heart J.* (2018) 39:119–77. doi: 10.1093/eurheartj/ehx393

26. Avis SR, Vernon ST, Hagström E, Figtree GA. Coronary artery disease in the absence of traditional risk factors: a call for action. *Eur Heart J.* (2021) 42:3822–4. doi: 10.1093/eurheartj/ehab474

27. Khan E, Brieger D, Amerena J, Atherton JJ, Chew DP, Farshid A, et al. Differences in management and outcomes for men and women with ST-elevation myocardial infarction. *Med J Aust.* (2018) 209:118–23. doi: 10.5694/mja17.01109

28. Entezarjou A, Mohammad MA, Andell P, Koul S. Culprit vessel: impact on short-term and long-term prognosis in patients with ST-elevation myocardial infarction. *Open Heart.* (2018) 5:e000852. doi: 10.1136/openhrt-2018-000852

29. Backhaus SJ, Kowallick JT, Stiermaier T, Lange T, Koschalka A, Navarra JL, et al. Culprit vessel-related myocardial mechanics and prognostic implications following acute myocardial infarction. *Clin Res Cardiol.* (2020) 109:339–49. doi: 10.1007/s00392-019-01514-x

30. Moon SH, Byun JH, Kim JW, Kim SH, Kim KN, Jung JJ, et al. Clinical usefulness of the angle between left main coronary artery and left anterior descending coronary artery for the evaluation of obstructive coronary artery disease. *PLoS ONE.* (2018) 13:e0202249. doi: 10.1371/journal.pone.0202249

31. Miranda E, Sousa LC, António CC, Castro CF, Pinto SIS. Role of the left coronary artery geometry configuration in atherosusceptibility: CFD simulations considering sPTT model for blood. *Comput Methods Biomech Biomed Eng.* (2021) 1488–1503.. doi: 10.1080/10255842.2021.1894555

32. Rakowski T, Dudek D, Dziewierz A, Yu J, Witzenbichler B, Guagliumi G, et al. Impact of infarct-related artery patency before primary PCI on outcome in patients with ST-segment elevation myocardial infarction: the HORIZONS-AMI trial. *EuroIntervention.* (2013) 8:1307–14. doi: 10.4244/EIJV8I11A199

33. De Luca G, Parodi G, Sciagrà R, Venditti F, Bellandi B, Vergara R, et al. Preprocedural TIMI flow and infarct size in STEMI undergoing primary angioplasty. *J Thromb Thrombolysis.* (2014) 38:81–6. doi: 10.1007/s11239-013-0977-x

34. Higuma T, Soeda T, Yamada M, Yokota T, Yokoyama H, Nishizaki F, et al. Coronary Plaque Characteristics Associated With Reduced TIMI (Thrombolysis in Myocardial Infarction) Flow Grade in Patients With ST-Segment-Elevation Myocardial Infarction: A Combined Optical Coherence Tomography and Intravascular Ultrasound Study. *Circ Cardiovasc Interv*. (2016) 9:e003913. doi: 10.1161/CIRCINTERVENTIONS.116.003913

35. Bulluck H, Carberry J, Carrick D, McEntegart M, Petrie MC, Eteiba H, et al. Redefining adverse and reverse left ventricular remodeling by cardiovascular magnetic resonance following ST-segment-elevation myocardial infarction and their implications on long-term prognosis. *Circ Cardiovasc Imaging.* (2020) 13:e009937. doi: 10.1161/CIRCIMAGING.119.009937

# Appendix

Table A1 Randomizations, total DANAMI-3, and CMR sub-population.

| **Total DANAMI-3 population** | **SMuRFless** ***n*** **= 283 (14%)** | **SMuRF > 0** ***n*** **= 1763 (86%)** | ***p*-value** |
|---|---|---|---|
| **Primary randomization** | | | |
| Randomized to deferred stenting, *n* (%). (DEFER) | 52 (18) | 508 (29) | <0.001 |
| Randomized to postconditioning, *n* (%). (iPOST) | 104 (37) | 472 (27) | <0.001 |
| Randomized to conventional treatment, *n* (%) | 127 (45) | 783 (44) | 0.88 |
| **Secondary randomization** | | | |
| Randomized to full-revascularization, *n* (% within secondary randomization). (PRIMULTI) | 26 (52) | 267 (51) | 0.85 |
| **CMR sub-population** | **SmuRFless** ***n*** **= 61 (8%)** | **SMuRF > 0** ***n*** **= 665 (92%)** | ***p*-value** |
| **Primary randomization** | | | |
| Randomized to deferred stenting, *n* (% within primary randomization). (DEFER) | 17 (28) | 222 (33) | 0.38 |
| Randomized to postconditioning, *n* (% within primary randomization). (iPOST) | 19 (31) | 160 (24) | 0.22 |
| Randomized to conventional treatment, *n* (%) | 25 (41) | 247 (42) | 0.58 |
| **Secondary randomization** | | | |
| Randomized to full-revascularization. (PRIMULTI) | 10 (48) | 136 (52) | 0.22 |

Table A2 Medical therapy at discharge, total DANAMI-3 and CMR sub-population.

| **Total DANAMI-3 population** | **SMuRFless** ***n*** **= 283 (14%)** | **SMuRF > 0** ***n*** **= 1,763 (86%)** | ***p*-value** |
|---|---|---|---|
| Antiplatelet therapy, *n* (%) | | | |
| Aspirin | 273 (96) | 1,732 (98) | 0.04 |
| Clopidogrel bisulfate | 74 (26) | 266 (15) | <0.001 |
| Prasugrel hydrochloride | 70 (25) | 946 (54) | <0.001 |
| Ticagrelor | 130 (46) | 530 (30) | <0.001 |
| Statin, *n* (%) | 271 (96) | 1,728 (98) | 0.01 |
| β-Blocker, *n* (%) | 245 (87) | 1,586 (90) | 0.08 |
| ACE/ARB, *n* (%) | 125 (44) | 799 (45) | 0.71 |
| **CMR sub-population** | **SmuRFless** ***n*** **= 61 (8%)** | **SMuRF > 0** ***n*** **= 665 (92%)** | **p-value** |
| Antiplatelet therapy, *n* (%) | | | |
| Aspirin | 61 (100) | 653 (98) | 0.29 |
| Clopidogrel bisulfate | 3 (5) | 40 (6) | 0.73 |
| Prasugrel hydrochloride | 43 (71) | 520 (78) | 0.17 |
| Ticagrelor | 14 (23) | 103 (13) | 0.13 |
| Statin, *n* (%) | 61 (100) | 661 (99) | 1.0 |
| β-Blocker, *n* (%) | 58 (95) | 613 (92) | 0.41 |
| ACE/ARB, *n* (%) | 23 (38) | 277 (42) | 0.54 |

# **Chapter 8.** Discussion - Overview of key findings and future directions

Despite significant advancements in the diagnosis, treatment and risk stratification of coronary artery disease, there are still a number of clinical challenges. In this thesis, I have addressed some of these challenges using cardiac imaging modalities including intravascular imaging and cardiac MRI.

1. A new method of assessment of infarct size and area at risk in a rodent model using 3D-MRI.
2. Identifying the clinical indications for use of OCT in cardiac catheterisation laboratory
3. Can 2D-QCA be used as an alternative to OCT in assessment of coronary artery lesion dimensions?
4. Assessed the plaque burden and progression in patients with no standard modifiable risk factors using IVUS
5. Clinical outcomes and infarct characteristics on cardiac MRI in patients with no standard modifiable risk factors

Below is an overview of the key findings and future directions.

## *Automated Quantification of Myocardial Salvage in a Rat Model of Ischemia–Reperfusion Injury using 3D High-Resolution Magnetic Resonance Imaging (MRI)*

The pathophysiology of coronary no-reflow after primary PCI is multifactorial and includes myocardial reperfusion injury that may occur after restoration of blood flow with accumulation of neutrophils and platelets that release inflammatory mediators and vasoconstrictors. Novel therapies targeting ischemia reperfusion injury are usually tested in small animal models. Therefore, an accurate assessment of infarct size and area at risk (AAR) is critical when assessing new therapies for myocardial ischemia reperfusion (IR) injury. In chapter 3, I aimed to develop and validate a high-resolution 3-dimensional (3D) magnetic resonance imaging (MRI) method for quantifying infarct size and AAR in a rodent model.

I addressed the problem of measuring the volume of infarction in animal models of ischemia reperfusion injury. In this study, I compared the standard Evan's Blue/TTC method of AAR/infarct delineation against a novel method that uses a combination of T2* contrast from MPIO to define the borders of the perfused/ unperfused myocardium, together with gadolinium-based T1- weighted enhancement to define the established infarct zone.

Current "gold standard" methods use a combination of selective perfusion of the heart with Evan's Blue and staining of the post-mortem sectioned heart with triphenyl tetrazolium chloride (TTC) to quantitate the area at risk and degree of completed infarct[1,2]. This method, although widely used and considered the "gold standard," has documented problems relating to the accurate and reproducible delineation of the border of the infarct and AAR zones[3].

A brief description of the procedure is as follows. Myocardial ischemia reperfusion injury was induced for 30 minutes by transient suture ligation of the left anterior coronary artery around 2 to 3 mm distal to the junction of pulmonary artery and left atrial appendage. The ligature was then released and the rats recovered for 48 hours. Under repeat anaesthesia, gadopentetate dimeglumine 0.15 mmol/kg was infused via the tail vein. After 10 minutes, the left anterior coronary artery was re-occluded and a solution containing MPIO (4.5 mg/kg body weight, as determined in pilot studies) mixed with 3% Evan's Blue, in a total volume of 5 mL, was infused. After a 2-minute interval, the heart was then excised, sectioned into 2-mm short-axis slices, and placed in TTC 1% in phosphate-buffered saline for 20 minutes at 37°C. Slices were photographed and then fixed in 10% normal buffered formalin.

Ex vivo MRI images of slices were acquired on a 9.4 Tesla magnet. The T2* data allowed visualization of AAR, with microparticle-associated signal loss in perfused regions. T1 data demonstrated gadolinium retention in infarcted zones. A Close correlation ($r=0.92$ to $0.94$; $P<0.05$) of MRI and Evan's Blue/TTC measures for both AAR and MI was observed when the combined techniques were applied to the same heart slice. However, 3D MRI acquisition and analysis of whole heart reduced intra-observer variability compared to assessment of isolated slices, and allowed automated segmentation and analysis, thus reducing interobserver variation. Anatomical resolution of 81 μm3 was achieved (versus ~ 2 mm with manual slicing). This novel, yet simple, MRI technique allowed precise assessment of infarct and AAR zones. It removed the need for tissue slicing and provided the opportunity for 3D digital analysis at high anatomical resolution.

The high-resolution 3D dataset achieved with this technique may help investigators assess the full impact of new therapies. Our technique has recently been adapted by Alqarni et al by

injecting gadolinium and iron oxide microparticles in a mouse model and performing 3D MRI ex-vivo to assess infarct size and area at risk with similar results[4].

**Future Directions:**

One of the challenges with current surgical technique of myocardial ischemia reperfusion models in rodents is the difficulty in performing the key step of ligating the left anterior descending artery in rodents. Recently Tong et al have described an improvement in the technique by using a polyvinyl chloride (PVC) tube and a unique knotting method [5]. In the current technique the myocardial tissue is ligated with a suture only which can tear the surrounding myocardial tissue or cause haemorrhage[5]. In the improved method by Tong et al, a soft PVC tube is used to apply pressure on the LAD, this prevents damage to the surrounding myocardial tissue and provides more consistent results[5]. The PVC tube is 2 mm in diameter and cut into 7 mm-length pieces. A 10 cm long 4-0 suture is inserted into the PVC tube, and tied at its ends, this helps with the insertion and removal of the PVC tube. A groove is cut in the middle of the PVC tube using ophthalmic scissors and the 6-0 suture is tied over the groove to prevent the PVC tube from falling off.

Another challenge with the traditional method of measuring AAR involves re-tying the LAD and injection of Evans blue via the tail vein to allow the Evans blue to perfuse the normal myocardium only and the absence of Evan's blue in the territory supplied by the LAD demarcates the boundary of AAR on tissue staining. This procedure has certain challenges. It requires re-operating on the animal especially if the study is intended for assessment of infarct size and AAR at longer time points e.g., 48 hours or 7 days. It requires re-tying the LAD at the same location at the time of second procedure which can be difficult to determine exactly and has the added risk of causing significant bleeding due to friable and oedematous tissue and

arrhythmias. The third challenge is injecting Evan's blue via the small tail vein. Unfortunately, our method of determining AAR by injecting MPIO's also requires these steps of re-operation, re-tying the LAD and injecting MPIO's via the tail vein.

An alternative method of measuring area at risk is by non-contrast T1 and T2 mapping by cardiac MRI which does not require these surgical steps to be performed. Ischemic injury due to occlusion of coronary vessel leads to an increase in edema or tissue water content which leads to an increase in myocardial T1 and T2 relaxation times. In a dog model of 2 hours of coronary occlusion followed by 4 hours of reperfusion, the area at risk was quantified by in-vivo T1 and T2 mapping[6]. AAR was defined as regions which had a T1 or T2 value (ms) greater than 2SD from remote. Both T1 and T2 mapping agreed well with each other and with the reference method using microspheres to determine the area at risk[6]. Although non-contrast T1 and T2 mapping has the potential to demarcate AAR in large animals, it can be very challenging to perform this technique in-vivo in small animal models.

The impact of Manganese on proton relaxation was first studied in 1962 and 1973[7]. It was the first MRI contrast agent assessed in mice in-vivo in the 1980s with significant cardiac, hepatic and renal uptake causing marked shortening of T1 relaxations[7]. Currently, Gadolinium is the most widely used contrast agent for myocardial infarction scar imaging as it accumulates in the extracellular space. Contrary to Gadolinium, Manganese can accumulate inside the myocytes by crossing myocardial L-type voltage-gated calcium channels and sodium-calcium exchangers as it is a calcium analogue[7]. Due to its ability to accumulate in viable myocytes, measurement of area at risk with manganese enhanced MRI (MEMRI) correlated well with fluorescent microspheres in a canine model, during and 2 hours after the occlusion of left anterior descending artery[8]. As Manganese accumulates in the normal viable myocytes and

shortens T1 relaxation, the area at risk and the infarcted area appear as a hypo-enhanced zone on MEMRI due to the absence of manganese in AAR and infarct[9]. When injected at time of occlusion of LAD in a rat model, the hypo-enhanced zone on MEMRI correlated with area at risk but when injected 6 hours after reperfusion, MEMRI correlated with infarct area on TTC staining [10]. The AAR maybe underestimated when Manganese is injected after reperfusion as Manganese may accumulate in the viable myocytes within the area at risk. Hence if MEMRI is used in rodent models, it would still require re-operation and re-tying of LAD in order to accurately assess the AAR.

The accurate assessment of AAR and infarct size in rodent models using cardiac MRI is challenging. Although our technique using Gadolinium and MPIO provides precise assessment of AAR and infarct along with a 3D assessment of whole heart, the surgical technique of the procedure remains a challenge. Improvements in surgical technique and MRI acquisition techniques may further improve assessment of infarct size and AAR in small animal myocardial ischemia reperfusion injury models.

### *Optical coherence tomography (OCT) as an adjunct to percutaneous coronary intervention; a single centre experience*

OCT is a relatively new intravascular imaging catheter in comparison to intravascular ultrasound [11] and indications for its use are not well defined. In **chapter 4**, I have tried to clarify the potentially under-appreciated clinical role that OCT may play in PCI. I reported a single centre experience where OCT was used to help guide management in routine clinical practice.

The main indications for use of OCT were categorised into 4 main sub-groups:

1 - To assess cause of stent thrombosis

2 - To assess in-stent restenosis

3 - To assess hazy or ambiguous lesions

4 - To optimise stent selection/size

OCT identified intracoronary pathologies like plaque rupture, intra-coronary dissection, cause of stent thrombosis and intracoronary thrombus. OCT added to angiographic interpretation in 70% cases and changed management in 49% cases. There were no complications related to the OCT procedures.

OCT provides cross sectional images of the coronary artery with a resolution up to 10 μm[12] which is approximately ten times higher than that of IVUS[12,13]. This allows OCT to demonstrate vessel morphology and stent deployment in greater detail then other currently clinically available technologies[14]. OCT demonstrates more clearly differentiation of lumen to arterial wall interface or the lumen border, when compared with IVUS [15]. This makes it superior to IVUS in identifying plaque rupture[16] coronary artery dissection and intracoronary thrombus[14,16]. In our case series it identified intraluminal pathologies like atheromatous plaque, coronary artery dissection, intracoronary thrombosis, plaque rupture and stent malapposition.

Our single centre study confirms that OCT is a safe procedure and can be used clinically to add to information obtained by coronary angiogram and to change management for the patient. Current guidelines also recommend using intravascular imaging for the indications used in our study[17].

A met-analysis of 9 randomised controlled trials showed that IVUS guided PCI reduced major adverse cardiac events and target lesion failure [18]. The clinical benefits of IVUS guided PCI were sustained at 5 years follow up[11]. There are no similar studies using OCT guided PCI vs. angiography guided PCI for clinical outcomes. However, OCT is non-inferior to IVUS guided PCI in terms of acute procedural results and mid-term clinical outcomes at 12 months in two randomised trials, ILUMIEN III and OPINION[19,20]. OCT has certain advantages over IVUS due to its higher resolution. OCT can detect stent malapposition, edge dissection, tissue coverage of stent struts and thrombus more clearly than IVUS[17]. OCT is more user friendly and images are easier to interpret. The main disadvantages of OCT are that it requires use of contrast and has limited ability to assess plaque burden due to lower tissue penetration especially in lipid rich plaque[17].

Current guidelines recommend intravascular imaging guided PCI for the following scenarios[17].

1. Long lesions, left main lesions and complex lesions.
2. IVUS guided PCI in chronic total occlusions.
3. OCT can be used to assess mechanism of stent failure (in-stent restenosis or stent thrombosis)

Current guidelines recommend the following approach when intravascular imaging guided PCI is used to optimise stent implantation[17].

**Pre-PCI assessment**

Intravascular imaging performed prior to PCI can identify plaque morphology and distribution. A heavily calcified lesion may require more aggressive lesion preparation with high pressure balloon dilatation or rotational atherectomy or intravascular lithotripsy. OCT allows better characterisation of calcification. IVUS can identify the arc of calcification but not the thickness

of calcification as the ultrasound waves are reflected off the calcified plaque[21]. An OCT based scoring system has been validated to determine which calcified lesions lead to under-expansion of stent, i.e. thickness >0.5mm, length of calcification >5mm and arc of calcium involving >50% (or >180 degrees) of the circumference of vessel[21]. Presence of all three factors increases the risk of stent under-expansion. A small observational study demonstrated greater stent expansion in lesions with fracture of coronary calcium after lesion preparation on OCT[22]. Demonstration of calcium fracture by OCT can be used as a goal for adequate lesion preparation.

Stent under-expansion is a strong predictor of in-stent restenosis and stent thrombosis, which emphasizes the importance of selecting the appropriate stent size[17]. An external elastic lamina [23] based diameter is preferable to lumen based diameter as it leads to a larger diameter stent without an increase in device related complications[21]. Stent size can be selected based on the proximal or distal reference diameter or an average of both[17]. Presence of significant plaque at the stent edge is associated with in-stent restenosis, stent thrombosis and major adverse cardiac events[17]. The appropriate length of stent should be based on avoiding a landing zone with >50% plaque burden[17].

**Post PCI optimisation of stent**

IVUS/OCT imaging post PCI can identify abnormalities related to deployment of stent, e.g., stent under-expansion, geographical miss, malapposition and edge dissection. Stent under-expansion is a strong predictor of stent failure. Stent expansion is defined as the minimum cross-sectional area or minimum stent area (MSA) which can be measured as an absolute value or relative to the reference diameter. A stent cross sectional area of 5.5mm2 is recommended based on IVUS studies and 4.5mm2 based on OCT studies for non-left main lesions[17]. For left

main lesions the cut-offs are higher, 7mm2 for distal left main and 8mm2 for proximal left main[17]. The drawback of using absolute values is that it may lead to under sizing in large vessels and failure to achieve target MSA in small vessels. The MSA relative to the proximal or distal reference segment has been used in clinical trials to overcome this. The various cut-offs used for relative minimum stent area (MSA) in clinical trials are; MSA greater than distal reference area, MSA >80% or >90% of the average (proximal and distal) reference area[17]. As it is usually difficult to achieve a relative MSA of > 90% in all cases, it is recommended to use a relative MSA of >80% in clinical practice. In the OCT based DOCTORS study, a relative MSA of >79.4% was associated with FFR >0.90[24].

OCT is superior to IVUS in detecting strut malapposition and edge dissection. Although acute stent malapposition is not a predictor of stent thrombosis in prospective studies as it may resolve over time. However, it is frequently seen as an underlying abnormality in cases of stent thrombosis in registries[17]. Current guidelines recommend that an acute malapposition that is <0.4mm in axial direction and <1mm in longitudinal direction does not need to be corrected[17]. However, this requires validation in prospective studies. Large dissections that are >60 degrees in lateral direction, involve the deeper layers or >2mm in depth are associated with adverse outcomes[17].

**Future directions:**

The OCT image acquisition requires injection of contrast to clear blood, which is not ideal in patients with renal failure. Low molecular weight dextran can produce comparable images but is also excreted via the kidneys and has the potential to cause renal injury. In a recent comparison of normal saline with contrast, it was possible to assess lesion morphology with saline flush but the clearance of blood was superior with contrast[25]. The lumen measurements

were smaller with saline OCT[25]. When saline flush measurements were corrected for the refractive index, the lumen dimension were larger with saline OCT[25]. An alternative flushing medium that has similar properties to contrast but less likely to cause renal injury is needed.

The presence of residual disease or dissection at stent edge is associated with in-stent restenosis or stent thrombosis. A software based, automated co-registration of OCT data with coronary angiogram reduces the errors with manual co-registration and may allow more precise stent deployment with full coverage of lesion. In a study of 398 patients treated with OCT guided PCI, the frequency of untreated lipid plaque within 5mm of proximal or distal stent edge was less in automated co-registration group than no co-registration group[26]. Automated co-registration is now available for clinical use.

A novel OCT based FFR has been developed and has good correlation and agreement with wire based FFR[27-29]. It uses the high-resolution images acquired by OCT to reconstruct the vessel dimensions precisely and then compute virtual FFR using a software[27]. In a study of 181 patients OCT based FFR was superior to angiography based quantitative flow ratio (QFR), when wire based FFR was used as a reference standard[28]. The diagnostic accuracy of OCT based FFR was not influenced by previous myocardial infarction or presence of stents[28]. OCT based FFR is promising as it allows assessment of coronary lesion morphology and ischemia with a single catheter.

Micro-OCT is the next generation OCT with a much higher resolution of 1-2μm and allows assessment of cellular morphology[30]. It was initially developed as a bench-top microscope system for in-vitro and ex-vivo studies[30]. Micro-OCT has been able to visualize endothelial cells, inflammatory cells, smooth muscle cells, micro-calcifications and cholesterol crystals in ex-vivo studies[30]. Recently the micro-OCT has been integrated into a coronary catheter, the

size of which is suitable for imaging human coronary arteries[31]. Its ability to visualise cellular and sub-cellular structures like macrophages, smooth muscle cells and cholesterol crystals was recently demonstrated in cadaver human coronary arteries and live rabbit aorta[31]. The development of an intracoronary micro-OCT catheter for clinical use in humans is awaited.

### *Comparison of two-dimensional quantitative coronary angiography (2D-QCA) with optical coherence tomography (OCT) in the assessment of coronary artery lesion dimensions*

An accurate assessment of intracoronary lumen dimensions is essential in the diagnosis and treatment of coronary artery disease. Although intravascular catheters like IVUS and OCT can provide an accurate assessment of the coronary artery lumen dimensions, they are invasive, expensive, time consuming and may require use of extra contrast. Also, these intravascular catheters may not be available in some cardiac catheterisation laboratories. 2D-QCA is available in most cardiac catheterisation laboratories as a software. It uses automated edge detection software to detect the contrast filled lumen of the coronary artery[32].

Previous studies comparing OCT and 2D-QCA show a good correlation, but how well the two agree with each other has not been well studied[33,34]. Chapter 5 shows a good correlation and agreement between 2D-QCA and OCT for estimating proximal and distal reference diameters. On average, the proximal reference diameter by 2D-QCA was 0.09 mm smaller and the distal reference diameter by 2D-QCA was 0.1 mm smaller than the OCT measurements. Importantly, most of the reference diameter measurements by 2D-QCA were within 0.5 mm of the OCT measurements. Although OCT is the gold standard in measuring coronary lumen dimensions, chapter 5 shows that in the absence or non-availability of OCT, 2D-QCA can be used to

estimate reference vessel diameters for sizing of stent prior to angioplasty. This is also supported by the ABSORB EXTEND study in which mandatory use of QCA prior to implantation of BVS showed a reduction in the under sizing of BVS[35].

QCA has the advantage of being non-invasive, inexpensive and less time consuming. The main technical challenge with QCA is selection of an appropriate image sequence. The accuracy of QCA is improved by selecting an image with minimal foreshortening and minimal overlap with other vessels or other radio-opaque structures[32]. The minimum luminal diameter (MLD) measured by QCA was significantly smaller compared to OCT. On average the MLD by QCA was 0.49 mm smaller than the OCT measurements. The possible reasons for this difference may be poor border detection by QCA or foreshortening of the image or incomplete filling of the vessel with contrast. In summary, there is a good correlation and agreement between 2D-QCA and OCT for measurement of proximal and distal reference diameters. However, the MLD was underestimated by 2D-QCA.

**Future directions:**

3D-QCA is a further improvement over 2D-QCA and was developed to overcome the limitations of 2D-QCA such as foreshortening and out of plane magnification errors. In order to perform 2D-QCA, the calibration procedure is required, which can increase measurement variability and introduce the so-called out-of-plane magnification error[36]. When the vessel of interest is not aligned in the same plane as the calibration object, lumen size can be overestimated or underestimated depending on the assessed position[36]. 3D-QCA allows reconstruction of a coronary artery in 3D from two angiographic views and reduces this error. While IVUS or OCT provides a wealth of information about plaque morphology, 3D QCA can

provide unique and complementary information including vessel tortuosity, curvature, and optimal viewing angles [37].

3D-QCA has been demonstrated to be more accurate than 2D-QCA in predicting physiologically significant coronary stenosis when FFR is used as a reference[38]. This was assessed in a substudy of FAVOR-II trial; a total of 645 vessels from 576 patients with 3D-QCA, 2D-QCA, and FFR were analyzed[38]. Using the conventional cut-off value of 50% for percent diameter stenosis, 3D-QCA was more accurate in predicting FFR ≤0.80 than 2D-QCA[38]. The study was based on data from prospectively enrolled consecutive patients with coronary lesions between 30% and 90% diameter stenosis and the overall optimal cut-off value for 3D-QCA was diameter stenosis of 50%[38].

Although, it's not possible to determine the exact ischemic potential of a lesion with coronary artery lesion dimension alone, the correlation between lesion severity and FFR has been shown in multiple studies[39]. A minimum luminal area (MLA) of 6mm2 and 4mm2 in left main and non-left main lesions on IVUS has been identified as a predictor of a functionally significant lesion on IVUS in multiple studies[39]. In a comparison study of 3D-QCA with IVUS for prediction of functionally significant coronary artery lesions i.e., FFR <0.8, 3D-QCA was non-inferior to IVUS[39]. The diagnostic accuracy of MLA was better than percentage diameter stenosis, as an area measurement may be closer to the true geometry of the lesion[39]. In this study of 175 lesions which were predominantly proximal LAD, the best cut-off value of 3D-QCA diameter stenosis percentage, 3D-QCA MLA, and IVUS MLA for ischemic FFR was 51.3%, 2.37 mm2 and 3.01 mm2, respectively[39].

**Quantitative flow ratio (QFR)**

Quantitative flow ratio (QFR) is a novel method for evaluating the functional significance of coronary stenosis by computation of FFR in the vessel based on 3-dimensional angiographic reconstruction and fluid dynamics algorithms[40]. Angiographic images are acquired at 15 frames/second and the contrast medium has to be injected manually with a forceful and stable injection or by the pump at a rate of approximately 4 ml/s[40]. It requires two angiographic image runs acquired at different angles ≥25 degrees apart. Images are then transferred by local network to the QFR system (AngioPlus, Pulse Medical Imaging Technology, Shanghai Co., Ltd., Shanghai, China) that uses algorithms for QFR computation[40]. The contrast flow model uses a frame count method to derive contrast flow velocity from coronary angiography[40].

**Diagnostic performance of QFR in comparison to FFR**

QFR was first evaluated in the single centre FAVOR pilot study and subsequently in FAVOR II China study, FAVOR Europe-Japan study and FAVOR III China study[40-43]. The multicentre FAVOR II China study enrolled 308 patients with at least 1 lesion with a stenosis of 30-90% in vessels ≥2mm in diameter. The lesions were assessed for QCA, QFR and FFR. The sensitivity and specificity of QFR was higher than QCA in predicting functionally significant stenosis when compared with FFR (sensitivity: 94.6% vs. 62.5%; $p < 0.001$; specificity: 91.7% vs. 58.1%; $p < 0.001$[40]. The patient- and vessel- level diagnostic accuracy of QFR was significantly higher than QCA at 92.4% and 92.7% respectively[40]. The FAVOR II Europe-Japan (Functional Assessment by Various Flow Reconstructions II Europe-Japan) was a prospective, observational study that enrolled 329 patients from 11 centres. FFR, QFR, and 2D-QCA was performed in 317 lesions. Sensitivity and specificity of QFR was significantly higher than 2D-QCA (sensitivity, 86.5% versus 44.2%; P<0.001; specificity, 86.9% versus 76.5%; P=0.002)[42]. The diagnostic accuracy of QFR was significantly higher for QFR compared with 2D-QCA (area under the receiver curve, 0.92 versus 0.64; P<0.001)[42].

A meta-analysis of 16 studies involving 3,335 vessels showed a good agreement and correlation between QFR and FFR[44]. The overall sensitivity, specificity, positive predictive value and negative predictive value were 0.84, 0.89, 0.80, and 0.92, respectively[44].

**Limitations of QFR**

Although QFR has good diagnostic performance, it has some limitations. In order to assess QFR in a coronary lesion, it requires two coronary angiogram images at least 25 degrees apart, no overlap of vessels and avoidance of short angiographic imaging time. Also, presence of coronary microvascular disease reduces the accuracy of QFR, however, it remains superior to angiography alone in the presence of microvascular disease[45]. In a multicentre registry, FFR and the index of microcirculatory resistance (IMR) were measured in 300 vessels[45]. When assessed according to microcirculatory status, a significantly lower AUC (area under the curve) of QFR were found in the high-IMR group as compared with the low-IMR group, AUC: 0.88 vs. 0.96, $p < 0.05$.

**Clinical applications of QFR**

QFR has the advantage of being a non-invasive wire-free and vasodilator-free method of assessing the functional significance of a coronary lesion. QFR can improve work flow as it also faster than performing an FFR. In FAVOR II Europe-Japan, the time to QFR computation was shorter than time to FFR (5.0 vs 7.0 min, $p < 0.001$)[42]. In the FAVOR III China study, QFR computation required $3.9 \pm 1.4$ min[43]. The clinical applications of QFR have been assessed in a number of trials.

FAVOR III China was a large multicentre, blinded, randomised, sham-controlled trial done at 26 hospitals in China that enrolled 3847 patients[43]. It compared angiography-guided PCI versus QFR based PCI in lesions with 50-90% diameter stenosis and vessel diameter at least 2.5mm by visual assessment[43]. Patients were randomised to QFR based PCI i.e., PCI was performed if QFR <0.8 versus angiography-guided PCI by standard visual assessment[43]. The primary endpoint was a composite of death from any cause, myocardial infarction, or ischaemia-driven revascularisation at 1 year. The 1-year primary endpoint occurred in 110 (5·8%) participants in the QFR-guided group and in 167 (8·8%) in the angiography-guided group, driven by fewer myocardial infarctions and ischaemia-driven revascularisations in the QFR-guided group[43].

**QFR in Multivessel Disease**

For patients with multivessel coronary artery disease, QFR of all three vessels maybe more practical than performing an invasive FFR. The prognostic significance of the sum of QFR of all three vessels was assessed in 549 patients with stable coronary artery disease who underwent an invasive coronary angiogram[46]. On multivariate analysis a three vessel sum of QFR <2.75 was one of the independent predictors of major cardiovascular adverse events[46]. In a retrospective analysis of 771 vessels from SYNTAX-II trial, achieving a post-PCI QFR of ≥0.91 was associated with lower vessel related adverse events at 2 years follow up[47].

**QFR in Acute Myocardial Infarction:**

The role of QFR has been assessed in patients with acute myocardial infarction (STEMI and NSTEMI). The post-PCI QFR of the culprit vessel was assessed in 186 patients at the time of staged PCI of non-culprit lesion more than 7 days after presenting with STEMI[48]. In these STEMI patients, a low post-PCI QFR in the culprit vessel was associated with higher vessel related adverse clinical events at 2 years follow up[48]. Hence, post-PCI QFR of the culprit vessel

in STEMI patients can be used as a predictor of prognosis. In patients with acute myocardial infarction (STEMI and NSTEMI) and multivessel coronary artery disease, complete revascularization with angiography guided or FFR guided PCI of the non-culprit lesion is superior to culprit-lesion-only PCI in reducing the risk of major cardiovascular events[49,50]. There is a concern that angiography guided PCI of non-culprit vessel in STEMI and NSTEMI patients may lead to unnecessary PCI. In a post-hoc analysis of FRAME-AMI trial, the clinical events post PCI of non-culprit lesions in STEMI and NSTEMI patients were assessed according to QFR. Patients were classified by non-culprit vessel QFR values into two groups i.e., QFR ≤0.80 and QFR >0.80. A total of 552 lesions were eligible for QFR analysis. In this analysis, 30.0% of angiography-guided PCI had QFR > 0.80 that resulted in un-necessary PCI for the non-culprit vessel, which was significantly associated with an increased risk of MACE than in those with deferred PCI for non-culprit vessel. Hence, QFR of non-culprit vessel in acute myocardial infarction is superior to angiography guided PCI.

***QFR in patients with myocardial bridge***

Myocardial bridge is a congenital anomaly in which the coronary artery takes an intramyocardial course and can get compressed during systole. It is usually considered a benign condition however in some cases it can be associated with myocardial ischemia, atrioventricular block, arrhythmias, and even sudden cardiac death[51]. The decision to perform surgical revascularisation in patients with a muscle bridge is clinically challenging. QFR was assessed in a retrospective observational study of 45 patients with a muscle bridge in mid LAD who had an invasive coronary angiogram[51]. Patients were initially treated with medical therapy and those refractory to medical therapy were surgically revascularized. Patients were retrospectively divided into a medical therapy group or a surgical therapy group. Due to the cyclical nature of stenosis in the myocardial bridge, the conventional QFR was not adequate.

QFR was assessed based on vessel geometry in end systole i.e., systolic geometry based QFR (SG-QFR) and in end diastole i.e., diastolic geometry based QFR (DG-QFR)[51]. The time-averaged QFR (TA-QFR) was defined as the average of SG-QFR and DG-QFR[51]. TA-QFR performed better than SG-QFR and DG-QFR in assessment of the functional significance of stenosis due to a myocardial bridge and is a novel index in guiding surgical intervention[51]. The optimal cut-off value of TA-QFR in predicting MB patients who require surgical intervention was 0.88, with an overall accuracy of 89%, sensitivity of 85%, specificity of 92%, PPV of 90%, and NPV of 89%[51].

***QFR in Drug Coated Balloon Angioplasty for In-stent restenosis***

Drug-coated balloons (DCB) are semi-compliant balloons covered with anti-proliferative drugs such as lipophilic paclitaxel that inhibits neointimal proliferation. Although DCBs are used as a treatment for in-stent restenosis (ISR), there is still a risk of recurrent ISR afterwards[52]. The prognostic role of QFR after DCB angioplasty has been assessed in two studies. In a study of 226 lesions treated with DCB for ISR, QFR value after DCB angioplasty was one of the predictors of recurrent restenosis after DCB angioplasty[52]. The optimal QFR cut-off value was determined to be 0.90 with a sensitivity of 0.94, specificity of 0.56, and accuracy of 0.79 in predicting recurrent restenosis[52]. Another study of 185 in-stent restenosis lesions treated with DCB angioplasty showed similar results[53]. A low QFR after DCB angioplasty in DES-ISR lesions was an independent predictor of adverse clinical events during a 1-year follow up[53]. Post PCI QFR cut-off of 0.94 was a better predictor than percentage diameter stenosis for vessel related clinical endpoints, defined as a composite of cardiac death, vessel-related myocardial infarction, and ischemia-driven target vessel revascularization[53].

**QFR to assess Microcirculatory function**

The index of microcirculatory resistance (IMR) is a measure of coronary microvasculature function and it is calculated by measuring the distal intracoronary pressure and the mean transit time during maximal hyperaemia with an invasive coronary pressure-wire[54] (reword). In STEMI patients, a post PCI IMR of >40U is associated with a higher rate of mortality and readmission for heart failure when measured at end of the procedure[54]. IMR is still considered a research tool and not used widely in clinical practice due to being invasive and requires additional time and cost. Recently, IMR derived from QFR called Angiography-derived index of microcirculatory resistance (IMRangio) has been proposed as an alternative to the wire based IMR[54]. The diagnostic accuracy of IMRangio was assessed in 145 patients with STEMI, NSTEMI and stable chronic coronary artery syndrome[55]. The IMRangio correlated well with invasive wire based IMR and demonstrated good diagnostic performance in predicting high IMR (STEMI AUC = 0.93; NSTEMI AUC = 0.77; CCS AUC = 0.88)[55]. IMRangio has the potential to be used more widely in clinical practice as it is wire-free, less expensive and shortens time of the procedure.

**vFFR**

vFFR is another angiography based FFR developed by CAAS, Pie Medical Imaging, Maastricht, the Netherlands and is obtained from two angiographic views at least 30° apart to generate the QCA[56-58]. The vFFR is calculated automatically by integrating the invasively measured aortic root pressure and the automatically generated 3D-QCA dimensions[56-58]. The pressure drop is calculated by applying the laws of physics including viscous resistance and separation loss effects present in coronary flow behavior[56-58]. A recent study of 334 patients demonstrated that 3D-QCA-based vFFR has excellent diagnostic performance to detect FFR

≤0.80[58]. This was a prospective observational multicentre study. Both site-determined and blinded independent core lab vFFR measurements were compared to FFR. The calculation of vFFR using 3D-QCA is promising and can reduce the need for using invasive measurement with FFR wire and improve work flow in the cardiac catheterisation laboratory. However, larger clinical trials are needed to further validate vFFR by 3D-QCA.

## *Progression of coronary atherosclerosis in patients without standard modifiable risk factors*

A number of large observational studies have shown, somewhat unexpectedly, that SMuRFless patients have higher in-hospital and 30-day mortality rates after myocardial infarction compared to patients with at least one of the major risk factors[59-64]. Analysis of 62,048 patients with first presentation ST-segment elevation myocardial infarction (STEMI) in the SWEDEHEART registry showed that SMuRFless patients had a ~1.5 times higher 30-day mortality rate compared to patients with >0 SMuRFs[63]. In a recent global metanalysis of 15 studies that included 1,285,722 patients, 11.56% were SMuRF-less[65]. The SMuRFless patients were 7.44% of non-ST-segment-elevation ACS patients and 12.87% of STEMI patients[65]. The proportion of SMuRFless patients presenting with STEMI (60.71%) tended to be higher than those with SMuRFs (49.21%)[65]. The SMuRFless patients had increased in-hospital mortality and cardiogenic shock despite lower body mass index and fewer comorbidities such as chronic kidney disease, peripheral arterial disease, stroke and heart failure[65]. A large retrospective analysis of 434,111 STEMI patients from the National Inpatient Sample database in the United States, identified 318,281 (73.4%) patients as SMuRF and 115,830 (26.6%) as SMuRFless patients[66]. The SMuRFless STEMI patients had higher odds of in-hospital mortality and in-hospital STEMI-related complications compared with SMuRF STEMI patients[66].

The reasons for the higher mortality rates in SMuRFless patients following myocardial infarction are not well understood. In order to better understand SMuRFless patients, I analysed their coronary plaque characteristics on IVUS (chapter 6) and myocardial infarct characteristics on cardiac MRI (chapter 7).

Greater plaque burden measured as PAV on baseline IVUS imaging in clinical trials has been shown to be associated with adverse cardiovascular events[67,68]. In an analysis of 4137 patients pooled from 6 clinical studies that used serial IVUS imaging, for each standard deviation increase in baseline PAV, there was a 1.3-fold increase in major adverse cardiovascular events[67]. The importance of baseline plaque burden has also been demonstrated in a post-hoc analysis of SATURN trial in which for each standard deviation increase in baseline PAV, there was 28% increase in major adverse cardiovascular events, despite achieving very low LDL-C levels of <70mg/dl[68].

In chapter 6, I utilised serial IVUS data from a pooled cohort of 5823 patients enrolled in ten clinical trials[69-78] to examine the rates of plaque progression in patients who had no standard modifiable risk factors versus individuals with risk factors who were matched on age, sex and use of statins. It is the first study comparing SMuRFless CAD patients with SMuRF explained CAD patients in terms of burden of coronary artery plaque and progression of plaque with comprehensive IVUS imaging. In chapter 6, baseline IVUS imaging showed that SMuRFless patients had less plaque burden compared to patients with SMuRFs.

Progression of plaque on serial IVUS imaging has also been shown to be associated with major adverse cardiovascular events[67]. Each standard deviation increase in PAV over a mean follow up of 21 months has been shown to be associated with a 1.2 fold increase in major adverse

cardiovascular events on serial IVUS imaging[67]. In chapter 6, there was no difference in the rate of progression of plaque between the two groups as determined by the change in PAV and the change in normalised TAV over a period of 12 months. This suggests the absence of traditional risk factors does not impact the potential modifiability of atherosclerotic plaque in these patients.

The role of intensive treatment of underlying risk factors to modify plaque in patients with standard modifiable risk factors is well established[79]. However, the absence of these risk factors in some patients presenting with myocardial infarction has stimulated the search to identify additional factors that may influence atherosclerosis. In our study, SMuRFless patients had lower CRP levels, suggesting that inflammation may not be the explanation for atherosclerosis in this group.

**Future Directions:**

The IVUS study in chapter 6 is limited by the lower resolution of IVUS and lacked information regarding plaque composition e.g., lipid rich or fibrotic. Other plaque features like necrotic cap and thin cap fibro atheroma were not assessed. Also, spotty calcification which is a marker of unstable lesions was not measured in these studies. An OCT based imaging study of the coronary plaque in SMuRFless patients is needed to provide more understanding of plaque morphology in these patients.

**Air Pollution:**

Further studies are required to identify additional risk factors that may be associated with atherosclerosis. For example, repetitive long-term exposure to air pollution promotes atherosclerosis and increases the risk of myocardial infarction[80]. Air pollution is a complex

mixture of gaseous phase and particulate constituents[80]. The particulate matter [74] in the air is categorized by aerodynamic diameter as <10 μm ($PM_{10}$), <2.5 μm ($PM_{2.5}$), <0.1 μm (ultrafine particles), and between 2.5 and 10 μm ($PM_{2.5-10}$)[80]. Fine particulate matter ($PM_{2.5}$) is the most important environmental contributor to global cardiovascular mortality and disability[80]. In a systematic review and meta-analysis of 34 studies, the risk of acute myocardial was increased after short-term air pollution exposures to $PM_{2.5}$, nitrogen dioxide, sulfur dioxide and carbon monoxide[81]. The relative risk of acute cardiovascular events can increase by 1% to 3% within a few days after short-term elevations in $PM_{2.5}$[80]. Long term exposure over several years may increase this risk by a larger magnitude (~10%)[80]. Repetitive long-term exposure is hypothesized to promote atherosclerosis[80]. The mechanisms of air pollution mediated cardiovascular risk maybe due to endothelial dysfunction, inflammation, prothrombotic pathways, autonomic imbalance and epigenomics[80].

**Genetic Risk:**

Genome wide association studies have identified more than 50 loci associated with risk of coronary artery disease and genetic risk score based on these alleles can identify individuals at high risk of coronary artery disease[82]. Polygenic risk scores have the potential to predict risk of developing coronary artery disease but the incremental benefit over the traditional risk factors is modest[83,84]. In an analysis of 7237 US adults of European ancestry, the polygenic risk score did not significantly improve risk reclassification when compared with standard modifiable risk factors[84]. The added value of combining a polygenic risk score with a risk score based on traditional risk factors was evaluated in a cohort of 352 660 participants with no history of cardiovascular disease over a follow up of 8 years[83]. The C statistic for discrimination of CAD for polygenic risk score, traditional risk factors, and both combined was 0.61, 0.76, and 0.78, respectively[83]. The change in C statistic between the latter 2 models was 0.02, which was statistically significant but the incremental benefit was very modest[83]. The

addition of the polygenic risk score to traditional risk factors resulted in a net reclassification improvement of 4.4% which was only a small proportion of cases[83]. As the incremental benefit of polygenic risk score on top of traditional risk factors model is only modest, the use of genetic information over the traditional risk factor score is still not ready for clinical implementation[83]. However, a potential advantage of a polygenic risk score maybe screening at a young age when traditional risk factors are absent and this may motivate individuals to make healthy lifestyle choices e.g., good diet and physical activity[84]. It is often assumed that the genetic predisposition to coronary artery disease is deterministic, however, it may be possible to attenuate the genetic risk of coronary artery by healthy lifestyle[82]. This was assessed in a study involving 55,685 participants, in which, genetic and lifestyle factors were independently associated with risk of developing coronary artery disease[82]. Interestingly, in this study, among subjects with high genetic risk, a favourable lifestyle reduced the relative risk of coronary artery disease by 50% when compared with unfavourable lifestyle[82]. It also included 4260 participants from the cross-sectional BioImage Study in whom subclinical coronary artery calcium was quantified in Agatston units[82]. Within low, intermediate and high genetic risk groups, a favourable lifestyle was associated with significantly less coronary-artery calcification[82]. Hence, a healthy lifestyle should be encouraged in every one but particularly in those with high genetic risk[82].

**Biomarkers to risk stratify SMuRFless patients**

The association between raised serum biomarkers and recurrent cardiovascular events in patients with ACS is well established[85]. These biomarkers represent different pathophysiological processes, BNP represents hemodynamic stress, high CRP (hs-CRP) and fibrinogen represents inflammation, d-dimer represents activated coagulation, uric acid (UA) represents endothelial activation, GGT (gamma-glutyl transferase) represents oxidative stress and Lipoprotein (a) or Lp(a) represents lipid disorders[85]. The role of these 7 biomarkers in risk

stratifying SMuRFless patients with ACS for recurrent cardiovascular events was recently assessed in a single centre retrospective observational study[85]. In this study, 81 of the 621 SMuRFless patients experienced a major adverse cardiovascular event (MACE) during a median follow up of 5 years[85]. MACE was defined as a composite of death, myocardial infarction and stroke. Out of the 7 biomarkers, higher fibrinogen, D-dimer, NT-proBNP and Lp(a) levels each were independently associated with increased risk of MACE[85]. However, hs-CRP, UA and GGT were not predictive of MACE on the multivariate analyses[85]. The risk of MACE was increased with increasing number of elevated biomarkers[85]. If all four biomarkers that were associated with increased risk of MACE were elevated, there was a 6-fold increased risk for MACE compared to those without any elevated biomarkers[85]. The predictive value of these 4 biomarkers varied significantly based on gender and the type of ACS, i.e., unstable angina, NSTEMI or STEMI indicating that these biomarkers may not be applicable to all ACS subgroups simultaneously[85]. D-dimer had the strongest association with MACE and was predictive in males, females and all subtypes of ACS, suggesting that activated coagulation may play an important role in progression of atherosclerosis in SMuRFless patients[85]. In the absence of traditional risk factors, a strategy of multiple biomarkers can potentially be used to identify patients at high risk of recurrent cardiovascular events[85].

**Metabolomics for coronary artery disease**

Metabolomics is the systematic identification and quantification of small molecules (up to 1.5 kDa) or metabolites in biological fluids[86]. The metabolites are the end products of cellular regulatory processes and capture a unique aspect of cellular homeostasis that reflects the gene and protein functional activity at a given point in time[87]. Hence, it reflects the metabolic state of the biological system at a given point in time. A systematic review of metabolomics studies identified 5 metabolites, acylcarnitine, dicarboxylacylcarnitine, trimethylamine N-oxide

(TMAO), phenylalanine, and glutamate that were associated with the incidence of cardiovascular disease[86]. In a study of 5768 participants, plasma dimethylguanidino valerate (DMGV) levels were associated with the incidence of type 2 diabetes mellitus, coronary artery disease and cardiovascular mortality[88]. Interestingly, the intake of sugar-sweetened beverages was associated with increased levels of DMGV, while intake of vegetables and the level of physical activity was associated with lower DMGV[88]. Hence, it's possible to modify levels of DMGV with lifestyle interventions.

Bio-HEART-CT is a prospective, longitudinal study to identify novel biomarkers of coronary artery disease across multiple centres in Australia[89]. It aims to recruit 5000 adults undergoing clinically indicated CT coronary angiogram and blood samples are assessed for novel biomarkers using state-of-the-art genomics, metabolomics, proteomics and immunophenotyping[89]. The identification of coronary atherosclerosis on CTCA in conjunction with serum biomarkers may improve the ability to detect new biomarkers and pathways for coronary artery disease. It may also help develop new risk models that incorporate the traditional risk factors and new biomarkers. A recent analysis of 1002 patients from Bio-HEART-CT study identified associations between four metabolites and coronary artery plaque phenotype on CTCA[86]. The four metabolites studied were TMAO, DMGV, glutamate, and phenylalanine. Out of these four metabolites, DMGV was most strongly associated with coronary artery disease plaque features[86]. DMGV was strongly associated with the presence of calcified plaque, obstructive coronary artery disease, and amount of coronary artery disease[86]. It also identified two metabolic pathways strongly associated with coronary artery disease, independent of traditional risk factors, the nucleotide metabolic pathway and the lipid metabolic pathway[86]. Further results from Bio-HEART-CT study may identify new biomarkers and mechanistic pathways of coronary artery disease.

**Plasma Proteomics based model**

Individual plasma biomarkers like pro-brain natriuretic peptide (BNP), high sensitivity troponins, and high sensitivity C-reactive protein (CRP) have limited value in predicting cardiovascular risk[90] This may be due to the fact that a single biomarker is part of a specific pathophysiological process but does not reflect the complexity of atherosclerosis[90]. Simultaneous measurement of a large number of plasma proteins may improve the risk prediction model. Widespread use of proteomics has been limited due to labour intensiveness, high costs, and the complex clinical interpretation[90]. Recently these limitations have been overcome by technical advancements[90]. Computational modelling allows interpretation of large data sets[90].

Recently a proteome-based model outperformed the traditional risk factor-based model in predicting the risk of myocardial infarction in a primary prevention setting[90]. The proteomics panel comprising of 368 proteins, related to pathways and/or risk factors involved in atherogenesis, to predict cardiovascular events was tested in 822 apparently healthy individuals in the United Kingdom[90]. A panel of 50 proteins was identified, which outperformed the clinical risk model in the prediction of myocardial infarction [area under the curve (AUC) 0.754 vs. 0.730; $P < 0.001$] during a median follow-up of 20 years[90]. The predictive value of the protein panel was also tested in another cohort of patients and confirmed to be superior to the clinical risk model (AUC 0.705 vs. 0.609; $P < 0.001$)[90].

The ability of proteome-based risk model in predicting recurrent cardiovascular events has also been tested in the setting of secondary prevention[91]. At first, 267 proteins were tested in a derivation cohort to construct a protein-based model comprising of 50 proteins with the highest

predictive value using machine learning[91]. The proteome-based model outperformed the clinical model in both the derivation cohort [area under the curve (AUC): 0.810 vs. 0.750; P < 0.001] and the validation cohort (AUC: 0.801 vs. 0.765; P < 0.001)[91]. It also identified a neutrophil dependent pathway in patients with low CRP, implying a residual inflammatory risk beyond the traditional IL-6 dependent pathway. The increased number of neutrophil-related proteins in the low CRP group with increased cardiovascular risk, also corresponds to the findings from LoDoCo2 (Low Dose Colchicine 2) trial in which proteins related to neutrophil-activation such as myeloperoxidase were reduced following colchicine treatment[91].

**Anatomic risk factors for coronary artery disease**

Atherosclerosis is a result of the complex interplay between systemic risk factors, anatomical risk factors and the physiological response of the arterial wall[92]. From the study of arterial bifurcation regions, it has been observed that the atherosclerotic plaque is more likely to build up and progress at certain geometric locations such as bifurcation sites despite the whole vascular tree being exposed to systemic risk factors[92]. The disturbance in flow and the low wall shear stress in these regions enhances the cellular and molecular processes towards atherosclerosis[92]. Hence, anatomic features maybe one of the risk factors that may explain the predisposition to coronary atherosclerosis in some individuals without traditional risk factors. The concept of high-risk geometry was first proposed by Friedman et al. in 1983 while studying pulsatile flow through casts of human aorta bifurcations[92]. Recent computational studies built on his initial work, has led to the discovery of several anatomical features that can influence wall shear stress e.g., inward curvature, marked angulating daughter branches, asymmetrical T-shaped bifurcation, bifurcation angle, cardiac curvature, vessel diameter, inflow angle and tortuosity[92].

There have been significant improvements in the spatial and temporal resolution of CT coronary angiography. Recently, a study (GeoCAD) has been proposed to better understand the relationship between high-risk anatomic features and risk of coronary artery disease[92]. It aims to develop a better coronary artery risk model by incorporating coronary artery geometry, coronary calcium score and traditional risk factors [92]. The recent improvements in computational processing power, large data storage and advancements in machine learning, may allow the translation of advanced imaging analysis into a practical coronary artery disease risk model that can be used clinically[92].

GeoCAD cohort study is a proof-of-concept study to address the risk of coronary artery disease in individuals with no traditional risk factors[92]. The primary aim is to identify novel anatomical biomarkers to improve the accuracy of prediction of coronary artery disease[92]. The secondary aims are:

1. To profile the CTCA images of a large population with respect to variations in anatomical shape and associated haemodynamic risk, comprising an individual's anatomical risk.
2. To develop a machine-learning algorithm for the rapid assessment of anatomical risk directly from unprocessed CTCA images.
3. To develop a novel CAD risk model combining traditional risk factors with anatomical risk.

It aims to retrospectively identify 1000 patients from the CTCA database at St. Vincent's Hospital, Sydney, Australia, who were referred for a CTCA for suspected coronary artery

disease[92]. Patients who have undergone at least two CTCA scans from 2010 onwards will be identified to allow comparison of geometry and plaque features over time[92].

**New Clinical pathway for SMuRFless patients**

Recently a clinical pathway has been proposed to guide physicians in the diagnosis and management of SMuRFless patients based on the currently available evidence by an international multidisciplinary team using a modified Delphi approach where clear evidence was not available[93]. The clinical pathway outlines the additional investigations and management that should be considered in SMuRFless patients with coronary artery disease. An international multicentre, prospective patient registry has been established through special clinics to measure the efficacy and cost-effectiveness of the pathway[93]. It will also report clinical outcomes. The diagnostic pathway will be implemented initially in 3 Australian states (New South Wales, Victoria, and South Australia) and later incorporated into additional clinics where SMuRFless patients may be found, including in Singapore and Mount Sinai Health System, New York[93]. The clinical pathway recommends the following four steps:

1) The first step is to confirm the presence of atherosclerotic coronary artery disease. In the setting of acute myocardial infarction, it requires the exclusion of non-atherosclerotic causes like spontaneous coronary artery dissection, coronary embolism and Takotsubu Cardiomyopathy. In the setting of stable angina, CT coronary angiogram or coronary calcium score can be used to confirm the presence of atherosclerosis.

2) The second step is to confirm the SMuRFless status. It proposes the following cut-offs to correctly discriminate SMuRFless patients from SMuRFs.

| | |
|---|---|
| Hypertension | Systolic blood pressure ≥140 mm Hg or<br>Diastolic blood pressure ≥90 mm Hg |
| Diabetes mellitus | HbA1c ≥ 6.5% or fasting blood glucose level ≥7.0 mmol/L or Oral Glucose Tolerance test with 2-hour blood glucose level >11.1 mmol/L |
| Hypercholesterolemia | Total cholesterol >5.5 mmol/L<br>Low density lipoprotein-C >3.5 mmol/L |
| Cigarette smoking | Current smoker (smoking within 12 months) |

3) Patients with coronary artery disease and no modifiable risk factors should receive guideline based secondary prevention medications irrespective of their cholesterol and blood pressure. The group advocates for the inclusion of SMuRFless patients with coronary artery disease in interventional and secondary prevention trials.

4) The clinical pathway recommends a systematic screening for additional risk factors known to be associated with atherosclerosis and cardiovascular mortality by taking a detailed history and physical examination. These risk factors are as follows:

a) **Obstructive Sleep Apnoea:** Untreated severe obstructive sleep apnoea (OSA) is associated with the incidence of coronary artery disease and major adverse cardiovascular events. The hypoxia and fragmented sleep from OSA are associated with altered cardiac and pulmonary vascular hemodynamics that drive sympathetic activation, systemic inflammation, endothelial dysfunction, and generation of reactive oxygen species, that promote the development of atherosclerosis. The pathway recommends screening of SMuRFless patients for OSA using clinical questionnaires and referring to a sleep physician for diagnosis and treatment if necessary.

b) **Nutrition:** Provide dietary advice as per guidelines. Encourage Mediterranean diet, replacement of saturated with unsaturated fat, increased consumption of plant-based foods rich in fibre, restricted consumption of processed meats, and consumption of fish.

c) **Physical Activity:** The International Physical Activity Questionnaire will be used to record physical activity and sedentary time for all patients. Patients will be encouraged to exercise regularly as per World Health Organisation guidelines, i.e. 150 to 300 minutes of moderate-intensity aerobic activity or 75 to 150 minutes of vigorous-intensity aerobic physical activity throughout the week.

d) **Oral health and periodontal disease:** Poor oral health is associated with coronary artery disease in observational studies. A meta-analysis of 22 studies, including 129,630 participants showed a 2-fold increased risk of myocardial infarction in those with periodontal disease after adjustment for traditional cardiovascular risk factors. However, there may be confounders like lower education and socioeconomic status. The pathway recommends screening for oral health with a self-reported questionnaire and referring to a dentist if necessary.

e) **Psychological and social factors:** Mental health and social factors are known to be associated with coronary artery disease. The pathway recommends screening all SMuRFless CAD clinic patients with a Patient Health Questionnaire to identify a depressive disorder.

f) **Inflammatory Disorders:** Systemic inflammatory diseases like systemic lupus erythematosus, rheumatoid arthritis, psoriasis, and inflammatory bowel diseases are known to be associated with increased risk of coronary artery disease. Patients will be

screened for these disorders by taking a detailed history and a limited set of screening tests including high-sensitivity C-reactive protein, rheumatoid factor, anti-cyclic citrullinated protein antibodies, antinuclear antibody, and antineutrophil cytoplasmic antibodies.

g) **Cardio-Oncology:** SMuRFless patients will be screened for a history of previous malignancy with a particular focus on childhood malignancy; mediastinal radiation; and chemotherapy agents, immunotherapies, and biologics.

h) **Sex-Specific Factors:** SMuRFless patients will be screened for pre-eclampsia, small for gestational age, preterm birth, gestational hypertension, gestational diabetes, endometriosis, polycystic ovary syndrome, ovarian insufficiency, menopause/hormonal status, use of hormone contraceptives, androgen deficiency, erectile dysfunction and use of anabolic or synthetic steroids.

i) **Metabolic and Vascular Health:** If the lab tests in step 2 shows an abnormality or are borderline, patients will be further assessed for insulin resistance using homeostatic model assessment by measuring fasting glucose and insulin levels. Glucose tolerance test will be considered 4 weeks post ACS to avoid false positive results. Lipoprotein (a) will be measured in all patients. Non–HDL-C will be calculated and reviewed as an alternative marker.

j) **Thrombotic factors:** Fibrinogen, Plasminogen activator inhibitor-1, and homocysteine will be measured in all SMuRFless patients with coronary artery disease.

Fibrinogen binds to platelets via glycoprotein IIb/IIIa receptors and promotes platelet aggregation. It is an independent risk factor for coronary artery disease and may mediate the effect of traditional risk factors as higher levels and activity are seen with age, smoking, diabetes and hyperlipidaemia.

Plasminogen activator inhibitor (PAI)-1 is required for the dissolution of insoluble fibrin in clots as it is the main physiologic inhibitor of tissue-type and urokinase-type plasminogen activator, which are responsible for the enzymatic activation of plasminogen. Polymorphisms in the gene for (PAI)-1 are associated with altered plasma PAI-1 concentrations and are associated with CAD.

Hyperhomocysteinemia has been associated with premature cardiovascular disease. It may occur due to genetic mutations to enzymes including cystathionine-β-synthase and methylenetetrahydrofolate reductase. Hyperhomocysteinemia can also result from nutritional deficiencies in folate, vitamin B12, and vitamin B6 and with metformin therapy (via reduction in B12 levels).

**k) Additional Vascular Studies:** Screening for atherosclerosis in other vascular territories will be considered if symptoms are suggestive of clinically relevant disease using duplex ultrasound for carotids and vertebral arteries and ankle-brachial index for lower limbs.

**l) Environmental factors:** Heavy metals (lead, cadmium, mercury, and arsenic) and particulate air pollution are associated with coronary artery disease and will be assessed by history or direct measurement. Exposure to common tick bites may lead to the

development of IgE antibodies to mammalian α-gal and is associated with >2-fold increase in the risk of coronary artery disease. IgE sensitivity to α-gal will be considered in some patients with a history of tick bite.

m) **Inherited risk, genetic analysis and polygenic risk scores:** SMuRFless patients will be screened for a family history of CAD, which is defined as an MI, stroke/transient ischemic attack, or peripheral artery disease in a first-degree relative who had an event before the age of 55 years if male or 65 years if female. In cases of a strong family history of premature CAD, screening for rare variants will be considered using whole-genome sequencing, whole-exome sequencing, or single-nucleotide polymorphism array.

In summary, the clinical pathway aims to perform a comprehensive assessment of SMurFless patients in dedicated clinics as part of a multicentre international registry. This approach aims to identify additional unknown risk factors that maybe modifiable.

### *Cardiovascular magnetic resonance characteristics and clinical outcomes of patients with ST-elevation myocardial infarction and no Standard Modifiable Risk Factors - A DANAMI-3 substudy.*

In order to understand the reasons for the observed high mortality in SMuRFless patients, we evaluated the clinical outcomes and CMR measures of infarct characteristics and LV remodelling in patients with and without SMuRFs who presented with first-presentation STEMI in chapter 7.

We identified 2046 patients from three randomized controlled STEMI trials performed at four large primary percutaneous coronary intervention [19] centres in Denmark; 14% were SMuRFless and 86% had >0 SMuRF. In terms of clinical outcomes, there was no difference in all-cause mortality, non-fatal reinfarction or hospitalization for heart failure at 30 days or at long-term follow-up. In the recent study of the SWEDEHEART Registry, 30-day mortality rates were ~50% higher in SMuRFless STEMI patients (11.3%) vs. those with at least one modifiable risk factor (7.9%; $p < 0.0001$)[63]. In comparison, the mortality rate was much lower overall in the DANAMI series (2%), and not significantly different between the groups. This lower mortality rate may reflect a degree of selection bias, with severely unwell patients being unsuitable for randomization to clinical trials, as well as potential higher rates of secondary prevention medications that are recognized to occur in the setting of a rigorous clinical trial vs. a "real-world" registry. It may also relate to the lower-than-expected proportion of women in the DANAMI study population, given women have an excess early mortality post STEMI[63,94]. On the other hand, register-based data are more prone to bias as regards the existence of comorbidities and risk factors, which may be even more pronounced among the most critically ill who also carry the highest mortality rate. The presence of multivessel disease in the overall population was higher in the SMuRF group (41 vs. 34%, $p = 0.02$), however, despite this the incidence of clinical outcomes like all-cause mortality, nonfatal reinfarction, or hospitalization for heart failure at 30 days or long-term follow up was not higher in the SMuRF group. Hence, the presence of higher multivessel disease in the SMuRF group probably did not have an effect on outcomes.

The SMuRFless patients had larger acute infarct size (17% vs. 13%, $p$=0.04) and smaller myocardial salvage index (42% vs. 50%, $p$=0.02). The most significant predictors of infarct size were a culprit LAD lesion and TIMI 0–1 flow pre-PCI. This is consistent with the previous

studies demonstrating that STEMI due to LAD as the culprit vessel is associated with larger infarct size, worse left ventricle function, and higher mortality when compared with STEMI due to non-LAD arteries [95,96]. Interestingly, the proportion of patients with culprit LAD and TIMI 0-1 flow pre-PCI was also significantly higher in SMuRFless patients similar to what was observed in the SWEDEHEART Registry[63], and CONCORDANCE[62] (Cooperative National Registry of Acute Coronary Syndrome Care) registry in Australia. In another pooled analysis of 2862 patients with individual level data from 10 randomised controlled trials, poor pre-PCI flow TIMI 0/1 was more frequent in SMuRFless patients compared to patients with at least 1 SMuRF (72% vs. 64%, OR: 1.35; 95% CI: 1.08-1.70)[97].

Poor pre-procedural TIMI flow in STEMI patients is well known to be associated with larger infarct size, higher fatal arrhythmia events, higher in-hospital, and one-year mortality[98-100]. Interestingly, in our multivariate analysis of predictors of TIMI 0-1 flow pre-PCI, SMuRFless status was one of the independent predictors. Whether SMuRFless patients truly have a higher predisposition for the involvement of LAD and if there are any biological mechanisms predisposing them to a higher incidence of poor flow (TIMI 0-1) pre-PCI requires further investigation.

A previous study has shown that adverse left ventricle remodelling after STEMI with ≥12% increase in both LVEDV and LVESV at 6 months was associated with worse clinical outcomes at 5 years in terms of all-cause mortality and hospitalization for heart failure in comparison to their counterparts[101]. The proportion of patients reaching this cut off was equivalent in both groups (11% of SMuRFless vs. 13% of patients with at least one SMuRF). There was no difference in MVO between the two groups. At baseline, the infarct size was larger in

SMuRFless patients even after adjusting for the area at risk. Infarct size, as a percent of LV mass, decreased equally over the 3 months in both groups by 1.5%.

**Future Directions:**

In summary, SMuRFless patients had a larger infarct size and smaller MSI following first-presentation STEMI, but this association was mediated by a higher proportion of LAD territory events and pre-PCI TIMI 0-1 flow. Despite of this observation, mortality was not significantly different. Whether the finding of LAD territory and flow reduction preponderance in SMuRFless STEMI patients is a chance finding or related to unknown differences in biology or plaque morphology requires further investigation.

The reasons for a higher early mortality in SMuRFless patients in observational studies remains unclear despite these patients having lower plaque burden and lower calcification (Chapter 6 and 7). The potential mechanisms maybe the absence of myocardial ischemic preconditioning, lack of pre-hospital therapy and less intensive early pharmacotherapy after the diagnosis of STEMI. The benefit of early pharmacotherapy with betablockers, lipid lowering therapies and ace inhibitors has been demonstrated in STEMI patients[102-104], although with some limitations that need further investigation.

**Beta Blockers**

In a randomised study of 270 patients with anterior STEMI, the METOCARD-CNIC trial, very early administration of intravenous metoprolol at time of diagnosis in the absence of heart failure and systolic BP >120 systolic, was associated with a reduction in infarct size on cardiac MRI at days 5 to 7 and higher ejection fraction on cardiac MRI at 6 months[105,106]. The extent of microvascular obstruction on cardiac MRI was significantly less in patients treated with

metoprolol. The extent of myocardial injury after a myocardial infarction is due to a combination of ischemia and reperfusion injury. The neutrophils bind to platelets and red blood cells and form plugs that are embolised to the microcirculation after reperfusion and contribute to microvascular obstruction. Secondly, the neutrophils infiltrating in the area of myocardial injury can have direct deleterious effects. The mechanism for the benefit of metoprolol in reducing infarct size may be due to stunning of neutrophils and dampening the inflammatory response rather than a direct action on the myocardium[107]. The mechanism of action of metoprolol was studied by Ibanez et al in in-vivo mouse models and in in-vitro experiments. The group observed a significant positive correlation between high neutrophil count and the extent of microvascular obstruction in METOCARD-CNIC trial. In contrast, there was no association between other sub-types of white blood cells and the extent of microvascular obstruction. In a mouse model of ischemia reperfusion injury, metoprolol treated mice had smaller infarct size, smaller microvascular obstruction and lower neutrophil infiltration into the infarct area. Metoprolol inhibited the recruitment of neutrophils into the area of myocardial injury. Further in-vitro experiments showed that metoprolol inhibits recruitment of neutrophils and production of reactive oxygen species (ROS) from neutrophils via the beta-1 adrenergic receptor on neutrophils. Metoprolol also inhibits PSGL-1, the receptor involved in neutrophil-platelet interaction, hence reducing the neutrophil-platelet plugs that can occlude microvessels in the myocardium[107].

The clinical benefit of beta blockers in patients with acute coronary syndrome and low ejection fraction is well established. However, the clinical benefit of beta blockers in patients with uncomplicated acute coronary syndrome and ejection fraction >40% is not known. Also, all the randomized trials that have demonstrated benefit of beta blockers after a myocardial infarction were done prior to the pre-perfusion era, except for CAPRICON trial but it only

recruited patients with EF <40%. In the current era of early reperfusion and revascularisation the clinical benefit of beta blockers is not known in patients with normal ejection fraction. In order to answer this clinical question, there are four ongoing prospective large-scale RCTs in Europe randomizing ACS patients without reduced LVEF to beta-blocker or a control group. These trials are:

- REBOOT (TREatment with Beta-blockers after myOcardial infarction withOut Reduced Ejection fracTion) which aims to randomize 8468 ACS patients with LVEF >40% (ClinicalTrials.gov identifier: NCT03596385)[108].

- REDUCE-SWEDEHEART (Evaluation of Decreased Usage of Betablockers After Myocardial Infarction in the SWEDEHEART Registry) aims to randomize 5000 ACS patients with LVEF ≥50% (ClinicalTrials.gov identifier: NCT03278509) ESC 2023[109].

- BETAMI (BEtablocker Treatment After Acute Myocardial Infarction in Patients Without Reduced Left Ventricular Systolic Function) which aims to randomize 10,000 ACS patients with LVEF >40% (EudraCT number 2018-000590-75)[110].

- DANBLOCK (Danish Trial of Beta Blocker Treatment After Myocardial Infarction Without Reduced Ejection Fraction) which aims to randomize 3570 patients with LVEF >40% after myocardial infarction, Clinicaltrials.gov identifier NCT03778554[111].

The optimal duration of treatment with beta-blockers after an acute coronary syndrome is also not known. There are two ongoing large-scale RCTs that will test the impact of beta-blocker withdrawal after 6–12 months following uncomplicated ACS and preserved LVEF:

- AβYSS trial (Beta Blocker Interruption After Uncomplicated Myocardial Infarction; NCT03498066) has randomized 3700 patients in 49 centres in France with a prior history of myocardial infarction and LVEF >40% to continued beta blocker therapy or interruption of beta blocker therapy after 1 year. It aims to assess if it is safe to withdraw beta blocker therapy after 1 year in uncomplicated stable post myocardial infarction patients[112].

- SMART-DECISION (Long-term Beta-blocker Therapy After Acute Myocardial Infarction) aims to recruit 2540 patients in Korea and investigate whether discontinuation of β-blocker after at least 1 year of β-blocker therapy is non-inferior to continuation of β-blocker in patients with LVEF >40% after acute myocardial infarction (ClinicalTrials.gov identifier NCT04769362).

**Lipid Lowering Therapies**

The benefit of statins in reducing the risk of cardiovascular death, non-fatal myocardial infarction, ischaemic stroke, and coronary revascularization by lowering LDL-C is well established. In a meta-analysis of 49 clinical trials with 312 175 participants, for every 1-mmol/L reduction in LDL-C level, there was a 23% relative risk reduction of major vascular events for statins and a 25% relative reduction for non-statin interventions that act primarily via upregulation of LDL receptor expression[113]. The benefit of more intensive reductions in LDL-C levels has also been demonstrated. In a meta-analysis of patients presenting with a median LDL-C of ≤1.8, there was a 21% relative risk reduction of major vascular events by starting statins or non-statin therapy[114]. There was no increased risk of serious adverse events, myalgias and/or myositis, elevation in aminotransferase levels, new-onset diabetes,

haemorrhagic stroke, or cancer even by achieving LDL-C levels as low as 0.5mmol/L[114]. In a recent metanalysis of 327,037 patients from 52 studies, there was a 19% relative risk (RR) reduction for major vascular events for each 1 mmol/L reduction in LDL cholesterol. Interestingly, there was a greater relative risk reduction in patients at lower 10-year atherosclerotic cardiovascular disease risk and in patients at younger age across a mean age of 50-75 years[115]. Based on the continued benefit at lower levels of cholesterol, the current guidelines recommend to lower LDL-C to <1.4mmol/L for secondary prevention[109].

**ACE Inhibitors**

The benefit of ACE inhibitors is well established in patients with heart failure and low ejection fraction[109]. In post myocardial infarction patients, the benefit of ACE inhibitors has mainly been demonstrated in those with heart failure and/or LVEF ≤40%, diabetes, chronic kidney disease, and/or hypertension[109]. However, these trials were performed more than 2.5 decades ago when coronary revascularisation was in its early phase. Current ESC guidelines give a Class IIa recommendation for use of ACE inhibitors after an ACS regardless of ejection fraction[109]. The benefit of ACE inhibitors in patients after a myocardial infarction with normal ejection fraction and absence of risk factors requires further investigation.

In patients with normal LV function but at high risk of coronary events, the benefit of ACE inhibitors was demonstrated in the HOPE and EUROPA trials[116,117]. In HOPE trial that included 9297 high risk patients who had vascular disease or diabetes plus at least one other cardiovascular risk factor, ramipril reduced the rates of death, myocardial infarction and stroke [116]. In EUROPA trial, among patients with stable coronary artery disease and normal LV function, there was a 20% relative risk reduction in cardiovascular death, myocardial infarction, or cardiac arrest[117]. In contrast, the addition of an ACE inhibitor did not reduce the risk of death

from cardiovascular causes, myocardial infarction, or coronary revascularization among patients with stable coronary artery disease and preserved LV function in the PEACE trial[118]. The lack of benefit in PEACE trial was probably due to the patient population being lower risk for cardiovascular events in comparison to HOPE and EUROPA trials.

**Transition from vulnerable plaque to vulnerable patients**

The association between plaque rupture and acute myocardial infarction has been demonstrated on pathology studies[119]. The vulnerable plaque is characterized by a large lipid or necrotic core and a thin fibrous cap <65μm in thickness[119]. A number of imaging and clinical studies have been performed to identify vulnerable plaques, in order to predict the risk of acute coronary events. In a large, prospective study of 697 patients that underwent coronary angiogram and IVUS virtual histology imaging, the PROSPECT (Providing Regional Observations to Study Predictors of Events in the Coronary Tree) trial, the recurrence of adverse cardiac events was adjudicated according to types of coronary atherosclerotic plaque[120]. At 3 years follow up, almost half of the recurrent major cardiovascular events occurred in non-culprit lesions, most of which appeared to be mild on coronary angiography[120]. Although, 596 vulnerable plaques with thin cap fibroatheroma (TCFA) were identified, the risk of myocardial infarction or sudden death related to these lesions was very low[119]. There were 6 events (6 myocardial infarctions and no deaths) after 3.4 years of follow-up among 1,005 coronary arterial sites with pathological intimal thickening and 595 thin-cap atheromas (TCFAs). Out of the total 3,160 plaques detected at baseline the event rate associated with each plaque would be only 0.06% per year. In patients with acute coronary syndrome, plaque rupture is frequently found in non-culprit lesions suggesting that vulnerability is spread throughout the coronary tree. Hence, the identification of vulnerable plaque maybe a marker of widespread inflamed coronary artery disease.

Several longitudinal IVUS and OCT based studies have demonstrated the dynamic nature of coronary artery plaque[119]. Thin cap fibroatheromas can heal over time and become thick cap fibroatheromas[121]. Conversely, thick cap fibroatheromas can progress to thin cap fibroatheroma[121]. OCT and IVUS imaging studies have demonstrated that many plaques can rupture without clinical symptoms[119]. Plaques that rupture and heal lead to progressive luminal obstruction[119]. The prevalence of sub-clinical plaque ruptures varies from 4 to 79% depending on the risk profile and the method of assessment in various studies[119]. The plaque ruptures that do lead to clinical events may depend on other patient factors like the pro-thrombotic milieu of the patient[119]. For example, patients with systemic inflammation and suppressed fibrinolysis maybe more pro-thrombotic[119]. Hence, acute coronary syndrome may occur in the setting of plaque rupture and a pro-thrombotic milieu that cannot contain the thrombosis within the vessel wall[119]. The next step in understanding acute coronary syndrome is to identify new risk factors and mechanisms that makes the patient more vulnerable to thrombosis in the setting of plaque rupture.

**Beyond-SMuRFs Study**

The ‘‘Beyond-SMuRFs Study’’ is a prospective, observational study designed to identify clinical, laboratory or imaging biomarkers that may be associated with acute myocardial infarction in SMuRFless patients[122]. It aims to recruit 500 consecutive patients presenting with STEMI or Non-STEMI (NSTEMI) at two academic hospitals in Thessaloniki, Greece, undergoing primary or emergency coronary angiography[122].

It aims to make a comprehensive in-depth assessment of the clinical profile of SMuRFless patients by collecting additional information on top of basic. Patients will be asked to complete

the International Physical Activity Questionnaire (IPAQ), to measure their physical activity as low, moderate or high. Obesity will be diagnosed by measuring body mass index (BMI; Kg/m2). Socioeconomic parameters like education, marital status, employment, income, migration background and ethnicity will be recorded. The health-related perception of quality of life before the acute myocardial infarction will be measured by the 36-item short form (SF-36) standardized questionnaire.

In terms of laboratory markers, the following will be measured during the hospital admission: total blood count, standard biochemistry parameters, coagulation tests, thyroid hormone and thyroid-stimulating hormone levels, HbA1c, NTproBNP, high sensitive troponin T, LP(a), apolipoproteins B and A1 (ApoB and ApoA1) interleukin-6 (IL-6) and soluble urokinase plasminogen activator receptor (suPAR).

Coronary angiograms will be assessed by two independent experienced cardiologists for lesion characteristics, coronary dominance and the SYNTAX score. All patients will have a detailed trans-thoracic echocardiogram that includes two-dimensional measurements, doppler and strain. Four different indices of myocardial work will be calculated, which are:

1) LV global work index (LVGWI, mmHg %), representing the total work within the LV pressure-strain loops,
2) LV global constructive work (LVGCW, mmHg %), defined as the work performed during myocardial shortening in systole and the work during myocardial lengthening in isovolumic relaxation,

3) LV global wasted work (LVGWW, mmHg %), representing the work contributing to the lengthening of the cardiac myocytes during systole and the shortening during isovolumic relaxation, and
4) LV global work efficiency (LVGWE, %), defining the percentage of effectively spend work by the LV myocytes and obtained by the following formula: (LVGCW/ [LVGCW + LVGWW]) × 100%.

The main aim of the study is to compare clinical, laboratory and imaging parameters between SMuRFless patients and patients with SMuRFs, thereby identifying clinical, laboratory, echocardiographic and angiographic biomarkers that maybe associated with SMuRFless patients in acute myocardial infarction.

Finally, in keeping with the continuous journey of discovery that is research, the work in this thesis has yielded important knowledge but has also generated many interesting questions and led to new avenues of inquiry. There is now a growing interest in the cardiology community to study SMuRFless patients with coronary artery disease. There are a number of clinical and basic science research studies that are ongoing to identify additional risk factors, new biomarkers and new mechanisms that maybe contributing to coronary artery disease in SMuRFless patients.

## *References:*


1. Gao E, Lei YH, Shang X, Huang ZM, Zuo L, Boucher M, Fan Q, Chuprun JK, Ma XL, Koch WJ. A novel and efficient model of coronary artery ligation and myocardial infarction in the mouse. *Circ Res*. 2010;107:1445-1453. doi: 10.1161/CIRCRESAHA.110.223925
2. Virag JA, Lust RM. Coronary artery ligation and intramyocardial injection in a murine model of infarction. *J Vis Exp*. 2011. doi: 10.3791/2581
3. Holmbom B, Näslund U, Eriksson A, Virtanen I, Thornell LE. Comparison of triphenyltetrazolium chloride (TTC) staining versus detection of fibronectin in experimental myocardial infarction. *Histochemistry*. 1993;99:265-275. doi: 10.1007/BF00269099
4. Alqarni F, Alsaadi M, Karem F. MR image analysis of ex-vivo mouse model of heart ischemia. *Saudi J Biol Sci*. 2021;28:1990-1998. doi: 10.1016/j.sjbs.2020.12.054
5. Tong HQ, Fan ML, Sun T, Zhang HW, Han J, Wang MX, Chen JD, Sun WX, Chen XH, Wu MH. Improved Rodent Model of Myocardial Ischemia and Reperfusion Injury. *J Vis Exp*. 2022. doi: 10.3791/63510
6. Ugander M, Bagi PS, Oki AJ, Chen B, Hsu LY, Aletras AH, Shah S, Greiser A, Kellman P, Arai AE. Myocardial edema as detected by pre-contrast T1 and T2 CMR delineates area at risk associated with acute myocardial infarction. *JACC Cardiovasc Imaging*. 2012;5:596-603. doi: 10.1016/j.jcmg.2012.01.016
7. Spath NB, Thompson G, Baker AH, Dweck MR, Newby DE, Semple SIK. Manganese-enhanced MRI of the myocardium. *Heart*. 2019;105:1695-1700. doi: 10.1136/heartjnl-2019-315227

8. Natanzon A, Aletras AH, Hsu LY, Arai AE. Determining canine myocardial area at risk with manganese-enhanced MR imaging. *Radiology*. 2005;236:859-866. doi: 10.1148/radiol.2363040413

9. Krombach GA, Saeed M, Higgins CB, Novikov V, Wendland MF. Contrast-enhanced MR delineation of stunned myocardium with administration of MnCl(2) in rats. *Radiology*. 2004;230:183-190. doi: 10.1148/radiol.2301020228

10. Daire JL, Hyacinthe JN, Tatar I, Montet-Abou K, Ivancevic MK, Masterson K, Jorge-Costa M, Morel DR, Vallée JP. In vivo myocardial infarct area at risk assessment in the rat using manganese enhanced magnetic resonance imaging (MEMRI) at 1.5T. *Magn Reson Med*. 2008;59:1422-1430. doi: 10.1002/mrm.21493

11. Hong SJ, Mintz GS, Ahn CM, Kim JS, Kim BK, Ko YG, Kang TS, Kang WC, Kim YH, Hur SH, et al. Effect of Intravascular Ultrasound-Guided Drug-Eluting Stent Implantation: 5-Year Follow-Up of the IVUS-XPL Randomized Trial. *JACC Cardiovasc Interv*. 2020;13:62-71. doi: 10.1016/j.jcin.2019.09.033

12. Tearney GJ, Regar E, Akasaka T, Adriaenssens T, Barlis P, Bezerra HG, Bouma B, Bruining N, Cho JM, Chowdhary S, et al. Consensus standards for acquisition, measurement, and reporting of intravascular optical coherence tomography studies: a report from the International Working Group for Intravascular Optical Coherence Tomography Standardization and Validation. *J Am Coll Cardiol*. 2012;59:1058-1072. doi: 10.1016/j.jacc.2011.09.079

13. Jang IK, Bouma BE, Kang DH, Park SJ, Park SW, Seung KB, Choi KB, Shishkov M, Schlendorf K, Pomerantsev E, et al. Visualization of coronary atherosclerotic plaques in patients using optical coherence tomography: comparison with intravascular ultrasound. *J Am Coll Cardiol*. 2002;39:604-609. doi: 10.1016/s0735-1097(01)01799-5

14. Bouma BE, Tearney GJ, Yabushita H, Shishkov M, Kauffman CR, DeJoseph Gauthier D, MacNeill BD, Houser SL, Aretz HT, Halpern EF, et al. Evaluation of intracoronary stenting by intravascular optical coherence tomography. *Heart*. 2003;89:317-320. doi: 10.1136/heart.89.3.317

15. Yamaguchi T, Terashima M, Akasaka T, Hayashi T, Mizuno K, Muramatsu T, Nakamura M, Nakamura S, Saito S, Takano M, et al. Safety and feasibility of an intravascular optical coherence tomography image wire system in the clinical setting. *Am J Cardiol*. 2008;101:562-567. doi: 10.1016/j.amjcard.2007.09.116

16. Kubo T, Imanishi T, Takarada S, Kuroi A, Ueno S, Yamano T, Tanimoto T, Matsuo Y, Masho T, Kitabata H, et al. Assessment of culprit lesion morphology in acute myocardial infarction: ability of optical coherence tomography compared with intravascular ultrasound and coronary angioscopy. *J Am Coll Cardiol*. 2007;50:933-939. doi: 10.1016/j.jacc.2007.04.082

17. Räber L, Mintz GS, Koskinas KC, Johnson TW, Holm NR, Onuma Y, Radu MD, Joner M, Yu B, Jia H, et al. Clinical use of intracoronary imaging. Part 1: guidance and optimization of coronary interventions. An expert consensus document of the European Association of Percutaneous Cardiovascular Interventions. *Eur Heart J*. 2018;39:3281-3300. doi: 10.1093/eurheartj/ehy285

18. di Mario C, Koskinas KC, Räber L. Clinical Benefit of IVUS Guidance for Coronary Stenting: The ULTIMATE Step Toward Definitive Evidence? *J Am Coll Cardiol*. 2018;72:3138-3141. doi: 10.1016/j.jacc.2018.10.029

19. Ali ZA, Maehara A, Généreux P, Shlofmitz RA, Fabbiocchi F, Nazif TM, Guagliumi G, Meraj PM, Alfonso F, Samady H, et al. Optical coherence tomography compared with intravascular ultrasound and with angiography to guide coronary stent

implantation (ILUMIEN III: OPTIMIZE PCI): a randomised controlled trial. *Lancet (London, England)*. 2016;388:2618-2628. doi: 10.1016/S0140-6736(16)31922-5

20. Kubo T, Shinke T, Okamura T, Hibi K, Nakazawa G, Morino Y, Shite J, Fusazaki T, Otake H, Kozuma K, et al. Optical frequency domain imaging vs. intravascular ultrasound in percutaneous coronary intervention (OPINION trial): one-year angiographic and clinical results. *Eur Heart J*. 2017;38:3139-3147. doi: 10.1093/eurheartj/ehx351

21. Ali ZA, Karimi Galougahi K, Mintz GS, Maehara A, Shlofmitz RA, Mattesini A. Intracoronary optical coherence tomography: state of the art and future directions. *EuroIntervention : journal of EuroPCR in collaboration with the Working Group on Interventional Cardiology of the European Society of Cardiology*. 2021;17:e105-e123. doi: 10.4244/EIJ-D-21-00089

22. Kubo T, Shimamura K, Ino Y, Yamaguchi T, Matsuo Y, Shiono Y, Taruya A, Nishiguchi T, Shimokado A, Teraguchi I, et al. Superficial Calcium Fracture After PCI as Assessed by OCT. *JACC Cardiovascular imaging*. 2015;8:1228-1229. doi: 10.1016/j.jcmg.2014.11.012

23. Wheeler A, Schrader G, Tucker G, Adams R, Tavella R, Beltrame JF. Prevalence of depression in patients with chest pain and non-obstructive coronary artery disease. *Am J Cardiol*. 2013;112:656-659. doi: 10.1016/j.amjcard.2013.04.042

24. Meneveau N, Souteyrand G, Motreff P, Caussin C, Amabile N, Ohlmann P, Morel O, Lefrançois Y, Descotes-Genon V, Silvain J, et al. Optical Coherence Tomography to Optimize Results of Percutaneous Coronary Intervention in Patients with Non-ST-Elevation Acute Coronary Syndrome: Results of the Multicenter, Randomized DOCTORS Study (Does Optical Coherence Tomography Optimize Results of

Stenting). *Circulation*. 2016;134:906-917. doi: 10.1161/CIRCULATIONAHA.116.024393

25. Gore AK, Shlofmitz E, Karimi Galougahi K, Petrossian G, Jeremias A, Sosa FA, Rahim HM, Stone GW, Mintz GS, Maehara A, et al. Prospective Comparison Between Saline and Radiocontrast for Intracoronary Imaging With Optical Coherence Tomography. *JACC Cardiovascular imaging*. 2020;13:2060-2062. doi: 10.1016/j.jcmg.2020.04.018

26. Kubo T, Ino Y, Shiono Y, Terada K, Emori H, Higashioka D, Takahata M, Wada T, Shimamura K, Khalifa AKM, et al. Usefulness of optical coherence tomography with angiographic coregistration in the guidance of coronary stent implantation. *Heart Vessels*. 2022;37:200-207. doi: 10.1007/s00380-021-01911-1

27. Yu W, Huang J, Jia D, Chen S, Raffel OC, Ding D, Tian F, Kan J, Zhang S, Yan F, et al. Diagnostic accuracy of intracoronary optical coherence tomography-derived fractional flow reserve for assessment of coronary stenosis severity. *EuroIntervention : journal of EuroPCR in collaboration with the Working Group on Interventional Cardiology of the European Society of Cardiology*. 2019;15:189-197. doi: 10.4244/EIJ-D-19-00182

28. Huang J, Emori H, Ding D, Kubo T, Yu W, Huang P, Zhang S, Gutiérrez-Chico JL, Akasaka T, Wijns W, et al. Diagnostic performance of intracoronary optical coherence tomography-based versus angiography-based fractional flow reserve for the evaluation of coronary lesions. *EuroIntervention : journal of EuroPCR in collaboration with the Working Group on Interventional Cardiology of the European Society of Cardiology*. 2020;16:568-576. doi: 10.4244/EIJ-D-19-01034

29. Gutiérrez-Chico JL, Chen Y, Yu W, Ding D, Huang J, Huang P, Jing J, Chu M, Wu P, Tian F, et al. Diagnostic accuracy and reproducibility of optical flow ratio for functional

evaluation of coronary stenosis in a prospective series. *Cardiology journal*. 2020;27:350-361. doi: 10.5603/CJ.a2020.0071

30. Nishimiya K, Tearney G. Micro Optical Coherence Tomography for Coronary Imaging. *Front Cardiovasc Med*. 2021;8:613400. doi: 10.3389/fcvm.2021.613400

31. Yin B, Piao Z, Nishimiya K, Hyun C, Gardecki JA, Mauskapf A, Jaffer FA, Tearney GJ. 3D cellular-resolution imaging in arteries using few-mode interferometry. *Light Sci Appl*. 2019;8:104. doi: 10.1038/s41377-019-0211-5

32. Garrone P, Biondi-Zoccai G, Salvetti I, Sina N, Sheiban I, Stella PR, Agostoni P. Quantitative coronary angiography in the current era: principles and applications. *Journal of interventional cardiology*. 2009;22:527-536. doi: http://dx.doi.org/10.1111/j.1540-8183.2009.00491.x

33. Okamura T, Onuma Y, Garcia-Garcia HM, van Geuns RJ, Wykrzykowska JJ, Schultz C, van der Giessen WJ, Ligthart J, Regar E, Serruys PW. First-in-man evaluation of intravascular optical frequency domain imaging (OFDI) of Terumo: a comparison with intravascular ultrasound and quantitative coronary angiography. *EuroIntervention*. 2011;6:1037-1045. doi: 10.4244/eijv6i9a182

34. Gutierrez-Chico JL, Serruys PW, Girasis C, Garg S, Onuma Y, Brugaletta S, Garcia-Garcia H, van Es GA, Regar E. Quantitative multi-modality imaging analysis of a fully bioresorbable stent: a head-to-head comparison between QCA, IVUS and OCT. *The international journal of cardiovascular imaging*. 2012;28:467-478. doi: http://dx.doi.org/10.1007/s10554-011-9829-y

35. Farooq V, Gomez-Lara J, Brugaletta S, Gogas BD, Garcia-Garcia HM, Onuma Y, van Geuns RJ, Bartorelli A, Whitbourn R, Abizaid A, et al. Proximal and distal maximal luminal diameters as a guide to appropriate deployment of the ABSORB everolimus-eluting bioresorbable vascular scaffold: a sub-study of the ABSORB Cohort B and the

on-going ABSORB EXTEND Single Arm Study. *Catheterization and cardiovascular interventions : official journal of the Society for Cardiac Angiography & Interventions*. 2012;79:880-888. doi: 10.1002/ccd.23177

36. Tu S, Xu L, Ligthart J, Xu B, Witberg K, Sun Z, Koning G, Reiber JH, Regar E. In vivo comparison of arterial lumen dimensions assessed by co-registered three-dimensional (3D) quantitative coronary angiography, intravascular ultrasound and optical coherence tomography. *The international journal of cardiovascular imaging*. 2012;28:1315-1327. doi: http://dx.doi.org/10.1007/s10554-012-0016-6

37. Tu S, Xu L, Ligthart J, Xu B, Witberg K, Sun Z, Koning G, Reiber JH, Regar E. In vivo comparison of arterial lumen dimensions assessed by co-registered three-dimensional (3D) quantitative coronary angiography, intravascular ultrasound and optical coherence tomography. *Int J Cardiovasc Imaging*. 2012;28:1315-1327. doi: 10.1007/s10554-012-0016-6

38. Ding D, Yang J, Westra J, Chen Y, Chang Y, Sejr-Hansen M, Zhang S, Christiansen EH, Holm NR, Xu B, et al. Accuracy of 3-dimensional and 2-dimensional quantitative coronary angiography for predicting physiological significance of coronary stenosis: a FAVOR II substudy. *Cardiovascular diagnosis and therapy*. 2019;9:481-491. doi: 10.21037/cdt.2019.09.07

39. Lee J, Seo KW, Yang HM, Lim HS, Choi BJ, Choi SY, Tahk SJ, Yoon MH. Comparison of three-dimensional quantitative coronary angiography and intravascular ultrasound for detecting functionally significant coronary lesions. *Cardiovascular diagnosis and therapy*. 2020;10:1256-1263. doi: 10.21037/cdt-20-560

40. Xu B, Tu S, Qiao S, Qu X, Chen Y, Yang J, Guo L, Sun Z, Li Z, Tian F, et al. Diagnostic Accuracy of Angiography-Based Quantitative Flow Ratio Measurements for Online

Assessment of Coronary Stenosis. *J Am Coll Cardiol*. 2017;70:3077-3087. doi: 10.1016/j.jacc.2017.10.035

41. Tu S, Westra J, Yang J, von Birgelen C, Ferrara A, Pellicano M, Nef H, Tebaldi M, Murasato Y, Lansky A, et al. Diagnostic Accuracy of Fast Computational Approaches to Derive Fractional Flow Reserve From Diagnostic Coronary Angiography: The International Multicenter FAVOR Pilot Study. *JACC Cardiovasc Interv*. 2016;9:2024-2035. doi: 10.1016/j.jcin.2016.07.013

42. Westra J, Andersen BK, Campo G, Matsuo H, Koltowski L, Eftekhari A, Liu T, Di Serafino L, Di Girolamo D, Escaned J, et al. Diagnostic Performance of In-Procedure Angiography-Derived Quantitative Flow Reserve Compared to Pressure-Derived Fractional Flow Reserve: The FAVOR II Europe-Japan Study. *Journal of the American Heart Association*. 2018;7. doi: 10.1161/JAHA.118.009603

43. Xu B, Tu S, Song L, Jin Z, Yu B, Fu G, Zhou Y, Wang J, Chen Y, Pu J, et al. Angiographic quantitative flow ratio-guided coronary intervention (FAVOR III China): a multicentre, randomised, sham-controlled trial. *Lancet (London, England)*. 2021;398:2149-2159. doi: 10.1016/S0140-6736(21)02248-0

44. Cortés C, Carrasco-Moraleja M, Aparisi A, Rodriguez-Gabella T, Campo A, Gutiérrez H, Julca F, Gómez I, San Román JA, Amat-Santos IJ. Quantitative flow ratio-Meta-analysis and systematic review. *Catheterization and cardiovascular interventions : official journal of the Society for Cardiac Angiography & Interventions*. 2021;97:807-814. doi: 10.1002/ccd.28857

45. Mejía-Rentería H, Lee JM, Lauri F, van der Hoeven NW, de Waard GA, Macaya F, Pérez-Vizcayno MJ, Gonzalo N, Jiménez-Quevedo P, Nombela-Franco L, et al. Influence of Microcirculatory Dysfunction on Angiography-Based Functional

Assessment of Coronary Stenoses. *JACC Cardiovasc Interv*. 2018;11:741-753. doi: 10.1016/j.jcin.2018.02.014

46. Hamaya R, Hoshino M, Kanno Y, Yamaguchi M, Ohya H, Sumino Y, Kanaji Y, Usui E, Murai T, Lee T, et al. Prognostic implication of three-vessel contrast-flow quantitative flow ratio in patients with stable coronary artery disease. *EuroIntervention : journal of EuroPCR in collaboration with the Working Group on Interventional Cardiology of the European Society of Cardiology*. 2019;15:180-188. doi: 10.4244/EIJ-D-18-00896

47. Kogame N, Takahashi K, Tomaniak M, Chichareon P, Modolo R, Chang CC, Komiyama H, Katagiri Y, Asano T, Stables R, et al. Clinical Implication of Quantitative Flow Ratio After Percutaneous Coronary Intervention for 3-Vessel Disease. *JACC Cardiovasc Interv*. 2019;12:2064-2075. doi: 10.1016/j.jcin.2019.08.009

48. Tang J, Chu J, Hou H, Lai Y, Tu S, Chen F, Yao Y, Ye Z, Gao Y, Mao Y, et al. Clinical implication of QFR in patients with ST-segment elevation myocardial infarction after drug-eluting stent implantation. *The international journal of cardiovascular imaging*. 2021;37:755-766. doi: 10.1007/s10554-020-02068-0

49. Mehta SR, Wood DA, Storey RF, Mehran R, Bainey KR, Nguyen H, Meeks B, Di Pasquale G, López-Sendón J, Faxon DP, et al. Complete Revascularization with Multivessel PCI for Myocardial Infarction. *The New England journal of medicine*. 2019;381:1411-1421. doi: 10.1056/NEJMoa1907775

50. Seung J, Choo EH, Kim CJ, Kim HK, Park KH, Lee SH, Kim MC, Hong YJ, Ahn SG, Doh JH, et al. Angiographic Severity of the Non-culprit Lesion and the Efficacy of Fractional Flow Reserve-guided Complete Revascularization in AMI Patients: FRAMI-AMI Substudy. *Circulation Cardiovascular interventions*. 2023. doi: 10.1161/CIRCINTERVENTIONS.123.013611

51. Qi Q, Liu G, Yuan Z, Liu L, Tu S, Zhao Q. Quantitative flow ratio-guided surgical intervention in symptomatic myocardial bridging. *Cardiology journal*. 2020;27:685-692. doi: 10.5603/CJ.a2019.0113

52. Cai X, Tian F, Jing J, Jin Q, Zhou S, Yin W, Chen Y, Wu Q, Fu Z. Prognostic value of quantitative flow ratio measured immediately after drug-coated balloon angioplasty for in-stent restenosis. *Catheterization and cardiovascular interventions : official journal of the Society for Cardiac Angiography & Interventions*. 2021;97 Suppl 2:1048-1054. doi: 10.1002/ccd.29640

53. Tang J, Hou H, Chu J, Chen F, Yao Y, Gao Y, Ye Z, Zhuang S, Lai Y, Liu X. Clinical implication of quantitative flow ratio to predict clinical events after drug-coated balloon angioplasty in patients with in-stent restenosis. *Clin Cardiol*. 2021;44:978-986. doi: 10.1002/clc.23630

54. De Maria GL, Scarsini R, Shanmuganathan M, Kotronias RA, Terentes-Printzios D, Borlotti A, Langrish JP, Lucking AJ, Choudhury RP, Kharbanda R, et al. Angiography-derived index of microcirculatory resistance as a novel, pressure-wire-free tool to assess coronary microcirculation in ST elevation myocardial infarction. *The international journal of cardiovascular imaging*. 2020;36:1395-1406. doi: 10.1007/s10554-020-01831-7

55. Scarsini R, Shanmuganathan M, Kotronias RA, Terentes-Printzios D, Borlotti A, Langrish JP, Lucking AJ, Ribichini F, Ferreira VM, Channon KM, et al. Angiography-derived index of microcirculatory resistance (IMR. *The international journal of cardiovascular imaging*. 2021;37:1801-1813. doi: 10.1007/s10554-021-02254-8

56. Masdjedi K, van Zandvoort LJC, Balbi MM, Gijsen FJH, Ligthart JMR, Rutten MCM, Lemmert ME, Wilschut JM, Diletti R, de Jaegere P, et al. Validation of a three-dimensional quantitative coronary angiography-based software to calculate fractional

flow reserve: the FAST study. *EuroIntervention : journal of EuroPCR in collaboration with the Working Group on Interventional Cardiology of the European Society of Cardiology*. 2020;16:591-599. doi: 10.4244/EIJ-D-19-00466

57. Masdjedi K, van Zandvoort LJ, Balbi MM, Nuis RJ, Wilschut J, Diletti R, de Jaegere PPT, Zijlstra F, Van Mieghem NM, Daemen J. Validation of novel 3-dimensional quantitative coronary angiography based software to calculate fractional flow reserve post stenting. *Catheterization and cardiovascular interventions : official journal of the Society for Cardiac Angiography & Interventions*. 2021;98:671-677. doi: 10.1002/ccd.29311

58. Masdjedi K, Tanaka N, Van Belle E, Porouchani S, Linke A, Woitek FJ, Bartorelli AL, Ali ZA, den Dekker WK, Wilschut J, et al. Vessel fractional flow reserve (vFFR) for the assessment of stenosis severity: the FAST II study. *EuroIntervention*. 2022;17:1498-1505. doi: 10.4244/eij-d-21-00471

59. Roe MT, Halabi AR, Mehta RH, Chen AY, Newby LK, Harrington RA, Smith SC, Jr., Ohman EM, Gibler WB, Peterson ED. Documented traditional cardiovascular risk factors and mortality in non-ST-segment elevation myocardial infarction. *Am Heart J*. 2007;153:507-514. doi: 10.1016/j.ahj.2006.12.018

60. Canto JG, Kiefe CI, Rogers WJ, Peterson ED, Frederick PD, French WJ, Gibson CM, Pollack CV, Jr., Ornato JP, Zalenski RJ, et al. Number of coronary heart disease risk factors and mortality in patients with first myocardial infarction. *Jama*. 2011;306:2120-2127. doi: 10.1001/jama.2011.1654

61. Nauta ST, Deckers JW, van der Boon RM, Akkerhuis KM, van Domburg RT. Risk factors for coronary heart disease and survival after myocardial infarction. *European journal of preventive cardiology*. 2014;21:576-583. doi: 10.1177/2047487312460514

62. Vernon ST, Coffey S, D'Souza M, Chow CK, Kilian J, Hyun K, Shaw JA, Adams M, Roberts-Thomson P, Brieger D, et al. ST-Segment-Elevation Myocardial Infarction (STEMI) Patients Without Standard Modifiable Cardiovascular Risk Factors-How Common Are They, and What Are Their Outcomes? *Journal of the American Heart Association*. 2019;8:e013296. doi: 10.1161/jaha.119.013296

63. Figtree GA, Vernon ST, Hadziosmanovic N, Sundström J, Alfredsson J, Arnott C, Delatour V, Leósdóttir M, Hagström E. Mortality in STEMI patients without standard modifiable risk factors: a sex-disaggregated analysis of SWEDEHEART registry data. *Lancet (London, England)*. 2021;397:1085-1094. doi: 10.1016/s0140-6736(21)00272-5

64. Vernon ST, Coffey S, Bhindi R, Soo Hoo SY, Nelson GI, Ward MR, Hansen PS, Asrress KN, Chow CK, Celermajer DS, et al. Increasing proportion of ST elevation myocardial infarction patients with coronary atherosclerosis poorly explained by standard modifiable risk factors. *European journal of preventive cardiology*. 2017;24:1824-1830. doi: 10.1177/2047487317720287

65. Kong G, Chin YH, Chong B, Goh RSJ, Lim OZH, Ng CH, Muthiah M, Foo R, Vernon ST, Loh PH, et al. Higher mortality in acute coronary syndrome patients without standard modifiable risk factors: Results from a global meta-analysis of 1,285,722 patients. *Int J Cardiol*. 2023;371:432-440. doi: 10.1016/j.ijcard.2022.09.062

66. Shamaki GR, Safiriyu I, Kesiena O, Mbachi C, Anyanwu M, Zahid S, Rai D, Bob-Manuel T, Corteville D, Alweis R, et al. Prevalence and Outcomes in STEMI Patients Without Standard Modifiable Cardiovascular Risk Factors: A National Inpatient Sample Analysis. *Curr Probl Cardiol*. 2022;47:101343. doi: 10.1016/j.cpcardiol.2022.101343

67. Nicholls SJ, Hsu A, Wolski K, Hu B, Bayturan O, Lavoie A, Uno K, Tuzcu EM, Nissen SE. Intravascular ultrasound-derived measures of coronary atherosclerotic plaque burden and clinical outcome. *J Am Coll Cardiol*. 2010;55:2399-2407. doi: 10.1016/j.jacc.2010.02.026

68. Puri R, Nissen SE, Shao M, Ballantyne CM, Barter PJ, Chapman MJ, Erbel R, Libby P, Raichlen JS, Uno K, et al. Coronary atheroma volume and cardiovascular events during maximally intensive statin therapy. *Eur Heart J*. 2013;34:3182-3190. doi: 10.1093/eurheartj/eht260

69. Nissen SE, Tuzcu EM, Brewer HB, Sipahi I, Nicholls SJ, Ganz P, Schoenhagen P, Waters DD, Pepine CJ, Crowe TD, et al. Effect of ACAT inhibition on the progression of coronary atherosclerosis. *The New England journal of medicine*. 2006;354:1253-1263. doi: 10.1056/NEJMoa054699

70. Nissen SE, Nicholls SJ, Sipahi I, Libby P, Raichlen JS, Ballantyne CM, Davignon J, Erbel R, Fruchart JC, Tardif JC, et al. Effect of very high-intensity statin therapy on regression of coronary atherosclerosis: the ASTEROID trial. *Jama*. 2006;295:1556-1565. doi: 10.1001/jama.295.13.jpc60002

71. Nissen SE, Tardif JC, Nicholls SJ, Revkin JH, Shear CL, Duggan WT, Ruzyllo W, Bachinsky WB, Lasala GP, Tuzcu EM. Effect of torcetrapib on the progression of coronary atherosclerosis. *The New England journal of medicine*. 2007;356:1304-1316. doi: 10.1056/NEJMoa070635

72. Nissen SE, Nicholls SJ, Wolski K, Nesto R, Kupfer S, Perez A, Jure H, De Larochellière R, Staniloae CS, Mavromatis K, et al. Comparison of pioglitazone vs glimepiride on progression of coronary atherosclerosis in patients with type 2 diabetes: the PERISCOPE randomized controlled trial. *Jama*. 2008;299:1561-1573. doi: 10.1001/jama.299.13.1561

73. Nissen SE, Nicholls SJ, Wolski K, Rodés-Cabau J, Cannon CP, Deanfield JE, Després JP, Kastelein JJ, Steinhubl SR, Kapadia S, et al. Effect of rimonabant on progression of atherosclerosis in patients with abdominal obesity and coronary artery disease: the STRADIVARIUS randomized controlled trial. *Jama*. 2008;299:1547-1560. doi: 10.1001/jama.299.13.1547

74. Nicholls SJ, Ballantyne CM, Barter PJ, Chapman MJ, Erbel RM, Libby P, Raichlen JS, Uno K, Borgman M, Wolski K, et al. Effect of two intensive statin regimens on progression of coronary disease. *The New England journal of medicine*. 2011;365:2078-2087. doi: 10.1056/NEJMoa1110874

75. Nicholls SJ, Puri R, Anderson T, Ballantyne CM, Cho L, Kastelein JJ, Koenig W, Somaratne R, Kassahun H, Yang J, et al. Effect of Evolocumab on Progression of Coronary Disease in Statin-Treated Patients: The GLAGOV Randomized Clinical Trial. *JAMA*. 2016;316:2373-2384. doi: 10.1001/jama.2016.16951

76. Nicholls SJ, Bakris GL, Kastelein JJ, Menon V, Williams B, Armbrecht J, Brunel P, Nicolaides M, Hsu A, Hu B, et al. Effect of aliskiren on progression of coronary disease in patients with prehypertension: the AQUARIUS randomized clinical trial. *JAMA*. 2013;310:1135-1144. doi: 10.1001/jama.2013.277169

77. Nissen SE, Tuzcu EM, Schoenhagen P, Brown BG, Ganz P, Vogel RA, Crowe T, Howard G, Cooper CJ, Brodie B, et al. Effect of intensive compared with moderate lipid-lowering therapy on progression of coronary atherosclerosis: a randomized controlled trial. *JAMA*. 2004;291:1071-1080. doi: 10.1001/jama.291.9.1071

78. Brener SJ, Ivanc TB, Poliszczuk R, Chen M, Tuzcu EM, Hu T, Frid DJ, Nissen SE. Antihypertensive therapy and regression of coronary artery disease: insights from the Comparison of Amlodipine versus Enalapril to Limit Occurrences of Thrombosis (CAMELOT) and Norvasc for Regression of Manifest Atherosclerotic Lesions by

Intravascular Sonographic Evaluation (NORMALISE) trials. *Am Heart J*. 2006;152:1059-1063. doi: 10.1016/j.ahj.2006.07.022

79. Andrews J, Puri R, Kataoka Y, Nicholls SJ, Psaltis PJ. Therapeutic modulation of the natural history of coronary atherosclerosis: lessons learned from serial imaging studies. *Cardiovascular diagnosis and therapy*. 2016;6:282-303. doi: 10.21037/cdt.2015.10.02

80. Rajagopalan S, Al-Kindi SG, Brook RD. Air Pollution and Cardiovascular Disease: JACC State-of-the-Art Review. *J Am Coll Cardiol*. 2018;72:2054-2070. doi: 10.1016/j.jacc.2018.07.099

81. Mustafic H, Jabre P, Caussin C, Murad MH, Escolano S, Tafflet M, Périer MC, Marijon E, Vernerey D, Empana JP, et al. Main air pollutants and myocardial infarction: a systematic review and meta-analysis. *JAMA*. 2012;307:713-721. doi: 10.1001/jama.2012.126

82. Khera AV, Emdin CA, Drake I, Natarajan P, Bick AG, Cook NR, Chasman DI, Baber U, Mehran R, Rader DJ, et al. Genetic Risk, Adherence to a Healthy Lifestyle, and Coronary Disease. *The New England journal of medicine*. 2016;375:2349-2358. doi: 10.1056/NEJMoa1605086

83. Elliott J, Bodinier B, Bond TA, Chadeau-Hyam M, Evangelou E, Moons KGM, Dehghan A, Muller DC, Elliott P, Tzoulaki I. Predictive Accuracy of a Polygenic Risk Score-Enhanced Prediction Model vs a Clinical Risk Score for Coronary Artery Disease. *JAMA*. 2020;323:636-645. doi: 10.1001/jama.2019.22241

84. Mosley JD, Gupta DK, Tan J, Yao J, Wells QS, Shaffer CM, Kundu S, Robinson-Cohen C, Psaty BM, Rich SS, et al. Predictive Accuracy of a Polygenic Risk Score Compared With a Clinical Risk Score for Incident Coronary Heart Disease. *JAMA*. 2020;323:627-635. doi: 10.1001/jama.2019.21782

85. Wang L, Cong HL, Zhang JX, Li XM, Hu YC, Wang C, Lang JC, Zhou BY, Li TT, Liu CW, et al. Prognostic performance of multiple biomarkers in patients with acute coronary syndrome without standard cardiovascular risk factors. *Front Cardiovasc Med*. 2022;9:916085. doi: 10.3389/fcvm.2022.916085

86. Vernon ST, Tang O, Kim T, Chan AS, Kott KA, Park J, Hansen T, Koay YC, Grieve SM, O'Sullivan JF, et al. Metabolic Signatures in Coronary Artery Disease: Results from the BioHEART-CT Study. *Cells*. 2021;10. doi: 10.3390/cells10050980

87. Martins AMA, Paiva MUB, Paiva DVN, de Oliveira RM, Machado HL, Alves LJSR, Picossi CRC, Faccio AT, Tavares MFM, Barbas C, et al. Innovative Approaches to Assess Intermediate Cardiovascular Risk Subjects: A Review From Clinical to Metabolomics Strategies. *Front Cardiovasc Med*. 2021;8:788062. doi: 10.3389/fcvm.2021.788062

88. Ottosson F, Ericson U, Almgren P, Smith E, Brunkwall L, Hellstrand S, Nilsson PM, Orho-Melander M, Fernandez C, Melander O. Dimethylguanidino Valerate: A Lifestyle-Related Metabolite Associated With Future Coronary Artery Disease and Cardiovascular Mortality. *Journal of the American Heart Association*. 2019;8:e012846. doi: 10.1161/JAHA.119.012846

89. Kott KA, Vernon ST, Hansen T, Yu C, Bubb KJ, Coffey S, Sullivan D, Yang J, O'Sullivan J, Chow C, et al. Biobanking for discovery of novel cardiovascular biomarkers using imaging-quantified disease burden: protocol for the longitudinal, prospective, BioHEART-CT cohort study. *BMJ Open*. 2019;9:e028649. doi: 10.1136/bmjopen-2018-028649

90. Hoogeveen RM, Pereira JPB, Nurmohamed NS, Zampoleri V, Bom MJ, Baragetti A, Boekholdt SM, Knaapen P, Khaw KT, Wareham NJ, et al. Improved cardiovascular

risk prediction using targeted plasma proteomics in primary prevention. *Eur Heart J*. 2020;41:3998-4007. doi: 10.1093/eurheartj/ehaa648

91. Nurmohamed NS, Belo Pereira JP, Hoogeveen RM, Kroon J, Kraaijenhof JM, Waissi F, Timmerman N, Bom MJ, Hoefer IE, Knaapen P, et al. Targeted proteomics improves cardiovascular risk prediction in secondary prevention. *Eur Heart J*. 2022;43:1569-1577. doi: 10.1093/eurheartj/ehac055

92. Adikari D, Gharleghi R, Zhang S, Jorm L, Sowmya A, Moses D, Ooi SY, Beier S. A new and automated risk prediction of coronary artery disease using clinical endpoints and medical imaging-derived patient-specific insights: protocol for the retrospective GeoCAD cohort study. *BMJ Open*. 2022;12:e054881. doi: 10.1136/bmjopen-2021-054881

93. Figtree GA, Vernon ST, Harmer JA, Gray MP, Arnott C, Bachour E, Barsha G, Brieger D, Brown A, Celermajer DS, et al. Clinical Pathway for Coronary Atherosclerosis in Patients Without Conventional Modifiable Risk Factors: JACC State-of-the-Art Review. *J Am Coll Cardiol*. 2023;82:1343-1359. doi: 10.1016/j.jacc.2023.06.045

94. Khan E, Brieger D, Amerena J, Atherton JJ, Chew DP, Farshid A, Ilton M, Juergens CP, Kangaharan N, Rajaratnam R, et al. Differences in management and outcomes for men and women with ST-elevation myocardial infarction. *The Medical journal of Australia*. 2018;209:118-123. doi: 10.5694/mja17.01109

95. Entezarjou A, Mohammad MA, Andell P, Koul S. Culprit vessel: impact on short-term and long-term prognosis in patients with ST-elevation myocardial infarction. *Open Heart*. 2018;5:e000852. doi: 10.1136/openhrt-2018-000852

96. Backhaus SJ, Kowallick JT, Stiermaier T, Lange T, Koschalka A, Navarra JL, Lotz J, Kutty S, Bigalke B, Gutberlet M, et al. Culprit vessel-related myocardial mechanics

and prognostic implications following acute myocardial infarction. *Clin Res Cardiol*. 2020;109:339-349. doi: 10.1007/s00392-019-01514-x

97. Figtree GA, Redfors B, Kozor R, Vernon ST, Grieve SM, Mazhar J, Thiele H, Patel MR, Udelson JE, Selker HP, et al. Clinical Outcomes in Patients With ST-Segment Elevation MI and No Standard Modifiable Cardiovascular Risk Factors. *JACC Cardiovasc Interv*. 2022;15:1167-1175. doi: 10.1016/j.jcin.2022.03.036

98. Hashimoto T, Ako J, Nakao K, Ozaki Y, Kimura K, Noguchi T, Yasuda S, Suwa S, Fujimoto K, Nakama Y, et al. Pre-Procedural Thrombolysis in Myocardial Infarction Flow in Patients with ST-Segment Elevation Myocardial Infarction. *International heart journal*. 2018;59:920-925. doi: 10.1536/ihj.17-518

99. Rakowski T, Dudek D, Dziewierz A, Yu J, Witzenbichler B, Guagliumi G, Kornowski R, Hartmann F, Lansky AJ, Brener SJ, et al. Impact of infarct-related artery patency before primary PCI on outcome in patients with ST-segment elevation myocardial infarction: the HORIZONS-AMI trial. *EuroIntervention : journal of EuroPCR in collaboration with the Working Group on Interventional Cardiology of the European Society of Cardiology*. 2013;8:1307-1314. doi: 10.4244/eijv8i11a199

100. De Luca G, Parodi G, Sciagrà R, Venditti F, Bellandi B, Vergara R, Migliorini A, Valenti R, Antoniucci D. Preprocedural TIMI flow and infarct size in STEMI undergoing primary angioplasty. *Journal of thrombosis and thrombolysis*. 2014;38:81-86. doi: 10.1007/s11239-013-0977-x

101. Bulluck H, Carberry J, Carrick D, McEntegart M, Petrie MC, Eteiba H, Hood S, Watkins S, Lindsay M, Mahrous A, et al. Redefining Adverse and Reverse Left Ventricular Remodeling by Cardiovascular Magnetic Resonance Following ST-Segment-Elevation Myocardial Infarction and Their Implications on Long-Term

Prognosis. *Circulation Cardiovascular imaging*. 2020;13:e009937. doi: 10.1161/circimaging.119.009937

102. Bugiardini R, Cenko E, Ricci B, Vasiljevic Z, Dorobantu M, Kedev S, Vavlukis M, Kalpak O, Puddu PE, Gustiene O, et al. Comparison of Early Versus Delayed Oral β Blockers in Acute Coronary Syndromes and Effect on Outcomes. *Am J Cardiol*. 2016;117:760-767. doi: 10.1016/j.amjcard.2015.11.059

103. Fonarow GC, Wright RS, Spencer FA, Fredrick PD, Dong W, Every N, French WJ, Investigators NRoMI. Effect of statin use within the first 24 hours of admission for acute myocardial infarction on early morbidity and mortality. *Am J Cardiol*. 2005;96:611-616. doi: 10.1016/j.amjcard.2005.04.029

104. ISIS-4: a randomised factorial trial assessing early oral captopril, oral mononitrate, and intravenous magnesium sulphate in 58,050 patients with suspected acute myocardial infarction. ISIS-4 (Fourth International Study of Infarct Survival) Collaborative Group. *Lancet (London, England)*. 1995;345:669-685.

105. Ibanez B, Macaya C, Sánchez-Brunete V, Pizarro G, Fernández-Friera L, Mateos A, Fernández-Ortiz A, García-Ruiz JM, García-Álvarez A, Iñiguez A, et al. Effect of early metoprolol on infarct size in ST-segment-elevation myocardial infarction patients undergoing primary percutaneous coronary intervention: the Effect of Metoprolol in Cardioprotection During an Acute Myocardial Infarction (METOCARD-CNIC) trial. *Circulation*. 2013;128:1495-1503. doi: 10.1161/CIRCULATIONAHA.113.003653

106. Pizarro G, Fernández-Friera L, Fuster V, Fernández-Jiménez R, García-Ruiz JM, García-Álvarez A, Mateos A, Barreiro MV, Escalera N, Rodriguez MD, et al. Long-term benefit of early pre-reperfusion metoprolol administration in patients with acute myocardial infarction: results from the METOCARD-CNIC trial (Effect of Metoprolol

in Cardioprotection During an Acute Myocardial Infarction). *J Am Coll Cardiol*. 2014;63:2356-2362. doi: 10.1016/j.jacc.2014.03.014

107. García-Prieto J, Villena-Gutiérrez R, Gómez M, Bernardo E, Pun-García A, García-Lunar I, Crainiciuc G, Fernández-Jiménez R, Sreeramkumar V, Bourio-Martínez R, et al. Neutrophil stunning by metoprolol reduces infarct size. *Nat Commun*. 2017;8:14780. doi: 10.1038/ncomms14780

108. Rossello X, Raposeiras-Roubin S, Latini R, Dominguez-Rodriguez A, Barrabés JA, Sánchez PL, Anguita M, Fernández-Vázquez F, Pascual-Figal D, De la Torre Hernandez JM, et al. Rationale and design of the pragmatic clinical trial tREatment with Beta-blockers after myOcardial infarction withOut reduced ejection fracTion (REBOOT). *Eur Heart J Cardiovasc Pharmacother*. 2022;8:291-301. doi: 10.1093/ehjcvp/pvab060

109. Byrne RA, Rossello X, Coughlan JJ, Barbato E, Berry C, Chieffo A, Claeys MJ, Dan G-A, Dweck MR, Galbraith M, et al. 2023 ESC Guidelines for the management of acute coronary syndromes: Developed by the task force on the management of acute coronary syndromes of the European Society of Cardiology (ESC). *European Heart Journal*. 2023;44:3720-3826. doi: 10.1093/eurheartj/ehad191

110. Munkhaugen J, Ruddox V, Halvorsen S, Dammen T, Fagerland MW, Hernæs KH, Vethe NT, Prescott E, Jensen SE, Rødevand O, et al. BEtablocker Treatment After acute Myocardial Infarction in revascularized patients without reduced left ventricular ejection fraction (BETAMI): Rationale and design of a prospective, randomized, open, blinded end point study. *Am Heart J*. 2019;208:37-46. doi: 10.1016/j.ahj.2018.10.005

111. Kristensen AMD, Bovin A, Zwisler AD, Cerquira C, Torp-Pedersen C, Bøtker HE, Gustafsson I, Veien KT, Thomsen KK, Olsen MH, et al. Design and rationale of the Danish trial of beta-blocker treatment after myocardial infarction without reduced

ejection fraction: study protocol for a randomized controlled trial. *Trials*. 2020;21:415. doi: 10.1186/s13063-020-4214-6

112. Silvain J, Cayla G, Ferrari E, Range G, Puymirat E, Delarche N, Collet JP, Dumaine R, Slama M, Payot L, et al. βeta blocker interruption after uncomplicated myocardial infarction: rationale and design of the randomized ABYSS trial. *Am Heart J*. 2023;258:168-176. doi: 10.1016/j.ahj.2023.01.014

113. Silverman MG, Ference BA, Im K, Wiviott SD, Giugliano RP, Grundy SM, Braunwald E, Sabatine MS. Association Between Lowering LDL-C and Cardiovascular Risk Reduction Among Different Therapeutic Interventions: A Systematic Review and Meta-analysis. *JAMA*. 2016;316:1289-1297. doi: 10.1001/jama.2016.13985

114. Sabatine MS, Wiviott SD, Im K, Murphy SA, Giugliano RP. Efficacy and Safety of Further Lowering of Low-Density Lipoprotein Cholesterol in Patients Starting With Very Low Levels: A Meta-analysis. *JAMA Cardiol*. 2018;3:823-828. doi: 10.1001/jamacardio.2018.2258

115. Wang N, Fulcher J, Abeysuriya N, Park L, Kumar S, Di Tanna GL, Wilcox I, Keech A, Rodgers A, Lal S. Intensive LDL cholesterol-lowering treatment beyond current recommendations for the prevention of major vascular events: a systematic review and meta-analysis of randomised trials including 327 037 participants. *Lancet Diabetes Endocrinol*. 2020;8:36-49. doi: 10.1016/S2213-8587(19)30388-2

116. Yusuf S, Sleight P, Pogue J, Bosch J, Davies R, Dagenais G, Investigators HOPES. Effects of an angiotensin-converting-enzyme inhibitor, ramipril, on cardiovascular events in high-risk patients. *The New England journal of medicine*. 2000;342:145-153. doi: 10.1056/NEJM200001203420301

117. Fox KM, Investigators EtOrocewPiscAd. Efficacy of perindopril in reduction of cardiovascular events among patients with stable coronary artery disease: randomised,

double-blind, placebo-controlled, multicentre trial (the EUROPA study). *Lancet (London, England)*. 2003;362:782-788. doi: 10.1016/s0140-6736(03)14286-9

118. Braunwald E, Domanski MJ, Fowler SE, Geller NL, Gersh BJ, Hsia J, Pfeffer MA, Rice MM, Rosenberg YD, Rouleau JL, et al. Angiotensin-converting-enzyme inhibition in stable coronary artery disease. *The New England journal of medicine*. 2004;351:2058-2068. doi: 10.1056/NEJMoa042739

119. Arbab-Zadeh A, Fuster V. The myth of the "vulnerable plaque": transitioning from a focus on individual lesions to atherosclerotic disease burden for coronary artery disease risk assessment. *J Am Coll Cardiol*. 2015;65:846-855. doi: 10.1016/j.jacc.2014.11.041

120. Stone GW, Maehara A, Lansky AJ, de Bruyne B, Cristea E, Mintz GS, Mehran R, McPherson J, Farhat N, Marso SP, et al. A prospective natural-history study of coronary atherosclerosis. *The New England journal of medicine*. 2011;364:226-235. doi: 10.1056/NEJMoa1002358

121. Kubo T, Maehara A, Mintz GS, Doi H, Tsujita K, Choi SY, Katoh O, Nasu K, Koenig A, Pieper M, et al. The dynamic nature of coronary artery lesion morphology assessed by serial virtual histology intravascular ultrasound tissue characterization. *J Am Coll Cardiol*. 2010;55:1590-1597. doi: 10.1016/j.jacc.2009.07.078

122. Moysidis DV, Daios S, Anastasiou V, Liatsos AC, Papazoglou AS, Karagiannidis E, Kamperidis V, Makedou K, Thisiadou A, Karalazou P, et al. Association of clinical, laboratory and imaging biomarkers with the occurrence of acute myocardial infarction in patients without standard modifiable risk factors - rationale and design of the "Beyond-SMuRFs Study". *BMC Cardiovasc Disord*. 2023;23:149. doi: 10.1186/s12872-023-03180-4